SEQUENCE STRATIGRAPHIC, PALEOENVIRONMENTAL, AND CHRONOLOGICAL ANALYSIS OF THE LATE NEOGENE WANGANUI RIVER SECTION, WANGANUI BASIN

A thesis submitted in fulfilment of the requirements for the degree

of

Doctor of Philosophy in Earth Sciences

at

The University of Waikato

The University of Waikato
Te Whare Wānanga o Waikato

SHAUN HAYTON

DEPARTMENT OF EARTH SCIENCES
THE UNIVERSITY OF WAIKATO
AUGUST 1998

ABSTRACT

Between Taranaki Basin and the central ranges of the North Island, New Zealand, lies the broadly elliptical, back-arc Wanganui Basin, half of which is onshore. This basin covers an area of about 22,000 km^2, and contains a Plio-Pleistocene sedimentary succession some 4 km thick. Ongoing south- to southeast-ward migration of the basin depocentre and thermally driven uplift to the north have resulted in the development of broad east-west trending stratal belts that young and dip to the south. The Wanganui River intersects these stratal belts and offers the potential to examine the entire late Miocene to late Pliocene succession in the western half of Wanganui Basin.

For the first time the Wanganui River section has been divided into five predominantly planktic foraminiferal biozones (*Globorotalia conomiozea* zone, *G. punticulata* zone, *G. inflata* zone, combined dextral *G. crassaformis* and *Cibicides molestus* zone, and dextral *G. crassaformis* zone), that are linked to the New Zealand stage classification system. The absolute ages implied by these biostratigraphic datums, combined with a magnetostratigraphy being developed for the section, form an age framework for the sedimentary succession exposed in the Wanganui River valley between Tieke and Parakino. The apparently diachronous nature of the datums traditionally tied to the Mangapanian-Waipipian Stage boundary are highlighted.

The lithostratigraphy of the approximately 3600 m thick sedimentary succession between Tieke and Parakino has been analysed and recorded. Three lithotypes (sandstone, siltstone, shellbed) have been identified, with each containing a number of lithofacies. These lithofacies represent a variety of paleoenvironments from nearshore (0-25 m) to slope type (200-600 m) depths, as determined by analysis of the benthic foraminiferal content and sedimentary structures. This study has resulted in the identification of key unit boundaries and has to some degree simplified the nomenclature assigned to this succession, with five discrete units being recognised.

The Matemateaonga Formation is an at least 1570 m-thick late Miocene (lower Kapitean) to Pliocene (mid Opoitian) succession with 31 discrete cyclothems being identified in the section studied. Each cyclothem displays a coarsening upward trend, with most being related to high-order (6th) glacio-eustatic sea-level fluctuations. Some differences are noted between these cyclothems and those modelled by Naish and Kamp (1997), notably the character of the basal boundary and the architecture of the transgressive systems tract.

The Pliocene (mid Opoitian and Waipipian) aged Tangahoe Formation in the Wanganui River valley is predominantly a deep-water (200-600 m) siltstone, within which occur three distinct sandstone-dominated units (Jerusalem, Matahiwi and Koroniti Sandstone Members). The depocentre, in which this unit was deposited, formed in a shallow continental seaway resulting in a foraminiferal signal that was both deep-water and neritic. The sandstone members are composed of multiple mass-emplaced sandstones interbedded with typical Tangahoe Formation siltstone and are interpreted as being slope and

basin floor (in terms of the depocentre, rather than a typical continental margin) fan deposits derived from quasi-steady state grain flows.

The Ahurangi Sandstone overlies the siltstone-dominated Tangahoe Formation, with the basal transition occurring over 15 m. The Ahurangi Sandstone is initially massive but becomes bedded in its upper half. This unit is interpreted as reflecting the rapid infilling of the deep-water basin responsible for the development of the Tangahoe Formation.

The Waipipian and Mangapanian aged cyclothemic Atene Formation overlies the Ahurangi Sandstone and records the return of high-order glacio-eustatic fluctuations as the dominant control on relative sea-level, and thus sedimentation, within a shelf environment.

The Mangaweka Mudstone is the uppermost unit within this study. The sedimentary succession as observed in the Wanganui River section is interpreted as being deposited in a "giant foreset" type of environment. Using foraminiferal data, the basal boundary of the Mangaweka Mudstone appears time transgressive across the Wanganui Basin.

The development of the Wanganui River valley succession between Tieke and Parakino can be subdivided into a series of six phases within an overall subsiding basin. The four complete phases (Ngaporo, Puraroto Caves, Pipiriki and Ranana) show a period of major deepening followed by shallowing before re-establishment of high-order glacio-eustatic sea-level fluctuations as the primary control on relative sea-level. These deepening events have been interpreted as representing stages of tectonically controlled depocentre development. The variability (lithological, architecture and size) in the phases is related to the proximity of the Wanganui River section to the loci of depocentre development. The Ranana phase is regarded as being centrally located, while the Ngaporo and Puraroto Caves phases represent more distal locations relative to their contemporary depocentre(s).

ACKNOWLEDGEMENTS

Firstly I would like to thank all the people that regard the Wanganui River valley as home for their help in this project. Although too many to thank individually there are a few I want to give special mention: Dennis and the team at Pipiriki D.o.C. for providing accommodation and helping to highlight and solve some of the local concerns; Baldy (Paul Haitana) for providing jet boat access on the river and for his never-ending hunting and fishing stories, as well as his knowledge of the river and its history; and the people of Mangapapapa and Tieke Maraes for their hospitality and for providing an insight into the spiritual importance of the Wanganui River.

To my supervisors, Peter Kamp and Cam Nelson, thanks for ongoing support and helping to get this project finished. To the Earth Sciences technical staff, especially Steve C., Laurie, Mike, Steve B., Bruce, Annette, Renat and the rest for the humour and down to earth attitude that has helped to keep things in perspective. To my fellow students thanks for the great discussions and help in various ways, especially to Martin who has put up with never-ending questions about forams and has taught me practically everything I know on that topic. Thanks also to the departmental secretaries Sydney, and Elaine, for their assistance and quiet advice.

A big thank you to family and friends that have assisted in numerous ways over the last few years. A special thanks to Ian for all his assistance with computers and other activities, and finally to Tai (N.Z.'s first CDX qualified Chow Chow) for his companionship.

Funding support from the Public Good Science Foundation grant UOW 607 is acknowledged.

Thanks everyone.

Shaun

CONTENTS

CHAPTER 4: TANGAHOE FORMATION AND THE DEEP-WATER, MASS-EMPLACED SANDSTONES

CHAPTER 5: AHURANGI SANDSTONE, ATENE FORMATION AND MANGAWEKA MUDSTONE: STRATIGRAPHY AND SEDIMENTOLOGY

CHAPTER 6: GEOLOGICAL SYNTHESIS

APPENDIX 1: METHODS

APPENDIX 2: DATA

LIST OF FIGURES

CHAPTER 1: INTRODUCTION

CHAPTER 2: BIOSTRATIGRAPHY AND CHRONOLOGY

Supplement 1

CHAPTER 3: STRATIGRAPHY, SEQUENCE STRATIGRAPHY AND PALEOENVIRONMENTS OF THE MATEMATEAONGA FORMATION

Supplement 1

Supplement 2

CHAPTER 4: TANGAHOE FORMATION AND THE DEEP-WATER, MASS-EMPLACED SANDSTONES

Supplement 1

CHAPTER 5: AHURANGI SANDSTONE, ATENE FORMATION AND MANGAWEKA MUDSTONE: STRATIGRAPHY AND SEDIMENTOLOGY

CHAPTER 6: GEOLOGICAL SYNTHESIS

LIST OF TABLES

CHAPTER 2: BIOSTRATIGRAPHY AND CHRONOLOGY

CHAPTER 3: STRATIGRAPHY, SEQUENCE STRATIGRAPHY AND PALEOENVIRONMENTS OF THE MATEMATEAONGA FORMATION

Supplement 2

CHAPTER 4: TANGAHOE FORMATION AND THE DEEP-WATER, MASS-EMPLACED SANDSTONES

Supplement 1

Supplement 2

CHAPTER 5: AHURANGI SANDSTONE, ATENE FORMATION AND MANGAWEKA MUDSTONE: STRATIGRAPHY AND SEDIMENTOLOGY

CHAPTER 6: GEOLOGICAL SYNTHESIS

LIST OF PLATES

CHAPTER 4: TANGAHOE FORMATION AND THE DEEP-WATER, MASS-EMPLACED SANDSTONES

CHAPTER 5: AHURANGI SANDSTONE, ATENE FORMATION AND MANGAWEKA MUDSTONE: STRATIGRAPHY AND SEDIMENTOLOGY

CHAPTER 1

INTRODUCTION

CHAPTER 1

INTRODUCTION

1:1 INTRODUCTION

South Wanganui Basin (of Katz, 1968; Anderton, 1981; referred to as the Wanganui Basin in this study as per recent studies e.g. Stern and Davey 1989; Naish *et al.*, 1996) is one of New Zealand's extensive Cenozoic sedimentary basins and lies behind the Hikurangi subduction zone in central New Zealand, west of the North Island axial ranges and east of Taranaki Basin (Figure 1:1). The broadly elliptical back-arc Wanganui Basin contains a Plio-Pleistocene marine sedimentary succession some 4 km thick (Anderton, 1981) and covers an area of about 22,000 km^2, approximately half of which is offshore. South- and southeast-ward migration of the basin depocentre has lead to onlapping of progressively younger strata onto Mesozoic basement rocks to the south. Coeval uplift to the north has resulted in roughly east/west trending stratal belts that dip gently (4-5°) towards the present depocentre (Anderton, 1981). The western boundary of this basin is clearly delineated by the Patea-Tongaporutu basement high and associated Taranaki Fault Zone, while in the east and northeast sediments either lap onto, or are in fault contact with, the Kaimanawa, Tararua and Ruahine Ranges (Figure 1:1). To the south, submarine Pleistocene sediments onlap the basement rocks of Marlborough Sounds (Anderton, 1981). However, the northern transition into the North Wanganui Basin is poorly defined, with more recent regional gravity analysis (Hunt, 1980) not supporting the existence of the Pipiriki High, which was proposed by Cope (1966) and subsequently used to subdivide the two basins (e.g. McQuillan, 1977).

Recently, the Wanganui Basin succession has been the impetus for numerous studies (e.g. Abbott and Carter, 1994; Naish and Kamp, 1995; Journeaux *et al.*, 1996; McIntyre and Kamp, 1998) relating late Pliocene and Pleistocene cyclic sedimentation in outcrop to glacio-eustatic sea-level fluctuations inferred from deep-sea oxygen isotope records (e.g. Tiedemann *et al.*, 1994; Shackleton *et al.*, 1995). The onland studies have utilised extensive coastal exposure and the deeply incised, southward flowing, rivers that progressively dissect and expose the stratigraphic succession. However, it is primarily the underlying late Miocene to late Pliocene strata that have been the emphasis of hydrocarbon exploration within the Wanganui Basin, both in terms of source rock potential and reservoir characteristics (e.g. Murphy *et al.*,

1994; Thompson *et al.*, 1994). Thus this study is based on increasing the body of knowledge and understanding of these potential hydrocarbon targets.

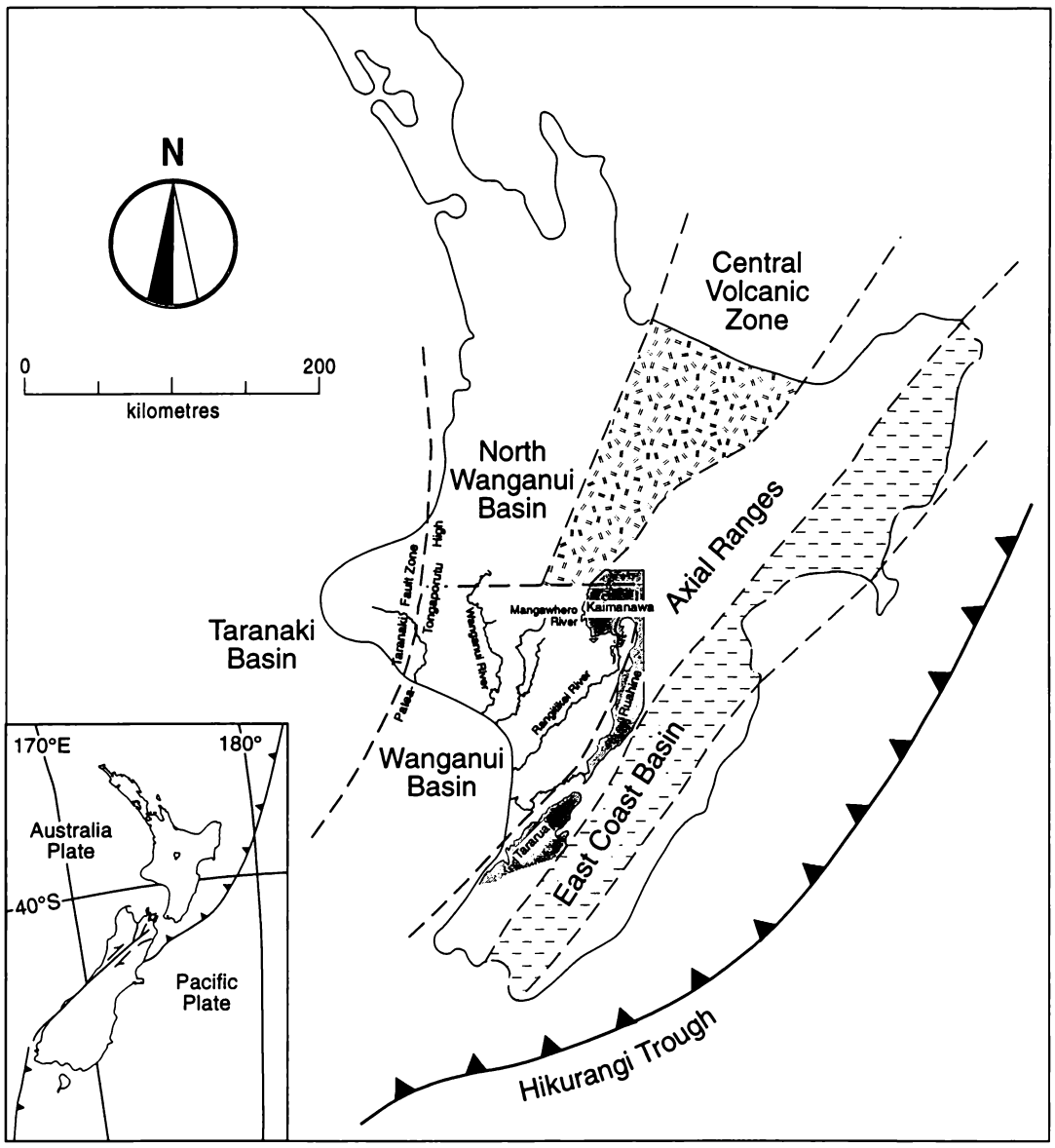

Figure 1:1. Location of the Wanganui Basin in North Island New Zealand. Some surrounding features of the Wanganui Basin as discussed in the text are shown.

1:2 STRUCTURAL DEVELOPMENT OF WANGANUI BASIN

Analyses of widespread seismic lines, acquired principally from the southern offshore portion of the Basin, have identified progressive onlap of younger sediments onto the Miocene unconformity from north to south (Anderton, 1981). Miocene uplift and erosion has largely removed inferred extensive pre-Miocene Cenozoic sediments, with some remnants possibly existing in structural depressions (Katz, 1988). Faulted outliers of Oligocene

sediments north of Wellington and in the Marlborough Sounds are thought to be remnants of such more extensive deposits (Stern *et al.*, 1992). Plio-Pleistocene downwarping and consequent development of the Wanganui Basin has been argued by Stern and Davey (1989; 1990) and Stern *et al.* (1992) to be a function of frictional shear between the Pacific and Australian Plates, where the "slab pull" force of the subducted Pacific Plate is harnessed to deform the overriding Australia Plate (Figure 1:2). This downwarping is equivalent to the wedge-flexure type mechanism of back-arc basin formation proposed by Davies (1981). Progressive downwarping and inundation to the south at the same time as thermally-driven uplift to the north, has resulted in the southward migration of a lithospheric scale "wave-like" structure (wave length and period of 200 km and 20 My, respectively; Stern *et al.*, 1992). The progressive southward migration of the downwarping has permitted the development of three depocentres for the period since the early Pliocene (Figure 1:3; Anderton, 1981).

1:3 THE WANGANUI RIVER SUCCESSION

The Wanganui River originates on the northern slopes of Mt. Tongariro and heads east to Taumarunui where it makes a right angle turn to flow south through the southern part of the North Wanganui Basin and through the western half of the Wanganui Basin (Figure 1:1). It is one of two major rivers in the basin, the other being the Rangitikei River. These and other rivers dissect the Plio-Pleistocene succession and provide an opportunity to observe the sedimentary sequences that infill the Wanganui Basin. Unlike the Rangitikei River, which has been the subject of numerous recent geological investigations (e.g. Seward *et al.*, 1986; Naish and Kamp, 1995; Journeaux *et al.*, 1996; Naish *et al.*, 1996), the Wanganui River is notable because of few recent publications concerning its surrounding geology. This situation may seem surprising considering that it intersects a comprehensive Miocene to Pleistocene sedimentary record. However, severe difficulties in accessing the area and frequently poor exposure in the more accessible areas have complicated study of the succession north of Parakino[1] (Figure 1:4). The river valley south of Parakino was part of Fleming's (1953) study, with the area around Parakino being more recently re-examined by McIntyre and Kamp (1998).

[1] May also be spelt Parikino, both spellings are widely used, however, the Parakino spelling is used in this study.

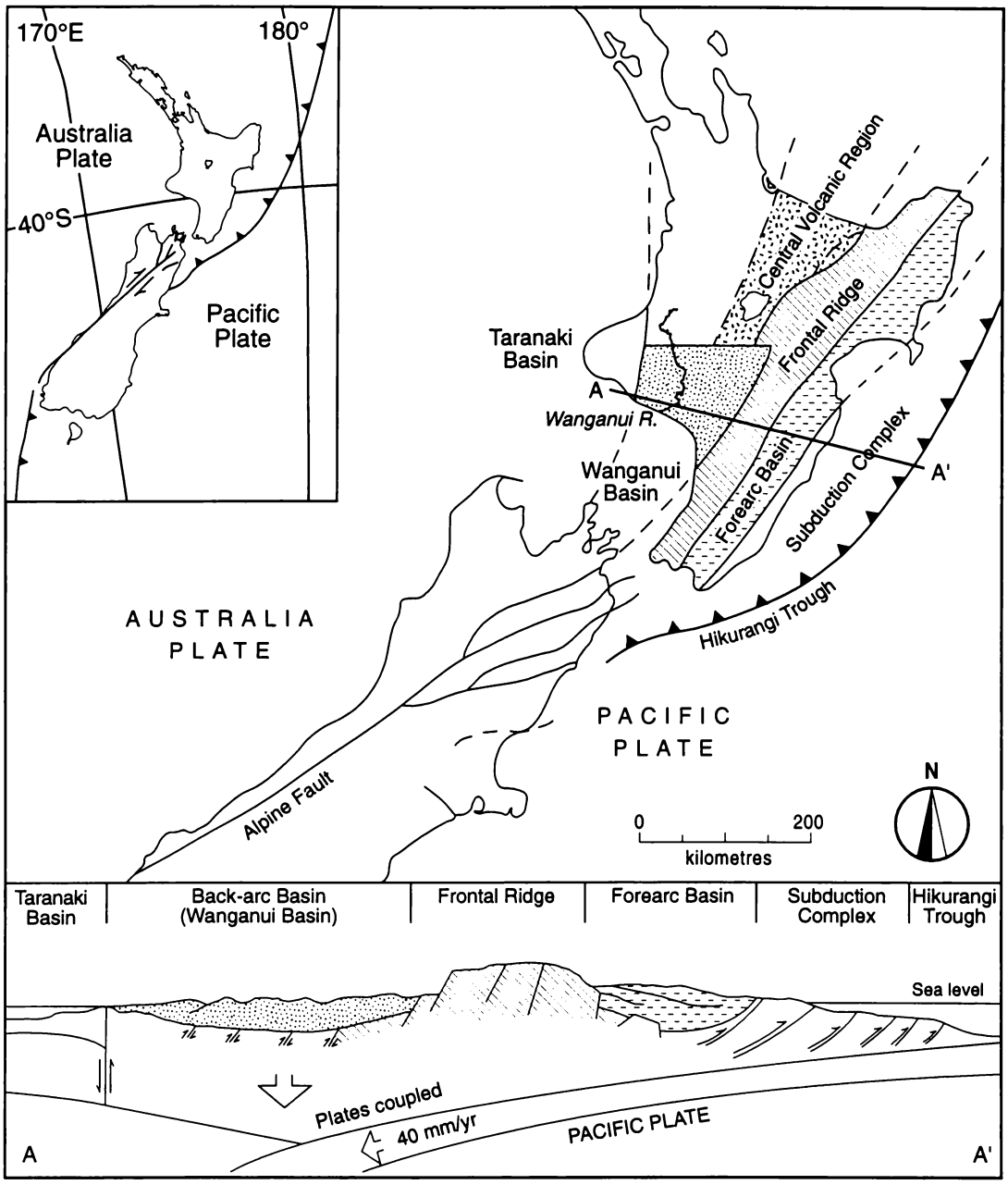

Figure 1:2. Regional tectonic setting of Wanganui Basin with respect to the main features of the Hikurangi Margin. Modified from Stern *et al.* (1992); Naish and Kamp (1995).

1:4 PRESENT STUDY AREA

Limited knowledge of the stratigraphy and structure of the western part of Wanganui Basin has hindered understanding of the development of the basin as whole. In this study the stratigraphic succession exposed in the Wanganui River valley between Tieke and Parakino (Figure 1:4) was chosen, as it offered the potential to examine the entire late Miocene (lower Kapitean; Chapter 2) to late Pliocene (Mangapanian; Chapter 2) record in the western

part of the basin. This study will complement studies undertaken elsewhere in the basin, allowing for better across-basin correlation and understanding of basin development. The northern limit of the study by Fleming (1953) forms the southern limit of the present study, which is principally confined to the river valley. Traditional mapping was not attempted because of the rugged, bush-clad terrain that dominates the study area, but beds and structures were mapped in the river channel and adjacent parts of the immediate valley (Chapter 2: Supplement 1).

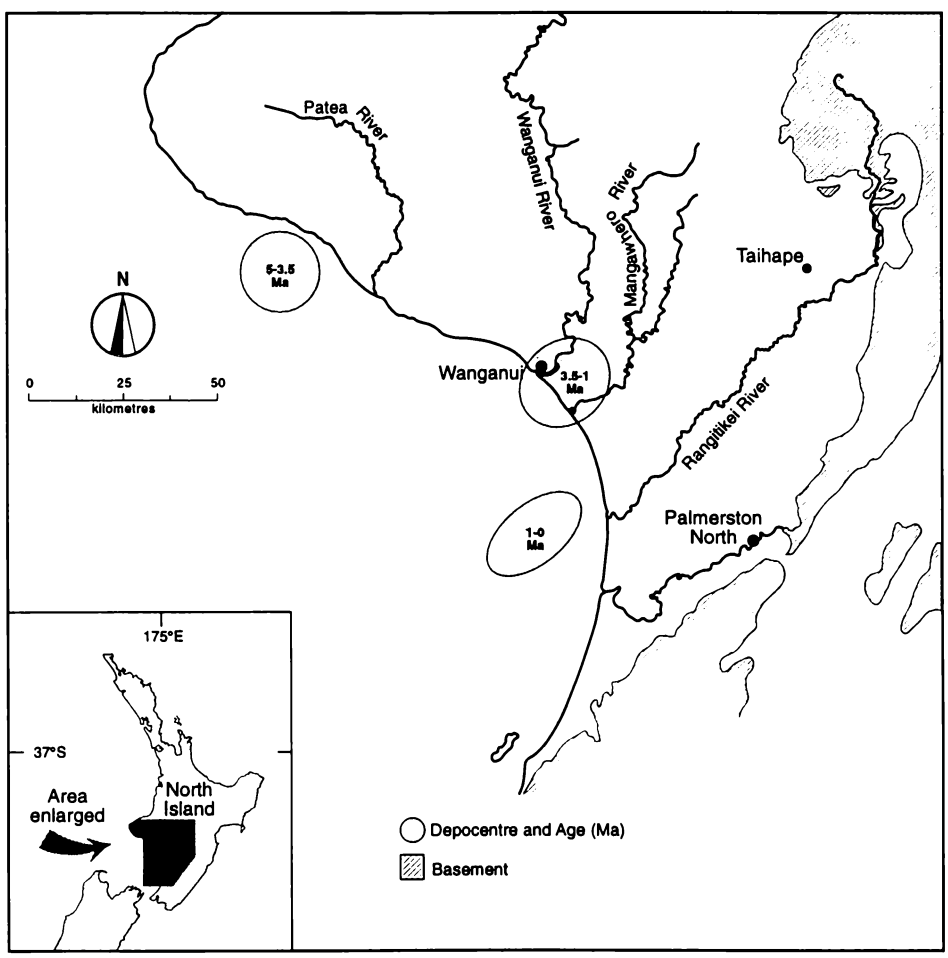

Figure 1:3. Map of Wanganui Basin showing location and age of depocentres since the early Pliocene. From Anderton (1981).

1:5 AIMS OF THIS STUDY

The principal aim of this study is to develop a conventional stratigraphic, sequence stratigraphic and paleoenvironmental interpretation of the late Miocene to late Pliocene beds exposed in the Wanganui Valley. To meet this aim, the lithostratigraphy of the sedimentary succession between Tieke and Parakino has been recorded in detail. This acts as the basis for further analyses, including revision of the stratigraphy and associated

nomenclature, determination of depositional environments, comparison of the sequence stratigraphic architecture in shelfal deposits against an established model, and development of the biostratigraphy and chronology.

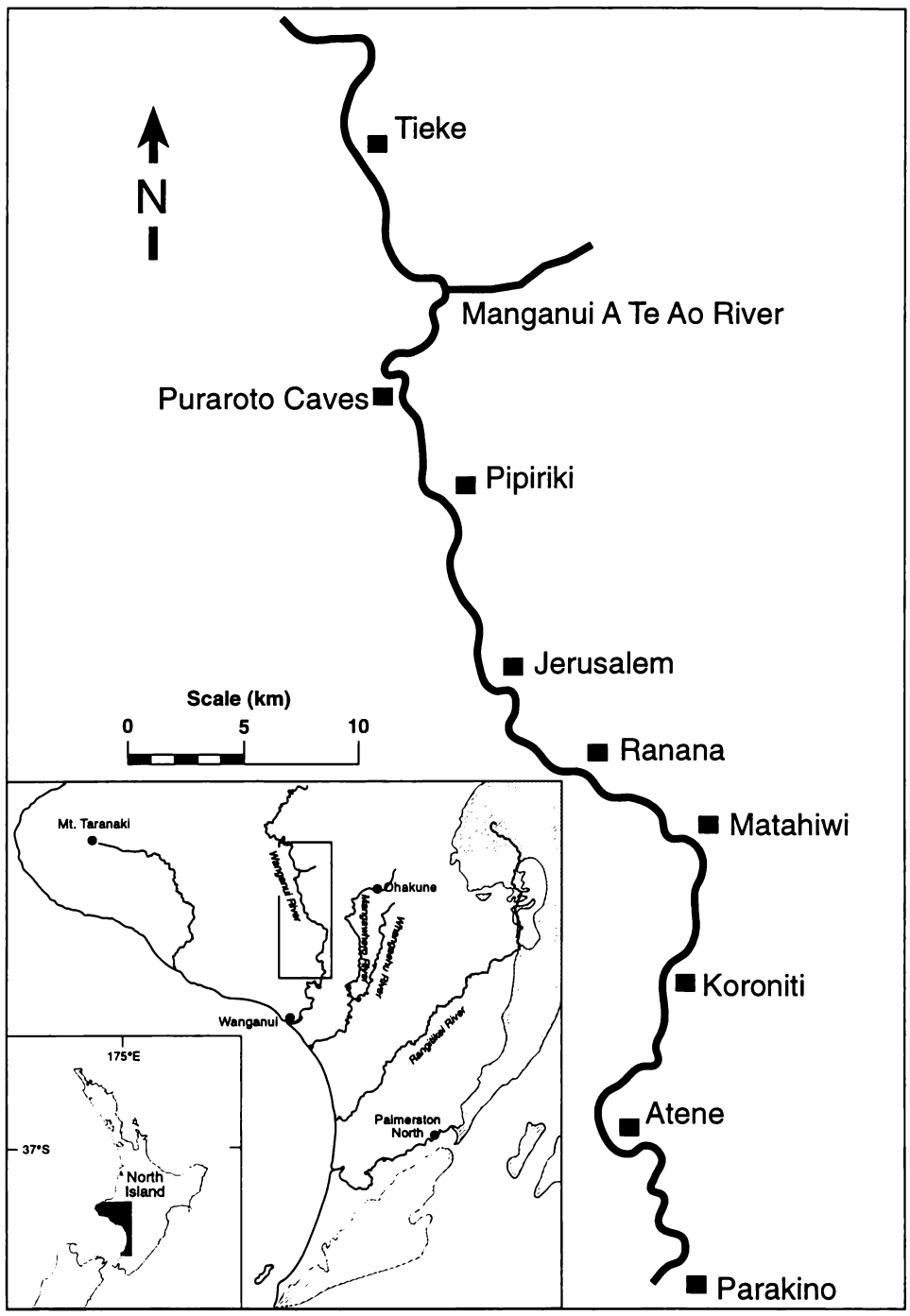

Figure 1:4. The section of Wanganui River valley forming the basis of this study. Key place names are shown.

1:6 THESIS OUTLINE

This thesis has been subdivided into a number of sections, with chapters defining each of the sections.

- Chapter 2: The biostratigraphy and chronology is developed for the late Miocene to late Pliocene Wanganui River section as a whole. Fourteen new maps and associated stratigraphic columns are presented as a supplement at the end of the chapter. Information developed in this chapter is used extensively throughout the rest of the thesis.

- Chapter 3: Matemateaonga Formation. Initially this section focuses on establishing the lithostratigraphy of that portion of this formation exposed in the study area. This is followed by an analysis of the paleoenvironments of the lithofacies and comparison of the cyclostratigraphy with established sequence stratigraphic models.

- Chapter 4: Tangahoe Formation. The lithostratigraphy for this formation is established and the nomenclature revised accordingly. Interpretation of the deep-water, mass-emplaced sandstones within the formation is an integral part of this chapter.

- Chapter 5: Ahurangi Sandstone, Atene Formation and Mangaweka Mudstone. These units are described and paleoenvironmental conditions interpreted.

- Chapter 6: Geological Synthesis.

CHAPTER 2

BIOSTRATIGRAPHY AND CHRONOLOGY

CHAPTER 2

BIOSTRATIGRAPHY AND CHRONOLOGY

2:1 INTRODUCTION

In any lithostratigraphic study it is important to have some age controls so as to be able to establish correlations and determine rates of processes. This study considers the lithostratigraphy of the Wanganui River section between Tieke in the north and Pitangi Stream near Parakino in the south (Figure 2:1). The aim of this chapter is to establish a reliable correlation with the New Zealand stage classification system and the global geomagnetic polarity timescale so as to derive numerical ages for the succession. Although considered separately, this chapter relies on the stratigraphy established in Chapters 3, 4 & 5. Sample location sites, tied to stratigraphic columns and maps, are presented in the supplement at the end of this chapter, with the columns used in this chapter being summaries of those supplement columns.

In this study, extensive foraminiferal studies have been undertaken to locate key biostratigraphic datums, upon which New Zealand stage boundaries have been correlated. Paleomagnetic samples were also taken as part of a larger study of the Wanganui Basin. The results applicable to the Wanganui River section will be used here. However, while the methodology is presented in Appendix 1, the details of the paleomagnetic studies will be presented in subsequent papers in conjunction with the people who generated the data. The absence of tephras in this section precludes the determination of radiometric ages on specific horizons.

2:2 BIOSTRATIGRAPHY

2:2:1 INTRODUCTION

The widespread occurrence of foraminifera in most marine sedimentary successions has placed them in a pre-eminent position in terms of biostratigraphy. This is especially so for planktic foraminifera, their wide distribution and low susceptibility to facies control, compared to benthic organisms making them particularly valuable for inter-regional correlation. Benthic foraminifera are useful in correlating basin-wide shelfal facies, where planktic foraminifera may be extremely rare. However, the environmental limits

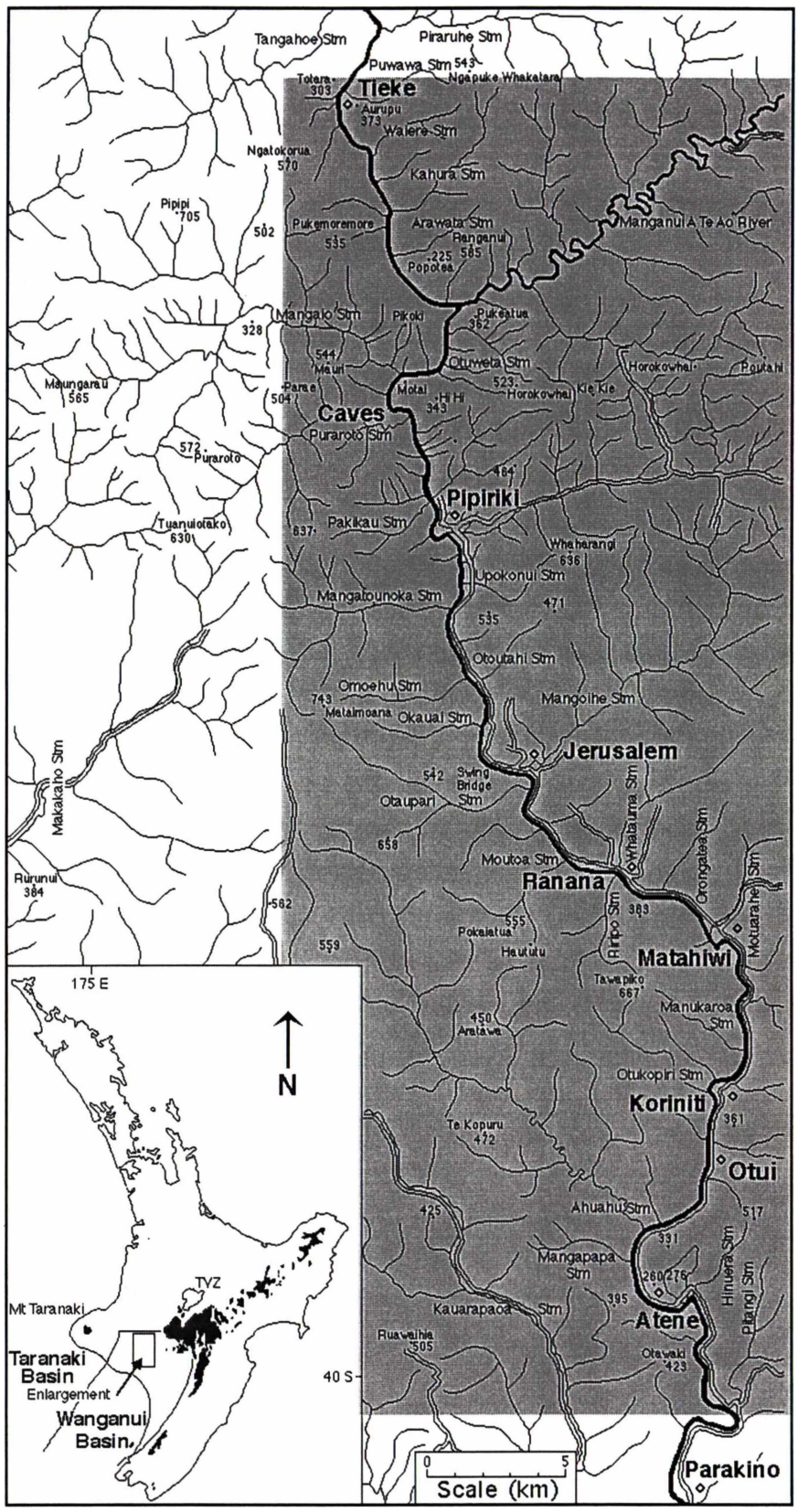

Figure 2:1. Locality map for the Wanganui River valley considered in this study. The grey tone approximates the section of river under study. Spot heights in metres. *Inset*: location of the study area relative to the Wanganui Basin. Topography over 1000 m is shown in black. TVZ = Taupo Volcanic Zone.

(depth, sediment type, etc.) on benthic foraminifera are a limiting factor in their usefulness for establishing a reliable chronological framework (Hornibrook *et al.*, 1989).

Macrofossils, particularly Mollusca, play an important role in establishing biostratigraphic datums (Beu and Maxwell, 1990). However, a working biostratigraphy based on Mollusca is generally limited to shallow-water nearshore facies where they are relatively abundant and diverse. Historically, macrofossils have formed the basis for much of the early work on New Zealand biostratigraphy, consequently many New Zealand stages are still defined on the basis of their macrofossil content (e.g. Beu and Maxwell, 1990; Beu, 1995). As macrofossils are extremely rare or absent throughout much of the section they have not been considered in this study. Recently there has been a move to redefine the New Zealand Neogene stages in terms of planktic microfossil datums so that better correlation between onshore and offshore regions, and ultimately global chronostratigraphy, can be established (Edwards, 1987; Morgans *et al.*, 1996).

Within the Wanganui River section north of Parakino, only Collen's (1972) study from Ranana to Parakino offers a detailed assessment of the biostratigraphy. He recognised three benthic foraminiferal biozones:

(a) *Hurupensis* zone (Wo), based on the presence of *Notorotalia hurupensis*.

(b) *Molestus* zone (Wp), based on the occurrence of *Notorotalia finlayi* and *Cibicides molestus*.

(c) *Finlayi* zone (Wm), based on *Notorotalia finlayi* following the extinction of *Cibicides molestus*.

Collen's work has been developed further in this study with the recognition of at least five well constrained biozones which are based primarily upon the occurrence and character of planktic foraminifera.

2:2:2 New Zealand stage boundaries

The late Miocene and Pliocene New Zealand stage boundaries and corresponding biostratigraphic zones are summarised in Figure 2:2 and discussed below. The Miocene-Pliocene boundary has been dated at 5.32 Ma by Berggren *et al.* (1995b), which is within the upper Kapitean (Figure 2:2). The Kapitean-Opoitian boundary closely approximates this international boundary.

2:2:2:1 Kapitean Stage (Tk)

The base of the Kapitean Stage is defined by the first appearance of the Mollusca *Sectipectin wollastoni* and *Austrofusus tuberculatus* (*coerulescens*) in the stratotype at Blind River in Marlborough (Finlay and Marwick, 1947). Roberts *et al.* (1994) tie the first appearance of these taxa to the base of paleomagnetic chron C3An2n. Although well established in the molluscan record, this boundary is poorly defined by planktic foraminifera. Hornibrook *et al.* (1989) adopted the first appearance of the planktic foraminiferan *Globorotalia conomiozea* as a deep-water proxy for the boundary. Recent work by Roberts *et al.* (1994) indicate that the first appearance datum (FAD) of the key Kapitean Mollusca occur 0.3 My before the first appearance of *G. conomiozea*. Thus the FAD of *G. conomiozea* can only be regarded as a proxy for the base of the Kapitean Stage.

The Kapitean is divided informally into two parts, upper and lower, based on the FAD of the planktic foraminiferan *Globorotalia sphericomiozea* (Roberts *et al.*, 1994). Two other key planktic foraminifera, namely *Globorotalia mons* and *G. pliozea,* are reported by Hornibrook *et al.* (1989) to appear for the first time within the upper Kapitean. Roberts *et al.* (1994) place the first appearance of *G. sphericomiozea* approximately one third of the way up through C3r, at c. 5.65 Ma.

2:2:2:2 Opoitian Stage (Wo)

Scott (1982) gives two options for the Opoitian-Kapitean boundary. Hornibrook *et al.* (1989) adopted the second of these options, where the FAD of *G. punticulata* and *G. crassaformis* defines the boundary. However, the first appearances of these two foraminifera are not simultaneous as "*they usually appear in close proximity, but their order is variable*" (Scott, 1982; pg. 475). Roberts *et al.* (1994) correlate this bioevent to the base of C3n.4n (5.23 Ma), making it a good proxy for the Miocene-Pliocene boundary dated at 5.32 Ma (Berggren *et al.*, 1995b).

Figure 2:2 (opposite page). Summary of first and last appearance datums (FAD and LAD, respectively) of key planktic and benthic foraminifera of biostratigraphic importance in the late Miocene to late Pliocene. Morgans *et al.* (1996) integrated the New Zealand Neogene stage classification system with the Berggren *et al.* (1995b) chronological time-scale. Information for compiling this diagram from Hornibrook (1981; 1982); Edwards (1987); Hornibrook *et al.* (1989); Journeaux (1995); and Morgans *et al.* (1996). S-sinistral, D-dextral.

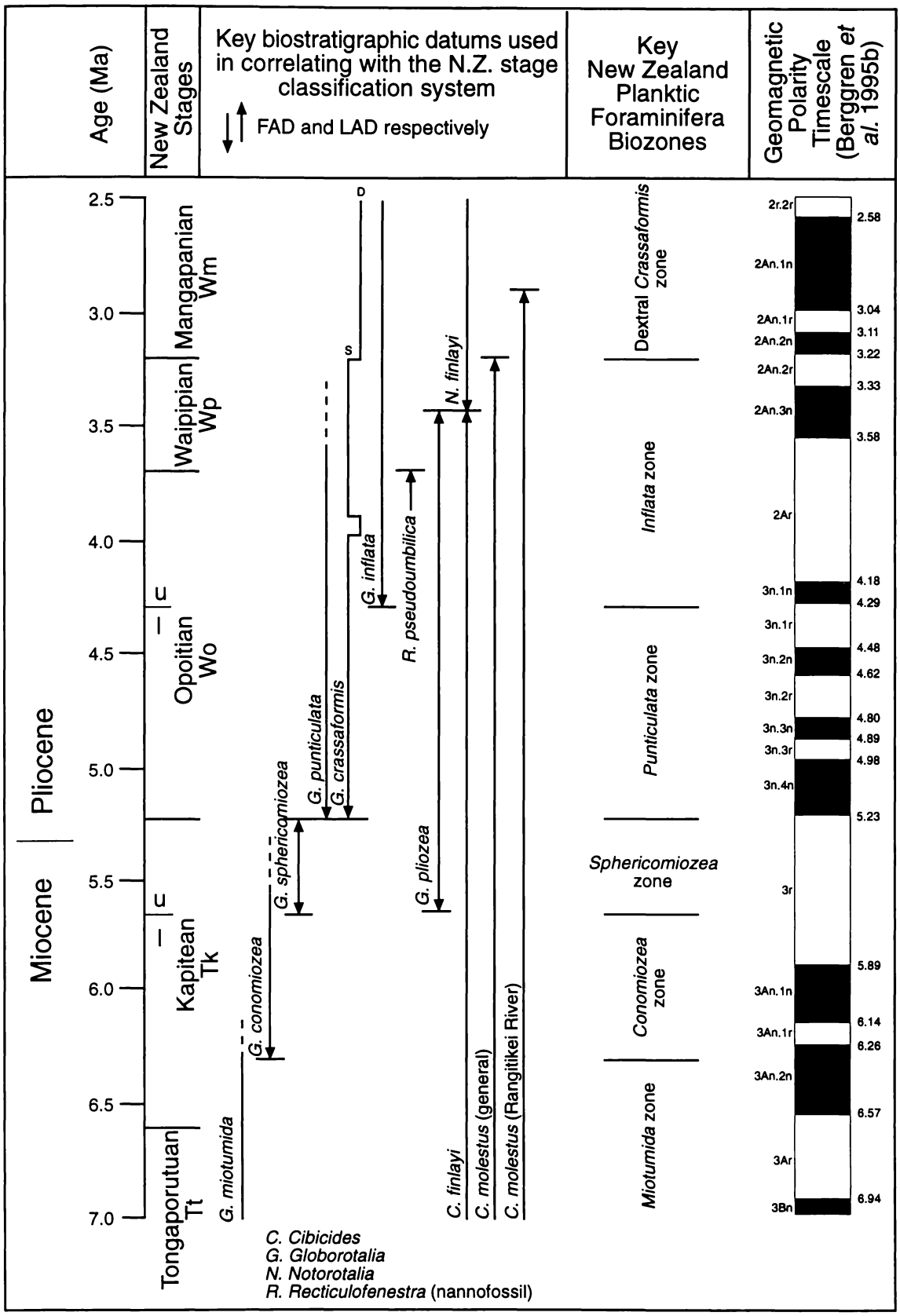
Age (Ma)
New Zealand Stages
Key biostratigraphic datums used in correlating with the N.Z. stage classification system
FAD and LAD respectively
Key New Zealand Planktic Foraminifera Biozones
Geomagnetic Polarity Timescale (Berggren et al. 1995b)
Miocene
Pliocene
Tongaporutuan Tt
Kapitean Tk
Opoitian Wo
Waipipian Wp
Mangapanian Wm
2.5
3.0
3.5
4.0
4.5
5.0
5.5
6.0
6.5
7.0
G. miotumida
G. conomiozea
G. sphericomiozea
G. punticulata
G. crassaformis
G. inflata
R. pseudoumbilica
G. pliozea
N. finlayi
C. finlayi
C. molestus (general)
C. molestus (Rangitikei River)
D
S
Miotumida zone
Conomiozea zone
Sphericomiozea zone
Punticulata zone
Inflata zone
Dextral Crassaformis zone
2r.2r
2An.1n
2An.1r
2An.2n
2An.2r
2An.3n
2Ar
3n.1n
3n.1r
3n.2n
3n.2r
3n.3n
3n.3r
3n.4n
3r
3An.1n
3An.1r
3An.2n
3Ar
3Bn
2.58
3.04
3.11
3.22
3.33
3.58
4.18
4.29
4.48
4.62
4.80
4.89
4.98
5.23
5.89
6.14
6.26
6.57
6.94
C. Cibicides
G. Globorotalia
N. Notorotalia
R. Recticulofenestra (nannofossil)

The Opoitian is informally divided into two parts, upper and lower, based on the FAD of good populations of *Globorotalia inflata*. The last appearance datum (LAD) of *Globorotalia mons* occurs within the lower Opoitian (Hornibrook *et al.*, 1989). Edwards (1987), upon re-evaluating the paleomagnetic stratigraphy of the Mangaopari Stream section (Wairarapa), placed the FAD of typical *G. inflata* at the base of chron 3n.1n (4.29 Ma).

2:2:2:3 Waipipian Stage (Wp)

While the Waipipian-Opoitian boundary has traditionally been defined on the basis of Mollusca, Hornibrook *et al.* (1989) note that the LADs of the planktic foraminiferan *Globorotalia pliozea* and the benthic foraminiferan *Cibicides finlayi,* and the FAD of the benthic foraminiferan *Notorotalia finlayi,* approximate the Waipipian-Opoitian boundary. Edwards (1987), however, cautions about the use of *C. finlayi,* as its LAD has been shown to be diachronous with respect to other biostratigraphic datums. The LAD of the calcareous nannofossil *Reticulofenestra pseudoumbilica* is noted by Morgans *et al.* (1996) as being a more reliable proxy for this boundary. Its LAD is dated at 3.7 Ma (Berggren *et al.*, 1995a).

Traditionally the LAD of the benthic foraminiferan *Cibicides molestus* has been used as a proxy for the Waipipian-Mangapanian boundary. However, the change from sinistral to dextral coiled populations of *Globorotalia crassaformis* has also been used (Hornibrook, 1981). A re-evaluation of the magnetostratigraphy for the Mangaopari Stream section (Wairarapa) by Edwards (1987) tied the FAD of dextral *Globorotalia crassaformis* to the base of chron 2An.2r (3.2 Ma).

2:2:2:4 Mangapanian Stage (Wm)

The Mangapanian Stage was formally defined by Fleming (1953) in the Wanganui Basin. The base of the stage coincides with the Mangapani Shell Conglomerate, which has a distinctive molluscan fauna (see Fleming, 1953). More commonly however, the benthic foraminiferan *Cibicides molestus* has been used as a proxy for the Waipipian-Mangapanian stage boundary and is considered to be coeval with the FAD of dextral *G. crassaformis* (Hornibrook, 1981). Subsequently the FAD of *G. crassaformis* has been reported in Edwards (1987) and Morgans *et al.* (1996) as correlating to the base of the paleomagnetic chron 2An.2n (3.22 Ma). Work in the Rangitikei River section by Journeaux (1995) and Naish *et al.* (1997) indicates that the LAD of *C. molestus* occurs at c. 2.9 Ma., significantly younger than the accepted date for the FAD of dextral *G. crassaformis* (which has not been positively identified in the Rangitikei River section). This brings into question

which of the foraminiferal datums truly approximates the Mangapanian-Waipipian stage boundary.

2:2:3 DATA SET

An extensive set of micropaleontological samples was collected from the Wanganui River section between Tieke and Pitangi Stream, north of Parakino (Figure 2:1). Foraminiferal census data were compiled on 69 samples, primarily for paleoenvironmental control (another 43 samples were examined and proved barren). The census samples also provided a general biostratigraphic framework for the lithostratigraphy. This was supplemented by a more detailed biostratigraphic analysis of 32 samples that were submitted to the Institute of Geological and Nuclear Sciences in Lower Hutt for analysis. All biostratigraphic and raw census data are presented in Appendix 2.

No detailed macrofauna work was undertaken in this study as Mollusca were extremely rare or absent throughout much of the section. However, some macrofaunal identification work was undertaken on shellbeds within the Matemateaonga Formation, the results of which are presented in Chapter 3.

2:2:4 BIOSTRATIGRAPHY OF THE WANGANUI RIVER SECTION

Detailed foraminiferal work, often on very large samples (10 kg or more), has resulted in the identification of a number of key planktic datums within the Wanganui River section. This is the first time that this section has been tied into a planktic foraminifera-based zonation linked to the New Zealand stage classification system. The biostratigraphy is discussed below and summarised in Figure 2:3. Detailed maps showing sample locations are presented in the supplement at the end of this chapter.

2:2:4:1 Tongaporutuan - lower Kapitean

The Tongaporutuan-Kapitean boundary was not identified in the section examined and presumably lies below the succession considered in this study. However, the lowest sample examined (W962002) contained at least three small, moderately compressed specimens of *Globorotalia miotumida* with at least 4.5-chambers in the outer whorl. Such specimens are shown in Hornibrook *et al.* (1989) as not extending above the lower half of the lower Kapitean.

2:2:4:2 Kapitean

The presence of 4 to 4.5 chambered, moderately ventroconical morphotypes of *Globorotalia conomiozea* within the lowermost part of the section examined (Figure 2:3) indicates that it is Kapitean in age (Hornibrook *et al.*, 1989). There is no faunal evidence to support the presence of upper Kapitean strata within this section (i.e. the *Globorotalia sphericomiozea* zone has not been identified). Samples W962046 and W962059 are dated as lower Kapitean and lower Opoitian respectively; if present, any upper Kapitean can be no more than 100 m thick (Figure 2:3). The possibility exists that all or part of the upper Kapitean (and possibly even part of the lower Kapitean) has not been deposited and/or eroded. If this is the case, then the unconformity with large-scale relief (>4 m) at the base of Matemateaonga Formation cyclothem 23 (Chapter 3: Supplement 1; shown in Figure 2:3) at the Puraroto Caves has to be a good candidate as the surface of erosion. The cause of this erosion is probably tied to glacio-eustatic fluctuations that have been identified from isotopic studies of deep-sea cores (e.g. Shackelton *et al.*, 1995). While recognising the limitations of the data described above, the 100 m thick zone between samples W962046 and W962059 is taken as being upper Kapitean.

Figure 2:3 (opposite page). Summary of key biostratigraphic information identified in this study. Columns 2, 3 and 4 show the distribution of key foraminifera (solid lines - continuos occurrences, solid circles - isolated occurrences, and ? - no occurrences). The resulting biozones have been linked to the New Zealand stage classification system and the international chronostratigraphic time-scale (far right of diagram). Other age important foraminifera are shown where they occur (e.g. Globorotalia miotumida occurs in sample W962002). In column 1 solid circles give the location of samples, with the sample numbers providing cross-referencing to the raw data contained in Appendix 2. Unnumbered, empty circles show the location of some of the barren samples examined in this study. For lithological details and geographic bounds of this column see the Maps in the supplement at the end of this Chapter. g - glauconite.

Wanganui River Section, Wanganui Basin, New Zealand

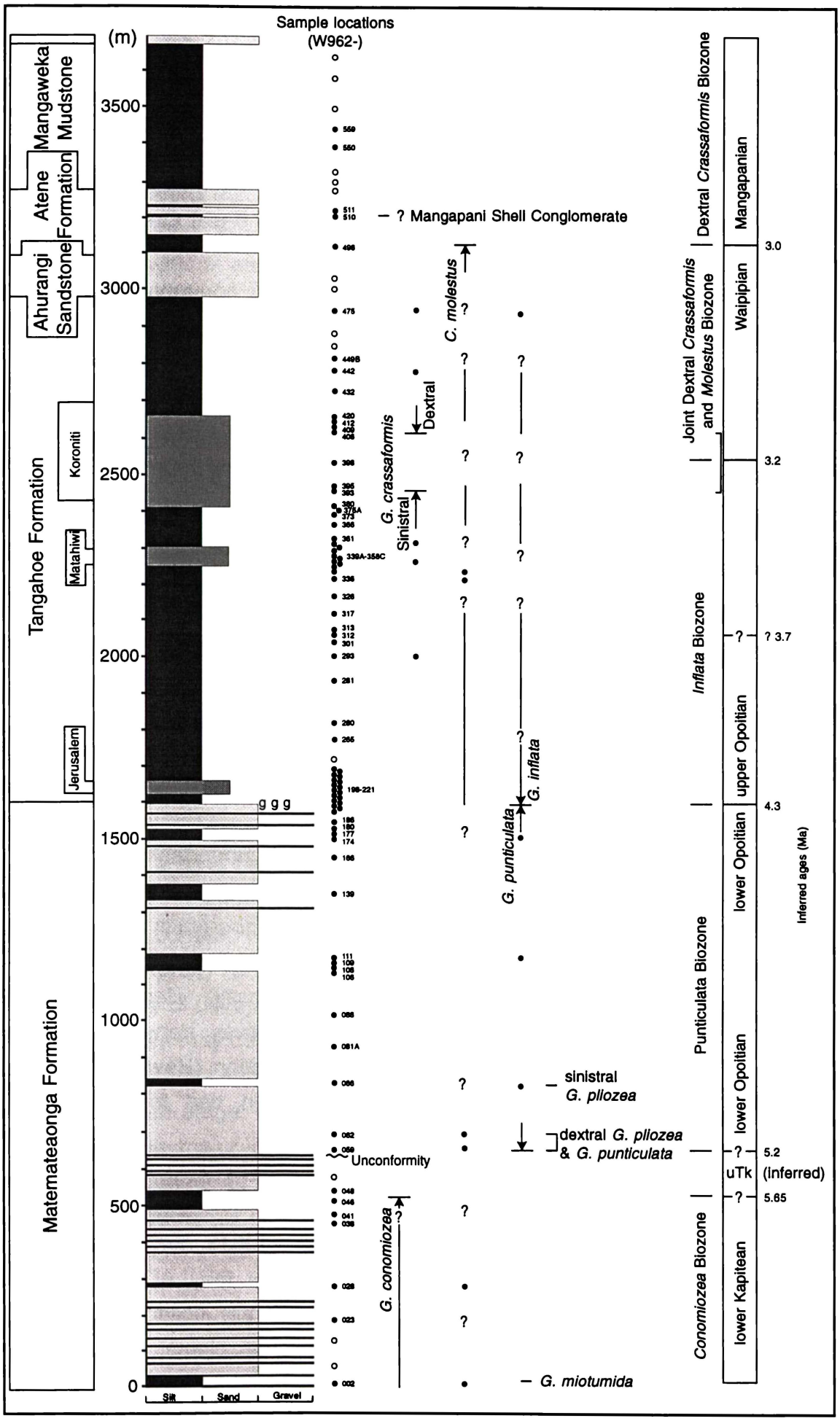

2:2:4:3 Opoitian

The joint occurrence of *Globorotalia punticulata* and dextral *G. pliozea* in samples W962059 and W962062 confirms the presence of basal Opoitian strata (Hornibrook, 1982) and implies very little, if any, Opoitian strata are missing within the possible unconformity at the Puraroto Caves. The lack of faunal identification of the upper Kapitean has meant that the Kapitean-Opoitian boundary is arbitrarily drawn at the lowermost basal Opoitian sample (W962059).

The first appearance of populations containing common *Globorotalia inflata* occurs at sample W962200. *Globorotalia punticulata*, the ancestor to *G. inflata*, is abundantly present within sample W962199. Populations dominated by *G. inflata* and *G. punticulata* occur above and below this point, respectively. Given these trends, and that only 5 m separate these two samples, this datum which informally divides the stage into lower and upper Opoitian is well constrained.

2:2:4:4 Waipipian

No reliable foraminiferal proxies for the base of the Waipipian have been identified within the Wanganui River section. The planktic foraminiferan *Globorotalia pliozea* has not been found above the level where populations of *G. inflata* appear. The benthic foraminiferan *Cibicides finlayi* is very rare, presumably because of unsuitable facies, and while *Notorotalia* are reasonably abundant there are taxonomic problems in identifying the transition from *Notorotalia hurupensis* to *N. finlayi*.

As a consequence, the Opoitian-Waipipian boundary is arbitrarily assigned to a position midway between the common occurrence of *G. inflata* and the base of the major zone of dextrally coiled *Globorotalia crassaformis*. Some indirect support for this is provided at DSDP site 284 (400 km west of New Zealand), where the calcareous nannofossil *Recticulofenestra pseudoumbilica* has its last appearance about midway between the two datums (Loman, 1986). In the Mangapoike River section (Hawke's Bay) the LAD of *Recticulofenestra pseudoumbilica* has been tied to the LAD of *Globorotalia pliozea* (Edwards, 1987).

2:2:4:5 Mangapanian

Subsequent to the work of Hornibrook (1981), the base of the Mangapanian has been variously assigned to either the LAD of *Cibicides molestus* and/or the base of a major zone of dextrally coiled *Globorotalia crassaformis.* Results from the present study however, clearly show that the LAD of *C. molestus* occurs at least 500 m above the base of the dextral *G.*

crassaformis zone. The first appearance of dextral *G. crassaformis* occurs within the upper part of the Koroniti Sandstone Member (sample W962406), while sinistral populations occur in the lower part of the member (sample W962393) with common populations of dextral and sinistral *G. crassaformis* above and below this point, respectively. However, *G. crassaformis* was not found in intervening samples. Consequently the datum is placed in the middle of the 150 m gap. Miscorrelation of the major zone of dextrally coiled *G. crassaformis* with an earlier Opoitian excursion noted by Hornibrook (1982) is not possible given the continuity of the zone up through the LAD of *Cibicides molestus*. The base of the major *G. crassaformis* dextral coiling event is reported in Edwards (1987) and Morgans *et al.* (1996) as being tied to the base of Chron 2An2n (3.2 Ma).

The LAD of *Cibicides molestus* is also not straight forward. Consistently good populations occur up to sample W962442, following which it is not present in two samples, but reappears in sample W962496. Its temporary absence, before its final appearance in sample (W962496) at the base of Atene Formation, is interpreted as being facies controlled. This explanation, however, is not entirely consistent as sample (W962449B) appears to be of an appropriate facies and the occurrence of *C. molestus* could be expected. The temporary disappearance of *C. molestus* immediately prior to its last appearance has not previously been reported in the Wanganui Basin. The highest occurrence of *C. molestus* is in the siltstone unit (Atene Formation siltstone member 1, Azm1) approximately 90 m below Acm2 (Atene Formation carbonate member 2), which is tentatively correlated on lithological evidence and across basin mapping to the Mangapani Shell Conglomerate (McIntyre pers. comm. and personal observation). Assuming that this correlation is correct, these new data support the use of the LAD of *C. molestus* as a proxy for the base of the Mangapanian Stage, and highlights the unsuitability of using the base of the dextrally coiled *G. crassaformis* zone. The latter datum may be better suited as an intra-Waipipian marker with a joint dextral *crassaformis* and *molestus* biozone defining an informal upper division of the Waipipian stage. Given that the LAD of *C. molestus* occurs well above the FAD of the major dextral coiling zone of *G. crassaformis* (>500 m), a significantly younger age must be applicable to this boundary. The 2.9 Ma age obtained by Journeaux (1995) and Naish *et al.* (1997) for the Rangitikei River section is regarded as a minimum age, as facies above the LAD in the Wanganui River section are unsuitable for the occurrence or preservation of *C. molestus,* and may have reduced its stratigraphic extent. Thus an age of 3 Ma has been arbitrarily assigned in this study to the LAD for *Cibicides molestus* in the Wanganui River section.

2:3 MAGNETOSTRATIGRAPHY

2:3:1 INTRODUCTION

Magnetostratigraphy and correlation to the geomagnetic polarity timescale offers the opportunity to obtain numerical ages for stratigraphic horizons, as the geomagnetic polarity reversals are contemporaneous world-wide phenomena for which ages have been established. The most recent compilation of the geomagnetic polarity time-scale is in Berggren *et al.* (1995b). This section presents the preliminary conclusions of a paleomagnetic study in the Wanganui River valley.

2:3:2 RESULTS

The results of new paleomagnetic data available (analyses undertaken at the paleomagnetic laboratory at Victoria University, Wellington) in this study are shown in Figure 2:4 and tabulated in Table 2:1. As this is still preliminary data, some samples are still prefaced with a question mark to designate a degree of uncertainty, while samples for which the results have not yet been obtained are shown in grey. Despite being provisional, any major variation in the magnetostratigraphic interpretation given here is unlikely. Due to technical difficulties at the laboratory to which samples were sent, the results for samples from the upper-half of the section are not yet available. Boundaries between reversals are defined as being the mid-point between samples of opposite polarity. Further paleomagnetic information from Wilson (1993) has been used to extend the magnetostratigraphy to above the Koroniti Sandstone Member. Sample positions relative to the stratigraphy have been estimated from the locations shown on the map given by Wilson (1993). Only Wilson's data described by him as excellent and good have been used here.

Figure 2:4 (opposite page). Location of all new paleomagnetic samples taken within the study area, and the preliminary results as at the time of writing. The resulting magnetostratigraphy is shown and has been extended to above the Koroniti Sandstone Member, using data from Wilson (1993).

Wanganui River Section, Wanganui Basin, New Zealand

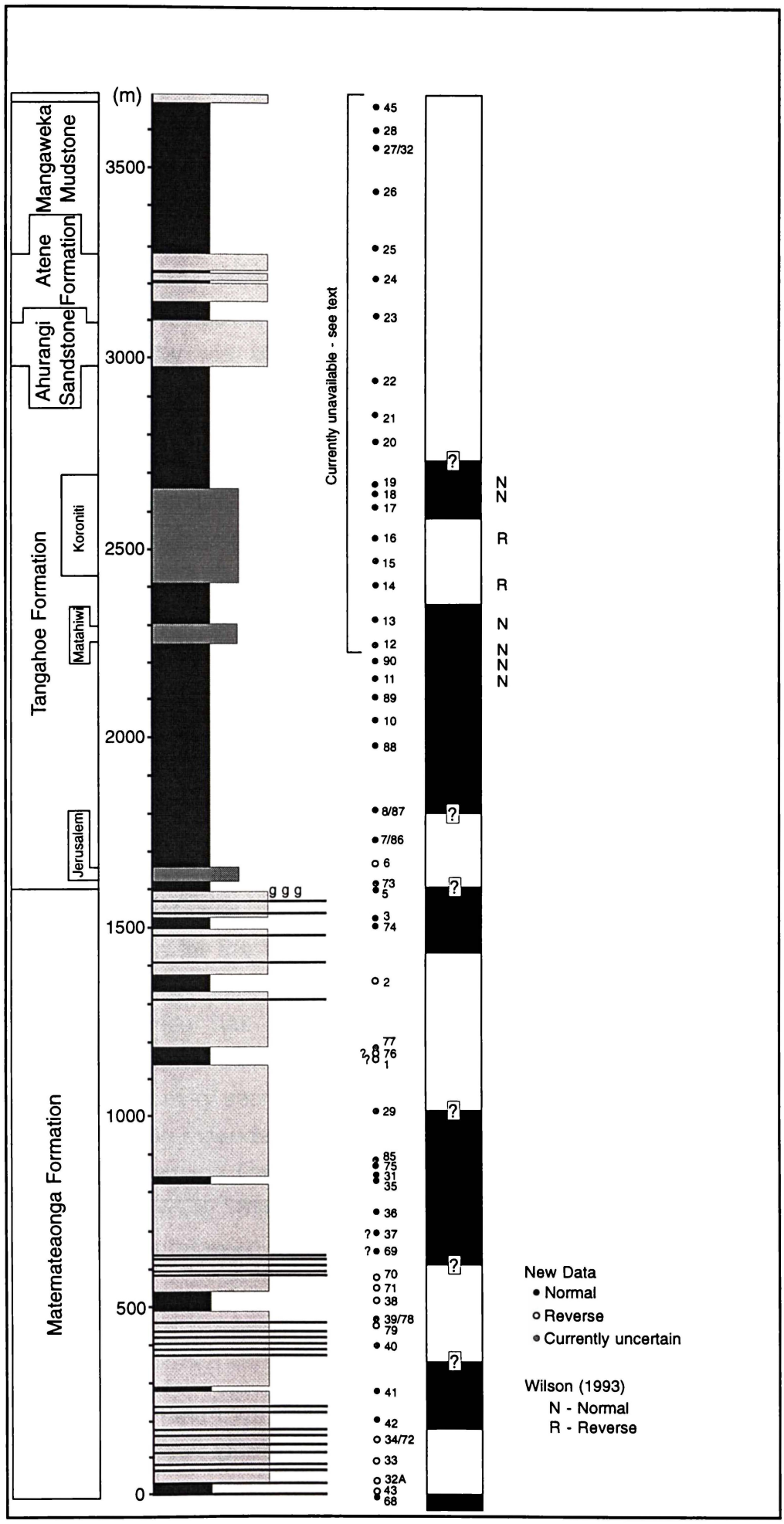

Table 2:1. Summary of the stratigraphic position and results of new paleomagnetic data.

Paleomag. Sample Number	Stratigraphic Height (m)	Result
68	2	Normal
43	8	Reverse
32A	40	Reverse
33	100	Reverse
34/72	146	Reverse
42	198	Normal
41	285	Normal
40	393	?
79	450	Reverse
39/78	464	?
38	532	Reverse
71	555	Reverse
70	575	Reverse
69	640	? Normal
37	690	? Normal
36	753	Normal
35	828	Normal
31	851	Normal
75	870	Normal
85	895	?
29	1009	?
1	1148	? Reverse
76	1160	? Reverse
77	1185	?
2	1346	Reverse
74	1495	Normal
3	1504	Normal
5	1573	?
73	1575	?
6	1654	Reverse
7/86	1734	?
8/87	1806	?
88	1960	Normal
10	2053	Normal
89	2080	Normal
11	2145	?
90	2160	Normal

2:4 AGE CONTROL

The right-hand side of Figure 2:5 contains the magnetostratigraphy for this section correlated against the geomagnetic polarity timescale of Berggren

et al. (1995b). This correlation is guided by the age of horizons inferred from biostratigraphic datums and stage boundaries as determined in other sections.

To develop the chronology for the Wanganui River section, central column of Figure 2:5, the biostratigraphic datums have been used to constrain the magnetostratigraphy. Dotted lines have been used to show the correlations between the magnetostratigraphy and the geomagnetic polarity timescale columns as determined in this study. Two short normal periods (C3n.3n and C3n.1n) have not been correlated. In both cases, the normal chrons above and below have been tied to normal periods on the magnetostratigraphy via biostratigraphic datums, with no normal polarity samples in-between to which the "missing chrons" can be correlated. One paleomagnetic datum and a biostratigraphic estimate have not been included in the adopted chronology. In the case of the paleomagnetic datum (top of C3n.2n) the boundary was poorly constrained compared to the biostratigraphic datum that occurred at approximately the same point. The 3.7 Ma biostratigraphic estimate was not included as it did not fit the better constrained magnetostratigraphy available. One independent age datum of 2.8 Ma has been assigned by McIntyre and Kamp (1998) to the top of the approximately 40 m thick Pitangi Sandstone, which overlies the Mangaweka Mudstone in the Wanganui River valley. It is expected that future localised studies will be able to key into this baseline study and further develop the relationships outlined in Figure 2:5.

Sediment accumulation rates are an integral part of age determinations as they offer the opportunity to determine the age of horizons between numerical age datum points. Figure 2:6 plots the sediment accumulation rates for the Wanganui River section considered in this study. Age relationships as determined from this figure are used throughout this study. No allowance has been made in Figure 2:6 for the unconformity suggested in section 2:2:4:2. If it were then the 0.24 m/ky section would not exist with the 1.77 m/ky section above being extended down and the 0.66 m/ky section below being extended up to a level equivalent to the unconformity. The separation between the lines would give an estimate of the duration of the unconformity. However, this would make no allowance for any change in sedimentation rate between the 5.65 and 5.2 Ma levels.

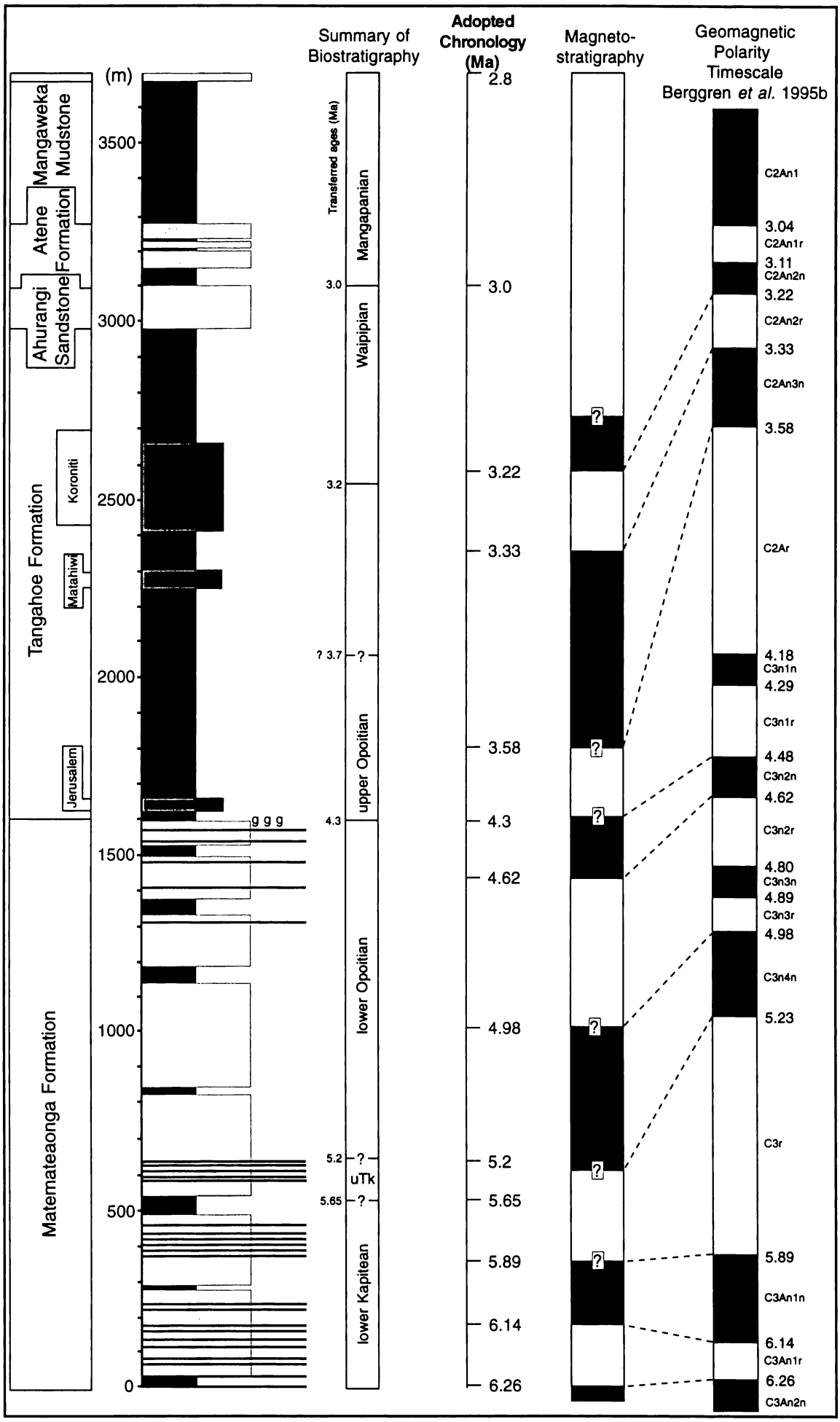
Mangaweka Mudstone
Atene Formation
Ahurangi Sandstone
Tangahoe Formation
Koroniti
Matahiwi
Jerusalem
Matemateaonga Formation
(m)
3500
3000
2500
2000
1500
1000
500
0
g g g
Summary of Biostratigraphy
Transferred ages (Ma)
Mangapanian
Waipipian
upper Opoitian
lower Opoitian
lower Kapitean
3.0
3.2
? 3.7
4.3
5.2
5.65
uTk
Adopted Chronology (Ma)
2.8
3.0
3.22
3.33
3.58
4.3
4.62
4.98
5.2
5.65
5.89
6.14
6.26
Magneto-stratigraphy
Geomagnetic Polarity Timescale Berggren et al. 1995b
C2An1
3.04
C2An1r
3.11
C2An2n
3.22
C2An2r
3.33
C2An3n
3.58
C2Ar
4.18
C3n1n
4.29
C3n1r
4.48
C3n2n
4.62
C3n2r
4.80
C3n3n
4.89
C3n3r
4.98
C3n4n
5.23
C3r
5.89
C3An1n
6.14
C3An1r
6.26
C3An2n

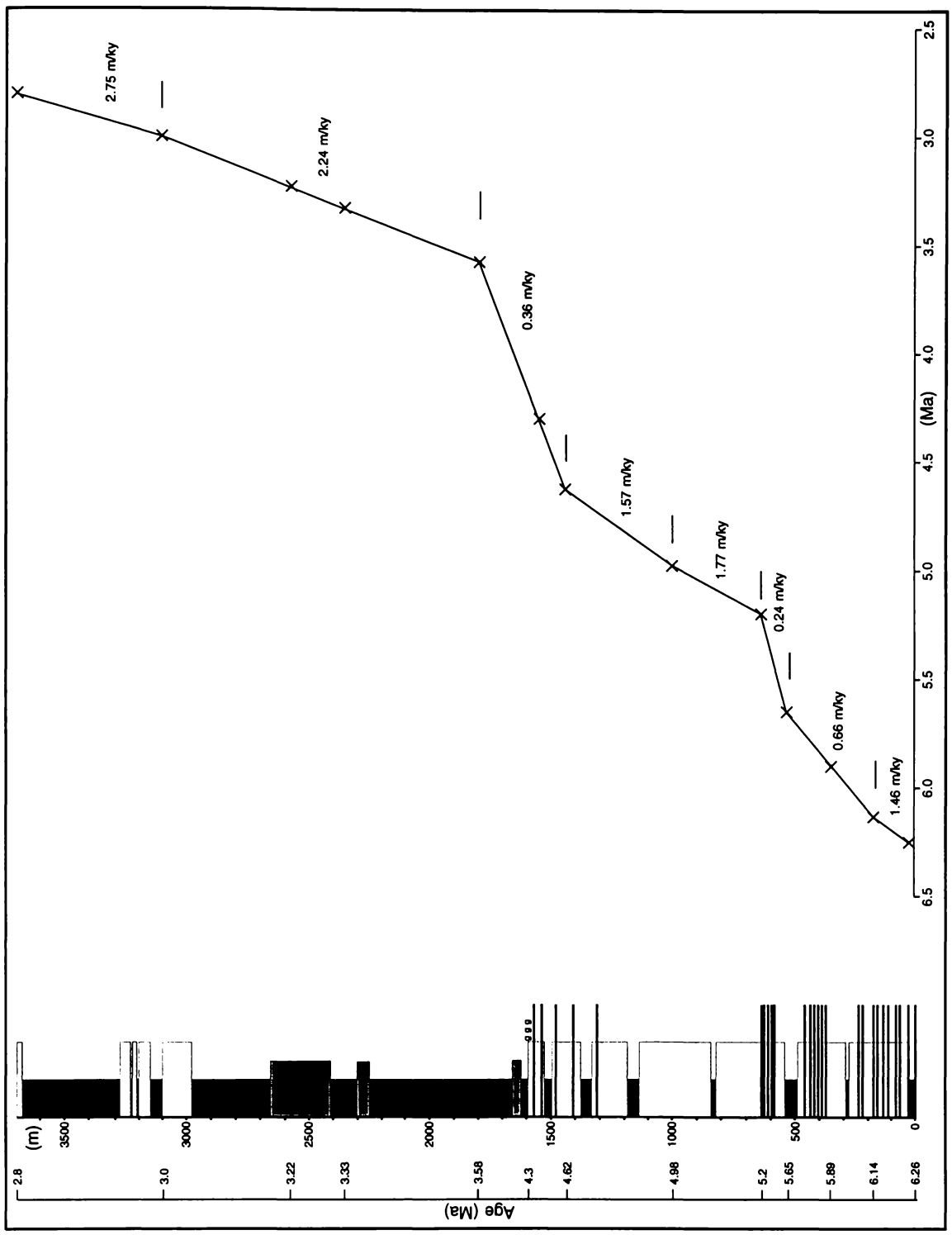

Figure 2:6. Sedimentation rates as calculated from the thickness of the stratigraphic interval between age datums as determined in this chapter.

Figure 2:5 (opposite page). Summary of all the available age controls and the resulting adopted chronology plotted against the lithostratigraphy. See the Maps in the Supplement at the end of this chapter for lithological details and geographical information.

CHAPTER 2: SUPPLEMENT 1

MAPS

The Wanganui River valley between Tieke and Pitangi Stream has been divided into 14 map sections shown in Figure C2S1:1. Each map section includes a 1:25,000 scale map and corresponding composite stratigraphic column. The maps show important boundaries, structural information and the location of key samples, overlying a drainage and grid pattern and geographical information derived from the NZMS 270 maps. The composite stratigraphic columns show from left to right (1) the magnetostratigraphy; (2) biozones and New Zealand stages; (3) absolute ages (Ma); (4) stratigraphic unit and subdivisions (i.e. members, cyclothems); (5) stratigraphic height (m); (6) generalised lithology; (7) sample information - paleomagnetic, general and foraminiferal; and (8) geographical features. A legend for all maps is shown in Figure C2S1:2. Numbers on the maps give the lower contacts of stratigraphic units identified on the sedimentary sections.

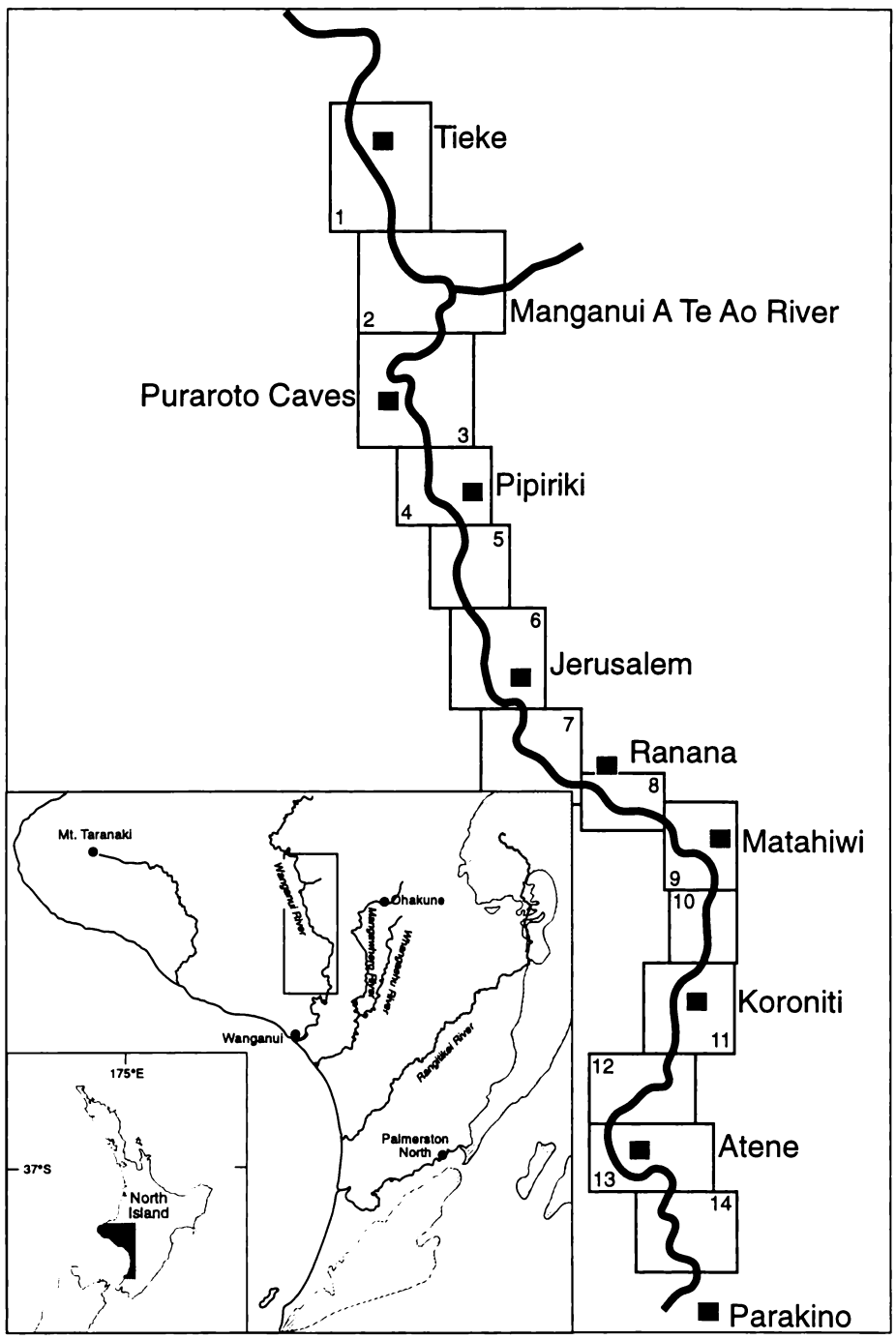

Figure C2S1:1. Section of the Wanganui River valley forming the basis of this study, showing the location of the 14 map sections presented in this chapter supplement.

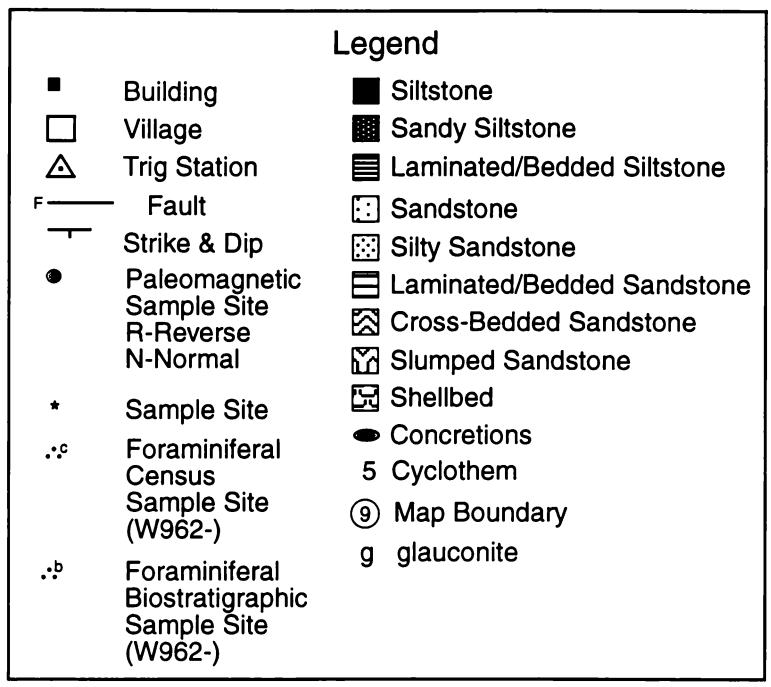

Figure C2S1:2. Legend for accompanying maps

MAP 1

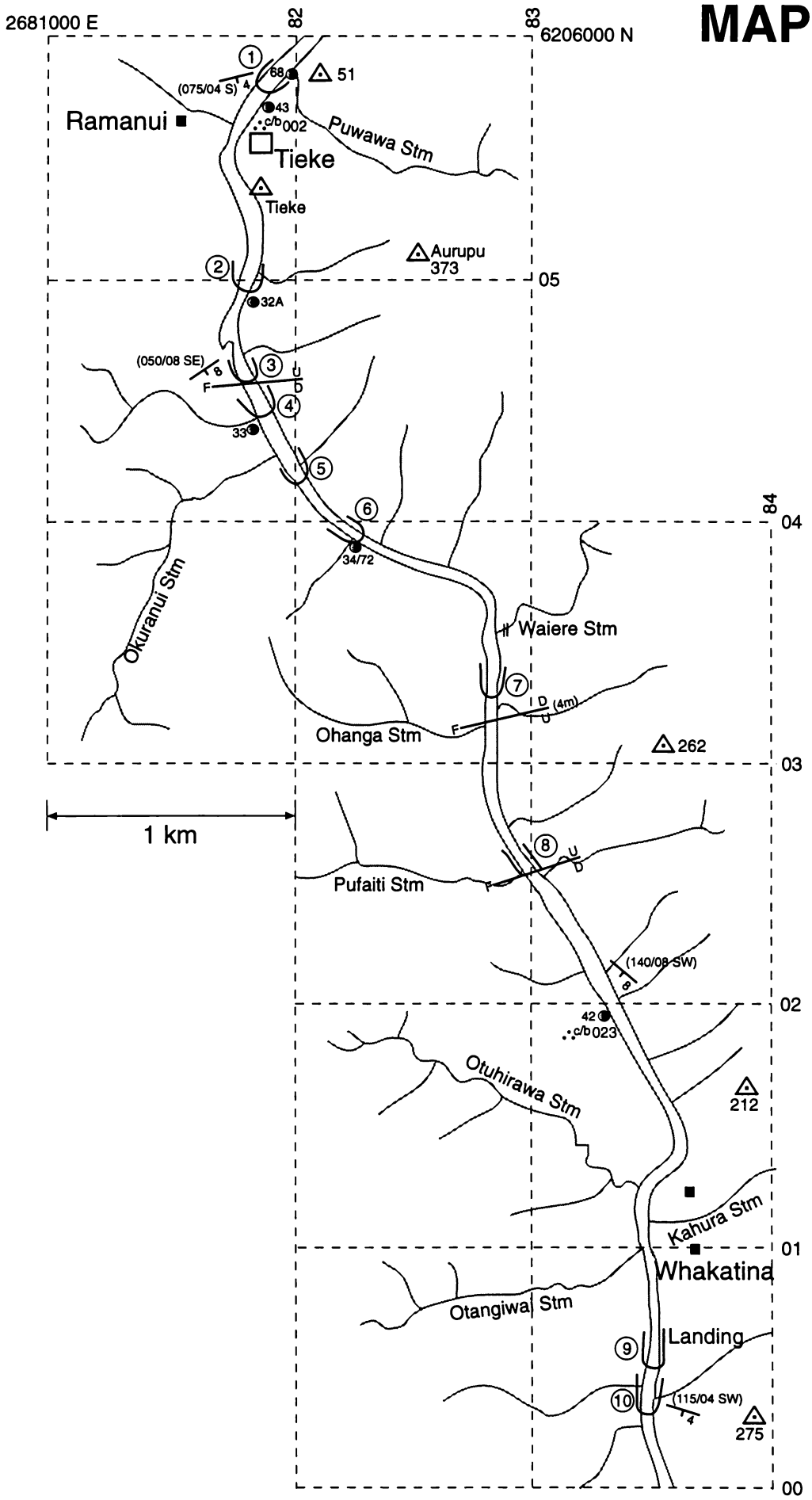
2681000 E
82
83
6206000 N
84
Ramanui
Tieke
Tieke
Puwawa Stm
51
68
43
c/b 002
(075/04 S)
Aurupu
373
05
32A
(050/08 SE)
33
34/72
Okuranui Stm
Waiere Stm
Ohanga Stm
(4m)
262
04
03
1 km
Pufaiti Stm
(140/08 SW)
42
c/b 023
02
Otuhirawa Stm
212
Kahura Stm
Whakatina
01
Otangiwa Stm
Landing
(115/04 SW)
275
00

Wanganui River Section, Wanganui Basin, New Zealand

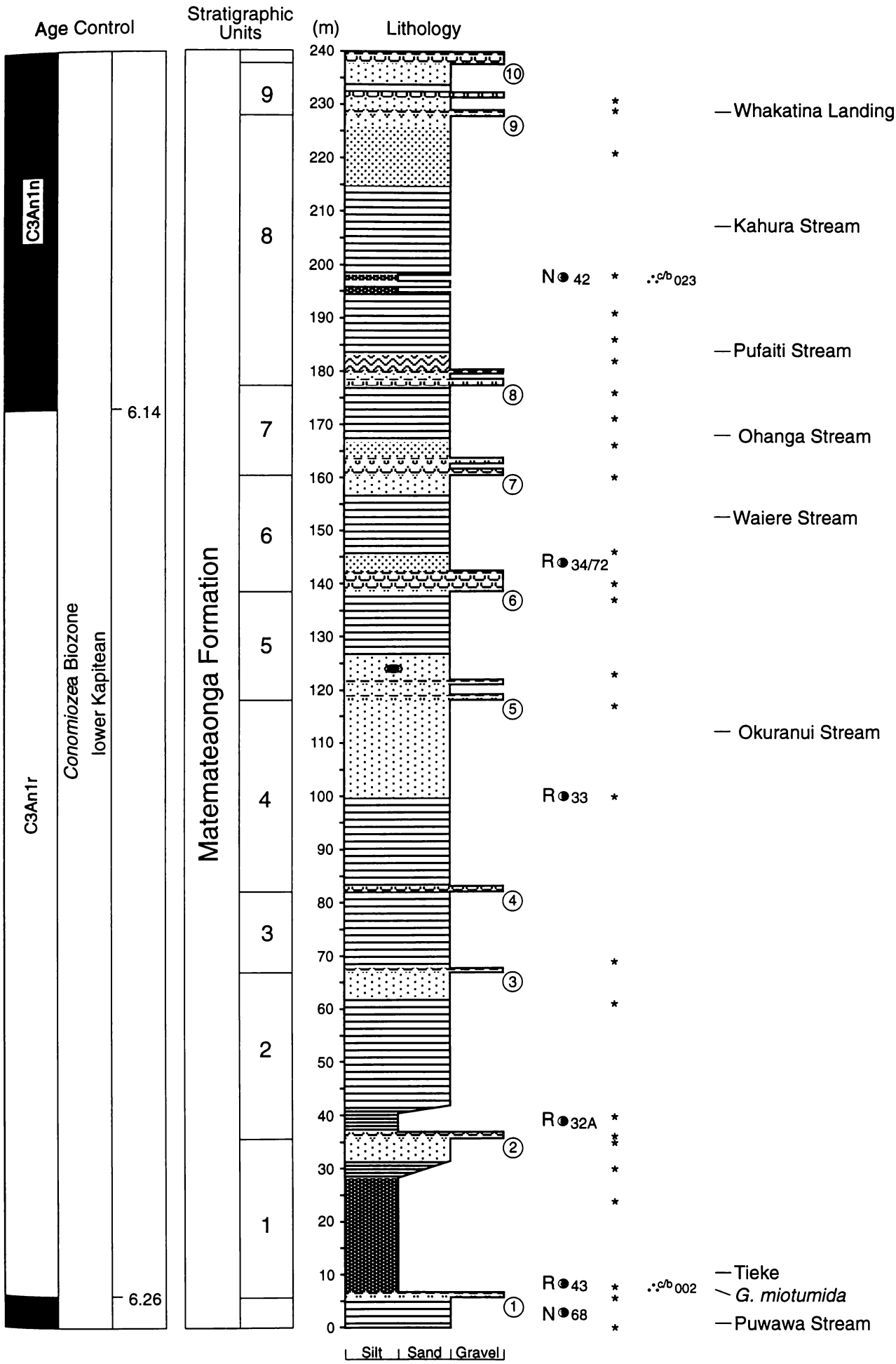

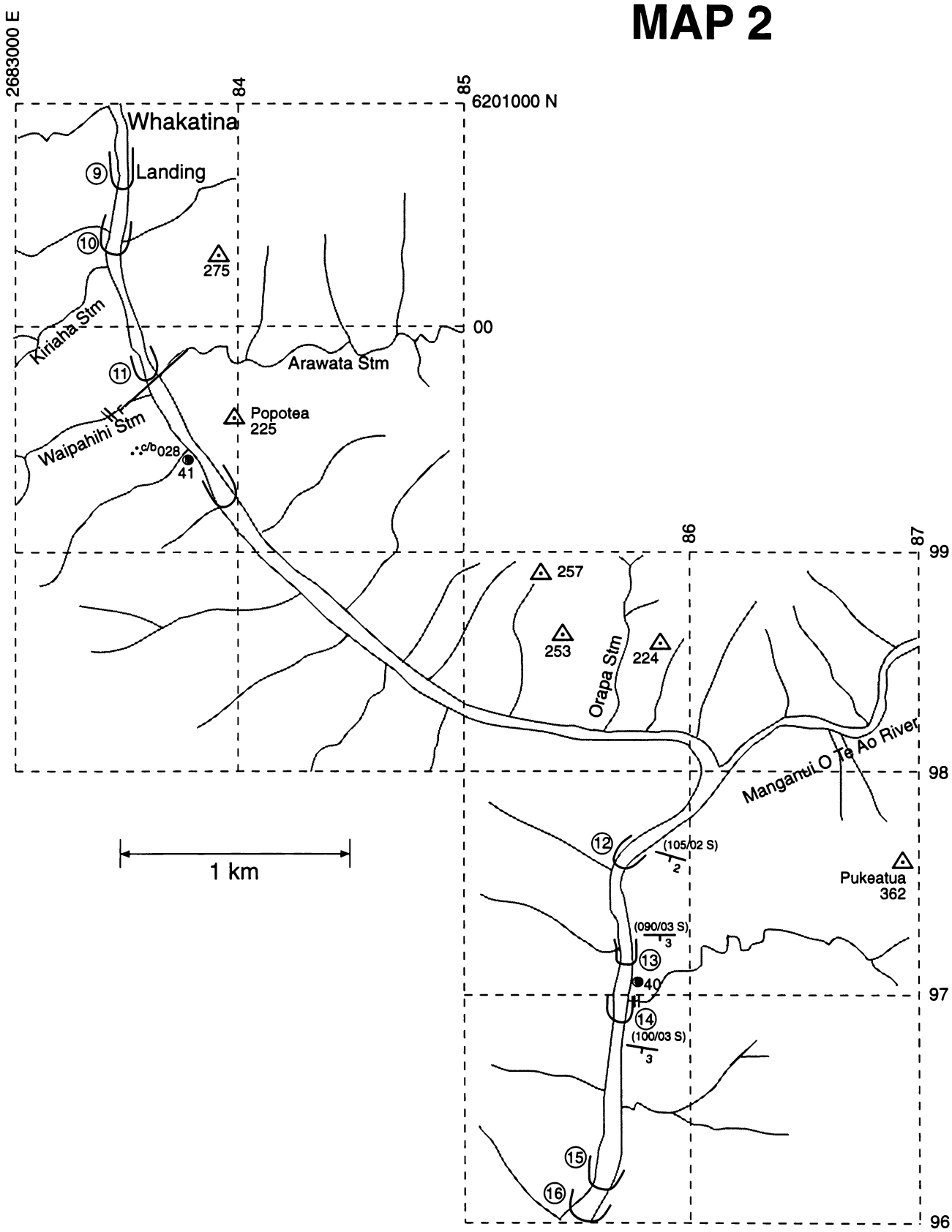
MAP 2
2683000 E
84
85
6201000 N
Whakatina
9
Landing
10
275
Kiriaha Stm
00
11
Arawata Stm
Popotea
225
Waipahihi Stm
028
41
86
87
99
257
253
224
Orapa Stm
Mangamuri O Te Ao River
98
1 km
12
(105/02 S)
2
Pukeatua
362
(090/03 S)
3
13
40
97
14
(100/03 S)
3
15
16
96

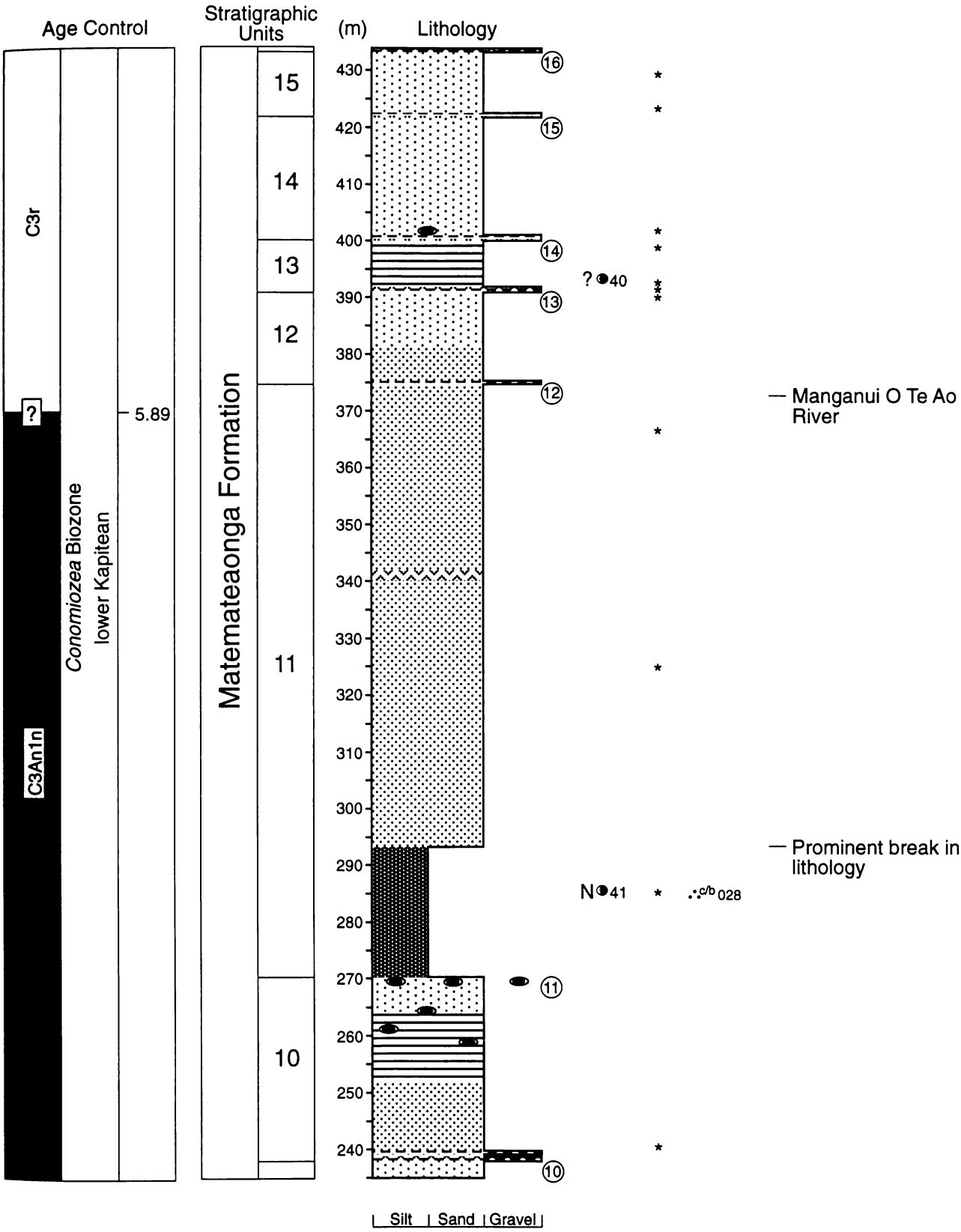
Age Control
Stratigraphic Units
(m)
Lithology
C3r
?
C3An1n
5.89
Conomiozea Biozone
lower Kapitean
Matemateaonga Formation
15
14
13
12
11
10
430
420
410
400
390
380
370
360
350
340
330
320
310
300
290
280
270
260
250
240
16
15
14
13
12
11
10
? 40
N 41
c/b 028
— Manganui O Te Ao River
— Prominent break in lithology
Silt
Sand
Gravel

MAP 3

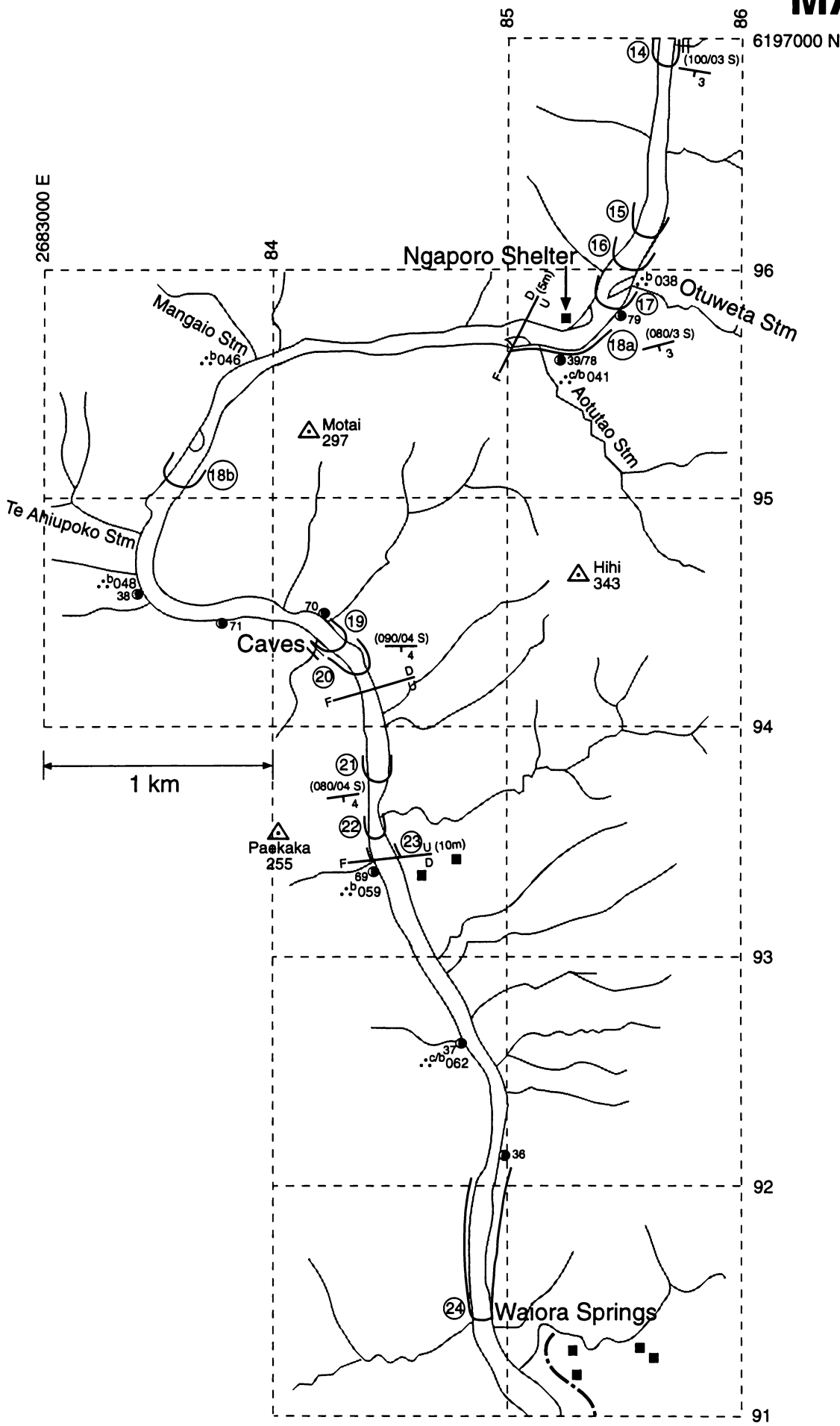
85
86
6197000 N
2683000 E
84
96
95
94
93
92
91
Ngaporo Shelter
Otuweta Stm
Mangaio Stm
Aotuitao Stm
Te Ahiupoko Stm
Motai
297
Hihi
343
Caves
Paekaka
255
Waiora Springs
1 km
(100/03 S)
(090/04 S)
(080/04 S)
(080/3 S)
U (5m)
U (10m)
D
U
F
b046
b038
b048
b059
c/b041
c/b062
14
15
16
17
18a
18b
19
20
21
22
23
24
79
39/78
38
70
71
69
37
36

Wanganui River Section, Wanganui Basin, New Zealand

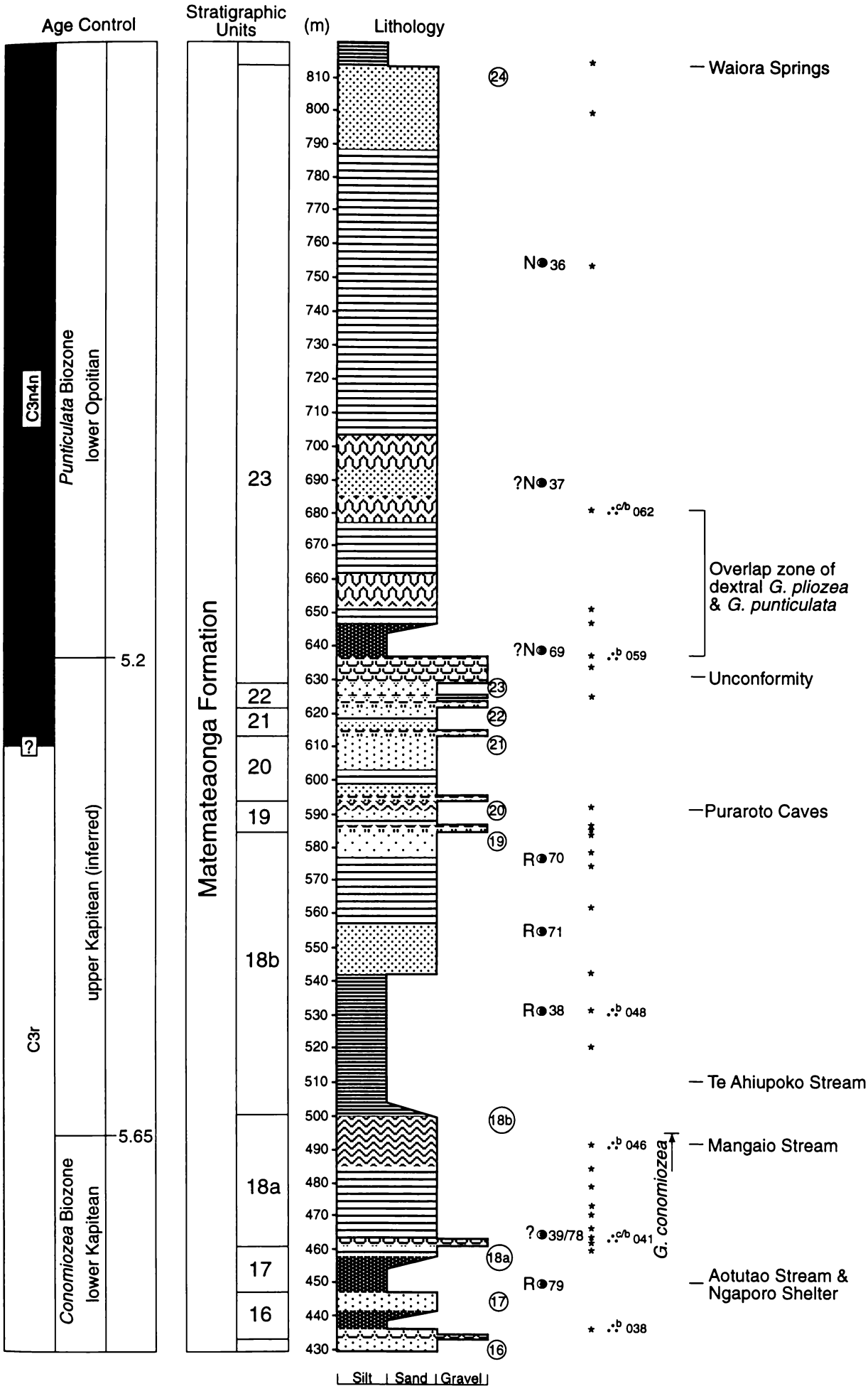

MAP 4

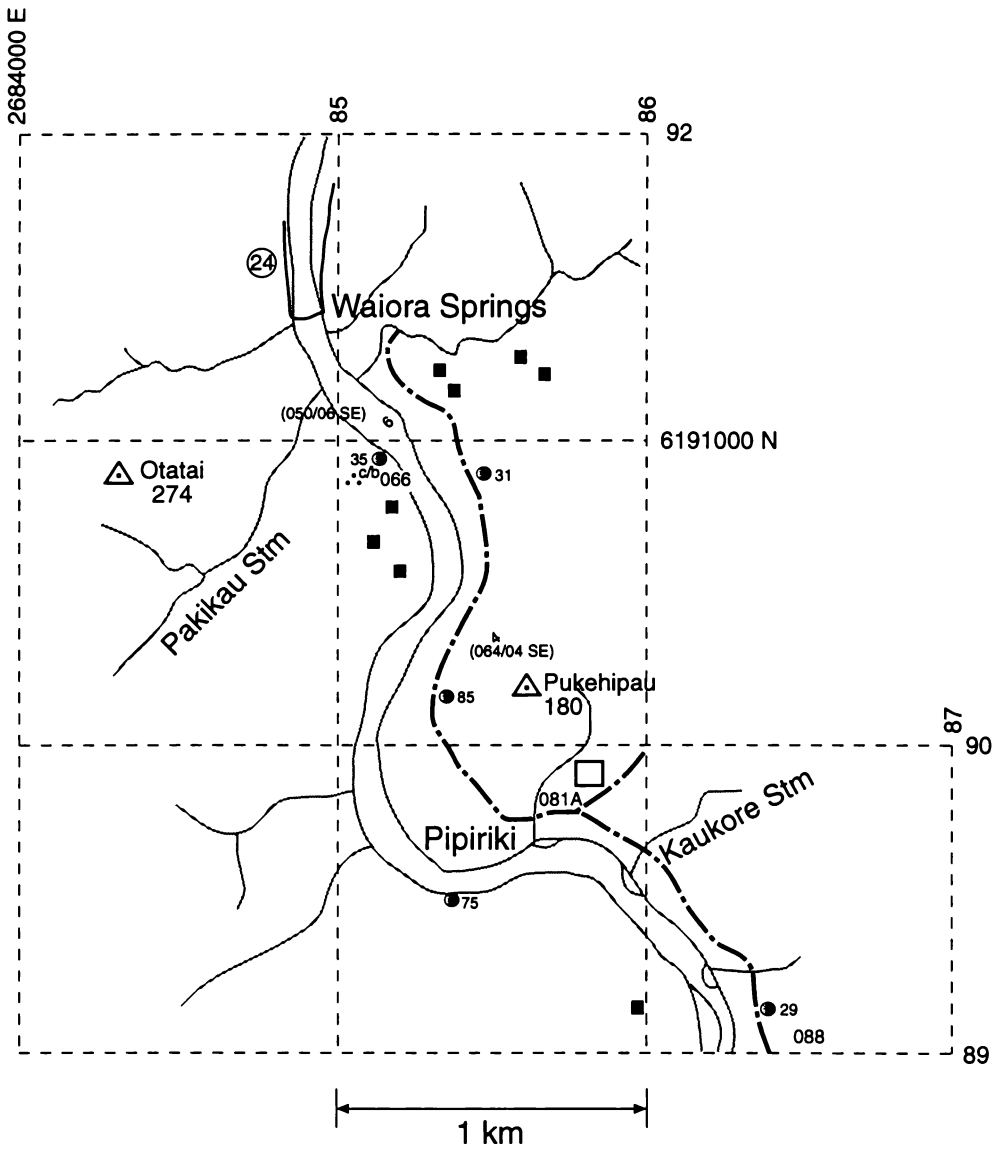
2684000 E
85
86
92
24
Waiora Springs
(050/06 SE)
6191000 N
Otatai
274
35
066
31
Pakikau Stm
(064/04 SE)
Pukehipau
180
85
87
90
081A
Pipiriki
Kaukore Stm
75
29
088
89
1 km

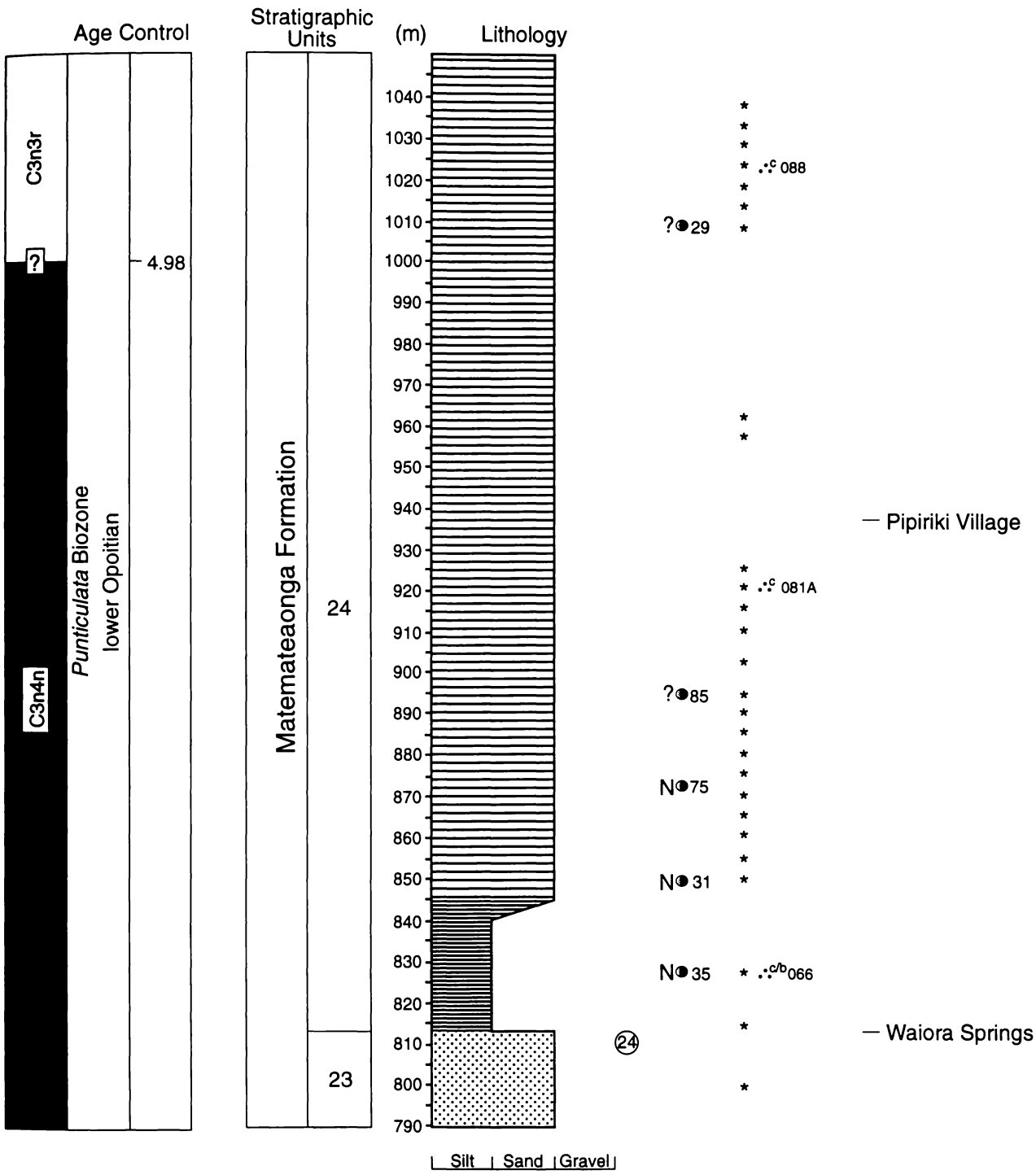
Age Control
Stratigraphic Units
(m)
Lithology
C3n3r
?
C3n4n
4.98
Punticulata Biozone
lower Opoitian
Matemateaonga Formation
24
23
1040
1030
1020
1010
1000
990
980
970
960
950
940
930
920
910
900
890
880
870
860
850
840
830
820
810
800
790
088
?29
081A
?85
N75
N31
N35
066
24
Pipiriki Village
Waiora Springs
Silt
Sand
Gravel

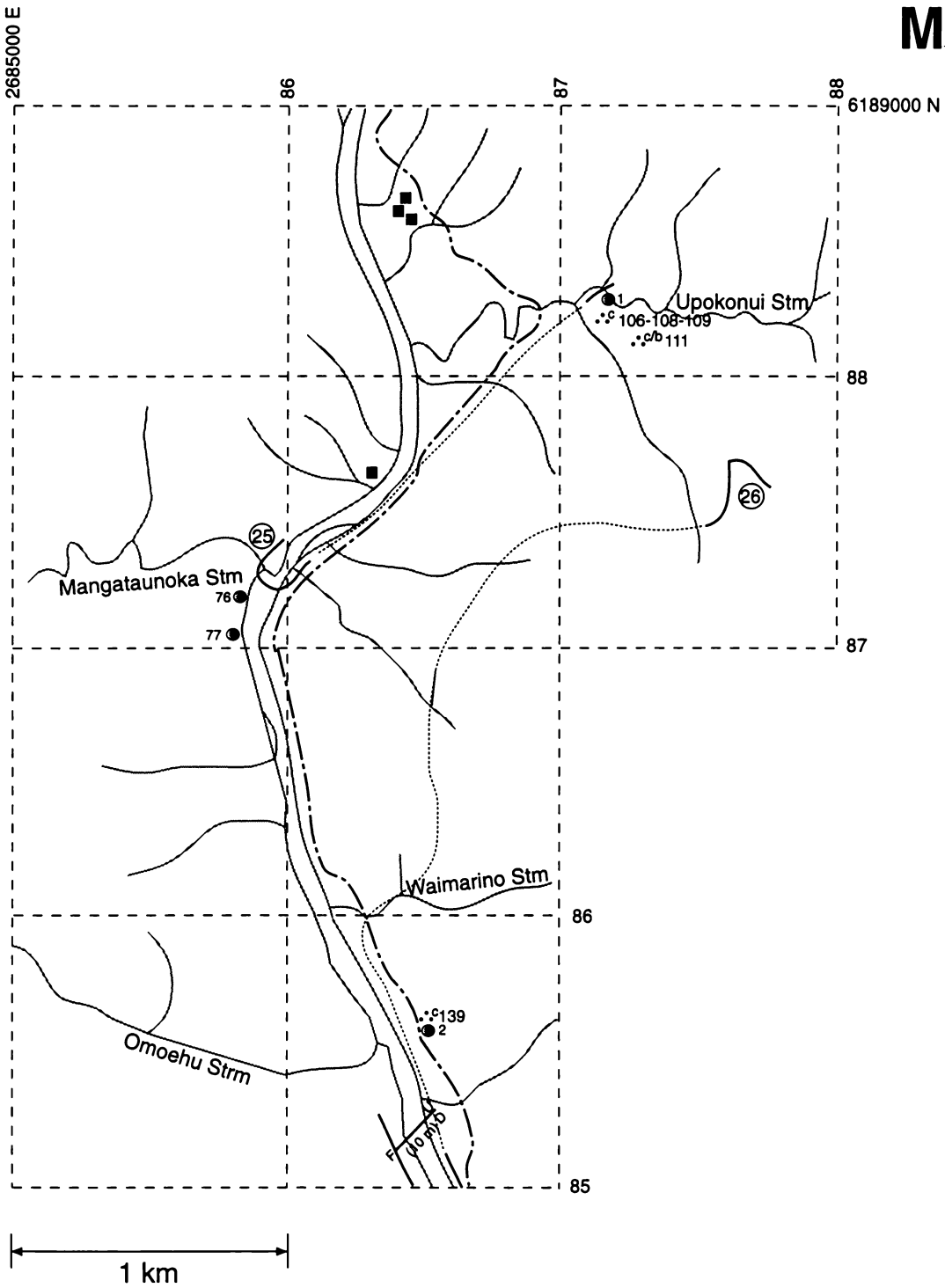
MAP 5
2685000 E
86
87
88
6189000 N
88
87
86
85
Upokonui Stm
1
c
106-108-109
c/b
111
26
25
Mangataunoka Stm
76
77
Waimarino Stm
c
139
2
Omoehu Strm
1 km

Wanganui River Section, Wanganui Basin, New Zealand

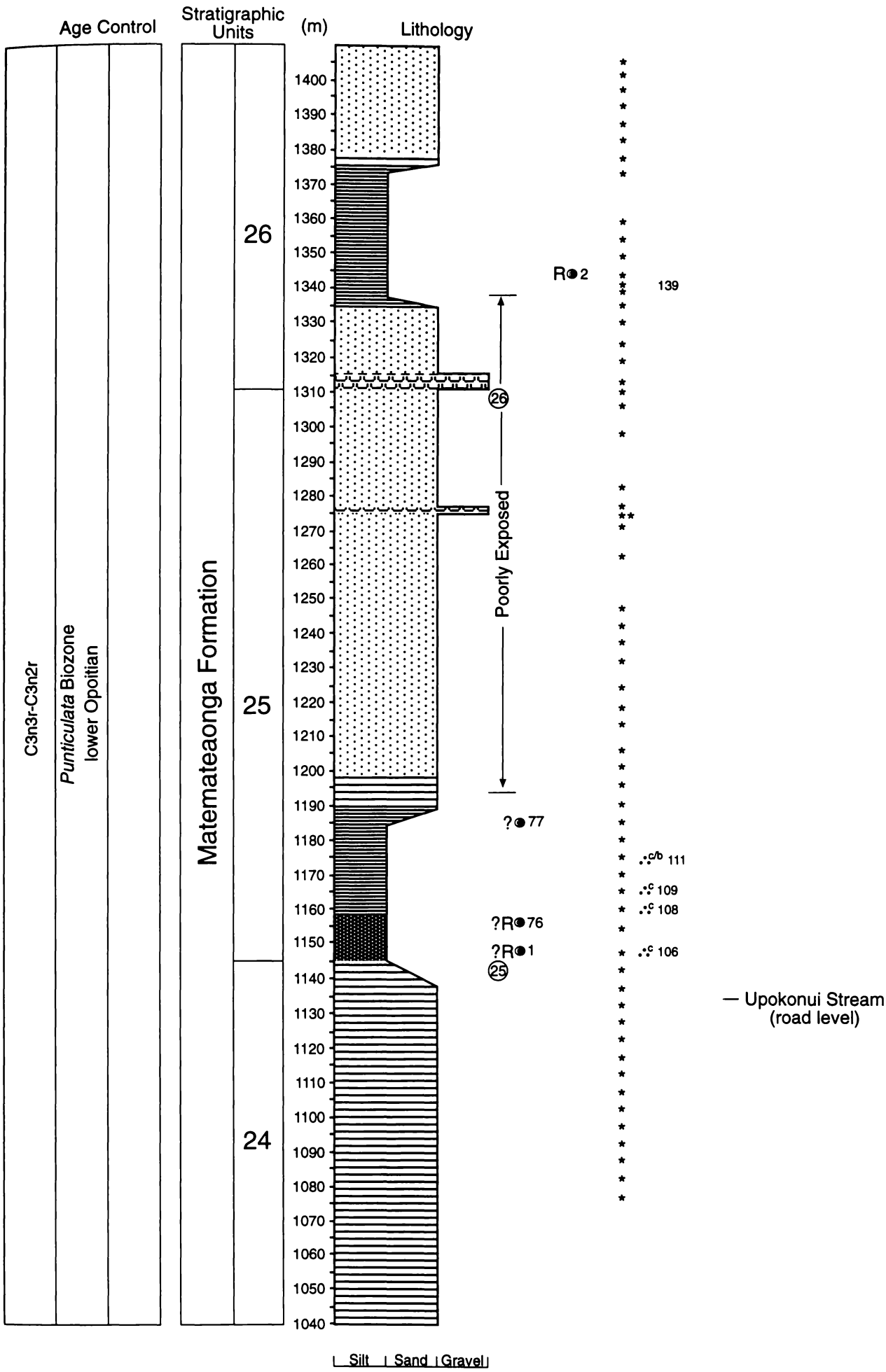

MAP 6

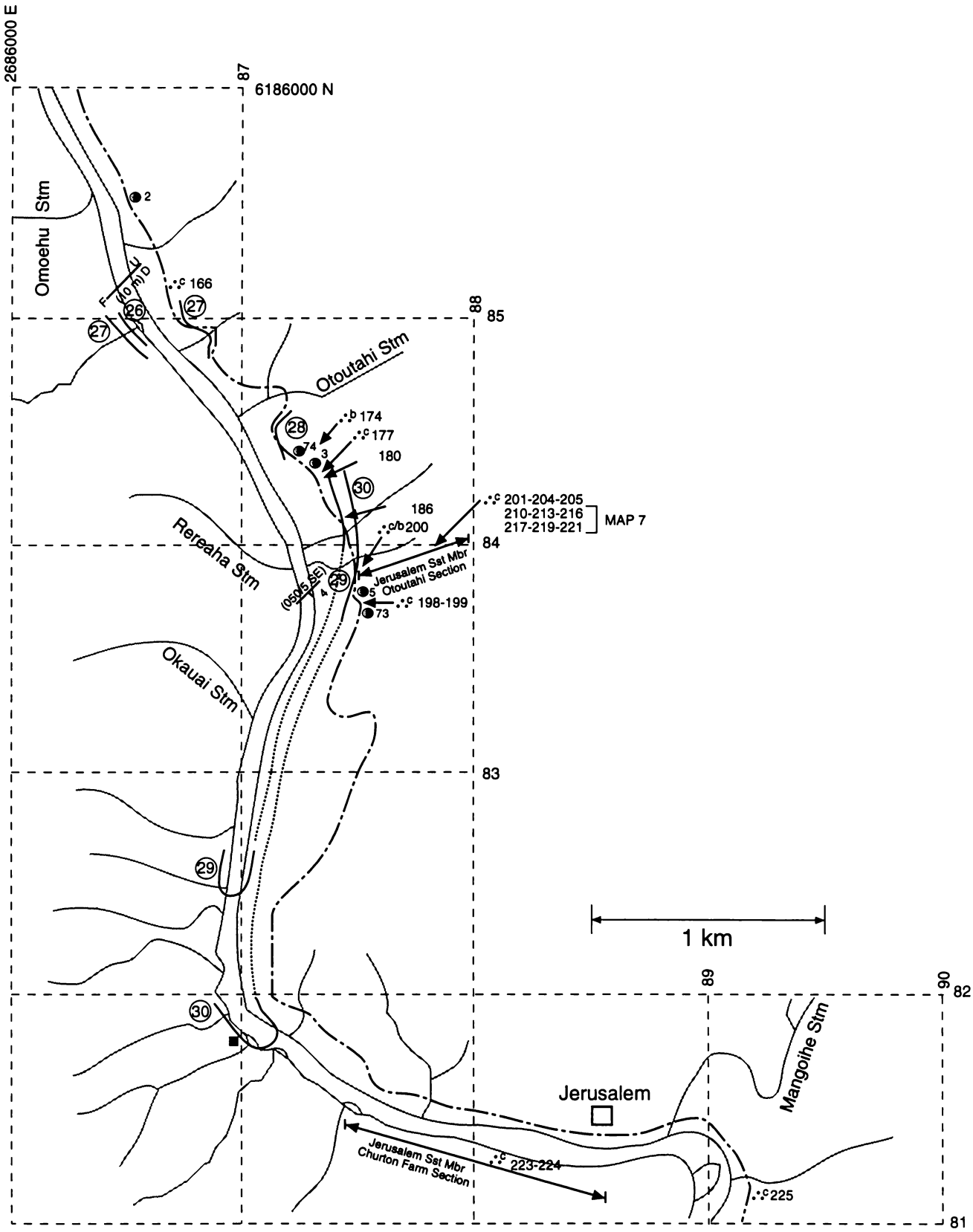
2686000 E
6186000 N
87
88
85
84
83
89
90
82
81
Omoehu Stm
Otoutahi Stm
Rerpaha Stm
Okauai Stm
Mangoihe Stm
Jerusalem
1 km
166
174
177
180
186
200
201-204-205
210-213-216
217-219-221
MAP 7
198-199
223-224
225
Jerusalem Sst Mbr
Otoutahi Section
Jerusalem Sst Mbr
Churton Farm Section

Wanganui River Section, Wanganui Basin, New Zealand

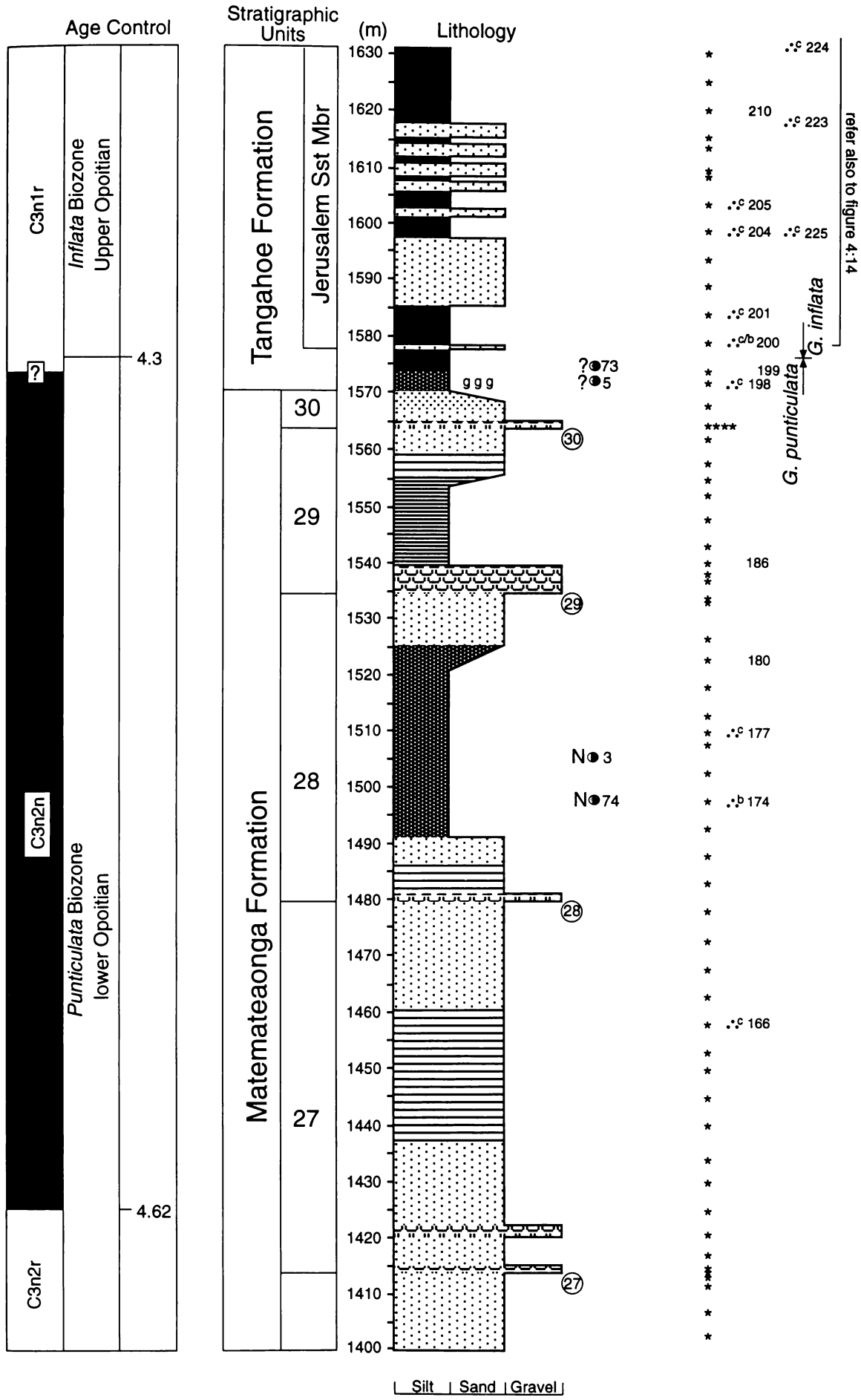

MAP 7

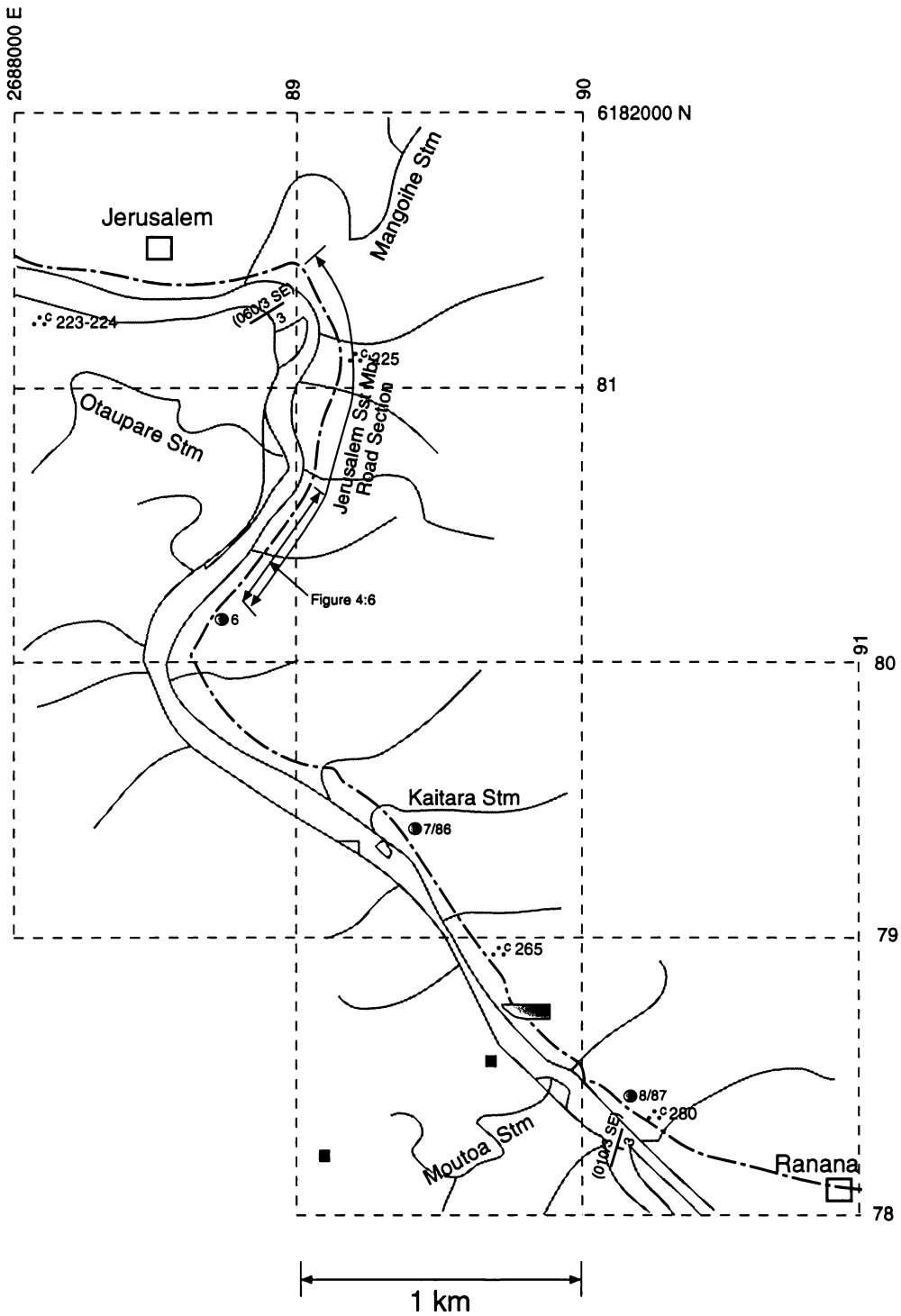
2688000 E
89
90
6182000 N
Jerusalem
Mangoihe Stm
223-224
(060)3 SE
3
225
81
Otaupare Stm
Jerusalem Sst Mbr
Road Section
Figure 4:6
6
91
80
Kaitara Stm
7/86
265
79
8/87
280
Moutoa Stm
(010)3 SE
3
Ranana
78
1 km

Wanganui River Section, Wanganui Basin, New Zealand

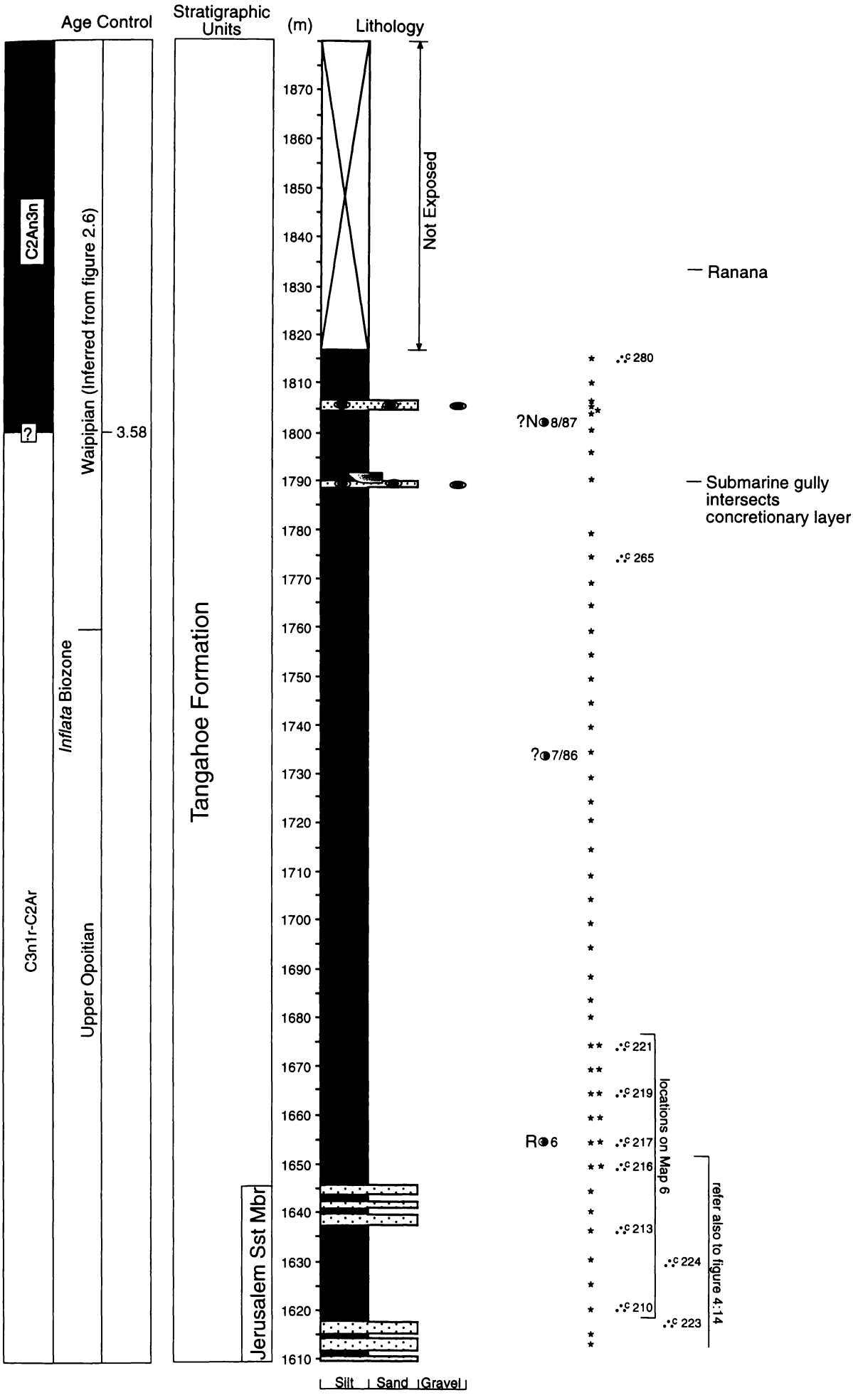

MAP 8

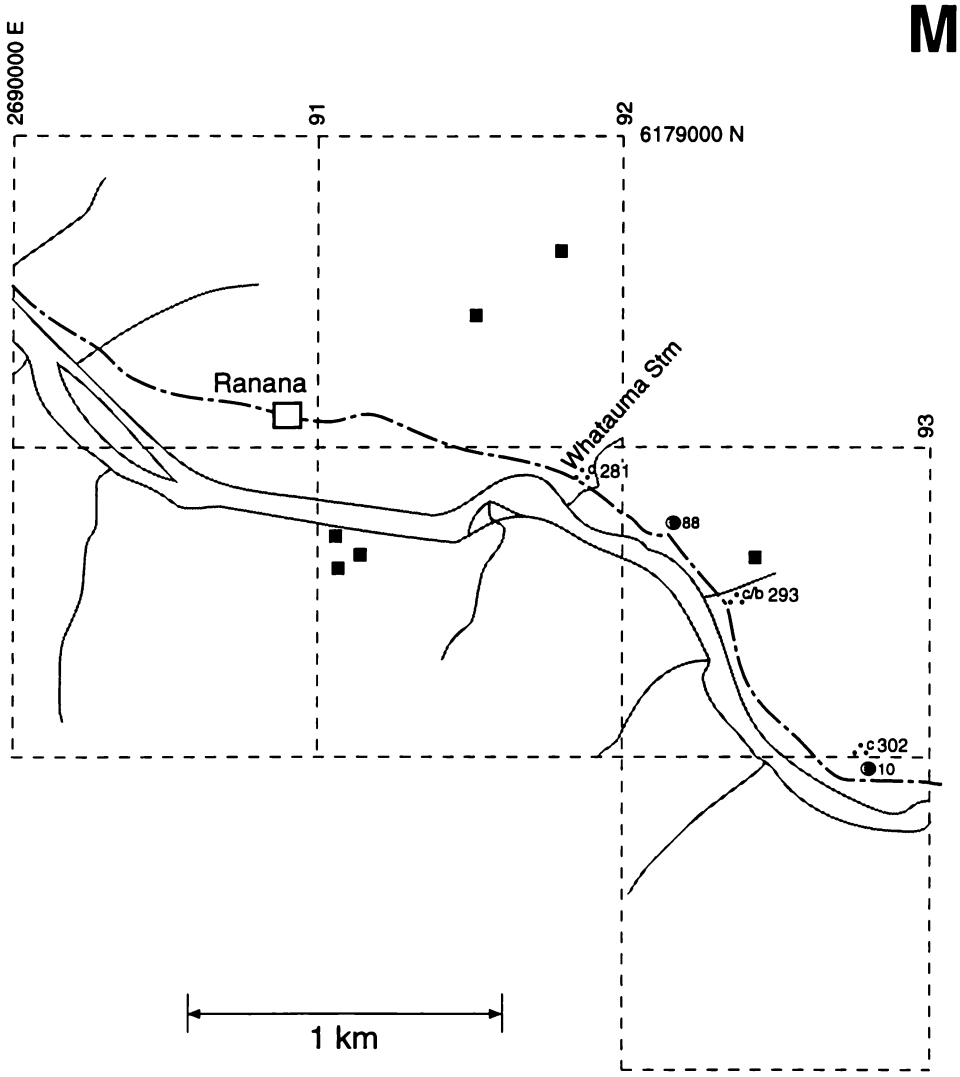
2690000 E
91
92
6179000 N
Ranana
Whatauma Stm
93
281
88
c/b 293
c 302
10
1 km

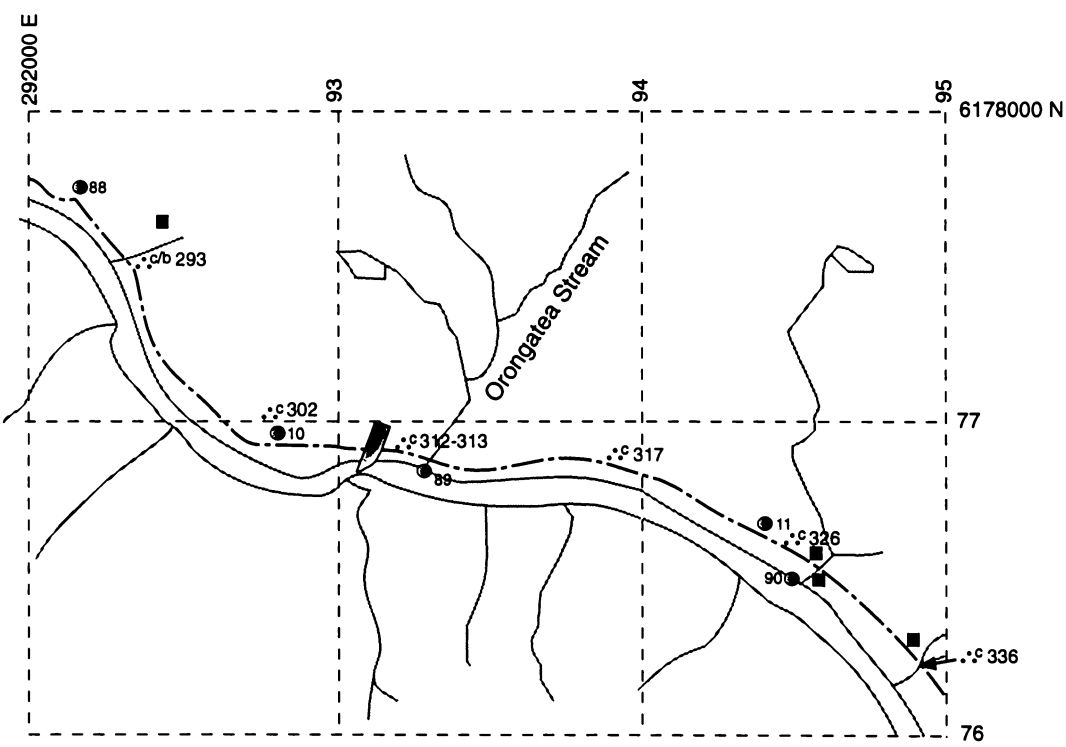
292000 E
93
94
95
6178000 N
88
c/b 293
Orongatea Stream
c 302
10
c 312-313
89
c 317
77
11
c 326
90
c 336
76

Wanganui River Section, Wanganui Basin, New Zealand

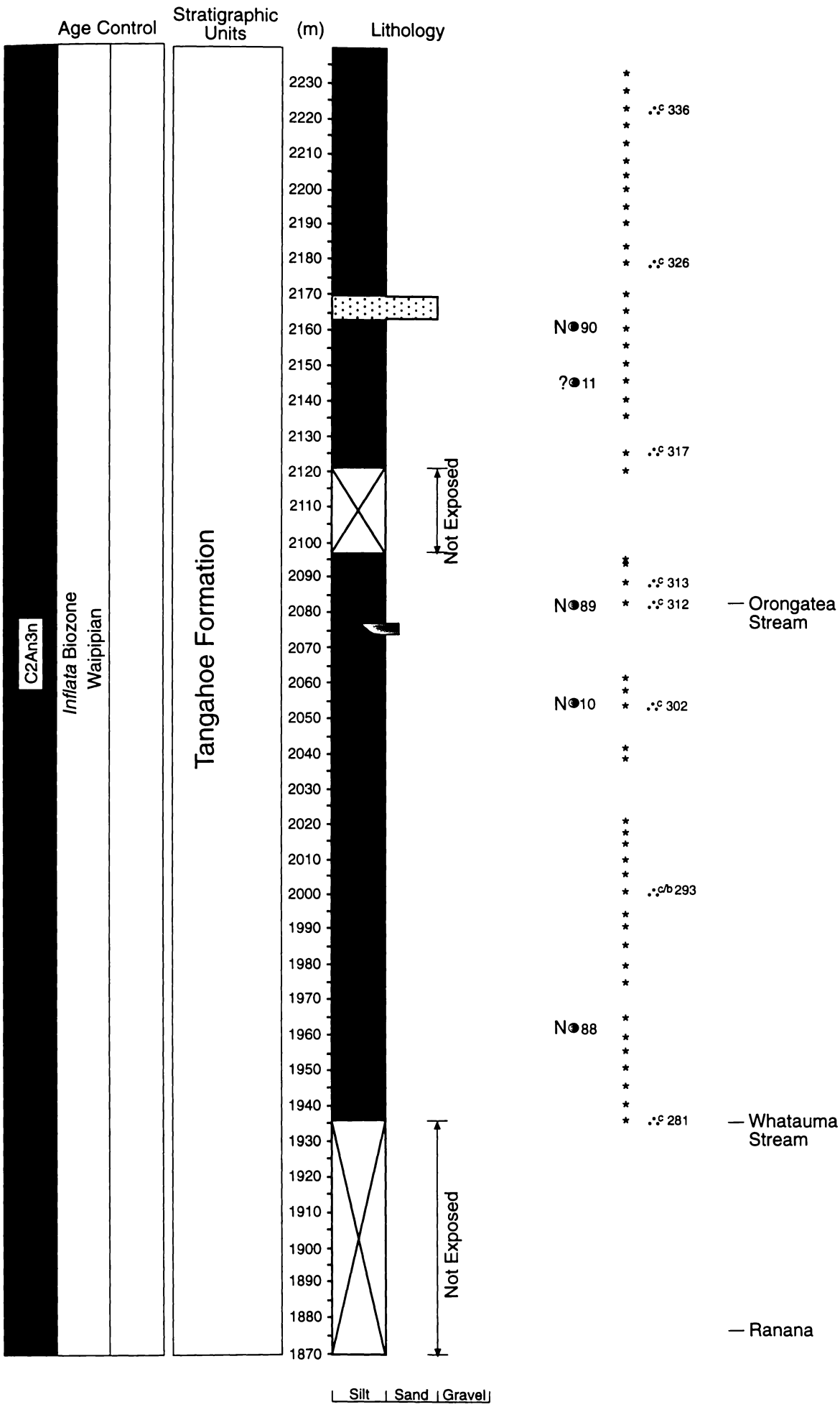

MAP 9

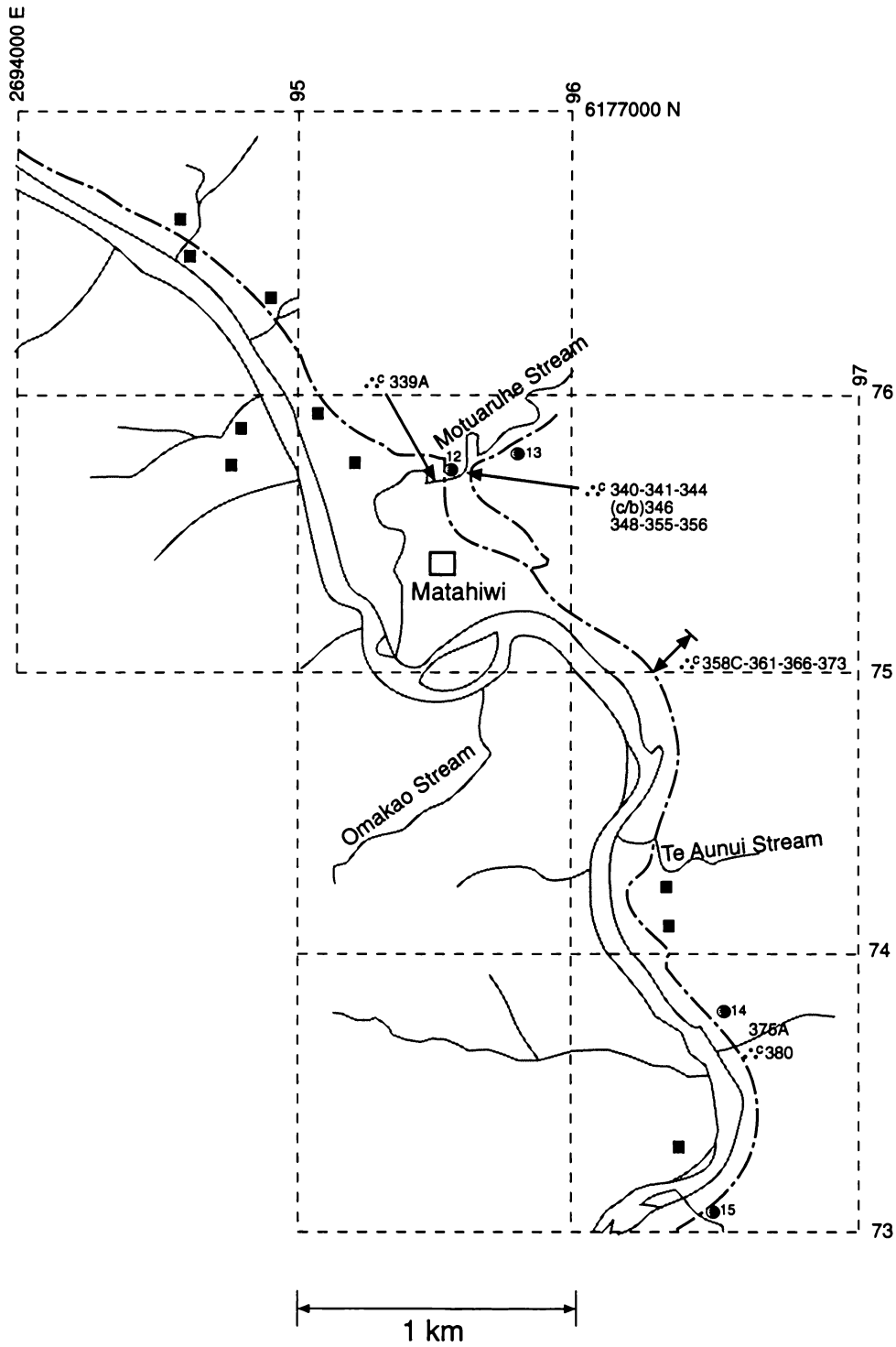
2694000 E
95
96
6177000 N
97
76
75
74
73
339A
Motuaruhe Stream
12
13
340-341-344
(c/b)346
348-355-356
Matahiwi
358C-361-366-373
Omakao Stream
Te Aunui Stream
14
376A
380
15
1 km

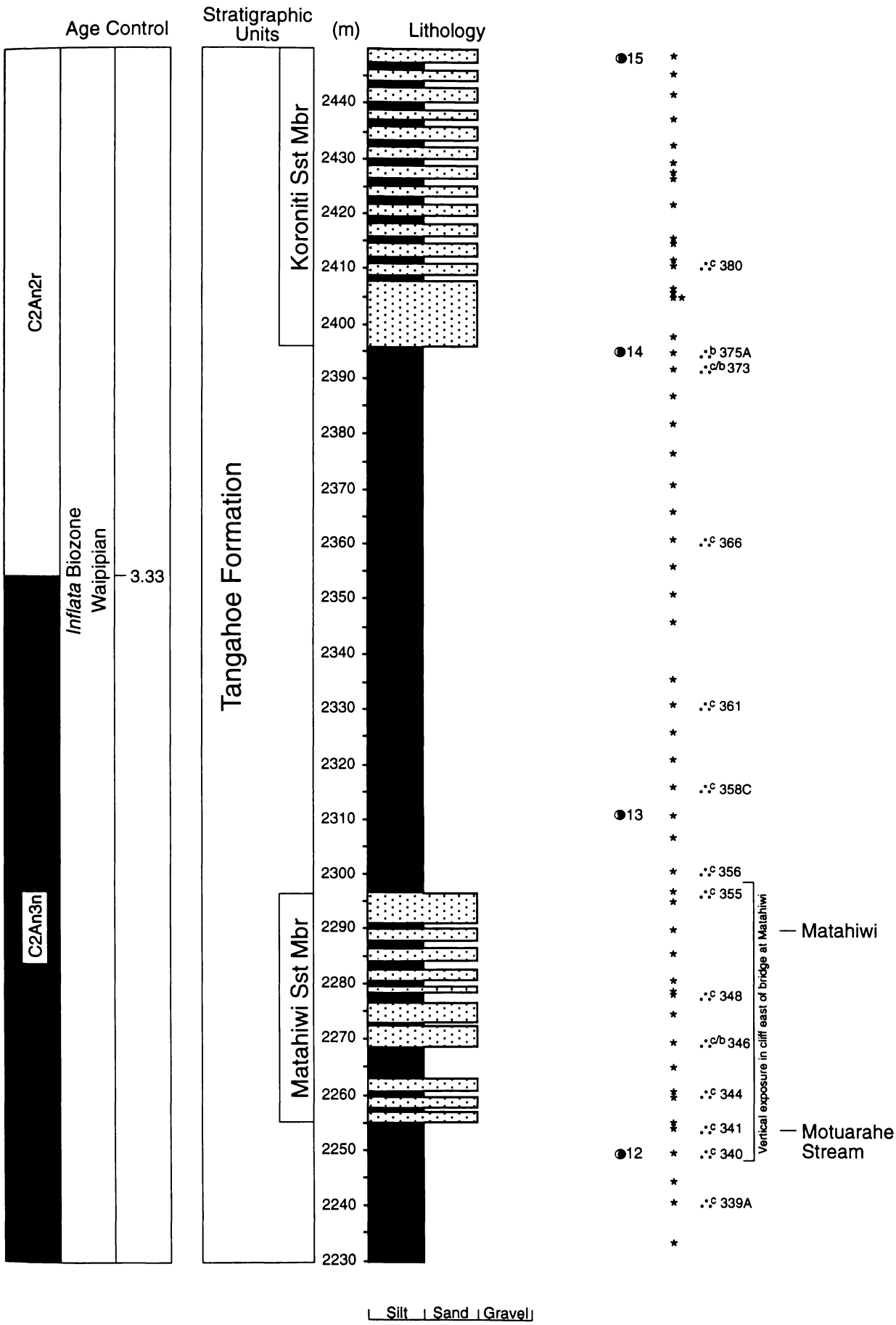
Age Control
Stratigraphic Units
(m)
Lithology
C2An2r
C2An3n
Inflata Biozone
Waipipian
3.33
Tangahoe Formation
Koroniti Sst Mbr
Matahiwi Sst Mbr
2440
2430
2420
2410
2400
2390
2380
2370
2360
2350
2340
2330
2320
2310
2300
2290
2280
2270
2260
2250
2240
2230
15
14
13
12
c 380
b 375A
c/b 373
c 366
c 361
c 358C
c 356
c 355
c 348
c/b 346
c 344
c 341
c 340
c 339A
Vertical exposure in cliff east of bridge at Matahiwi
Matahiwi
Motuarahe Stream
Silt
Sand
Gravel

MAP 10

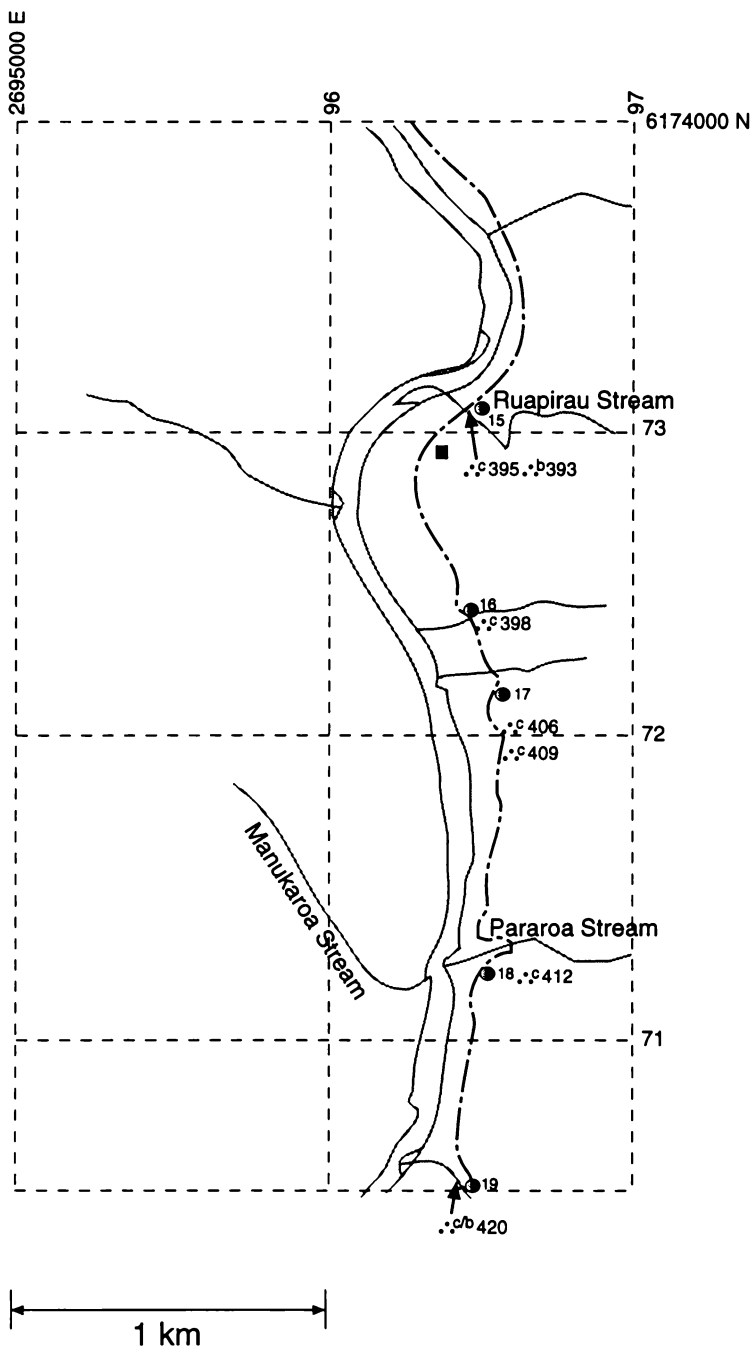
2695000 E
96
97
6174000 N
Ruapirau Stream
15
73
c395
b393
16
c398
17
c406
c409
72
Manukaroa Stream
Pararoa Stream
18
c412
71
19
c/b420
1 km

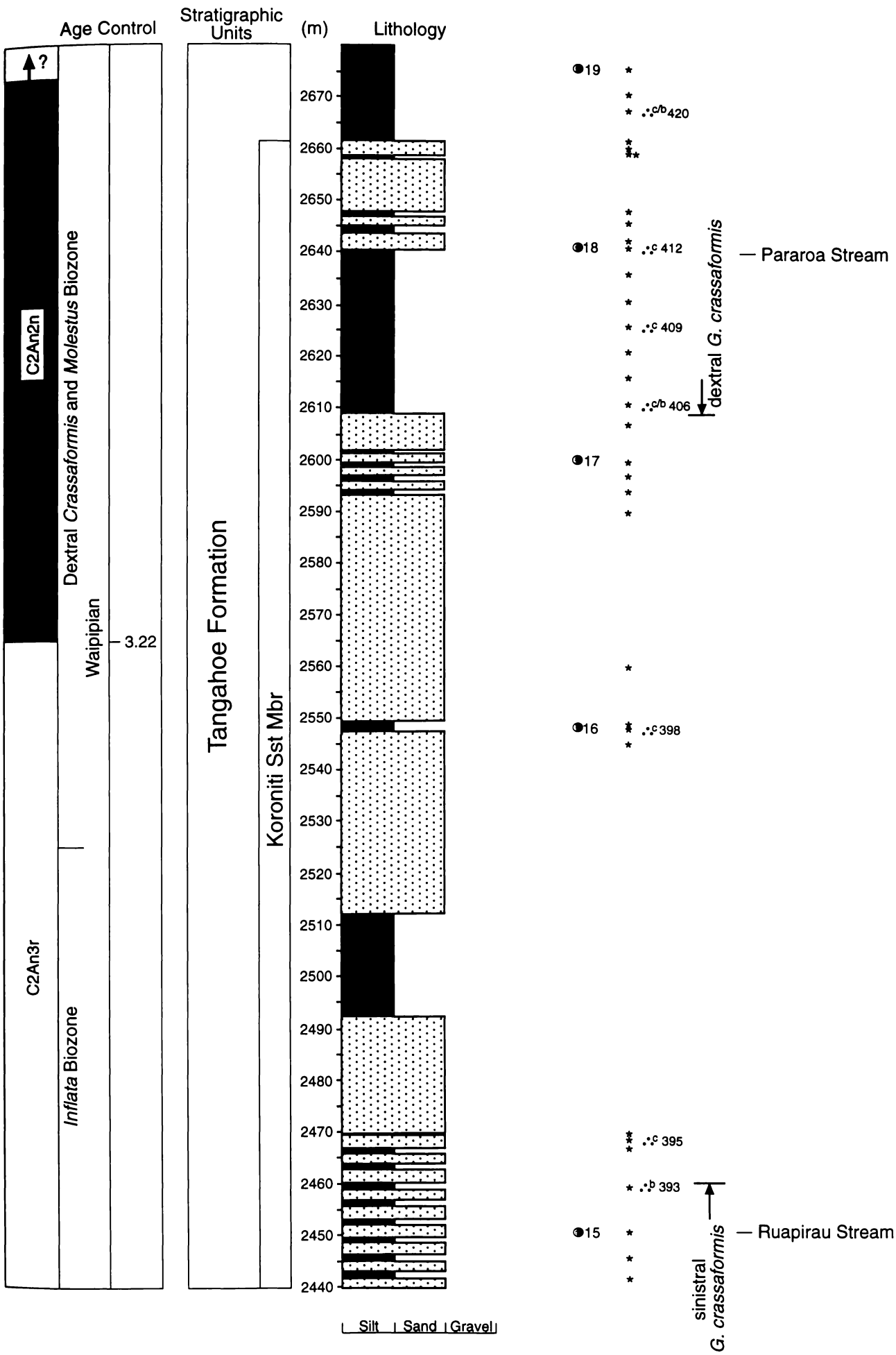
Wanganui River Section, Wanganui Basin, New Zealand
Age Control
Stratigraphic Units
(m)
Lithology
?
C2An2n
C2An3r
Dextral Crassaformis and Molestus Biozone
Inflata Biozone
Waipipian
3.22
Tangahoe Formation
Koroniti Sst Mbr
2670
2660
2650
2640
2630
2620
2610
2600
2590
2580
2570
2560
2550
2540
2530
2520
2510
2500
2490
2480
2470
2460
2450
2440
19
18
17
16
15
c/b 420
c 412
c 409
c/b 406
c 398
c 395
b 393
dextral G. crassaformis
— Pararoa Stream
sinistral G. crassaformis
— Ruapirau Stream
Silt
Sand
Gravel

MAP 11

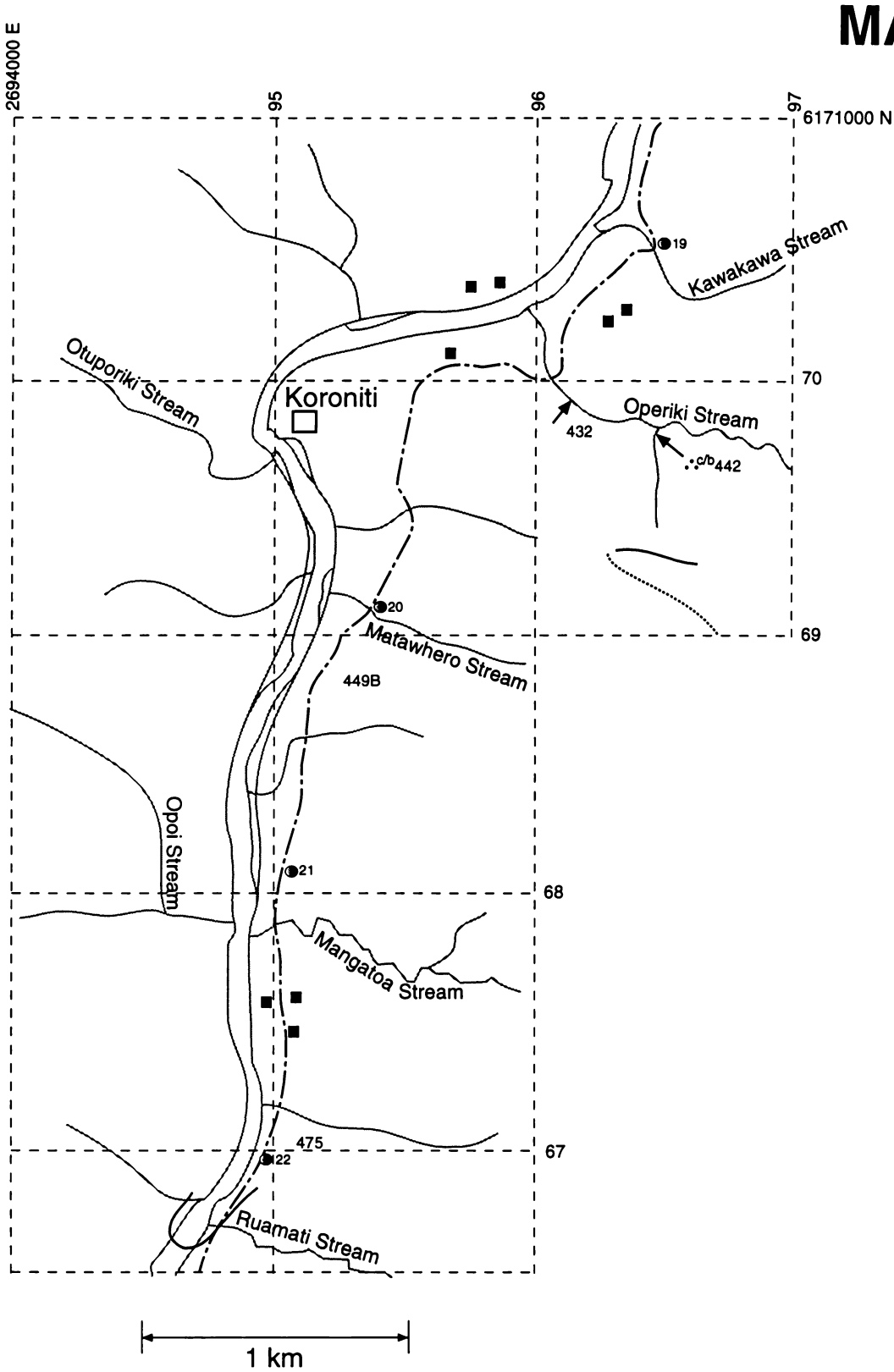
2694000 E
95
96
97
6171000 N
70
69
68
67
Kawakawa Stream
19
Otuporiki Stream
Koroniti
Operiki Stream
432
c/b442
20
Matawhero Stream
449B
Opoi Stream
21
Mangatoa Stream
475
22
Ruamati Stream
1 km

Wanganui River Section, Wanganui Basin, New Zealand

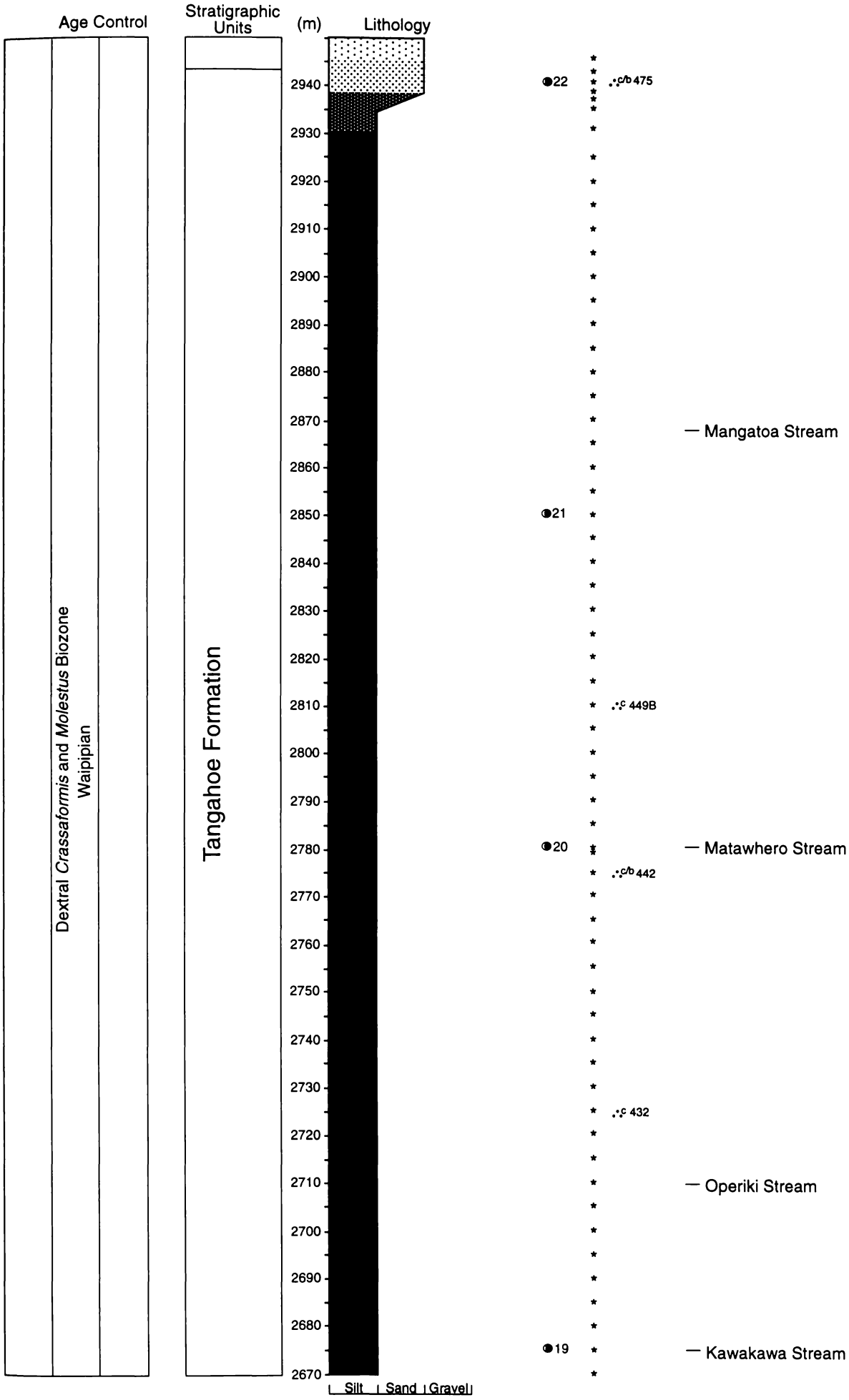

MAP 12

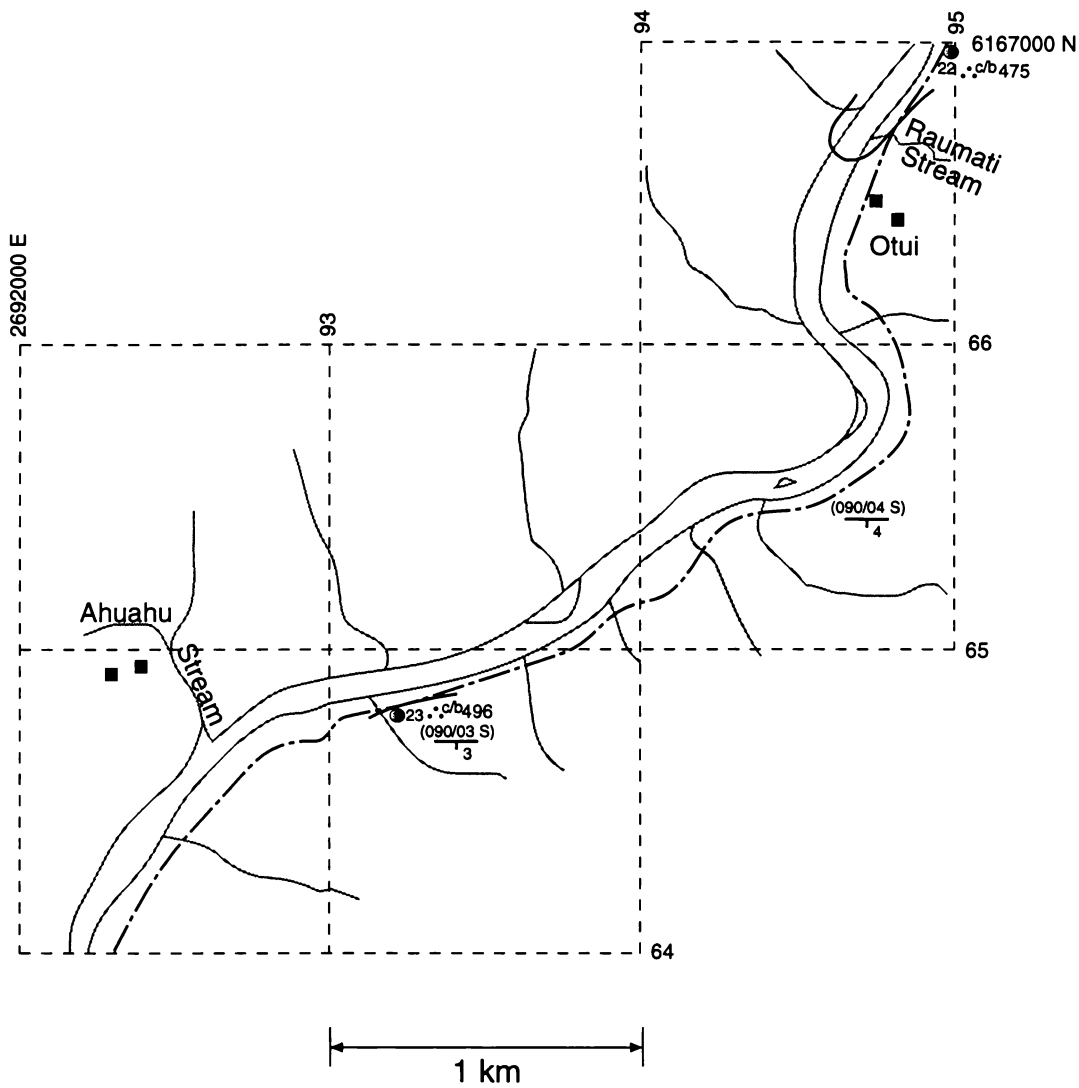
94
95
6167000 N
22 c/b 475
Raumati Stream
Otui
2692000 E
93
66
(090/04 S)
4
Ahuahu
Stream
65
23 c/b 496
(090/03 S)
3
64
1 km

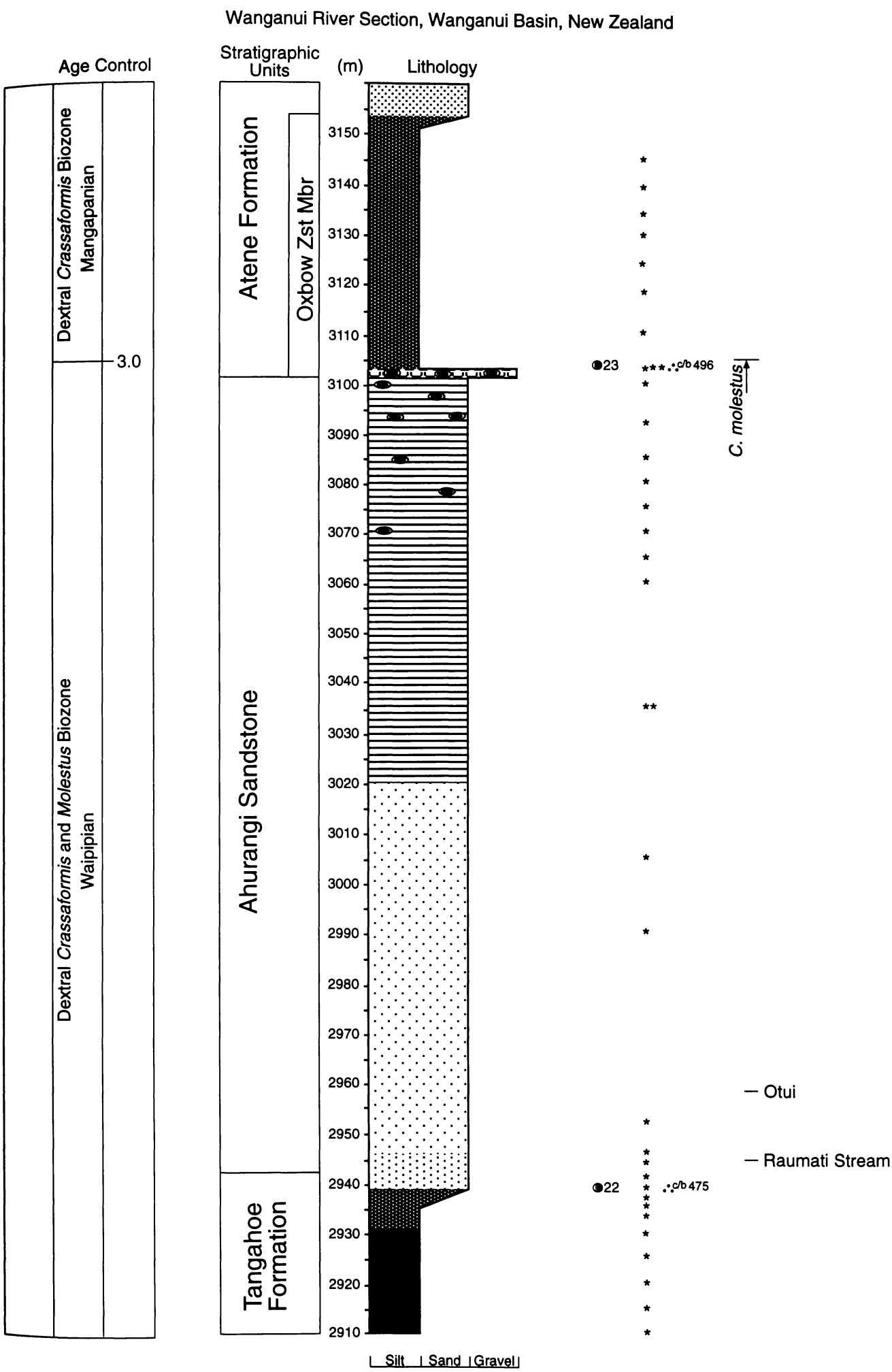
Wanganui River Section, Wanganui Basin, New Zealand
Age Control
Stratigraphic Units
(m)
Lithology
Dextral Crassaformis Biozone
Mangapanian
3.0
Dextral Crassaformis and Molestus Biozone
Waipipian
Atene Formation
Oxbow Zst Mbr
Ahurangi Sandstone
Tangahoe Formation
3150
3140
3130
3120
3110
3100
3090
3080
3070
3060
3050
3040
3030
3020
3010
3000
2990
2980
2970
2960
2950
2940
2930
2920
2910
23
c/b 496
C. molestus
22
c/b 475
— Otui
— Raumati Stream
Silt
Sand
Gravel

MAP 13

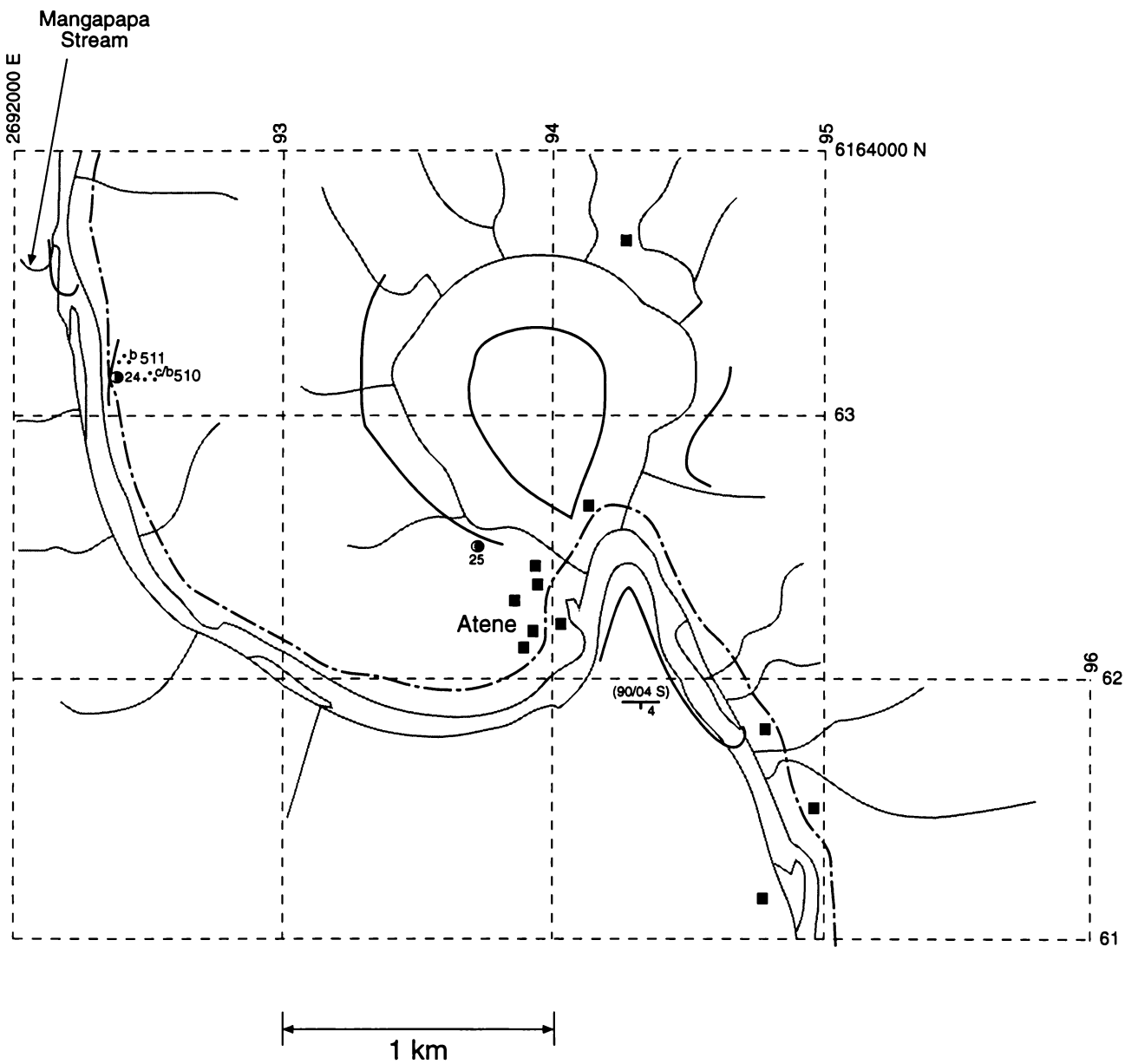
Mangapapa
Stream
2692000 E
93
94
95
6164000 N
63
62
61
96
511
24
510
25
Atene
(90/04 S)
1 km

Wanganui River Section, Wanganui Basin, New Zealand

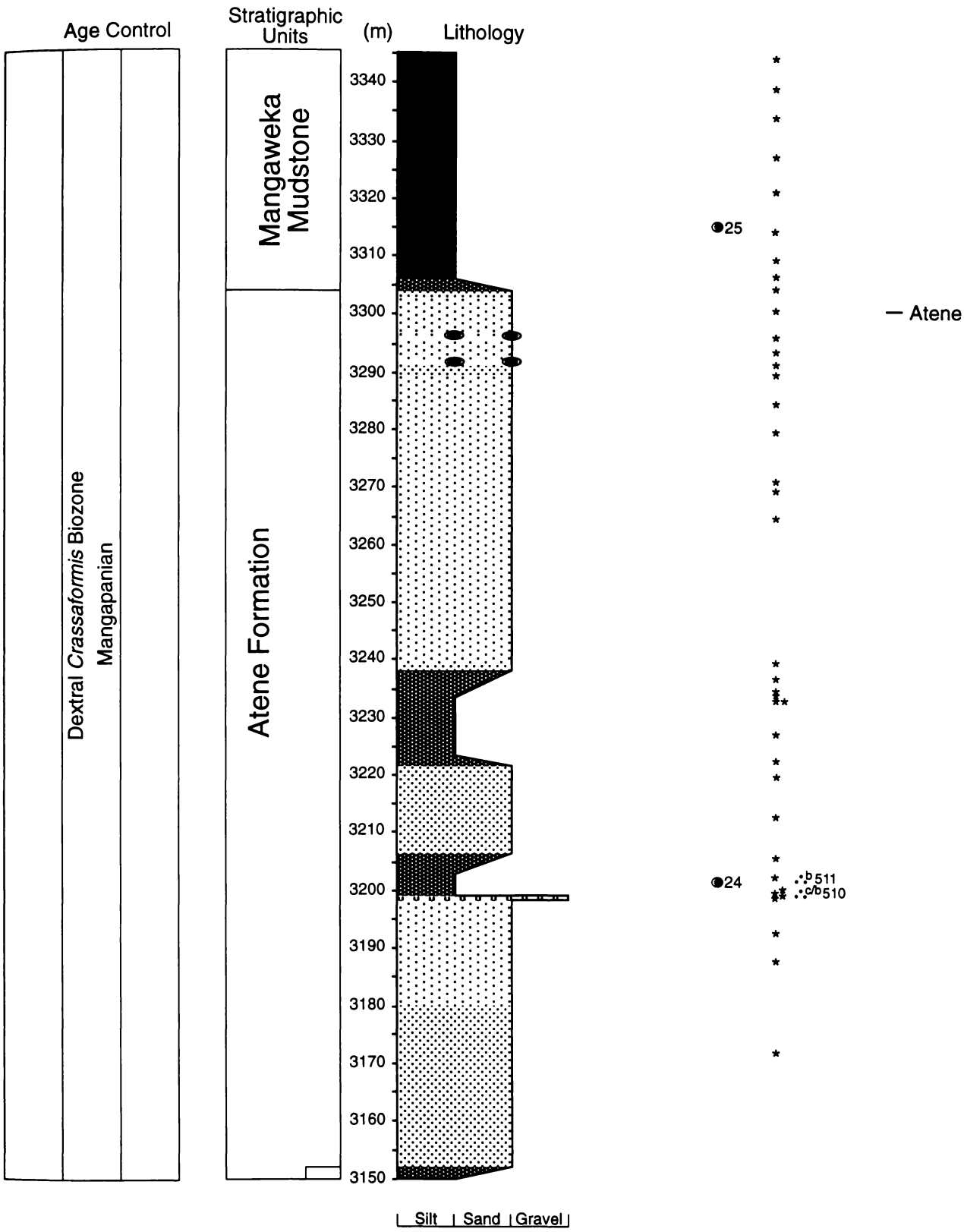

MAP 14

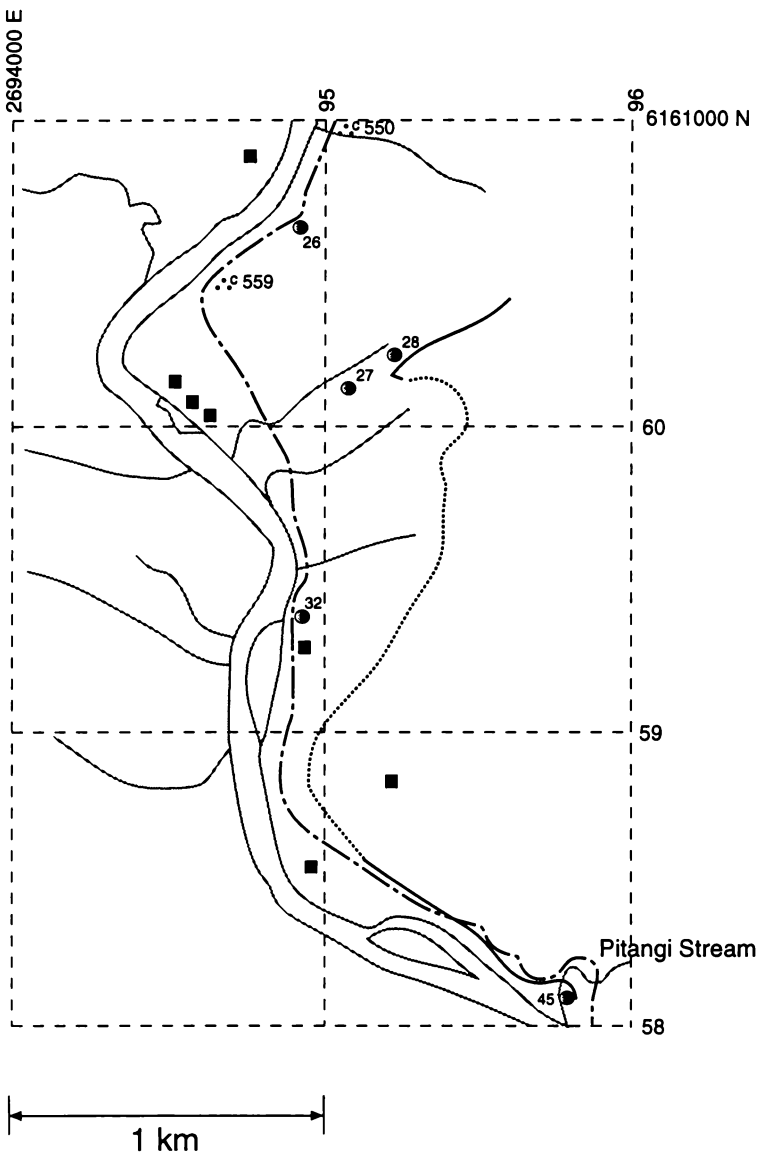
2694000 E
95
96
6161000 N
550
26
559
28
27
60
32
59
Pitangi Stream
45
58
1 km

Wanganui River Section, Wanganui Basin, New Zealand

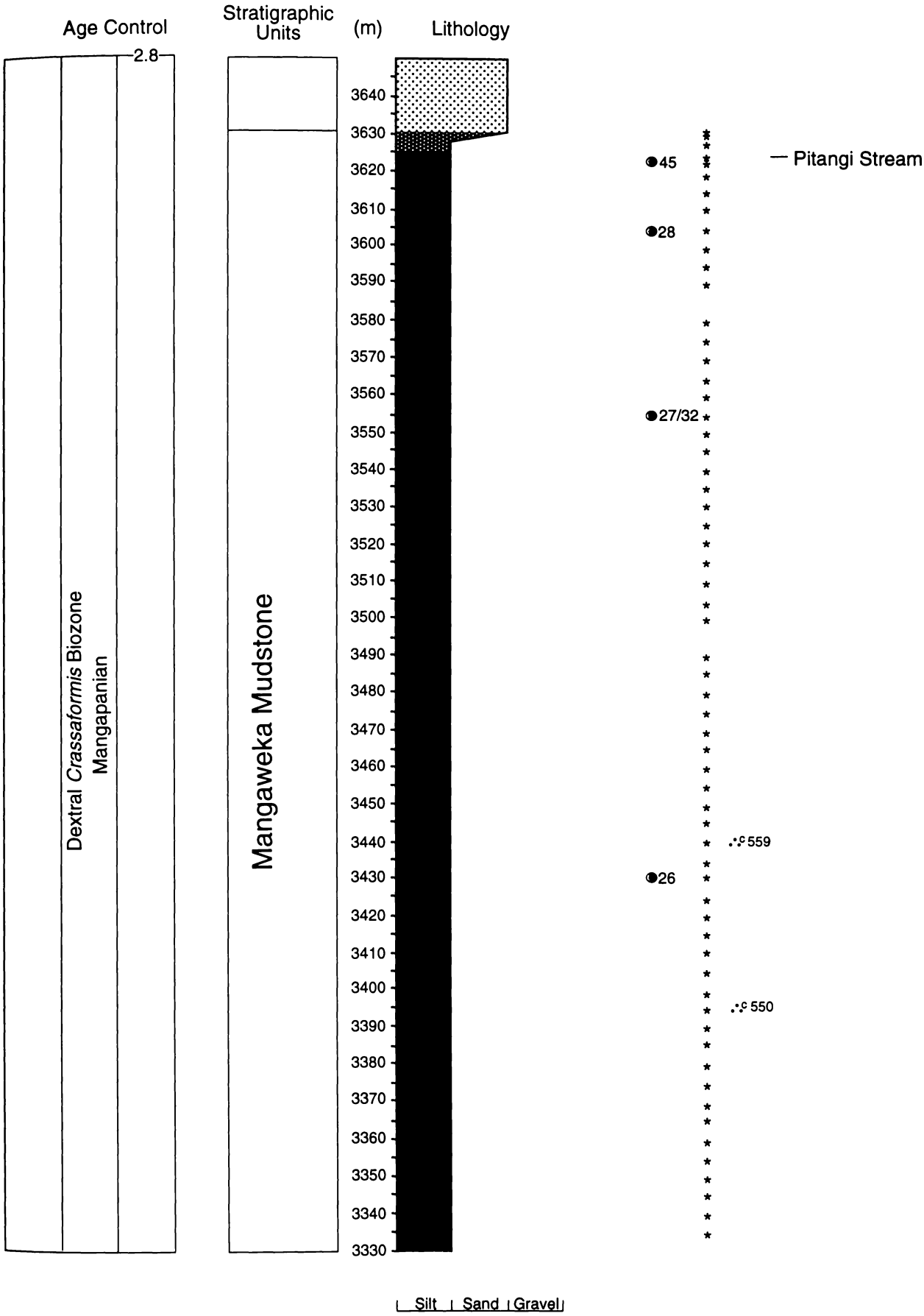

CHAPTER 3

STRATIGRAPHY, SEQUENCE STRATIGRAPHY AND PALEOENVIRONMENTS OF THE MATEMATEAONGA FORMATION

CHAPTER 3

STRATIGRAPHY, SEQUENCE STRATIGRAPHY AND PALEOENVIRONMENTS OF THE MATEMATEAONGA FORMATION

3:1 INTRODUCTION

The Matemateaonga Formation is extensively exposed across the deeply incised, northern part of Wanganui Basin (Figure 3:1). More restricted exposure to the east is due to young volcanic deposits blanketing these areas. It is the lowermost unit considered in this study and is dominated by cyclothemic shelf sandstones that are overlain by the deep water siltstones of the Tangahoe Formation (the topic of Chapter 4).

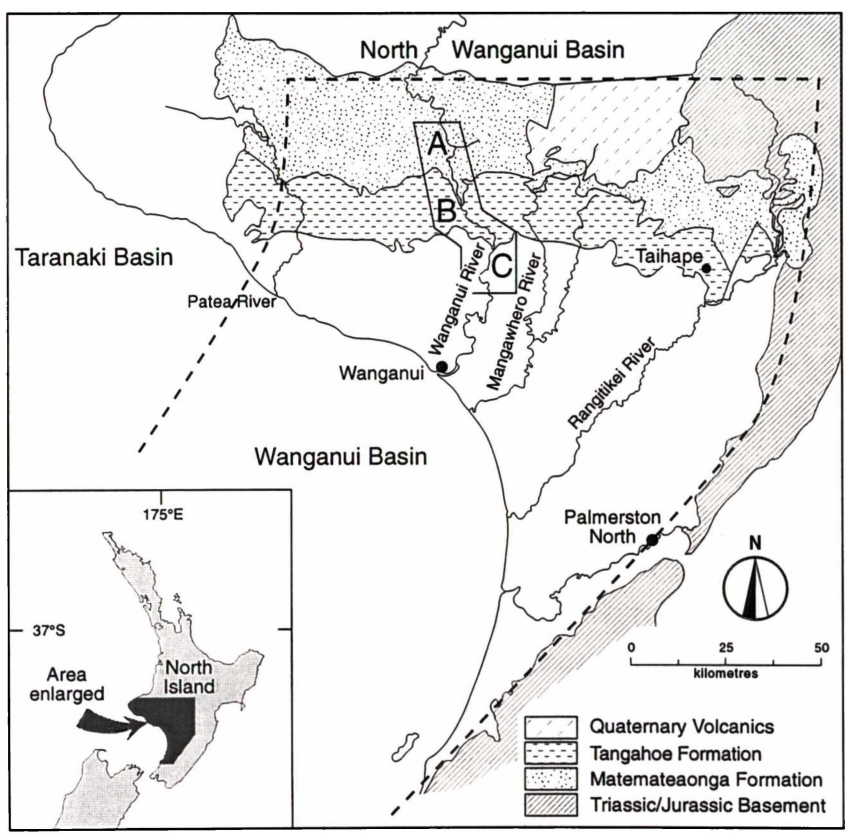

Figure 3:1. Distribution of the Matemateaonga Formation and other units across the northern part of Wanganui Basin (after Hay, 1967; Katz and Leask, 1989; Murphy *et al.*, 1994). A = Chapter 3; B = Chapter 4; and C = Chapter 5.

Given the regional east-west trending stratal belts (Figure 3:1) that dip to the south (Anderton, 1981), the north-south trending Wanganui River offers the best continuous exposure through the Matemateaonga Formation.

Between Tieke and Jerusalem (Figure 3:2) an approximately 1570 m thick south to southeast-ward dipping late Miocene (lower Kapitean) to early Pliocene (mid Opoitian) terrigenous-dominated marine succession is well exposed within the Wanganui River valley. Composite stratigraphic columns, tied to appropriate map sections and showing sample locations, are included as a supplement at the end of Chapter 2.

The emphasis of this chapter is on the presentation of a formal lithostratigraphy for the succession between Tieke and Jerusalem, along with a description of the lithofacies it contains and interpretation of depositional paleoenvironments represented, and a comparison of the sequence stratigraphic architecture of the cyclothemic sandstones with the Naish and Kamp (1997) model for sixth-order Plio-Pleistocene cyclothems in the Rangitikei River, Wanganui Basin, New Zealand.

3:2 STRUCTURE OF THE MATEMATEAONGA FORMATION IN THE WANGANUI RIVER VALLEY

The late Miocene (lower Kapitean) and early Pliocene (mid Opoitian) sedimentary succession, exposed in the study area between Tieke and Jerusalem (Figure 3:2), forms an east-west to southeast-northwest striking monocline which dips to the south-southeast. Structural information obtained in this study is shown on Maps 1-6 (Chapter 2) as dip and strike and fault occurrences. The beds dip at 2° to 8° S with 3 to 4° S being typical values. Strike data were usually obtained by measuring the attitude of shellbeds where they intersected the river level.

Faults, usually of normal type and down-thrown to the south, are occasionally observed within this section, with throws from a few metres to a few tens of metres (Maps 1-6). Strike directions for the fault planes are only approximate, as they are commonly occupied by small streams. Most of the faults are identified by the displacement of shellbeds. Hence the lithological variability of the Matemateaonga Formation assisted in the identification of fault offsets. An important point is that, apart from tilting, the Matemateaonga Formation is very weakly deformed, enabling an almost continuous stratigraphic column to be compiled from mainly river bank exposures.

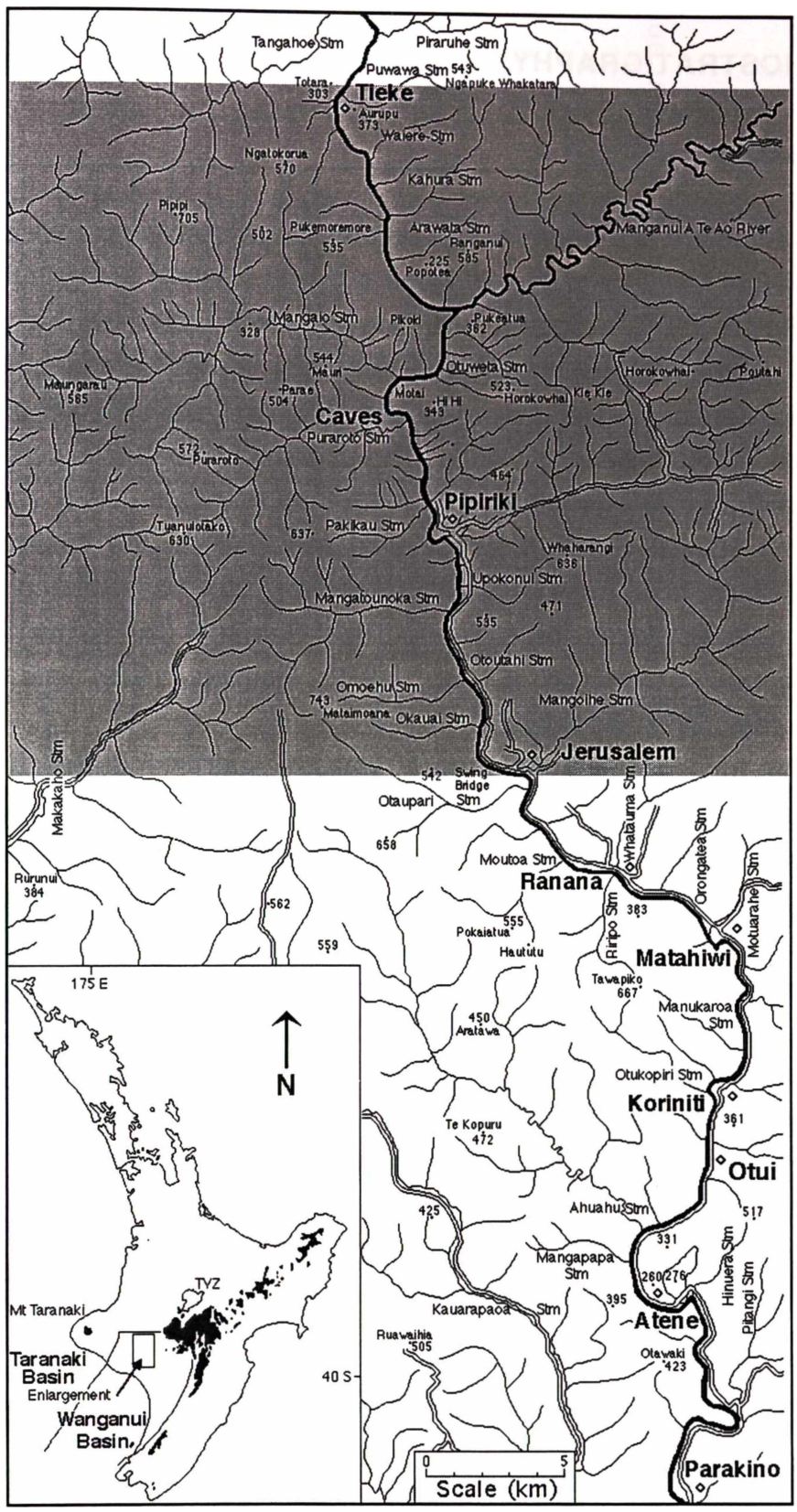

Figure 3:2. Locality map for the Wanganui River valley considered in this study. The grey tone approximates the section of river under study in this Chapter. Spot heights in metres. *Inset*: location of the study area within Wanganui Basin. Topography over 1000 m is shown in black. TVZ = Taupo Volcanic Zone.

3:3 LITHOSTRATIGRAPHY

3:3:1 HISTORY

A summary of the formational nomenclature used by previous workers to describe late Miocene to late Pliocene strata in western Wanganui Basin is given in Figure 3:3. The Superior Oil Company N.Z. Ltd report (Feldmeyer *et al.*, 1943) is the earliest significant reference to the stratigraphy of the Wanganui River valley. The lowermost unit of interest, discussed in that report, was named the Reef-Bearing Sands. The uppermost "reef" (No. 1 Reef of the Reef-Bearing Sands) was mapped by them from Wanganui River eastward to the Ruahine Range. Subsequent studies, especially in the eastern part of Wanganui Basin, have used a variety of names for the Reef-Bearing Sands. It has been referred to as the Waiouru (Reef-Bearing) Sandstone (Fleming, 1959), Waiouru Sandstone (Collen, 1972; Fleming, 1978) and Waiouru Formation (Ker, 1991; Beu, 1995).

The name Matemateaonga Formation was introduced by Arnold (1957) to describe the late Miocene and early Pliocene rocks cropping out in southern and central Taranaki Peninsula. Subsequently this unit has been recognised as being continuous with the Reef-Bearing Sands of Feldmeyer *et al.* (1943), which lead Hay (1967) to produce Sheet 7 of the 1:250,000 geological map series of New Zealand showing the Matemateaonga Sandstone as being continuous across the Taranaki and Wanganui Basins. Recent workers have persisted with the name Matemateaonga Formation rather than Matemateaonga Sandstone (e.g. Katz and Leask, 1989; Morris, 1994; Murphy *et al.*, 1994; Thompson *et al.*, 1994; King and Thrasher, 1996), and have continued to recognise the Waiouru Formation as an eastern correlative of the Matemateaonga Formation. Formational status for the Matemateaonga was formalised by Morris (1994), who nominated a stratotype location in central Taranaki.

3:3:2 REFERENCE SECTION

In central Taranaki, Morris (1994) designated the type section of the Matemateaonga Formation as the stratigraphic interval between the upper and lower contacts of the Matemateaonga Formation in the Tangahoe River section (top Q21 383882: base Q21 385933) and Pohokura Saddle section (top R19 511243: base R19 508238), respectively. Arnold (1957) did not

Age	Feldmeyer *et al.* (1943)	Fleming (1953)	Collen (1972)		Ker (1973)	Wilson (1993)		This Study
Wm	Mangaweka Formation	Mangaweka Mst		Pitangi Mst	Mangaweka Formation	Paparangi Group	Otawake Zst	Mangaweka Mudstone
	Atene Sands		Mangaweka Mst	Atene Sands	Atene Sst	Whenuakura Group	Atene Sst	Atene Formation
				Mangapapa Zst	Oxbow Zst		Oxbow Zst	Oxbow Siltstone Mbr
	Ahu Ahu Sands			Ahuahu Sands	Ahurangi Sst		Ahurangi Sst	Ahurangi Sandstone
Wp				Raumati Mst	Otui Zst		Otui Zst	Tangahoe Formation
	Koroniti Beds		Koroniti Sst		Koroniti Sst	Tangahoe Group	Koroniti Sst	Koroniti Sandstone Mbr
	Taihape Mst		Taihape Mst		?unnamed Zst		Raupirau Zst	
	Matahiwi Sands						Matahiwi Sst	Matahiwi Sandstone Mbr
							Ranana Mst	
uWo	Jerusalem Sands					Matemateaonga Group	Jerusalem Sst	Jerusalem Sandstone Mbr
lWo	Reef-Bearing Sands						Otuitahi Sst	Matemateaonga Formation
	Pipiriki Sands						Mangataunoka Zst	
uTk							Kahanui Mst	Various divisions
lTk							Popotea Sst	defined (see Chapter 3)
							Kabura Zst	
							Ramanui Sst	

NB: The upper Kapitean (uTk) - lower Opoitian (lWo) boundary approximates the Miocene-Pliocene boundary.

Figure 3:3. Historical lithostratigraphic nomenclature for the latest Miocene and Pliocene strata of the Wanganui River section and that proposed in this study. Dashed lines indicate approximate lowermost extent of study.

define a specific type section for the Matemateaonga Formation, but defined the Matemateaonga Ranges as the type area. A reference section (no column provided) for the Matemateaonga Formation was given by Ker (1991) in eastern Wanganui Basin.

Given the substantial difference in thickness and variability in character of the Matemateaonga Formation in western and eastern parts of the Wanganui Basin (e.g. this study cf. Murrell (1998) and Oulton (1998) respectively), it is necessary to define a reference section within western Wanganui Basin. I propose that the stratigraphic interval between the upper (R21 847839) and lower boundaries (not identified in this study) of the Matemateaonga Formation as exposed within the Wanganui River valley be a reference section for this formation.

3:3:3 Lower and Upper Boundaries

The Matemateaonga Formation is generally regarded as the lowermost unit within Wanganui Basin (e.g. Anderton, 1981; Thrasher, 1993; Murphy *et al.*, 1994; Thompson *et al.*, 1994). However, this assumption is based on offshore seismic and a few exploration wells drilled on basement highs, all of which are in the southern part of Wanganui Basin. Thus in the northern part of the basin the oldest rocks at depth are unknown, but probably include at least lateral equivalents of the Urenui Siltstone that Hay (1967) mapped as being in conformable contact with the base of the Matemateaonga Formation. This present study extends as far north as Tieke (R20 816057), but the lower boundary of the Matemateaonga Formation occurs north of this locality.

Feldmeyer *et al.* (1943) defined the upper boundary of the Matemateaonga Formation as occurring at the top of the uppermost shellbed (No. 1 reef of Feldmeyer *et al.* (1943)) which was traced by Feldmeyer *et al.* (1943) across the Wanganui Basin. Boundaries as drawn in that report coincide with the location of the uppermost shellbed as identified in this study. However, the nature of the sediments between the shellbed and the siltstones that characterise the overlying Tangahoe Formation may vary considerably, even over short distances (Figure 3:4). In this study the upper boundary is placed at the base of a 1 m thick glauconitic siltstone (Map 6; Figure 3:4) which corresponds to the base of the Tangahoe Formation. This glauconitic siltstone marks an abrupt change from sandstone to siltstone above the uppermost Matemateaonga Formation shellbed. While it is recognised that the glauconitic horizon is not an obvious unit in outcrop, it has been found in the Mangawhero River valley some 20 km east of Wanganui River valley

(Dickinson, 1998), so it is a widely distributed feature which, taken together with the underlying sandstone and shellbed, can be mapped regionally.

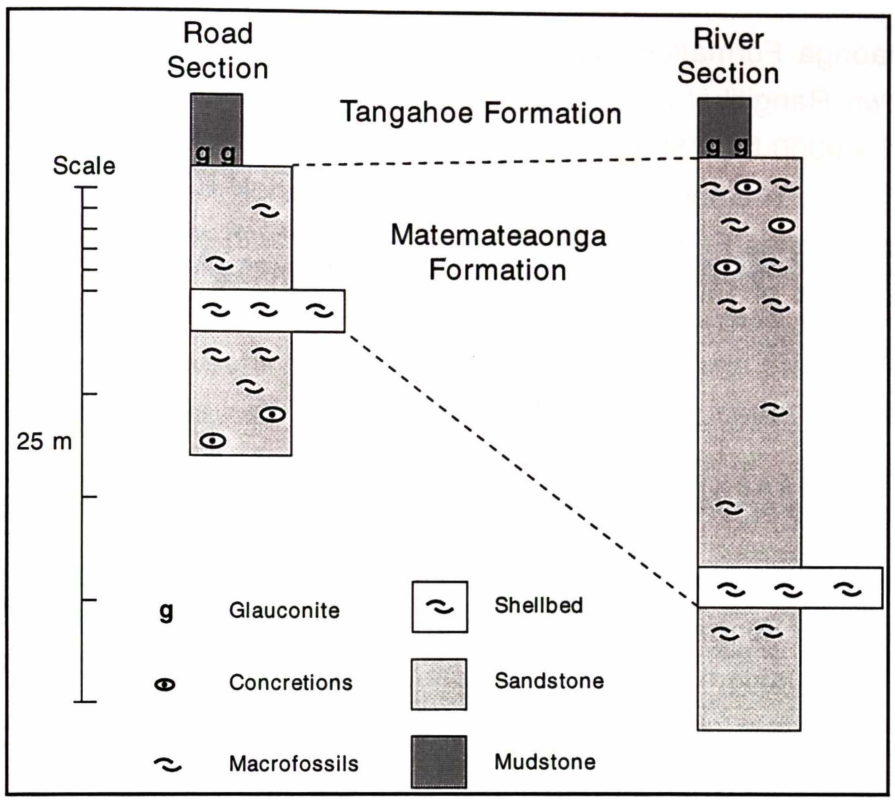

Figure 3:4. Correlation of the uppermost shellbed of the Matemateaonga Formation and the glauconitic siltstone at the base of the Tangahoe Formation at the road (R21 847839) and river (R21 876815) locations.

The upper boundary of the Matemateaonga Formation is well exposed at road level, just south of the bridge over the unnamed stream at R21 847839, (Map 6; in 1996-98 the bridge over the stream carried a label: Otoutahi Stream; however, no name is used on either the NZMS 260 or 270 series maps). The Matemateaonga/Tangahoe boundary is also accessible, but poorly exposed, at river level along the western bank of the Wanganui River, with the glauconitic siltstone dipping below water level about 200 m south of the Churton Farm swing bridge (R21 876815), some 1.5 km north of Jerusalem village.

3:3:4 THICKNESS

The total thickness of Matemateaonga Formation in the Wanganui River section has not been determined because the lower boundary does not occur within the confines of the study area. However, between Tieke and the upper boundary there is 1570 m of succession (Figure 3:5). Feldmeyer *et al.*

(1943) also had problems defining the base of the Matemateaonga Formation, with his 8150 ft thick TW4 section described as definitely being of the Reef-Bearing Sands. Subsequent reports involving thickness of the Matemateaonga Formation within the Wanganui Basin have either used the better known Rangitikei section (e.g. Thrasher, 1993; Murphy *et al.*, 1994) or have used a 9000 ft (2750 m) approximation based on Feldmeyer *et al.* (1943) (e.g. Hay, 1967; Thompson *et al.*, 1994). In the Taranaki Basin the thickness of the Matemateaonga Formation is well defined from both outcrop and well data with thicknesses of 1500 m (Morris, 1994) and 1400 m (King and Thrasher, 1996) respectively.

3:3:5 STRATIGRAPHY

For the first time, this study presents a detailed lithostratigraphy for the Matemateaonga Formation as exposed in the Wanganui River valley between Tieke and Jerusalem. Figure 3:5 summarises the exposed stratigraphy. However, the scale of this section is such that to accurately illustrate and record the detailed lithostratigraphy it has been necessary to subdivide the stratigraphic column into six map sections. Each of the six maps illustrates a detailed stratigraphic column, with pertinent sample information, tied to the appropriate map section (Maps 1-6).

A notable feature of the stratigraphic section derived from the Matemateaonga Formation in the Wanganui River valley is the cyclical repetition of the major lithologic facies, namely siltstones, sandstones and shellbeds. Such regularly repeated facies are known as sedimentary cycles or cyclothems (Clifton *et al.*, 1988) which in recent years have been increasingly linked to facies development during changes in sea-level associated with glacio-eustatic fluctuations, although cyclicity controlled by tectonics and sediment supply are also recognised (Dodd and Stanton, 1991). Certainly cyclothems have been widely identified in the Plio-Pleistocene sediments elsewhere in Wanganui Basin (Fleming, 1953; Kamp and Turner, 1990; Abbott and Carter, 1994; Naish and Kamp, 1995; Journeaux *et al.* 1996; McIntyre and Kamp, 1998).

The 31 cyclothems identified in this study (Figure 3:5, Maps 1-6) are described individually within Supplement 1 at the end of the Chapter. The information contained in this Supplement includes the vertical distribution of facies and the extent of members. The subdivision into cyclothems forms the basis for subsequent paleoenvironmental and sequence stratigraphic analysis. To assist in the identification of individual lithological units in later

discussions, each cyclothem has been subdivided into a number of members. Given the large number of units that can be usefully defined within the Matemateaonga Formation, the alpha-numeric system of Naish and Kamp (1995) has been adopted.

3:3:6 Facies Characteristics

Within the Matemateaonga Formation, 13 lithofacies have been identified and have been grouped into three major lithotypes using standard facies parameters and are named siltstone, sandstone and shellbed after the prominent lithology as noted in the field. The diagnostic characteristics of the lithofacies are described according to their (a) physical description, (b) paleontological content (full listings in Appendix 2: Forams), and (c) an interpretation of depositional environments (all three are summarised in Table 3:1). Analysis of the depositional paleoenvironment for all census samples from the Matemateaonga Formation is shown in Supplement 2 (summarised in Table 3:2) and is based on the identification of key ecologically restricted taxa (Figure 3:6) rather than by statistical analysis as discussed in Appendix 1. In terms of physical features, the interpretation of these is constrained by the occurrence of these lithofacies in a shallow-marine succession.

3:3:6:1 Siliciclastic siltstone lithotype

FACIES Z2 - (a) Weakly lithified, blue-grey, massive, bioturbated, micaceous (<1%), fine sandy siltstone. Barren to sparsely fossiliferous and rarely concretionary.

(b) *Anomalinoides parvumbilius*, *A. sphericus*, *Astrononion parki*, *Cassidulina neocarinata*, *Evolvocassidulina orientalis*, *Lenticulina* spp., *Sphaeroidina bulloides,* and *Uvigerina miozea* group being the benthic foraminifera species typically encountered.

(c) Microfaunal analyses indicate a predominantly outer-shelf (100-200 m) to possibly mid-shelf (50-100 m) depositional environment.

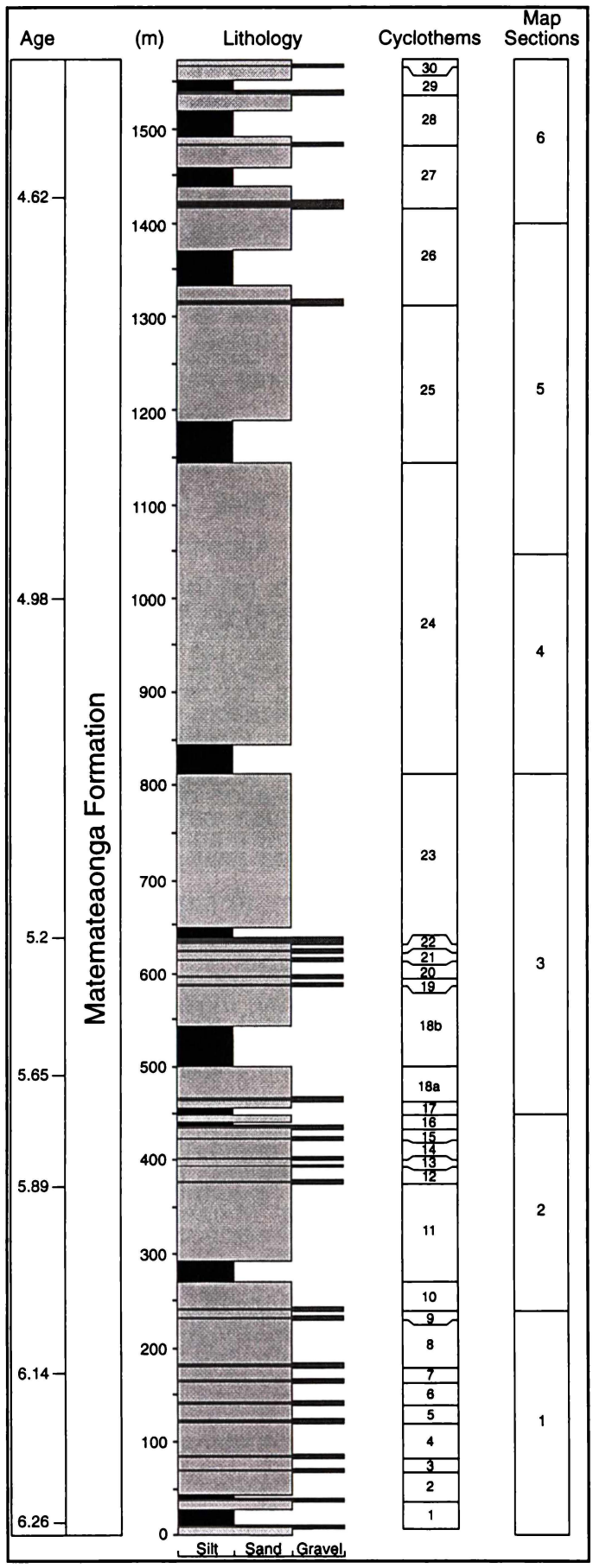
Age
(m)
Lithology
Cyclothems
Map Sections
Matemateaonga Formation
4.62
4.98
5.2
5.65
5.89
6.14
6.26
1500
1400
1300
1200
1100
1000
900
800
700
600
500
400
300
200
100
0
30
29
28
27
26
25
24
23
22
21
20
19
18b
18a
17
16
15
14
13
12
11
10
9
8
7
6
5
4
3
2
1
6
5
4
3
2
1
Silt
Sand
Gravel

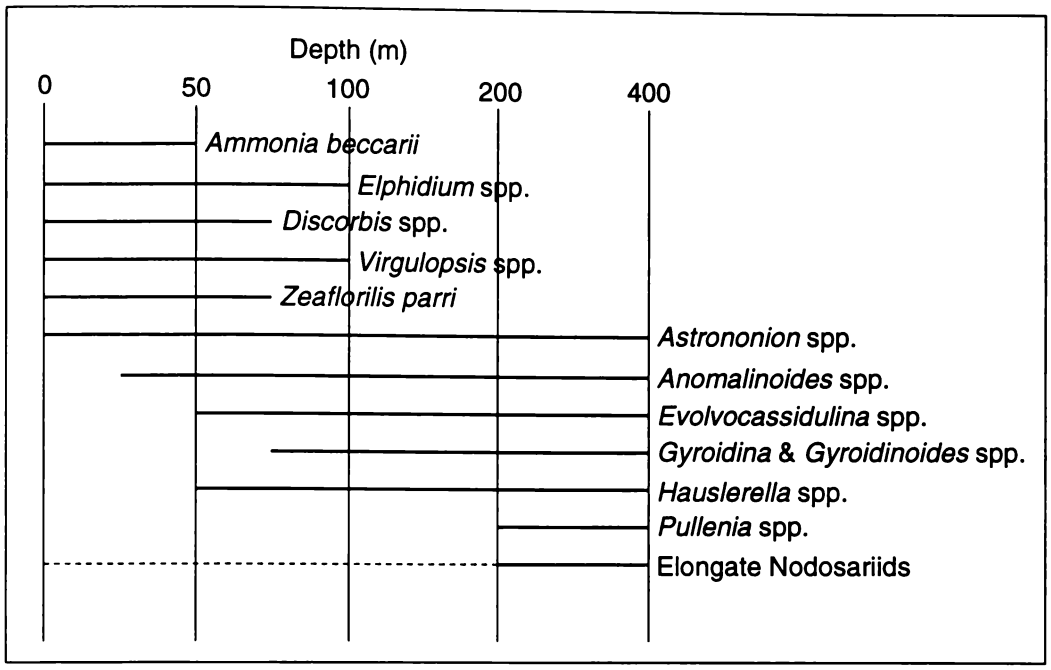

Figure 3:6. Depth range of some key benthic foraminifera used in the interpretation of paleoenvironments (after Hayward, 1986; Hornibrook *et al.*, 1989; Crundwell *et al.*, 1994; and Hayward *et al.*, 1997).

FACIES Z3 - (a) Weakly lithified, wavy to horizontally laminated / thinly bedded (mm/cm), micaceous (<1%), fine sandy siltstone with few burrows. Very fine sands forming mm thick laminations, which may show occasional shallow (<10 cm) troughs. Barren to sparsely fossiliferous and variably concretionary.

(b) *Cassidulina neocarinata*, *Elphidium charlottense*[1], *Evolvocassidulina orientalis* and *Nonionella flemingi* being the common benthic foraminifera.

(c) Microfaunal analysis indicates a predominantly mid-shelf (50-100 m; Table 3:2) depositional environment.

Figure 3:5 (opposite page). Composite stratigraphic column for the Matemateaonga Formation within the Wanganui River section showing the stratigraphic distribution of cyclothems and relevant maps. Details on thickness and lithologies of individual cyclothems are presented in Supplement 1 to this chapter, while the maps appear at the end of Chapter 2. The chronology on Figure 3:5 is derived from information presented in Chapter 2.

[1] Commonly called *E. charlottensis*

3:3:6:2 Siliciclastic sandstone lithotype

FACIES S1 - (a) Loose to weakly lithified, barren to sparsely fossiliferous, variably concretionary, massive, bioturbated, micaceous (1-5%), silty fine sandstone.

(b) Benthic foraminifera *Astrononion parki*, *Evolvocassidulina orientalis* and *Notorotalia* spp. commonly observed.

(c) Microfaunal analysis of one sample indicates an outer-shelf (100-200 m) depositional environment.

FACIES S2 - (a) Soft, barren to sparsely fossiliferous, moderately to well sorted, massive, variably concretionary, bioturbated, micaceous (1-5%), fine to medium sandstone.

FACIES S3 - (a) Loose to weakly lithified, barren to sparsely fossiliferous, wavy to horizontally laminated, variably concretionary, micaceous (1-5%), fine silty sandstone.

(b) *Astrononion parki*, *Cassidulina neocarinata*, *Elphidium charlottense, Evolovocassidulina orientalis*, *Notorotalia depressa* group and *Virgulopsis pustulata* being the commonly encountered benthic foraminifera.

(c) Microfaunal analyses indicate a mid to outer-shelf (50-200 m) depositional environment.

FACIES S4 - (a) Soft, barren to sparsely fossiliferous, wavy to horizontally thinly bedded, variably concretionary, micaceous (1-5%), fine sandstone.

(c) Such thinly bedded fine sandstones have been regarded as deposited in a mid- to outer-shelf environment (e.g. Driese *et al.*, 1991).

FACIES S5 - (a) Soft, barren to sparsely fossiliferous, trough cross-bedded, variably concretionary, micaceous (1-5%), medium to fine sandstone.

(c) Trough cross-bedding has been regarded as representative of a subtidal shore-face environment (e.g. Driese *et al.*, 1991; Naish and Kamp, 1997).

FACIES S6 - (a) Soft, barren to sparsely fossiliferous, low-angle tabular cross-bedded, variably concretionary, micaceous (1-5%), medium to fine sandstone.

(c) A subtidal shore-face depositional environment is the typically defined paleoenvironment for low-angle tabular cross-bedding (e.g. Driese *et al.*, 1991; Naish and Kamp, 1997).

FACIES S7 - (a) Loose to weakly lithified, slumped, variably concretionary, micaceous, silty fine sandstone to fine sandstone. Where laminations or thin bedding are preserved, they show that post-depositional movement has occurred as the laminations / thin beds are wavy, overturned and contourted (Plate 3:1?). No water escape structures are observed in the overlying parallel laminated / thinly bedded sediments. Thus movement appears to have occurred at or near the sediment / water interface.

(b) The benthic foraminifera *Astrononion parki*, *Cassidulina neocarinata*, *Elphidium charlottense*, *E. simplex aoteanum*, elongate Nodosariids, *Evolovocassidulina orientalis, Notorotalia* spp. and *Virgulopsis* spp. are observed.

(c) Microfaunal analyses are interpreted as representing an initial deposition on the mid-shelf (50-100 m), with slumping carrying the mid-shelf material to an outer-shelf environment. The apparent mix of mid (initial) and outer (final) shelf depositional environments, suggest earthquake activity may well have been the trigger mechanism rather than oversteepening on a shelf edge.

3:3:6:3 Shellbed lithotype

FACIES Cs1 - (a). Closely packed shells, initially bivalve-dominated, but grading to a variable mixture of pectens, oysters and other bivalves within massive densely cemented sandstone. The ratio of bioclastic components to terrigenous-dominated matrix varies up through these shellbeds. Typically the matrix dominates the upper and lower parts of the shellbed, while bioclastic components make up the bulk of the central section. The shells are commonly disarticulated and variably abraded and bored.

(b) Including *Maorimactra* sp., *Phialopecten marwicki* and *Crassostrea ingens*..

(c) The taxa indicate a high energy shore-face to inner-shelf depositional paleoenvironment (Beu and Maxwell, 1990; Gillespie and Nelson, 1996).

FACIES Cs2 - (a) Closely packed shells, predominantly bivalves other than pectens and oysters within densely cemented sandstone. Typically terrigenous-dominated matrix forms the bulk of the upper and lower parts of the shellbed, with bioclastic components dominating the central section. The shells are generally disarticulated and variably abraded and bored.

(b) Predominantly *Maorimactra* sp..

(c) The taxa indicate a high energy shore-face to inner-shelf depositional paleoenvironment (Beu and Maxwell, 1990; Gillespie and Nelson, 1996).

Table 3:1. Summary of sedimentary facies in late Miocene - early Pliocene Matemateaonga Formation cyclothems.

Code	Description	Depositional environment	Example (Cyclothem & Mbr)
Siliciclastic siltstone lithotype			
Z2	Massive fine sandy siltstone	Mid- to outer-shelf	Cyclothem 1 Mtzm1 (lower 10 m)
Z3	Laminated fine sandy siltstone	Mid-shelf	Cyclothem 18 Mtzm8
Siliciclastic sandstone lithotype			
S1	Massive, micaceous, silty fine sandstone	Mid- to outer-shelf	Cyclothem 10 Mtsm18 (lower 10 m)
S2	Massive, micaceous, medium to fine sandstone	Inner- to mid-shelf	Cyclothem 4 Mtsm5 (upper 20 m)
S3	Laminated, micaceous, silty fine sandstone	Mid- to outer-shelf	Cyclothem 24 Mtsm36
S4	Thinly bedded, micaceous, fine sandstone	Mid- to outer-shelf	Cyclothem 5 Mtsm7 (upper 5 m)
S5	Trough-cross bedded fine sandstone	Subtidal shore-face	Cyclothem 18a Mtsm28 (upper 15 m)
S6	Low angle, tabular, cross-bedded fine sandstone	Subtidal shore-face	Cyclothem 19 Mtsm30 (upper 2 m)
S7	Slumped silty fine sandstone to fine sandstone	Initially mid-shelf	Cyclothem 23 Mtsm35 (lower 50 m)
Shellbed lithotype			
Cs1	Variable abundance of oysters, pectens and other bivalves in a densely cemented sandstone matrix (matrix to shell to matrix dominated)	Shore-face to inner-shelf	Cyclothem 29 Mtcm34
Cs2	Predominantly bivalves other than pectens and oysters in a densely cemented sandstone matrix (matrix to shell to matrix dominated)	Shore-face to inner-shelf	Cyclothem 27 Mtcm31
Cs3	Variable abundance of bivalves, including pectens and oysters in a densely cemented sandstone matrix (shell dominated)	Inner-shelf	Cyclothem 27 Mtcm32
Cs4	Bands, clumps and scattered shells in a fine silty sandstone matrix (matrix dominated)	Inner to mid-shelf	Cyclothem 8 Mtcm12

FACIES Cs3 - (a) Closely packed shells, consisting of a variable mixture of bivalves, including pectens and oysters within densely cemented bioturbated sandstone (shell dominated). The oysters are typically articulated although other shells are disarticulated. There is minimal if any abrasian or boring.

(b) Including *Maorimactra* sp., *Phialopecten marwicki* and *Crassostrea ingens*.

(c) The taxa indicate a high energy inner-shelf depositional paleoenvironment (Beu and Maxwell, 1990; Gillespie and Nelson, 1996).

FACIES Cs4 - (a) Bands, clumps and scattered shells that are commonly broken within massive fine silty sandstone to sandstone, matrix dominated and variably concretionary.

(c) The rarity of taxa and more delicate nature of the shells suggests a lower energy inner- to mid-shelf depositional paleoenvironment (Beu and Maxwell, 1990; Gillespie and Nelson, 1996).

Table 3:2. Paleobathymetric interpretation using the benthic foraminifera from Matemateaonga Formation census samples. Summary of interpretations made in Chapter Supplement 2. Raw data presented in the Appendix 2: Forams.

Sample No. W962-	Stratigraphic Height (m)	Cyclothem: Member: Facies	Inferred Water Depth (m)
002	8	1: Mtzm1: Z2	100-200
023	198	8: Mtzm4: Z2	100-200
028	285	11: Mtzm5: Z2	100-200
041	464	18a: Mtsm28: S1	100-200
062	681	23: Mtsm35: S7	50-200
066	828	24: Mtzm10: Z3	100-200
081A	919	24: Mtsm36: S3	50-100
088	1024	24: Mtsm36: S3	100-200
106	1148	25: Mtzm11: Z2	50-100
108	1161	25: Mtzm11: Z3	50-100
109	1166	25: Mtzm11: Z3	50-100
111	1176	25: Mtzm11: Z3	50-100
139	1341	26: Mtzm12: Z3	50-100
166	1459	27: Mtsm41: S3	50-100
177	1511	28: Mtzm13: Z2	50-100
180	1524	28: Mtzm13: Z2	50-100
186	1540	29: Mtzm14: Z3	50-100
198	1571	30: Mtsm45: S1	100-200

3:3:7 Facies Associations and Cyclothems

Within the Matemateaonga Formation, lithofacies show a repetitive, cyclic distribution (Maps 1-6), with individual cycles equivalent to the cyclothems depicted in the Supplement at the end of this Chapter. While the Matemateaonga Formation as a whole shows considerable repetition in

lithofacies, the internal architecture of individual cyclothems shows a common progressive change in lithofacies. Typically cyclothems have one or two well cemented shellbeds (carbonate members) at their base. In cases where two shellbeds occur, they are separated by a massive fine to medium sandstone (e.g. cyclothems 5, 9 and 22). Above the shellbeds, the cyclothems fall into three basic patterns: (1) siltstone or silty fine sandstone sitting upon the uppermost shellbed (e.g. cyclothems 1, 4 and 10); (2) a sandstone of variable thickness lies between the uppermost shellbed and the overlying siltstone/silty fine sandstone (e.g. cyclothems 5, 8 and 16); or rarely (3) only sandstone exists between the uppermost shellbed and the overlying cyclothem (cyclothems 13, 14 and 15). These features are illustrated in an idealised model shown in Figure 3:7 and discussed further in Section 3:4.

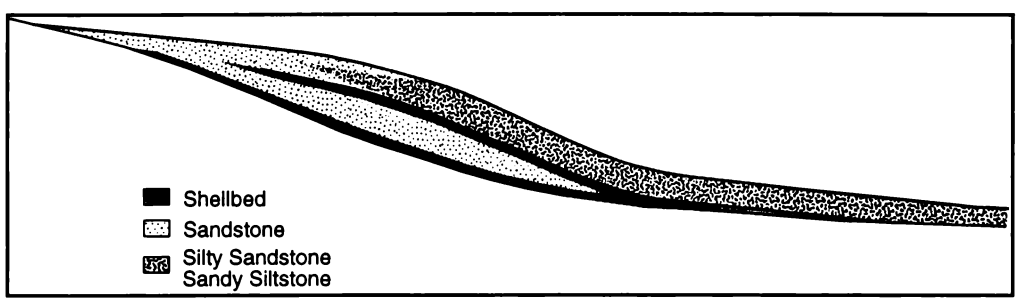

Figure 3:7. Idealised model showing the stratal architecture of the Matemateaonga Formation cyclothems, with individual cyclothems as observed in the field representing various points along the cross-section.

With the exception of cyclothems 13, 14 and 15 a coarsening upwards trend in lithofacies is observed from the first siltstone/silty fine sandstone lithofacies occurrence. Commonly this coarsening upward trend ends in a fine or medium sandstone, which occasionally has bedding structure (e.g. cyclothem 19).

3:3:8 PALEOENVIRONMENTAL SYNTHESIS

Paleoenvironmental interpretation of sedimentary successions is commonly undertaken on the basis of two sets of features: (1) physical - grainsize and bedding structures; and (2) faunal - both macro- and microfauna. In this study both lines of evidence have already been used to determine depositional environments for most of the lithofacies (Section 3:3:6). In this section, the aim is to consider the trends in depositional environment representative of the Matemateaonga Formation cyclothems.

The shellbeds that typically form the basal lithofacies of the cyclothem are extremely difficult to work with because of their well cemented nature. In general, however, they contain varying abundances of bivalves, oysters and pectens, including *Maorimactra* sp., *Phialopecten marwicki, Crassostrea ingens, Chlamys gemmulata* and ?*Ruditapes* sp.. Using information from Beu and Maxwell (1990) and Gillespie and Nelson (1996), these taxa indicate the shellbeds typically formed in a shallow-water, nearshore to inner-shelf environment. The occasional occurrence of conglomerate (predominantly greywacke), clasts normally less than 5 cm in diameter although clasts up to 30 cm in diameter have been observed (cyclothem 23), supports a moderate to high energy, nearshore depositional environment. Large conglomerate, as in the case of cyclothem 23, may well be a transgressive lag deposit above an unconformity.

The finest grained lithofacies of each cyclothem sits upon (i.e. cyclothem 23), or just above (i.e. cyclothem 28), the basal carbonate member(s), or is the basal lithofacies where no carbonate member is present (i.e. cyclothem 17). The finest grained lithofacies in each cyclothem is typically a fine sandy siltstone (Z2 or Z3) or silty fine sandstone (S1 or S3). Analysis of the benthic foraminifera within these lithofacies (Table 3:2) indicates that they represent mid- to outer-shelf (50-200 m) deposits. Cyclothems 14, 15 and 22 are exceptions to this generalisation, with only massive fine to medium sandstone occurring above their respective basal carbonate members. While this may be due to erosion of finer lithologies, as is the case for cyclothem 22, cyclothems 14 and 15 probably represent situations where water depths were never sufficiently deep to deposit finer-grained lithologies.

The coarsening upward trend in each cyclothem represents a progressive shallowing from a mid- or outer shelf environment. While the lack of bedding structures (e.g. cross-bedding) typically implies that the minimum water depths are below wave base, the well sorted nature of these sandstones means that bedding structures may not be particularly obvious. Given the paleoenvironmental interpretations of the confining fine-grained lithologies and the shellbeds, these sandstones probably represent paleoenvironments no deeper than inner-shelf. Microfaunal analyses were attempted on samples from the upper sandy lithologies, but they all proved to be barren (Appendix 2: Summary).

3:4 SEQUENCE STRATIGRAPHY

Sequence stratigraphy is the study of repetitive, genetically related strata, bounded by unconformities, or their correlative conformities, within a

chronostratigraphic framework, with the fundamental unit being the sequence (Figure 3:8; Van Wagoner *et al.*, 1988). Each depositional sequence is usually subdivided into systems tracts (Posamentier *et al.*, 1988), where each system tract is bounded by a physical surface (Figure 3:8) and is composed of discrete parasequence association patterns (Vail *et al.*, 1991). The fundamental concepts involved in sequence stratigraphy were developed from seismic-reflection studies of third-order passive-margin successions where systems tracts were delineated by the nature of reflector terminations (i.e. onlap, backlap, downlap and toplap). The relationship between sea-level changes and particular systems tracts is commonly inferred on the basis of the stratal geometry, which is characteristic of each systems tract. "*However, sequence stratigraphy must be viewed as a tool or approach rather than a template*" (Posamentier and James, 1993 pg. 3). Subsequently the sequence stratigraphic model has been applied in a wide variety of environments (e.g. Sarg, 1988; Postma *et al.*, 1993; Pasquier and Strasser, 1997), highlighting the variability of stratal architecture (Helland-Hansen and Gjelberg, 1994). This variability is a feature of local conditions (Posamentier *et al.*, 1988; Posamentier and Allen, 1993), with the effect of sediment supply being particularly highlighted (e.g. Schlager, 1993; Church and Gawthorpe, 1997; Rivenaes, 1997).

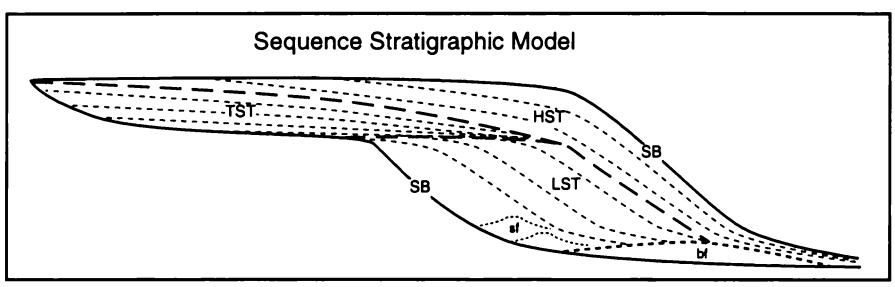

Figure 3:8. Sequence stratigraphic model showing sequence boundaries (SB) and systems tracts: LST - Lowstand systems tract (sf - slope fan, bf - basin floor fan); TST - Transgressive systems tract; HST - Highstand systems tract, and parasequence patterns (after Vail *et al.*, 1991).

Recently there has been a shift to consider younger, higher-order (6^{th}) cyclicity (e.g. Haywick *et al.*, 1992; Ito, 1992). This is highlighted by recent studies in the Wanganui Basin (e.g. Kamp and Turner, 1990; Carter *et al.*, 1991; Abbott and Carter, 1994; McIntyre and Kamp, 1998). Figure 3:9 compares various idealised sequence stratigraphic architectures used to describe cyclothems in the Wanganui Basin. While this comparison reveals that there are many similarities in general stacking patterns, the Naish and Kamp (1997) model recognises the Regressive Systems Tract (RST) that is not recognised in previous studies. As the general stratal pattern of the Naish

and Kamp (1997) model appears to best fit the general nature of the Matemateaonga Formation (Section 3:3:7), this is the model that will be used in the comparison against the outcrop patterns observed in the Matemateaonga Formation.

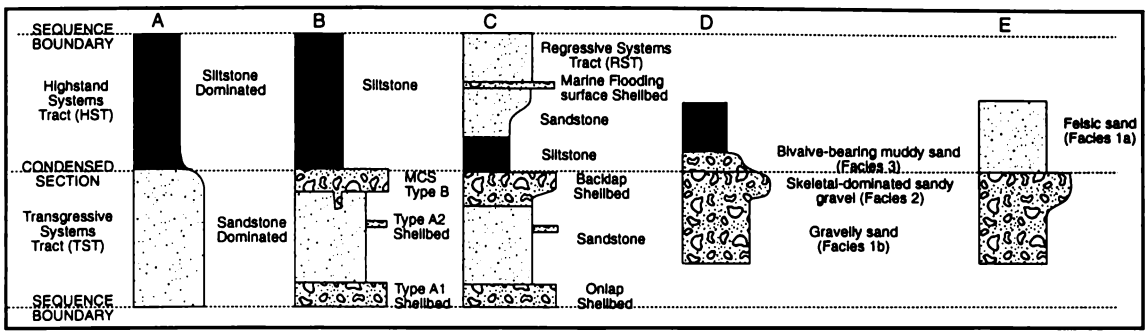

Figure 3:9. Schematic logs illustrating the idealised sequence stratigraphic architecture for: (A) Onshore coastal sections (Beu and Edwards, 1984); (B) Typical mid-Pleistocene Castecliff cyclothem (Abbott and Carter 1994); (C) Typical late Pliocene symmetrical Rangitikei cyclothem (Naish and Kamp 1997); (D) Modern mid to deep-water Wanganui shelf (Gillespie *et al.* in press); and (E) Modern shallow-water Wanganui shelf (Gillespie *et al.* in press).

Work by Naish and Kamp (1997) has resulted in the development of a two-dimensional sequence stratigraphic model for sixth-order late Pliocene-Pleistocene shelf cyclothems in the Wanganui Basin (Figure 3:10). In this model five fundamental architectural elements are defined: (1) a basal sequence boundary that is coincident with either the transgressive surface of erosion or its correlative conformity; (2) a transgressive systems tract composed of either a thick deepening upward mixed carbonate-siliciclastic succession or a thin condensed fossiliferous facies deposited on a sediment starved shelf; (3) a sharp downlap surface separating condensed fossiliferous facies of the transgressive systems tract from terrigenous siltstones of the superjacent highstand systems tract; (4) a highstand systems tract of aggradational shelf siltstone; and (5) a progradational regressive systems tract. In the Naish and Kamp (1997) model, the use of condensed deposits, especially shellbeds, as indicators of sequence architecture have been refined from earlier studies (e.g. Kidwell, 1991; Abbott and Carter, 1994). Four distinct shellbed accumulations were described: (1) associated with the transgressive surface of erosion; (2) at the top of the transgressive system tract; (3) at marine flooding surfaces; and (4) where the transgressive surface of erosion and transgressive system tract accumulations become superimposed. These shellbeds are referred to as the onlap, backlap, flooding surface and compound shellbeds, respectively.

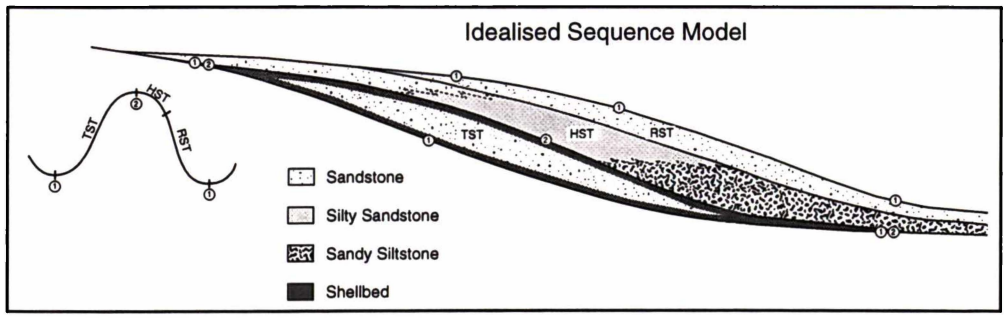

Figure 3:10. Idealised interpretation of the Naish and Kamp (1997) model of sixth-order shelf sequence showing the sequence boundaries and system tracts. TST - Transgressive systems tract; HST - Highstand systems tract; RST - Regressive systems tract.

3:4:1 COMPARISON WITH THE MATEMATEAONGA FORMATION CYCLOTHEMS

Each of the architectural elements as defined by Naish and Kamp (1997) are, in stratigraphic order, considered below in relation to the features displayed by the Matemateaonga Formation cyclothems. Detailed columns for all of the cyclothems observed in this study, showing their sequence stratigraphic interpretation, are presented in Supplement 1 to this Chapter.

3:4:1:1 Basal Sequence Boundary

The basal sequence boundary of the Matemateaonga Formation cyclothems is typically a planar surface across regressive systems tract sandstone of the underlying cyclothem. Each sequence boundary is inferred to coincide with the transgressive surface of erosion (ravinement surface) or its deep water correlative conformity (e.g. Nummendal and Swift, 1987; Walker and Wiseman, 1995). While in nine of the cyclothems an erosional boundary has been identified, the presence or absence of an erosional sequence boundary in the remaining cyclothems is difficult to define with confidence. Naish and Kamp (1997) tend towards defining, in the late Pliocene Rangitikei Group, all planar surfaces across sandstone as erosional surfaces.

Some of the basal boundary Matemateaonga Formation shellbeds show a gradational increase in shell material, rather than a sudden dominance characteristic of an erosional boundary. This raises the question as to whether or not all apparent planar surfaces at the base of the Matemateaonga Formation cyclothems are erosional. The cemented nature of the shellbeds further complicates this problem as (a) detailed examination of the boundary is commonly an examination of the basal limit of cementation, which may or may not be the same plane, and (b) the tabular nature of the

shellbeds is over-emphasised by the cementation fronts (i.e. the planar surfaces may be diagenetic in origin). It is probably such difficulties that lead Walker (1992, pg. 10) to comment "*that in the field, "evidence" for subaerial exposure may be inferred rather than real*". As there appears to be no way to definitively resolve the dilemma over the presence or absence of erosional basal boundaries, the illustrations in Supplement 1 of this chapter show erosional boundaries only where they have been clearly identified in the field. The basal boundaries of the other cyclothems are shown simply as a planar surface with no implication as to whether or not they are erosionally based and are referred to as "appearing to be conformable".

3:4:1:2 Transgressive Systems Tract

Three distinct transgressive system tract motifs are recognised, with three types of shellbed; namely onlap, backlap and compound shellbeds. The nature of the shellbeds is summarised in Table 3:3.

MOTIF 1: In this motif a compound shellbed is overtopped by silty lithologies (e.g. cyclothems 1, 6 and 23). This situation recognises a high rate of relative sea-level rise and/or low sediment supply, resulting in sediment starvation on the shelf until the silty lithologies of the highstand systems tract downlap onto the compound shellbed.

MOTIF 2: In this motif an onlap and backlap shellbed are separated by massive fine to medium sandstones. The massive nature of this sandstone interval means that evidence for parasequence stacking patterns within the wedge is not evident. However, "*parasequences within the transgressive-systems tract onlap onto the sequence boundary in a landward direction and downlap onto the transgressive systems tract in a basinward direction*" (Van Wagoner *et al.*, 1988, pg. 44). This situation recognises a low rate of relative sea-level rise and/or a moderate to high rate of terrigenous sediment supply. It results in a sediment-saturated transgressive systems tract, characterised by an onlap and backlap shellbed separated by massive fine to medium sandstone of the nearshore siliciclastic wedge. While the name nearshore siliciclastic wedge may imply a nearshore location, if sediment supply is greater than the accommodation space generated by the transgression, the parasequences of the nearshore siliciclastic wedge will prograde across the onlap shellbed and may well reach locations basinward of the contemporary wave-base.

In the Naish and Kamp (1997) model, the backlap shellbed is typically overtopped by downlapping silty lithologies of the highstand systems tract.

While this certainly occurs (e.g. cyclothems 7 and 9), there are situations where the backlap shellbed is overtopped by massive fine to medium sandstone before silty lithologies more representative of the highstand systems tract occur (e.g. cyclothems 5, 8 and 27). In this case it is assumed that the sandstones are derived from a short-lived regressive parasequence at the base of the highstand systems tract, with any associated transgression being to a point basinward of the original shoreline. As the physical boundary between the transgressive systems tract and the highstand systems tract is the maximum flooding surface (Vail *et al.*, 1991), the downlap surface (surface 2 in Figure 3:8) is defined as occurring at the top of the backlap shellbed.

MOTIF 3: In this motif the onlap shellbed is overtopped by massive fine to medium sandstones, which are in turn overlain by silty lithologies (e.g. cyclothems 2, 16 and 26). In this situation the backlap shellbed has not formed due to high sediment input. The maximum flooding surface, and therefore the downlap surface, are assumed to be at the contact of the sandstone and silty lithologies.

Another unusual situation in the Matemateaonga Formation is the presence of five cyclothems with no lithofacies characteristic of the transgressive systems tract (cyclothems 11, 17, 18b, 24 and 25). The absence of typical transgressive systems tract strata would tend to indicate an extremely rapid transgression and re-establishment of sedimentation so as to prevent its development. The driving force of such rapid fluctuations may be glacio-eustatic if a very high sediment flux exists. However, other possibilities such as tectonic movements have to be considered given the unusual stratal architecture and size of these cyclothems in comparison to the typical Matemateaonga Formation situation, discussion continued in Section 3:5.

3:4:1:3 Highstand and Regressive Systems Tracts

In the Matemateaonga Formation cyclothems, the start of the highstand is characterised by silty lithofacies (typically Z2 and Z3), which typically grade up into massive fine to medium sandstone. In the nearshore situation the start of the regressive systems tract will be characterised by strongly progradational shoreline facies, as described by Naish and Kamp (1997) for the Rangitikei River section. However, in more basinward locations, there may not be any lithological evidence on which to define the boundary between these two systems tracts. Given this variability in possible locations for the highstand/regressive system tract contact, and the lack of any clear way of consistently defining the boundary between these systems tracts, the cyclothems illustrated in Supplement 1 at the end of this Chapter show the

highstand and regressive systems tracts as a continuum rather than as distinct zones or contacts.

Table 3:3. Characteristics and sequence stratigraphic significance of shellbeds in the Matemateaonga Formation cyclothems.

Shellbed type	Lithofacies	Depositional environment	Sedimentary dynamics	Stratal relationship	Systems tract	Example
Onlap	Cs2	Inner-shelf to shore-face	Sediment starvation during onlap	Rests on TSE or correlative conformity	Base of TST	Cyclothem 27 Mtcm31
Backlap	Cs3	Inner-shelf to shore-face	Sediment starvation during onlap	Conformably overlies TST sandstone	Upper TST	Cyclothem 27 Mtcm32
Flooding surface	Cs4	Inner- to mid-shelf	Sediment starvation during minor flooding	Associated with minor flooding events	HST / RST	Cyclothem 8 Mtcm12
Compound	Cs1	Inner-shelf to shore-face	Sediment starvation	Rests on TSE or correlative conformity	TST	Cyclothem 29 Mtcm34

3:5 ORIGIN OF CYCLICITY

Progressive and ongoing subsidence within the Wanganui Basin during the deposition of the Matemateaonga Formation has been necessary to accommodate and preserve the thick (<1500 m) succession of cyclic sedimentary sequences observed within the Wanganui River valley. Despite such ongoing regional subsidence, rapid variability in relative sea-level has been necessary to develop the observed cyclicity. Extrapolation of compacted sediment accumulation rates (Figure 3:11) suggest that, with the exception of cyclothem 23, shellbed-based cyclothems are derived from a 40 ky cyclicity (multiply sedimentation rate by thickness). The most likely cause of such cyclicity is high-order glacio-eustatic fluctuations. Isotopic analysis of deep-sea cores (Shackleton *et al.* 1995) indicate that fluctuations of this magnitude have been occurring over the time period considered here (Figure 3:11). Cyclothems 11, 18b, 23, 24 and 25 differ significantly as they are substantially thicker than the aforementioned cyclothems and with the exception of cyclothem 23 have no distinctive lithofacies representative of a transgressive systems tract. Extrapolation of generalised sedimentation rates suggest that development of these cyclothems has occurred over periods of approximately

100 - 200 ky. These lower-order cyclothems may have been derived from glacio-eustatic fluctuations although it would be expected that if they did, they would occur (a) at some regular interval or (b) all together as a discrete period of time. An alternative is that they are related to the tectonic development of the basin. Phases of rapid tectonically driven subsidence would overshadow smaller scale glacio-eustatic fluctuations and result in randomly spaced cyclothems of varying duration depending upon the degree and duration of the subsidence. Such a mix of cycle types has been reported in other tectonically active basins (Dodd and Stanton, 1991).

No direct correlation between the isotope curve shown in Figure 3:9 and the cyclicity in the Matemateaonga Formation has been attempted as the age data available are insufficiently precise to reliably relate individual cyclothems to particular points on the isotope curve. The reversal stratigraphy for the isotope curve has been aligned with the Geomagnetic Polarity Time-scale developed in Berggren *et al.* (1995a, b).

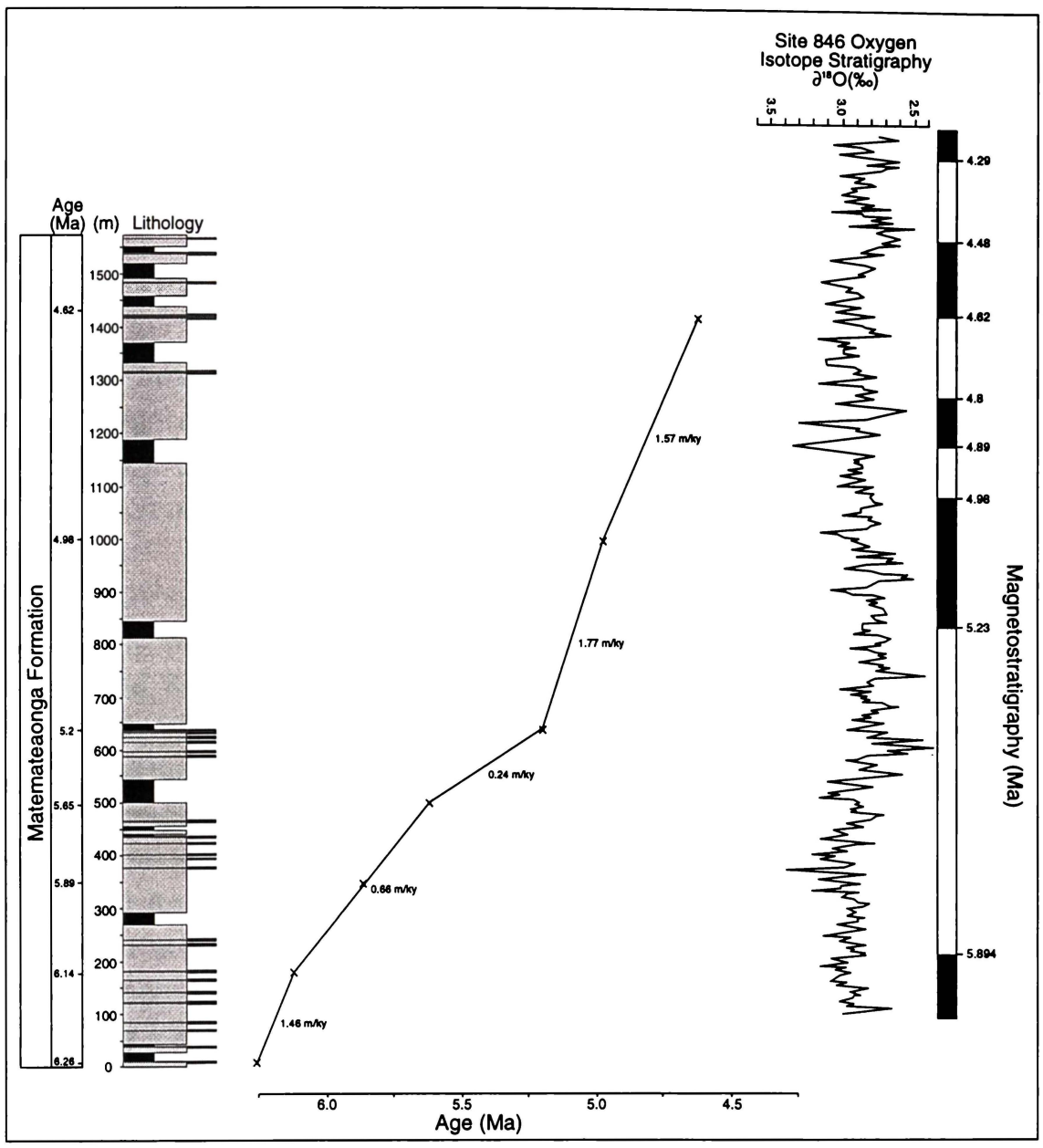

Figure 3:11. Generalised sediment accumulation rates for the late Miocene - early Pliocene Matemateaonga Formation in the Wanganui River valley. Ages used on the column are based on data in Chapter 2. The oxygen isotope record is derived from ODP site 846 (Shackleton *et al.*, 1995). The chronology of polarity reversals on the magnetostratigraphy beside the oxygen isotope record are based on the Geomagnetic Polarity Timescale of Berggren *et al.* (1995a, b).

CHAPTER 3: SUPPLEMENT 1

COLUMNS AND DESCRIPTIONS OF MATEMATEAONGA FORMATION CYCLOTHEMS

This chapter supplement provides detailed lithofacies descriptions for each of the 31 cyclothems identified within the Matemateaonga Formation between Tieke and Jerusalem. Each cyclothem is composed of lithological units assigned member status. The characteristics of the members define the detailed cyclothem architecture and provide the essential link between the lithostratigraphy and the sequence stratigraphy of the Matemateaonga Formation.

Given the large number of members that can be usefully defined within the Matemateaonga Formation, the alpha-numeric code system of Naish and Kamp (1995) has been adopted. The code consists of (1) an abbreviation for the Matemateaonga Formation (Mt), (2) an abbreviated lithological term (i.e. sm = sand member), and (3) a numerical value denoting the stratigraphic order of the member within the Matemateaonga Formation.

The patterns and other features shown on the graphical logs, illustrated for each cyclothem, are the same as those used in the Maps presented at the end of Chapter 2. Erosional boundaries have only been drawn where they have been positively identified on direct field evidence. Otherwise a planar surface is illustrated, with the boundary regarded as being conformable (i.e. appear to be conformable), although some other work (e.g. Naish and Kamp, 1997) would suggest that many of these planar boundaries are erosional (see Section 3:4:1:1). The facies codes used are as discussed in Section 3:3:6 and summarised in Table 3:1. The sequence stratigraphic interpretation relates to the Naish and Kamp (1997) model, with the sequence stratigraphic coding used equivalent to that shown in Figure 3:10, and reproduced over the page as Figure C3S1:1.

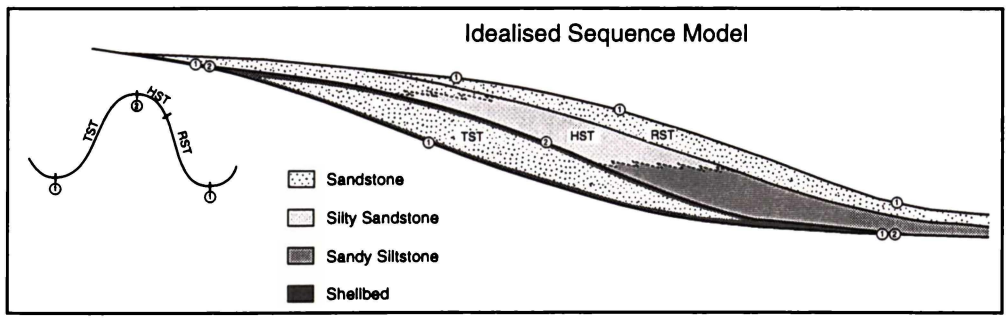

Figure C3S1:1. (reproduced Figure 3:10). Idealised interpretation of the Naish and Kamp (1997) model of sixth-order shelf sequence showing the sequence boundaries, system tracts and relative sea level curve. TST - Transgressive systems tract; HST - Highstand systems tract; RST - Regressive systems tract. (No scale implied)

CYCLOTHEM 1

Cyclothem 1 appears to be in conformable contact with the underlying sedimentary succession and has at it's base an approximately 20 cm-thick, cemented, shellbed (Mtcm1). Mtcm1 has a well cemented sandstone matrix and is over-lain by massive, fine sandy siltstone (Mtzm1). Mtzm1 grades into a massive medium to fine sandstone (Mtsm1) via a horizontally laminated, fine sandy siltstone. The mid-section of this cyclothem is poorly exposed.

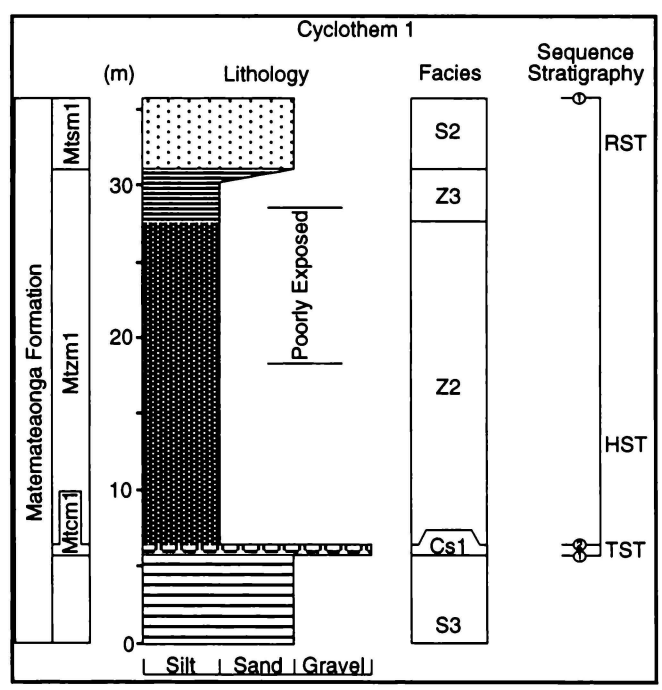

CYCLOTHEM 2

An approximately 20 cm-thick, shellbed (Mtcm2) appears to conformably overly Mtsm1. Mtcm2 is conformably over-lain by massive medium to fine sandstone (Mtsm2). The TST is placed at the top of Mtsm2, TST motif 3. Laminated, fine sandy siltstone of Mtzm2 is in sharp but conformable contact with Mtsm2. Mtzm2 grades up into the horizontally laminated silty fine sandstone that forms much of Mtsm3. In the top third of Mtsm3 there is a transition to a massive medium to fine sandstone.

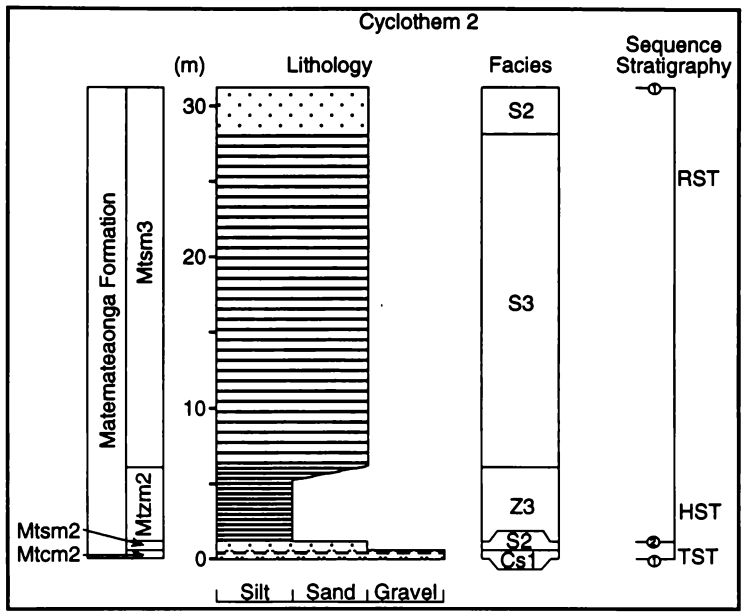

CYCLOTHEM 3

Cyclothem 2 appears to be conformably overlain by the approximately 50 cm-thick shellbed (Mtcm3) at the base of cyclothem 3. Mtcm3 grades rapidly into Mtsm4. The lower part of Mtsm4 consists of laminated silty fine sandstone before grading into thinly bedded fine sandstone about halfway through cyclothem 3.

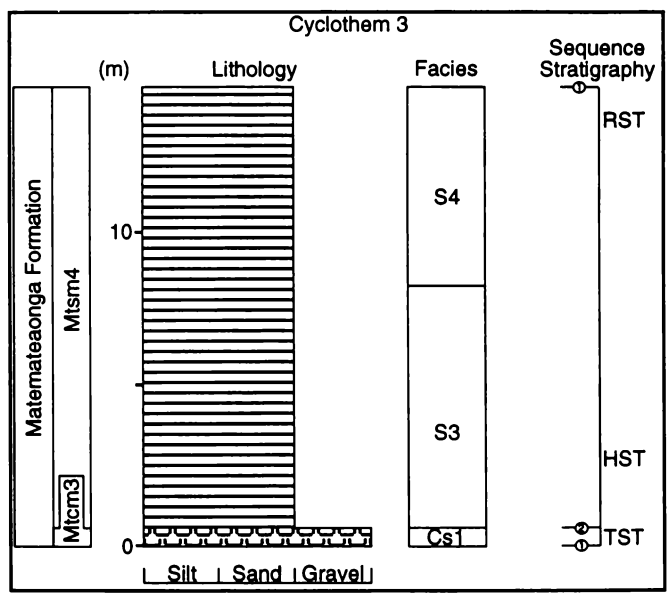

CYCLOTHEM 4

Cyclothem 4 appears to conformably overlie cyclothem 3 and has at its base a shellbed (Mtcm4). Mtcm4 is composed of bivalves, oysters and common large pectins in a well cemented sandstone matrix which contains gravel sized conglomerate. Mtcm 4 rapidly grades into the laminated silty fine sandstone of Mtsm5. Within Mtsm5 there is a progressive increase in sand concentration from the laminated silty fine sandstone at the base to the massive medium to fine sandstone that makes up the upper half of cyclothem 4.

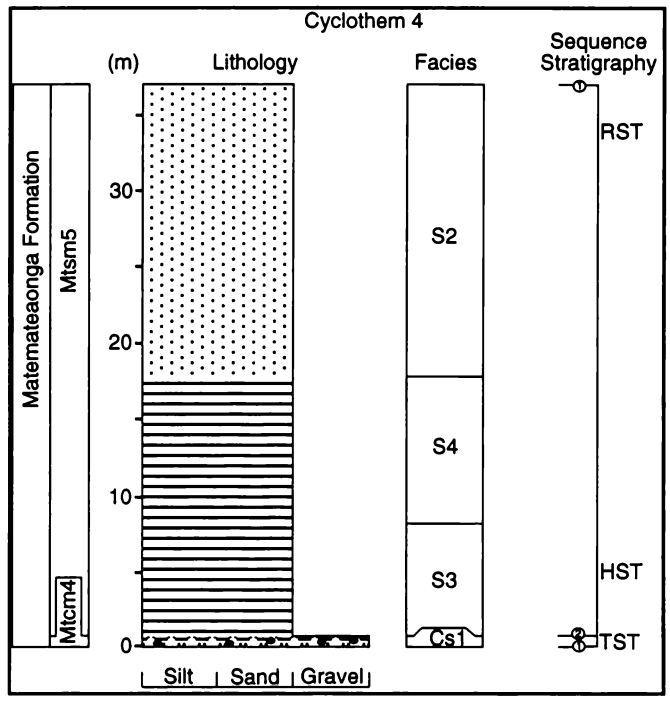

CYCLOTHEM 5

Cyclothem 5 contains two shellbeds (Mtcm5 & 6) separated by approximately 2 m of massive medium to fine sandstone (Mtsm6). Both shellbeds have a well cemented sandstone matrix and grade rapidly into uncemented massive medium to fine sandstone (Mtsm6 & 7; respectively). The lower-most shellbed within cyclothem 5 (Mtcm5) appears to be in conformable contact with Mtsm5 of cyclothem 4. Mtsm7 shows a fining to coarsening trend as it grades from the massive medium to fine sandstone to a thinly bedded medium to fine sandstone via a laminated silty fine sandstone.

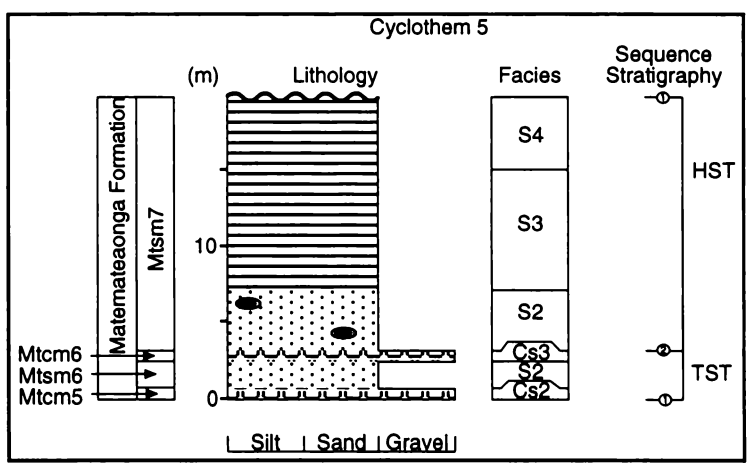

CYCLOTHEM 6

The approximately 3 m thick, variably cemented, oyster dominated (*Crassostrea*) shellbed (Mtcm7) has a wavy basal boundary that appears to conformably overlie cyclothem 5. Mtcm7 grades into a massive silty fine sandstone, the basal lithofacies of Mtsm8. A distinct break occurs where the massive silty fine sandstone becomes a laminated silty fine sandstone within Mtsm8. Up section from the prominent break, there is a progressive increase in sand content until a massive medium to fine sandstone lithology is reached approximately 1 m from the top of the cyclothem.

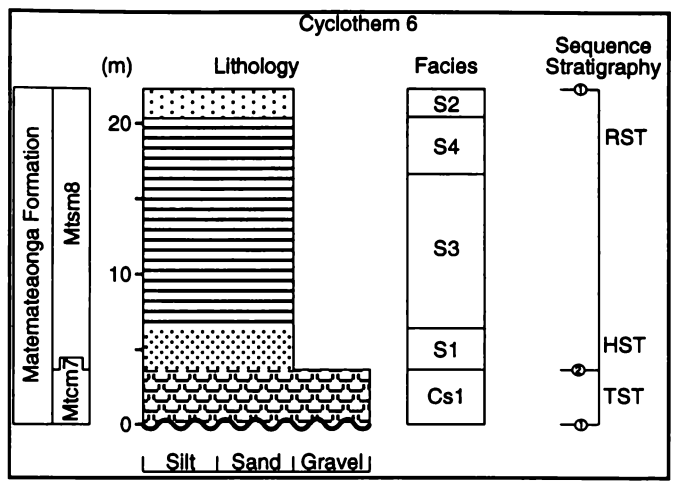

CYCLOTHEM 7

Cyclothem 7 contains two shellbeds (Mtcm8 & 9) separated by approximately 2 m of massive medium to fine sandstone (Mtsm9). Both shellbeds have a well cemented sandstone matrix. Mtcm8 appears to conformably overlie Mtsm8 and grades into Mtsm9, which is in turn conformably overlain by Mtcm9. Mtcm9 grades into the silty fine sandstone lithofacies at the base of Mtsm10, which has a decreasing then increasing sand content as it changes to a thinly bedded fine sandstone via a laminated silty fine sandstone.

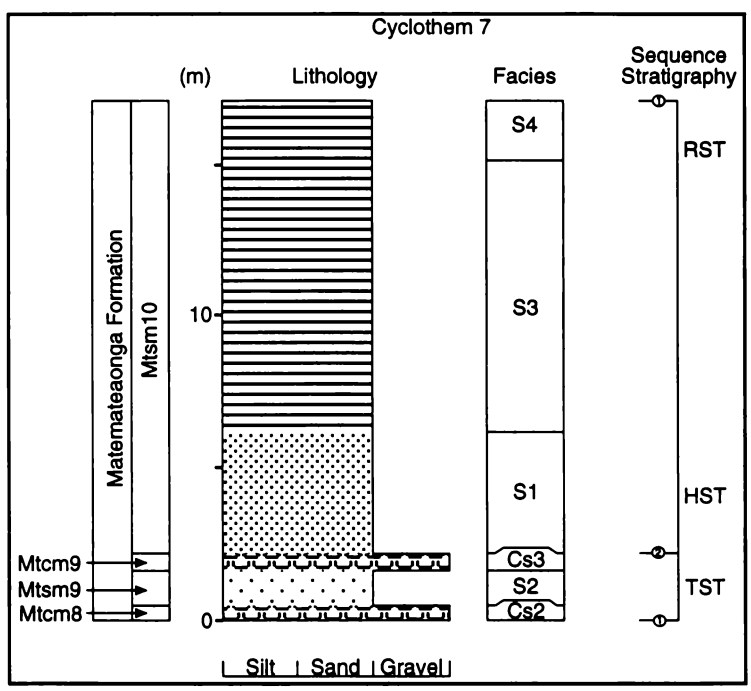

CYCLOTHEM 8

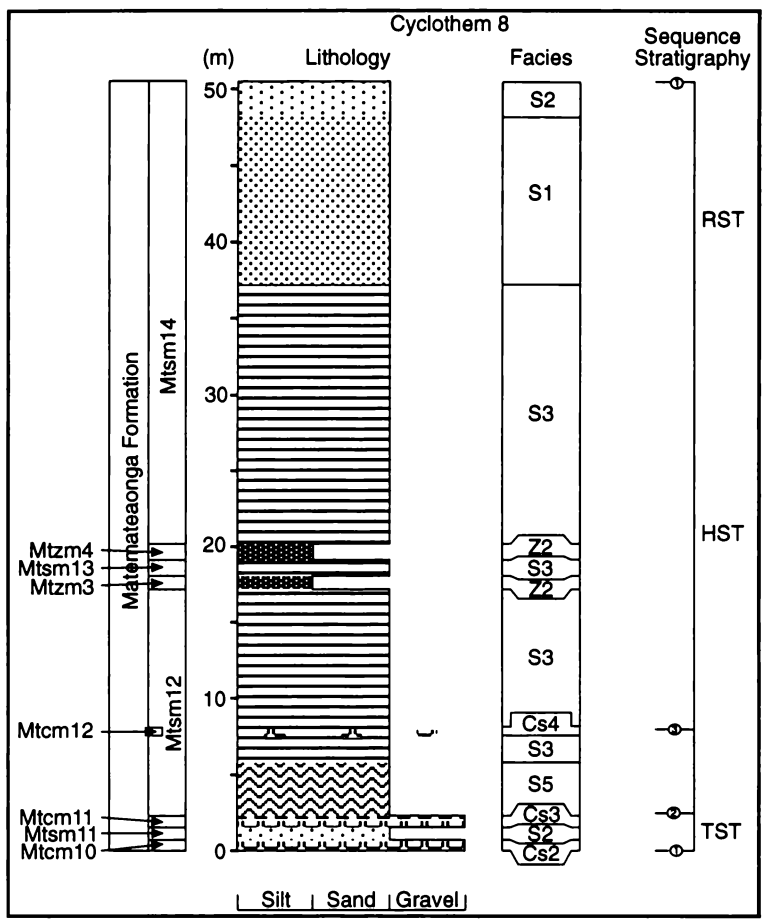

Cyclothem 8 contains two shellbeds (Mtcm10 & 11) separated by approximately 1 m of massive medium to fine sandstone (Mtsm11). Both shellbeds have a well cemented sandstone matrix. Mtcm10 appears to conformably overly cyclothem 7 and grades into Mtsm11, which is capped by Mtcm11. Mtcm11 is over-lain by Mtsm12, which is a cross-bedded medium to fine sandstone that grades into a laminated silty fine sandstone, within which occurs a discontinuous layer of clumped macrofossil (predominantly fragments; Mtcm12), equivalent to a flooding surface shellbed, sequence stratigraphic surface number (3). Cyclothem 8 is divided by two approximately 1 m-thick prominent fine sandy siltstone beds (Mtzm3 & 4) which grade from and into laminated silty fine sandstone (Mtsm12, 13 &14). The uppermost member of cyclothem 8, Mtsm14 has a progressively increasing sand content as it grades from a laminated silty fine sandstone through a massive silty fine sandstone to a massive medium to fine sandstone.

CYCLOTHEM 9

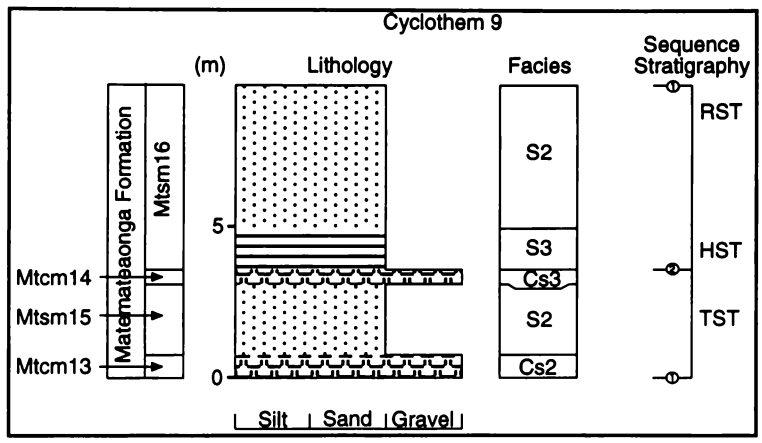

The two shellbeds of cyclothem 9 (Mtcm13 & 14) are conformably separated by approximately 2 m of massive medium to fine sandstone (Mtsm15). Both shellbeds have a well cemented sandstone matrix. The basal boundary of the lower shellbed (Mtcm13) appears to be in conformable contact with cyclothem 8, while Mtcm14 grades into the laminated silty fine sandstone of Mtsm16. Mtsm16 shows increasing sand content as it grades rapidly into a massive medium to fine sandstone.

CYCLOTHEM 10

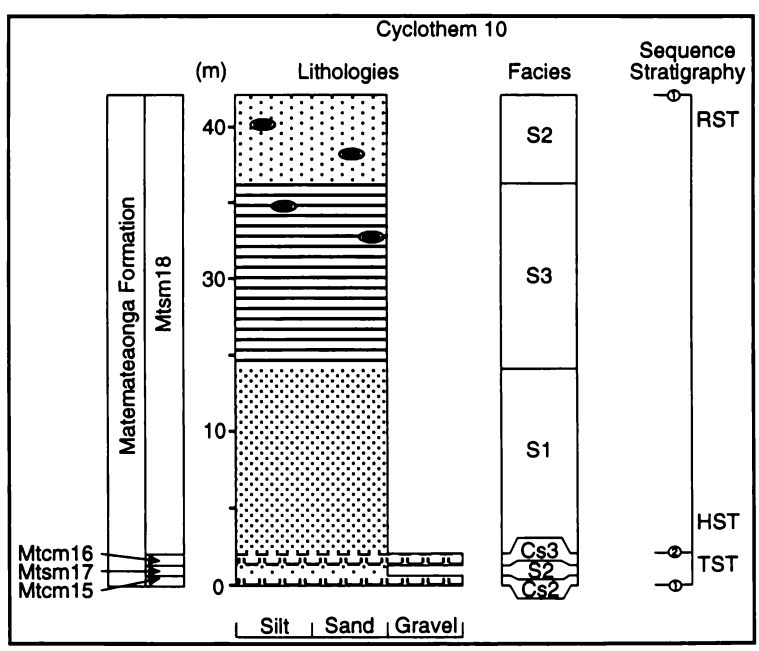

Cyclothem 10 contains two shellbeds (Mtcm15 & 16) separated by approximately 1 m of massive medium to fine sandstone (Mtsm17). Both shellbeds have a well cemented sandstone matrix. Mtcm15 appears to be in conformable contact with Mtsm16 of cyclothem 9, while Mtcm16 grades into a massive silty sandstone that is the basal lithofacies of Mtsm18. Mtsm18 transforms from this basal lithofacies to a concretionary massive medium to fine sandstone via a concretionary laminated silty fine sandstone.

CYCLOTHEM 11

The basal siltstone member (Mtzm5) of cyclothem 11, conformably, but sharply overlies Mtsm18 of cyclothem 10. this situation is unusual as no shellbed marks the start of this cyclothem. The transition from Mtzm5 to the overlying massive silty fine sandstone (Mtsm19) is marked by a prominent break in the lithology. Approximately halfway through Mtsm19 occurs a zone of post-depositional movement (lithofacies S7), there is no apparent change in grain-size leading into, through or out of the slump zone, nor is there any other contact apparent in outcrop.

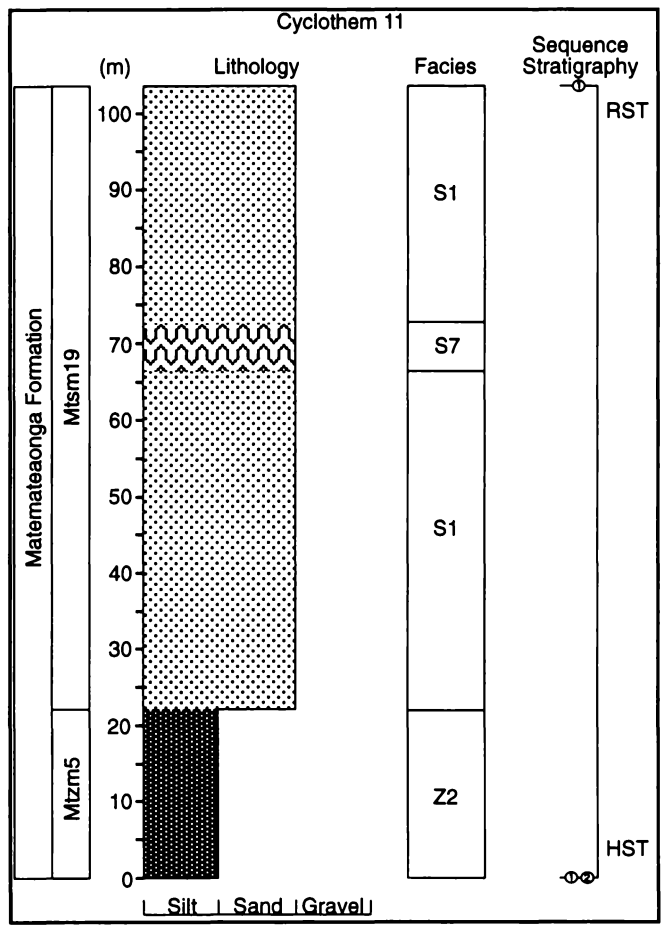

CYCLOTHEM 12

Cyclothem 11 appears to be conformably overlain by the approximately 15 cm-thick shellbed (Mtcm17) at the base of cyclothem 12. Mtcm17 has a well cemented sandstone matrix and grades rapidly into the silty fine sandstone at the base of Mtsm20. The sandstones of Mtsm20 are massive, although silty in the lower parts.

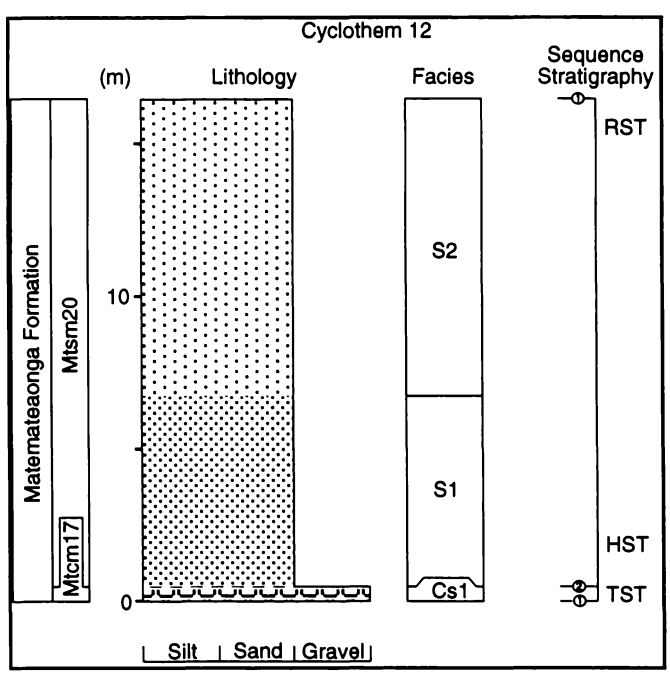

CYCLOTHEM 13

Cyclothem 13 has at its base a approximately 50 cm-thick oyster (*Crassostrea*) rich shellbed (Mtcm18), in a variably cemented sandstone matrix that appears to conformably overlie cyclothem 12. Mtcm18 rapidly grades into the laminated silty fine sandstone of Mtsm21. Cyclothem 13 is only 10 m thick.

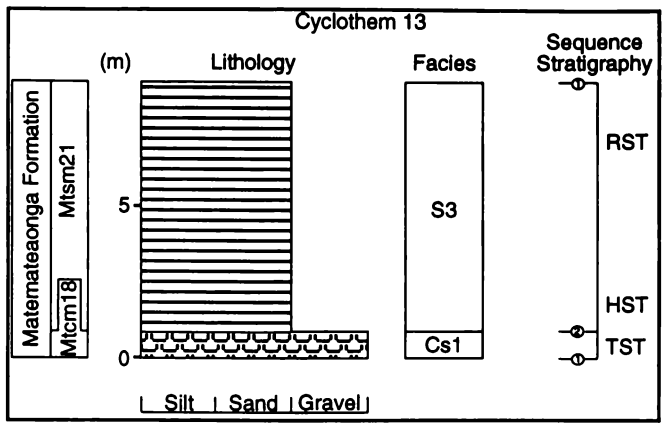

CYCLOTHEM 14

The approximately 20 cm-thick member Mtcm19 has a well cemented sandstone matrix and appears to conformably overlie cyclothem 13. Mtcm19 grades into the massive medium to fine sandstone of the overlying sandstone member (Mtsm22). Approximately 1 m above the Mtcm19/Mtsm22 transition occurs a prominent concretionary horizon.

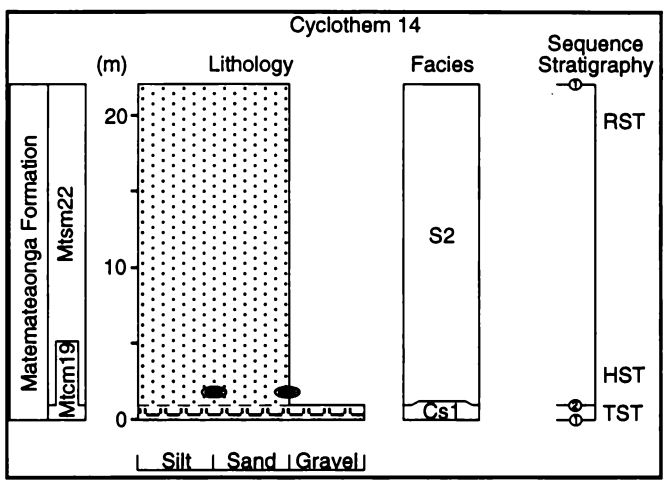

CYCLOTHEM 15

The basal member of cyclothem 15, an approximately 50 cm-thick shellbed (Mtcm20), appears to conformably overlie cyclothem 14. Mtcm20 has a well cemented sandstone matrix and rapidly grades into the overlying massive medium to fine sandstone (Mtsm23).

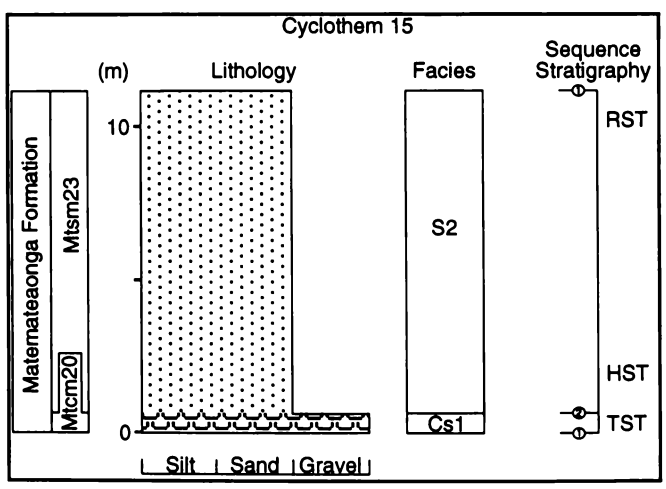

CYCLOTHEM 16

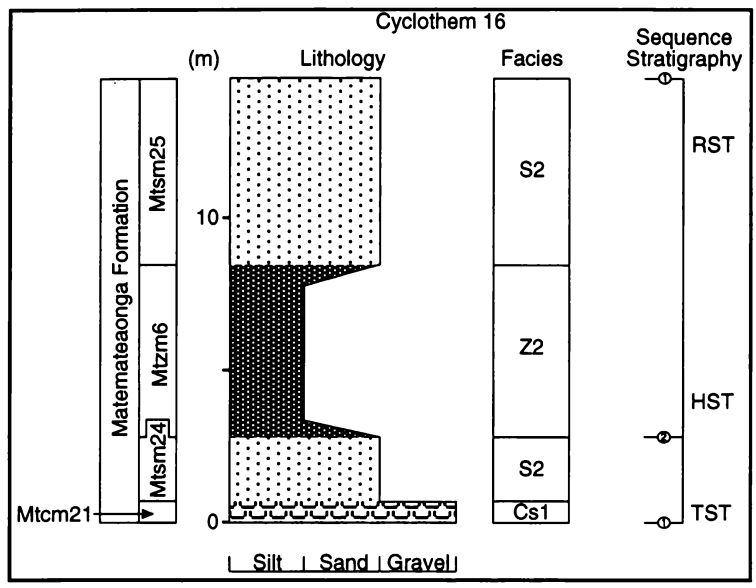

Cyclothem 15 appears to be conformably overlain by the approximately 20 cm-thick shellbed (Mtcm21) at the base of cyclothem 16. Mtcm21 is composed of large oysters (*Crassostrea*) and pectins in a well cemented sandstone matrix which grades rapidly into the overlying massive medium to fine sandstone of Mtsm24. The top of the TST is placed at the top of Mtsm24, TST motif 3. The massive sandstone becomes progressively finer upsection and grades into the massive fine sandy siltstone of Mtzm6. An increasing sand content up section leads to a transition from Mtzm6, back to a massive medium to fine sandstone of Mtsm25.

CYCLOTHEM 17

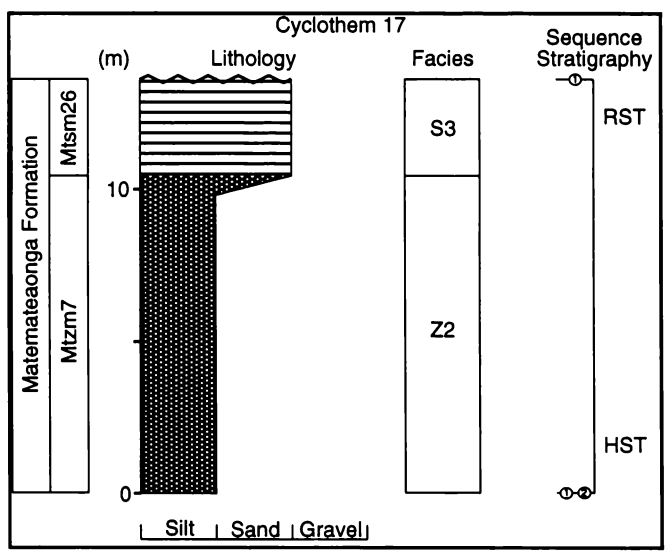

The basal massive fine sandy siltstone member (Mtzm7) of cyclothem 17, conformably, but sharply overlies Mtsm25 of cyclothem 16 and grades into the laminated silty fine sandstone of Mtsm26. This cyclothem is one of the few unusual cyclothems that do not have a basal shellbed.

CYCLOTHEM 18a

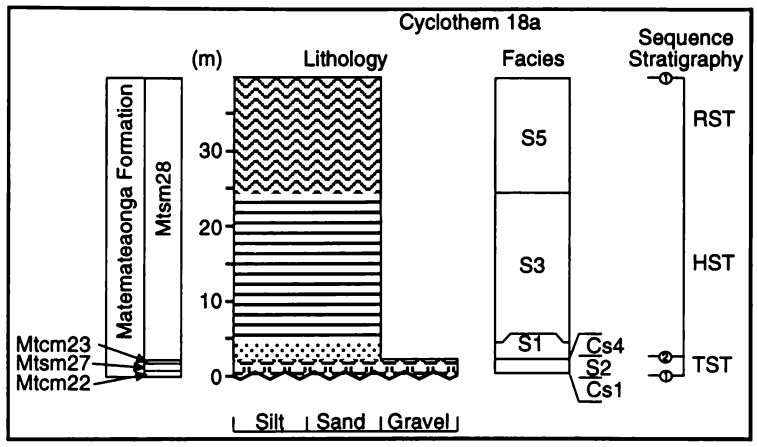

Cyclothem 18a contains two shellbeds (Mtcm22 & 23; approximately 25 & 10 cm-thick respectively) conformably separated by approximately 80 cm of massive medium to fine sandstone (Mtsm27). Although both shellbeds have a variably cemented sandstone matrix, Mtcm22 is predominantly composed of cross-bedded bivalves layers and delineates an eroded contact with the underlying Mtsm26 of cyclothem 17, while the poorly developed Mtcm23 grades into the silty fine sandstone of Mtsm28 which becomes cross-bedded over the top 15 m.

CYCLOTHEM 18b

The concretionary siltstone Mtzm8 marks the base of cyclothem 18b and appears to conformably overly cyclothem 18a. The transition from Mtzm8 to Mtsm29 is marked by a prominent break in the slope, with Mtsm29 grading from a massive silty fine sandstone to a massive medium to fine sandstone via a laminated silty fine sandstone lithofacies.

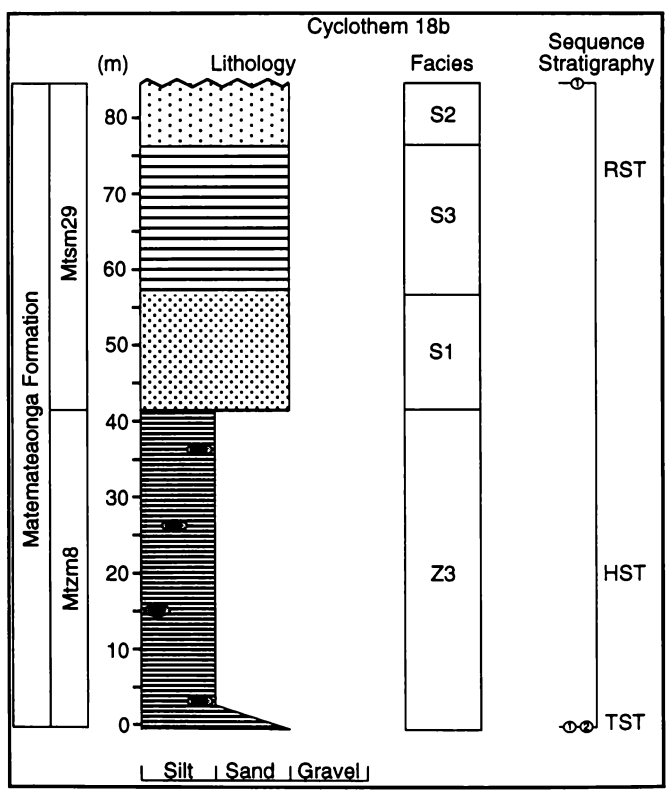

CYCLOTHEM 19

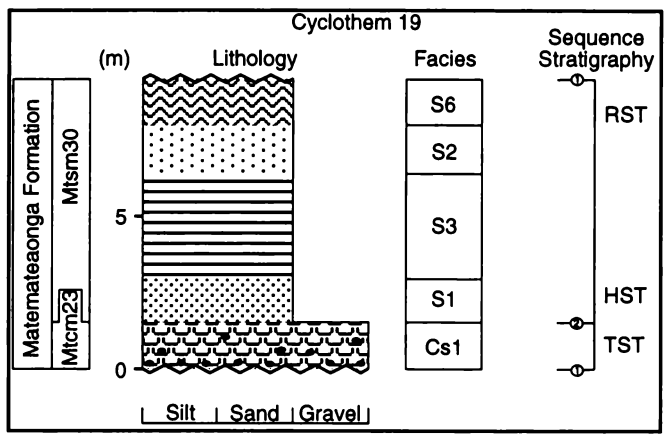

The basal member of cyclothem 19, an approximately 1 m thick shellbed (Mtcm23), sits upon the eroded boundary with cyclothem 18. Mtcm23 is composed of the typical fauna in a well cemented, conglomeratic, sandstone matrix and rapidly grades into the overlying massive silty fine sandstone (Mtsm30). Mtsm30 grades from its initial massive silty fine sandstone nature to a laminated silty fine sandstone then a massive medium to fine sandstone which becomes cross-bedded near the top of the cyclothem.

CYCLOTHEM 20

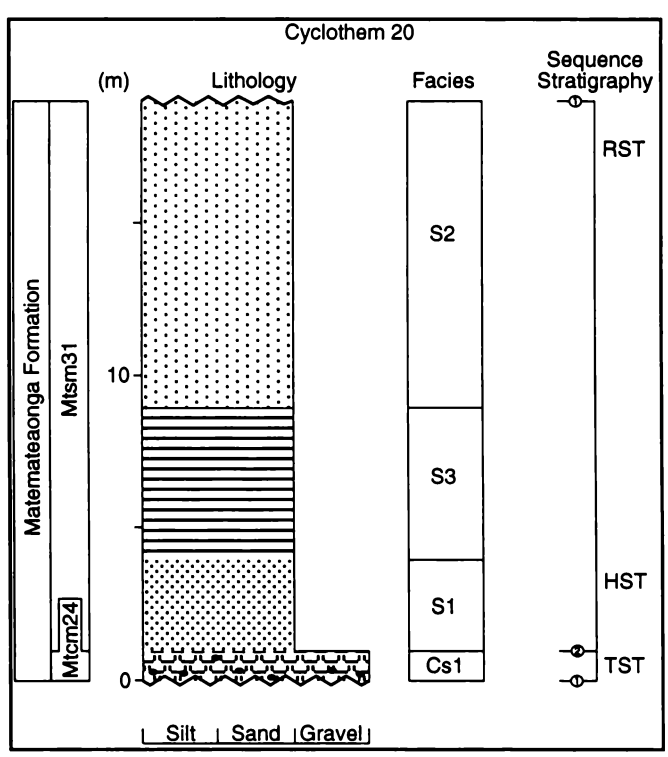

The approximately 1 m thick, shellbed at the base of cyclothem 20 (Mtcm24) lies upon the eroded boundary between cyclothems 19 & 20. Mtcm24 has a well cemented, conglomeratic sandstone matrix and is conformably over-lain by massive silty fine sandstone (Mtsm31). Mtsm31 grades from a massive silty fine sandstone to a massive medium to fine sandstone via a laminated silty fine sandstone lithofacies.

CYCLOTHEM 21

The approximately 1 m-thick, shellbed at the base of cyclothem 21 (Mtcm25) lies upon the eroded boundary between cyclothems 20 & 21. Mtcm25 has a well cemented sandstone matrix which is conformably over-lain by massive silty fine sandstone (Mtsm32). Mtsm32 grades from a massive silty fine sandstone to a massive medium to fine sandstone via a thinly bedded fine sandstone lithofacies.

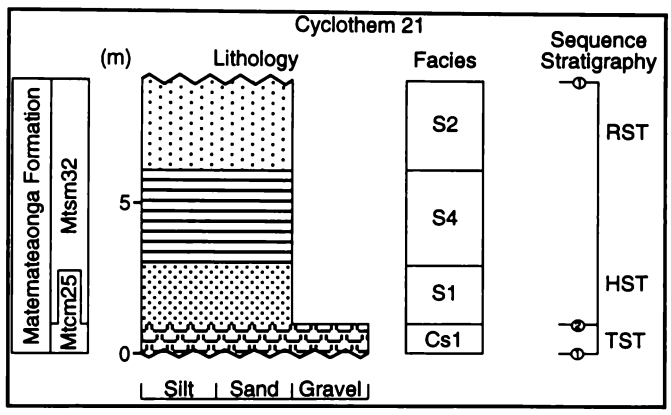

CYCLOTHEM 22

Cyclothem 22 contains two shellbeds (Mtcm26 & 27; approximately 1 m & 30 cm-thick respectively) conformably separated by approximately 1.5 m of massive medium to fine sandstone (Mtsm33). Both shellbeds have a well cemented sandstone matrix. Mtcm26 sits upon the eroded contact with Mtsm32 of cyclothem 21, while Mtcm27 grades into the massive medium to fine sandstone of Mtsm34. Cyclothem 22 has a highly variable thickness of 7m (mid value of observed thickness) due to the extensively eroded nature of the upper boundary.

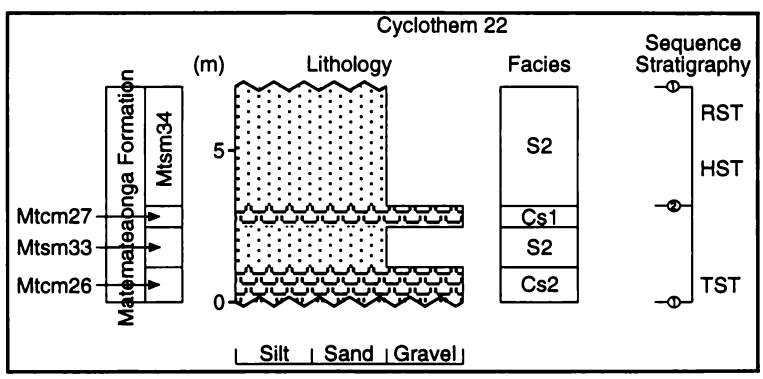

CYCLOTHEM 23

The approximately 7 m thick, shellbed at the base of cyclothem 23 (Mtcm28) lies upon the eroded boundary between cyclothems 23 & 24. Relief of up to approximately 4 m was observed on this boundary. Mtcm28 has a well cemented, conglomeratic (boulders up to 30 cm in diameter were observed) sandstone matrix and is conformably over-lain by the massive fine sandy siltstone of Mtzm9. Mtzm9 grades into Mtsm35 which is predominantly composed of laminated, concretionary, silty fine sandstone. Three prominent packages of material that has undergone post-depositional movement (lithofacies S7) break-up the lower half of Mtsm35 while the top of the member is capped by a massive silty fine sandstone. There is no obvious change in grainsize leading into, through or out of the slump zones, nor is there any other contact apparent in outcrop.

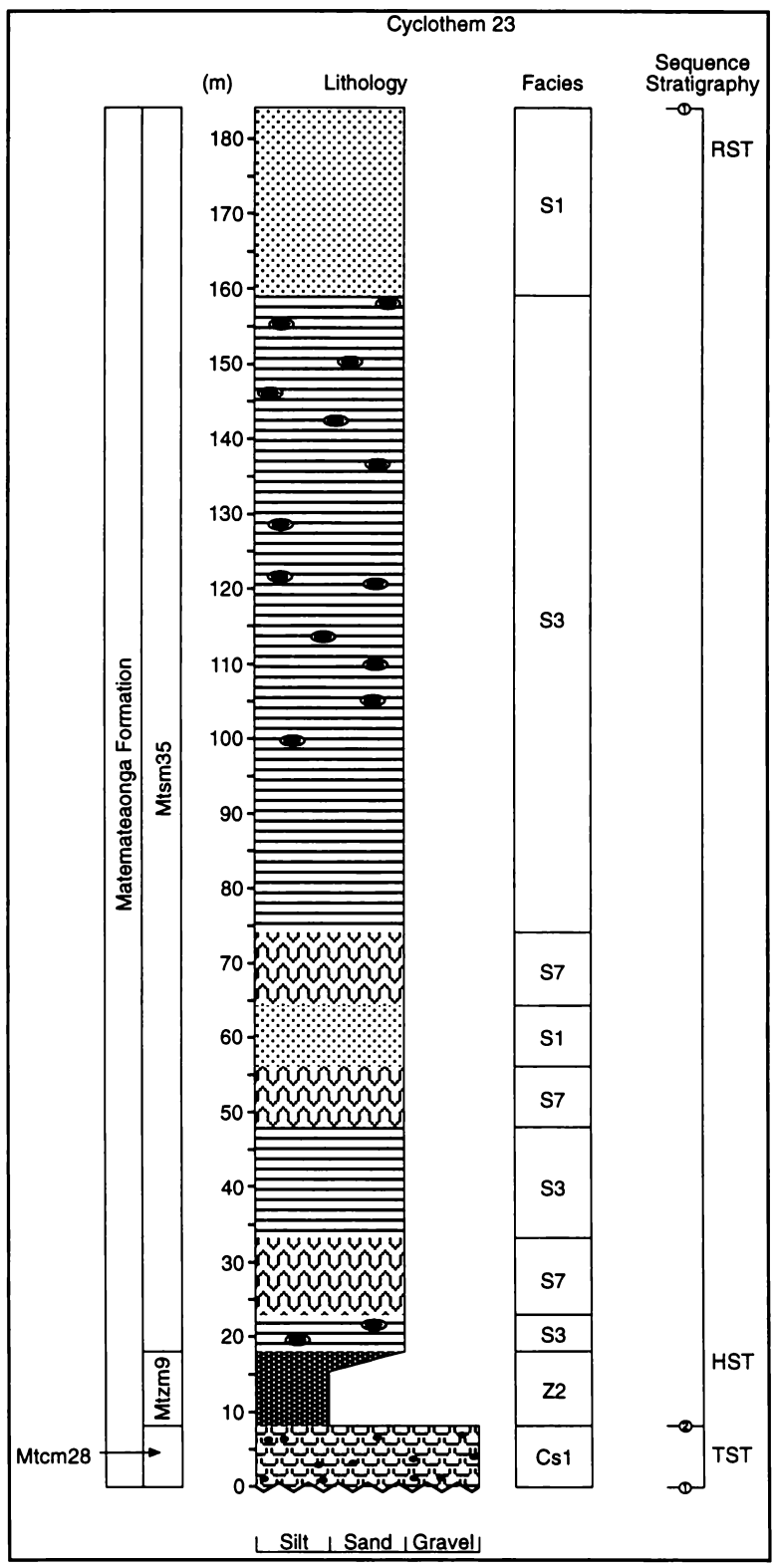

CYCLOTHEM 24

The basal laminated fine sandy siltstone member (Mtzm10) of cyclothem 24, conformably overlies Mtsm35 of cyclothem 23 and grades into the laminated silty fine sandstone of Mtsm36. This cyclothem is unusual given it's uniformity, sheer thickness, approximately 330 m and lack of basal shellbed or other distinctive horizon related to the transgressive systems tract.

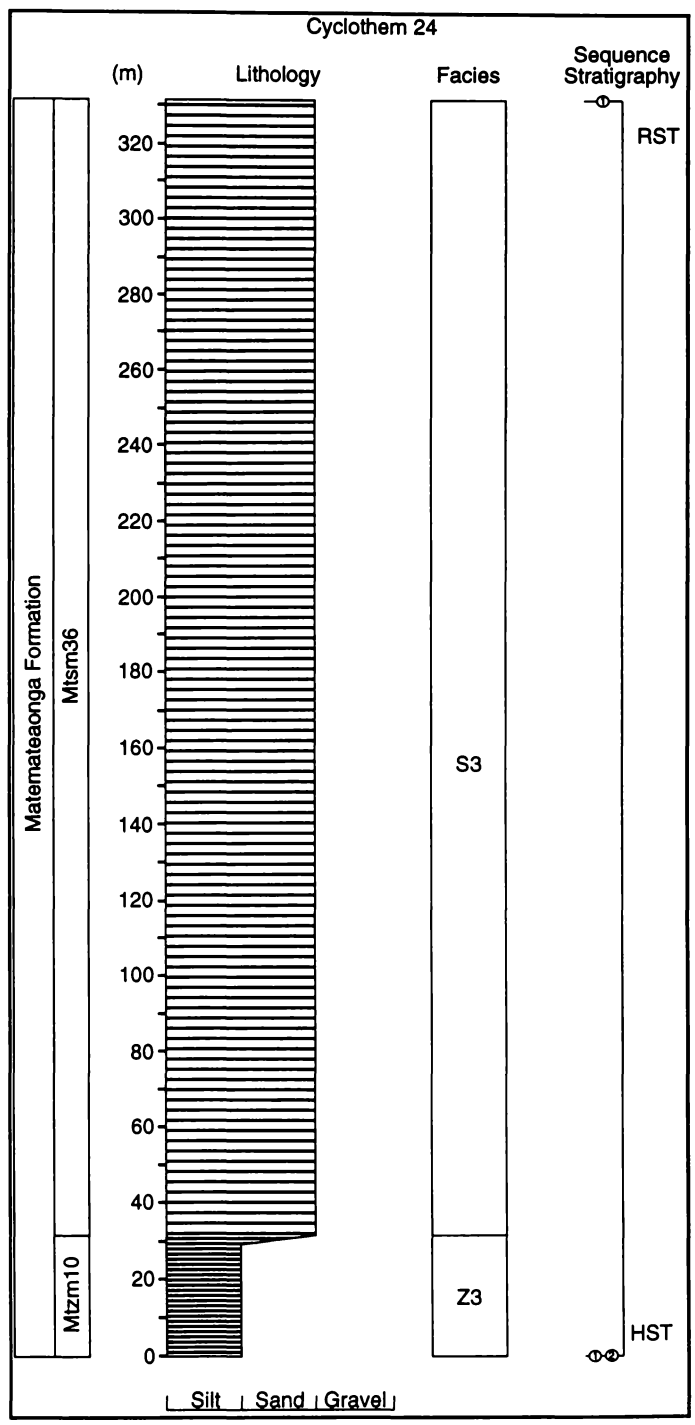

CYCLOTHEM 25

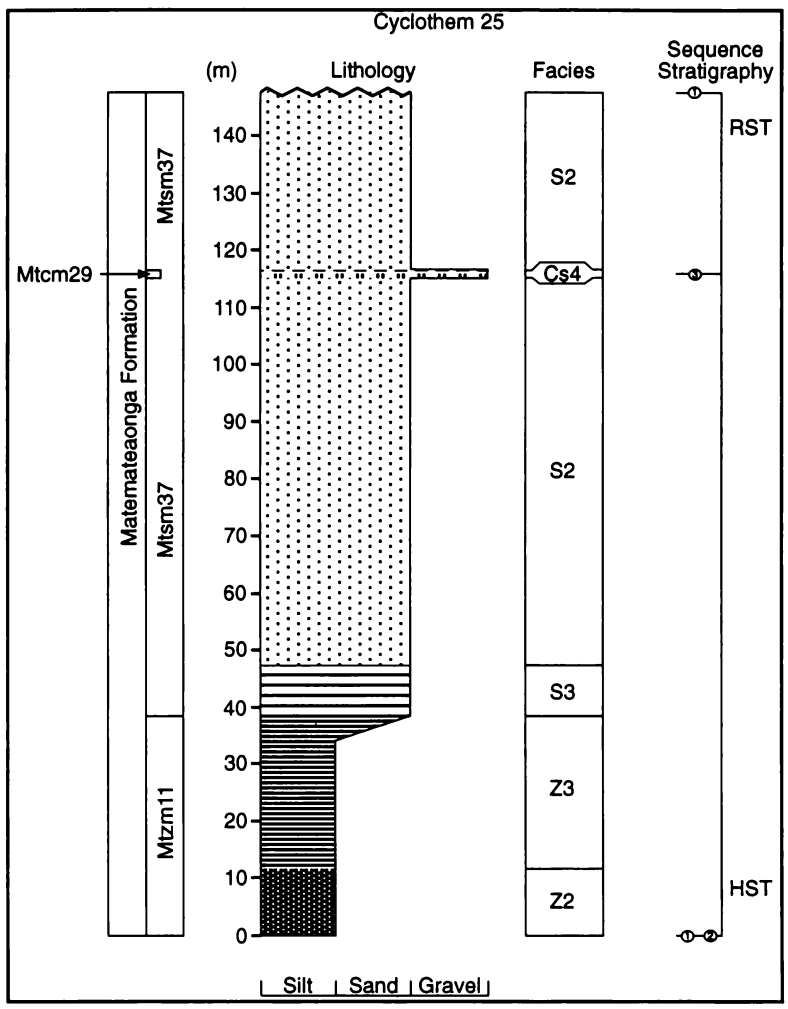

The basal massive fine sandy siltstone of Mtzm11 is in sharp contact with the underlying Mtsm36 of cyclothem 24, again no facies characteristic of the transgressive systems tract appears to be present. Within Mtzm11 there is a transition from massive to laminated fine sandy siltstone. The progressive increase in sand content continues upsection with the transition to a laminated silty fine sandstone (Mtsm37) and finally a massive medium to fine sandstone. Approximately two thirds the way through Mtsm37, the massive medium to fine sandstone is broken by the lensoidal, variably concreted shell hash of Mtcm29. The Mtsm37 is regarded as continuous either side of Mtcm29 because of the lensoidal and discontinuous nature of this shellbed, which is regarded here as a flooding surface shellbed - sequence stratigraphic surface number (3).

CYCLOTHEM 26

The approximately 4 m thick, shellbed at the base of cyclothem 26 (Mtcm30) lies upon the eroded boundary between cyclothems 25 & 26. Mtcm30 has a well cemented sandstone matrix and is conformably over-lain by massive medium to fine sandstone (Mtsm38) which has been included into the TST - motif 3. The laminated fine sandy siltstone of Mtzm12 conformably overlies Mtsm38 and grades into the overlying massive fine sandstone of Mtsm39 via a laminated silty fine sandstone lithofacies.

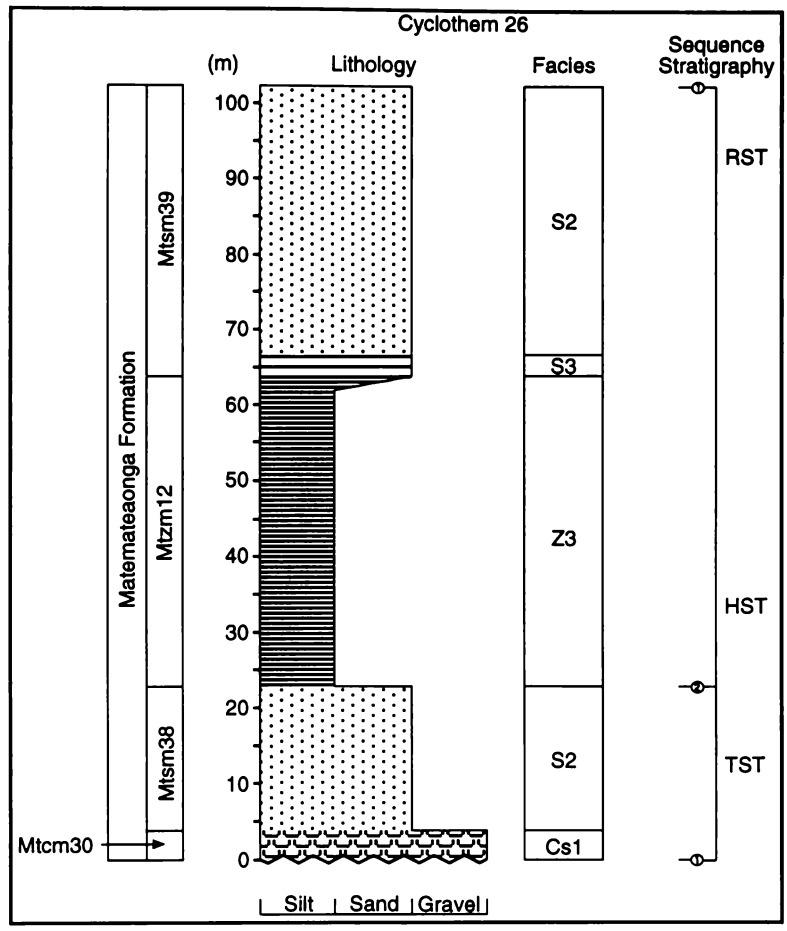

CYCLOTHEM 27

Cyclothem 27 contains two shellbeds (Mtcm31 & 32; approximately 1 m & 75 cm-thick respectively) conformably separated by approximately 5 m of massive medium to fine sandstone (Mtsm40). Both shellbeds have a well cemented sandstone matrix. Mtcm31 sits upon what appears to be a conformable contact with Mtsm39 of cyclothem 26, while Mtcm32 grades into the massive medium to fine sandstone of Mtsm41. Mtsm41 shows a decreasing to increasing sand content as it passes through a laminated silty fine sandstone before returning to a massive medium to fine sandstone.

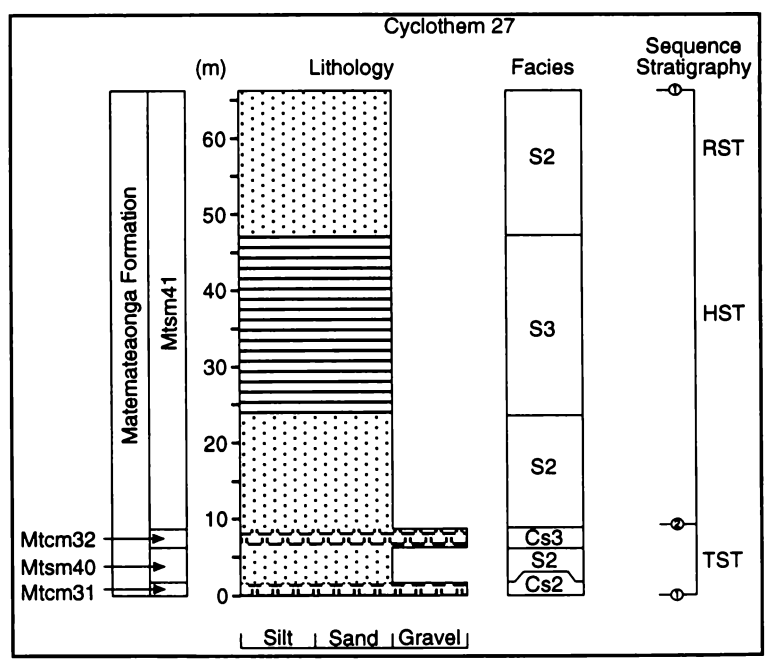

CYCLOTHEM 28

The basal member of cyclothem 28, an approximately 20 cm-thick lensoidal shellbed (Mtcm33), appears to sit conformably upon with cyclothem 27. Mtcm33 grades into the overlying laminated silty fine sandstone of Mtsm42. Mtsm42 grades into a massive medium to fine sandstone which is sharply over-lain by massive fine sandy siltstone of Mtzm13. The siltstone grades into the massive medium to fine sandstone of Mtsm43. Mtsm42 has been included in the TST - motif 3.

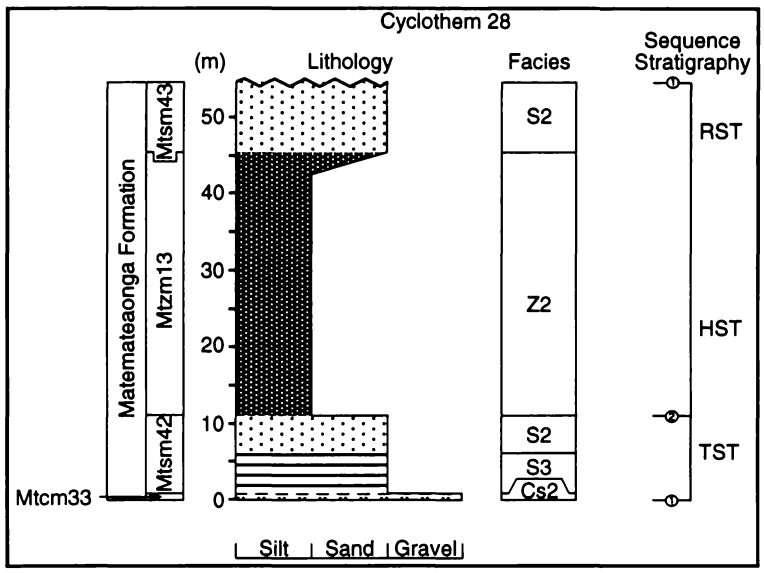

CYCLOTHEM 29

The approximately 4 m thick, shellbed at the base of cyclothem 29 (Mtcm34) lies upon the eroded boundary with cyclothems 28. Mtcm34 has a well cemented, conglomeratic sandstone matrix and appears to be conformably over-lain by a macrofossil rich (*Nemocardium*), laminated fine sandy siltstone (Mtzm14). Mtzm14 grades into the massive fine sandstone of Mtsm44 via a laminated silty fine sandstone lithofacies.

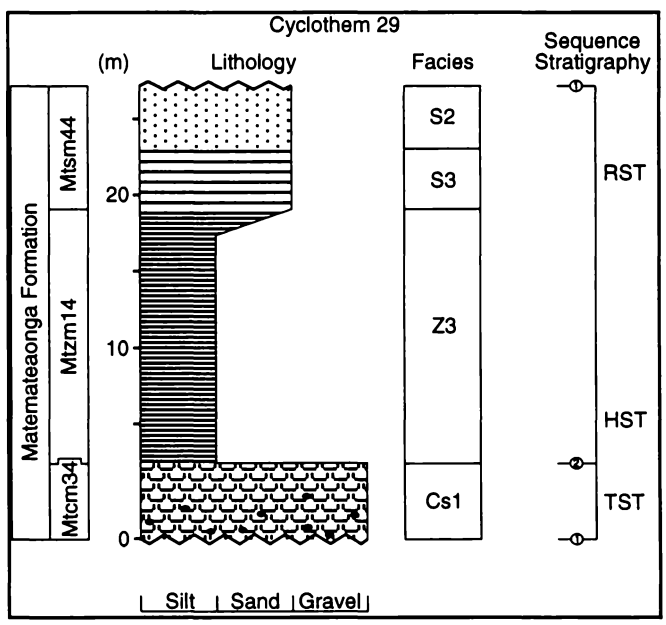

CYCLOTHEM 30

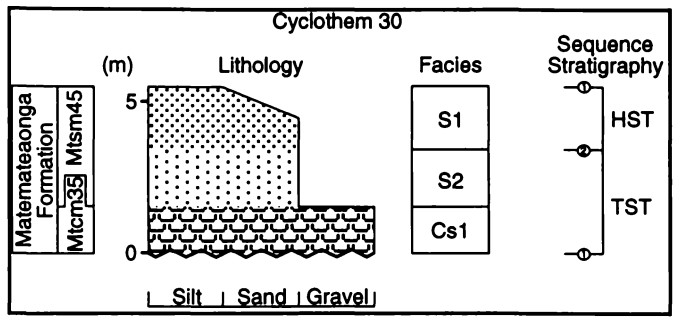

The basal member of cyclothem 30, an approximately 1 m thick shellbed (Mtcm35), sits upon the eroded contact with cyclothems 29. Mtcm35 has a well cemented, conglomeratic, sandstone matrix and grades into the overlying massive medium to fine sandstone of Mtsm45. Mtsm45 grades into a massive silty fine sandstone forming the top of the Matemateaonga Formation. The massive medium to fine sandstones of Mtsm45 have been included in the TST - motif3.

CHAPTER 3: SUPPLEMENT 2

PALEOENVIRONMENTAL INTERPRETATION

This chapter supplement provides a summary of the benthic foraminiferal composition of samples from the Matemateaonga Formation to aid interpretation of depositional paleoenvironments. The raw data are contained in Appendix 2: Forams.

Typically paleoenvironmental determination is undertaken by comparing the benthic fauna contained in a sample against tables showing the known depth ranges for those taxa. Census samples of approximately 200 specimens of benthic foraminifera were picked from the greater than 125 μm sample fraction (full methodology given in Appendix 1). However, samples from the Matemateaonga Formation were commonly barren or contained very poor foraminiferal assemblages, with a significant amount of time required to obtain even small numbers of foraminifera from large amounts of sediment. To maximise the amount of information available for the formation, census samples with less than 100 specimens have been included. The number of foraminifera making up these small samples is noted.

To simplify analysis of the census samples, benthic foraminifera typical of the Matemateaonga Formation have been compared to the depositional depth ranges given in Hayward (1986); Hornibrook *et al.* (1989); Crundwell *et al.* (1994); and Hayward *et al.* (1997). From this comparison, five groupings of fauna that characterise specific paleodepth zones have been developed. The relative occurrence of these groups in any one sample is used to determine the paleobathymetry. Table C3S2:1 gives the composition of the groupings while Figure C3S2:1 illustrates the depositional ranges of the benthic foraminifera used in Table C3S2:1. Interestingly, the groupings developed here, are similar to the assemblages obtained from foraminiferal studies on the modern Lincoln Shelf, South Australia (Li *et al.*, 1996).

Table C3S2:1. Environmental groupings used to determine inferred depositional depths.

Depositional environment	Key depth diagnostic fauna
Nearshore to inner-shelf (0-50)	*Ammonia beccarii*
Nearshore to mid-shelf (0-100 m)	*Elphidium* spp. *Discorbis* spp. *Discorbinella* spp. *Zeaflorilis parri* *Virgulopsis* spp.
Shelf and uppermost bathyl	*Anomalinoides* spp. *Astrononion* spp.
Not inner-shelf (>50 m)	*Evolvocassidulina* spp. *Gyroidina* spp. *Gyroidinoides* spp. *Hauslerella* spp.
Not Shelf (>200m)	*Pullenia* spp. Elongate Nodosariids

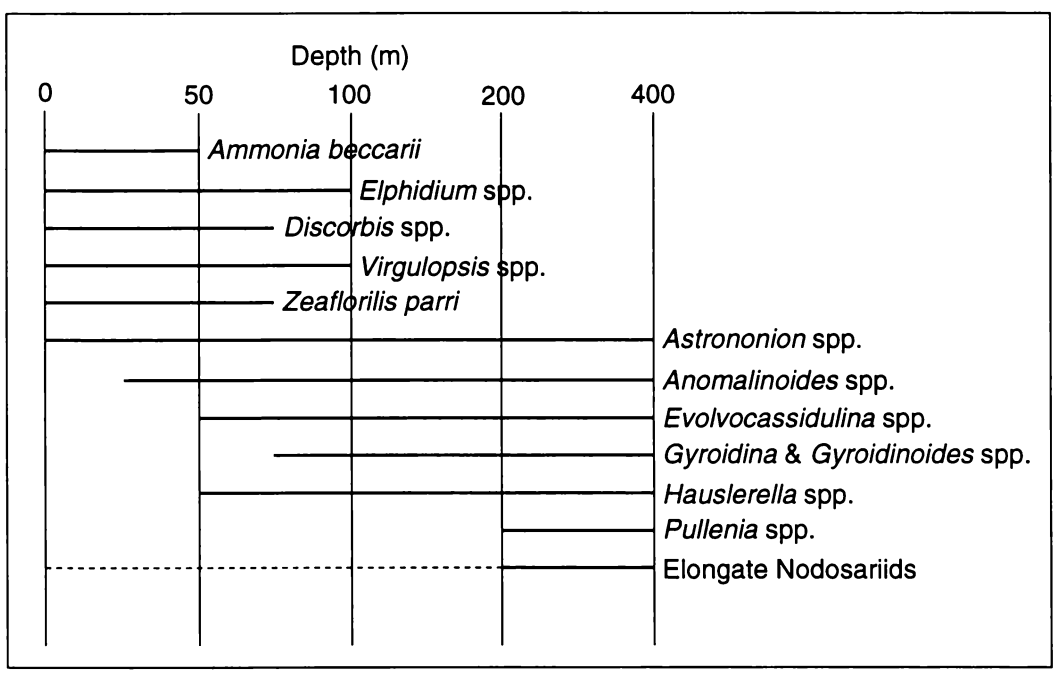

Figure C3S2:1. Depth range of benthic foraminifera used in the environmental groupings in Table C3S2:1 (after Hayward, 1986; Hornibrook *et al.*, 1989; Crundwell *et al.*, 1994; and Hayward *et al.*, 1997).

Sample W962002

Planktic percentage	5%	Neritic
Near-shore to inner-shelf	absent	>50 m
Near-shore to mid-shelf	absent	>100 m
Shelf and uppermost bathyl	abundant	0-400 m
Not inner-shelf	common	>50 m
Not Shelf	absent	<200 m
Interpretation		100-200 m

Sample W962023

Planktic percentage	11%	Neritic
Near-shore to inner-shelf	absent	>50 m
Near-shore to mid-shelf	rare	≈100 m
Shelf and uppermost bathyl	common	0-400 m
Not inner-shelf	common	>50 m
Not Shelf	absent	<200 m
Interpretation		100-200 m

Sample W962028 - foraminifera rare - 93 specimens

Planktic percentage	-	Neritic
Near-shore to inner-shelf	absent	>50 m
Near-shore to mid-shelf	rare	≈100 m
Shelf and uppermost bathyl	abundant	0-400 m
Not inner-shelf	common	>50 m
Not Shelf	absent	<200 m
Interpretation		100-200

Sample W962041 - foraminifera very rare - 39 specimens

Planktic percentage	2.5%	Neritic
Near-shore to inner-shelf	absent	>50 m
Near-shore to mid-shelf	rare	≈100 m
Shelf and uppermost bathyl	common	0-400 m
Not inner-shelf	common	>50 m
Not Shelf	absent	<200 m
Interpretation		100-200

Sample W962062

Planktic percentage	4 %	Neritic
Near-shore to inner-shelf	absent	>50 m
Near-shore to mid-shelf	common	0-100 m
Shelf and uppermost bathyl	common	0-400 m
Not inner-shelf	common	>50 m
Not Shelf	rare	≈200 m
Interpretation		50-200

Note: slumped unit - initially deposited at inner-shelf depths before being redeposited at outer-shelf depths.

Sample W962066

Planktic percentage	1%	Neritic
Near-shore to inner-shelf	absent	>50 m
Near-shore to mid-shelf	rare	≈100 m
Shelf and uppermost bathyl	abundant	0-400 m
Not inner-shelf	common	>50 m
Not Shelf	absent	<200 m
Interpretation		100-200

Sample W962081A

Planktic percentage	1%	Neritic
Near-shore to inner-shelf	absent	>50 m
Near-shore to mid-shelf	common	0-100 m
Shelf and uppermost bathyl	common	0-400 m
Not inner-shelf	common	>50 m
Not Shelf	absent	<200 m
Interpretation		50-100

Sample W962088

Planktic percentage	1%	Neritic
Near-shore to inner-shelf	absent	>50 m
Near-shore to mid-shelf	absent	>100 m
Shelf and uppermost bathyl	common	0-400 m
Not inner-shelf	common	>50 m
Not Shelf	absent	<200 m
Interpretation		100-200

Sample W9620106 - foraminifera very rare - 16 specimens

Planktic percentage	-	Neritic
Near-shore to inner-shelf	absent	>50 m
Near-shore to mid-shelf	present	0-100 m
Shelf and uppermost bathyl	absent	
Not inner-shelf	present	>50 m
Not Shelf	absent	<200 m
Interpretation		50-100

Sample W962108 - foraminifera rare - 83 specimens

Planktic percentage	2 %	Neritic
Near-shore to inner-shelf	present	>50 m
Near-shore to mid-shelf	present	0-100 m
Shelf and uppermost bathyl	absent	
Not inner-shelf	rare	>50 m
Not Shelf	absent	<200 m
Interpretation		50-100

Sample W962109

Planktic percentage	4.5%	Neritic
Near-shore to inner-shelf	absent	>50 m
Near-shore to mid-shelf	present	0-100 m
Shelf and uppermost bathyl	present	0-400 m
Not inner-shelf	present	>50 m
Not Shelf	absent	<200 m
Interpretation		50-100

Sample W962111 - foraminifera very rare - 21 specimens

Planktic percentage	19 %	Neritic
Near-shore to inner-shelf	absent	>50 m
Near-shore to mid-shelf	common	0-100 m
Shelf and uppermost bathyl	absent	
Not inner-shelf	rare	>50 m
Not Shelf	absent	<200 m
Interpretation		50-100

Sample W962139 - foraminifera rare - 74 specimens

Planktic percentage	14 %	Neritic
Near-shore to inner-shelf	absent	>50 m
Near-shore to mid-shelf	common	0-100 m
Shelf and uppermost bathyl	common	0-400 m
Not inner-shelf	rare	>50 m
Not Shelf	absent	<200 m
Interpretation		50-100

Sample W962166

Planktic percentage	5%	Neritic
Near-shore to inner-shelf	absent	>50 m
Near-shore to mid-shelf	common	0-100 m
Shelf and uppermost bathyl	rare	0-400 m
Not inner-shelf	common	>50 m
Not Shelf	absent	<200 m
Interpretation		50-100

Sample W962177 - rare foraminifera - 75 specimens

Planktic percentage	2.5%	Neritic
Near-shore to inner-shelf	present	≈50 m
Near-shore to mid-shelf	abundant	0-100 m
Shelf and uppermost bathyl	rare	0-400 m
Not inner-shelf	rare	>50 m
Not Shelf	absent	<200 m
Interpretation		50-100

Sample W962180 - rare foraminifera - 58 specimens

Planktic percentage	1.5%	Neritic
Near-shore to inner-shelf	rare	≈50 m
Near-shore to mid-shelf	abundant	0-100 m
Shelf and uppermost bathyl	absent	
Not inner-shelf	rare	>50 m
Not Shelf	absent	<200 m
Interpretation		50-100

Sample W962186

Planktic percentage	1.5%	Neritic
Near-shore to inner-shelf	absent	>50 m
Near-shore to mid-shelf	abundant	0-100 m
Shelf and uppermost bathyl	rare	0-400 m
Not inner-shelf	present	>50 m
Not Shelf	absent	<200 m
Interpretation		50-100

Sample W962198

Planktic percentage	13.5%	Neritic
Near-shore to inner-shelf	absent	>50 m
Near-shore to mid-shelf	absent	>100 m
Shelf and uppermost bathyl	rare	0-400 m
Not inner-shelf	present	>50 m
Not Shelf	absent	<200 m
Interpretation		100-200

CHAPTER 4

TANGAHOE FORMATION AND THE DEEP-WATER, MASS-EMPLACED SANDSTONES

CHAPTER 4

TANGAHOE FORMATION AND THE DEEP-WATER, MASS-EMPLACED SANDSTONES

4:1 INTRODUCTION

The siltstone-dominated, early to late Pliocene (late Opoitian and Waipipian) Tangahoe Formation occurs as a broad east-west trending belt across the central part of Wanganui Basin (Figure 4:1), and dips towards the southern depocentre (Anderton, 1981). Between Jerusalem and Otui (Figure 4:2) the north-south trending Wanganui River exposes a 1350 m-thick terrigenous-dominated marine succession. The Tangahoe Formation (B in Figure 4:1) has upper-slope depth affinities and separates the underlying clearly cyclothemic sandstones of the Matemateaonga Formation (A, Figure 4:1) from the overlying less obviously cyclothemic sandstones of zone C (Figure 4:1). These features are discussed in more detail later in the chapter and elsewhere in the thesis (Matemateaonga Formation in Chapter 3 and zone C in Chapter 5). Composite stratigraphic columns, tied to appropriate map sections showing sample locations, are given at the end of Chapter 2.

The emphasis of this chapter is on the presentation of a formal lithostratigraphy for the succession between Jerusalem and Otui, along with a description of lithofacies and interpretation of their depositional paleoenvironments.

4:2 STRUCTURE OF THE TANGAHOE FORMATION IN THE WANGANUI RIVER VALLEY

The general lack of lithological variability in this section of the Wanganui River valley has limited the number of opportunities to obtain structural information. This Pliocene sedimentary succession forms an approximately east-west striking monocline, with regional strike values ranging from 010 to 060° and dip values of 3 to 5° SE. Fault identification is extremely difficult, although Collen (1972) proposed that the highly fractured nature of the Tangahoe Formation south of Ranana is possibly related to the presence of the Nukumaru Fault Zone. This is the only suspected fault recognised within the Tangahoe Formation. While small faults undoubtedly occur, lithological variability has been insufficient to highlight their occurrence.

Structural information obtained in this study is shown on Maps 6-11 (Chapter 2).

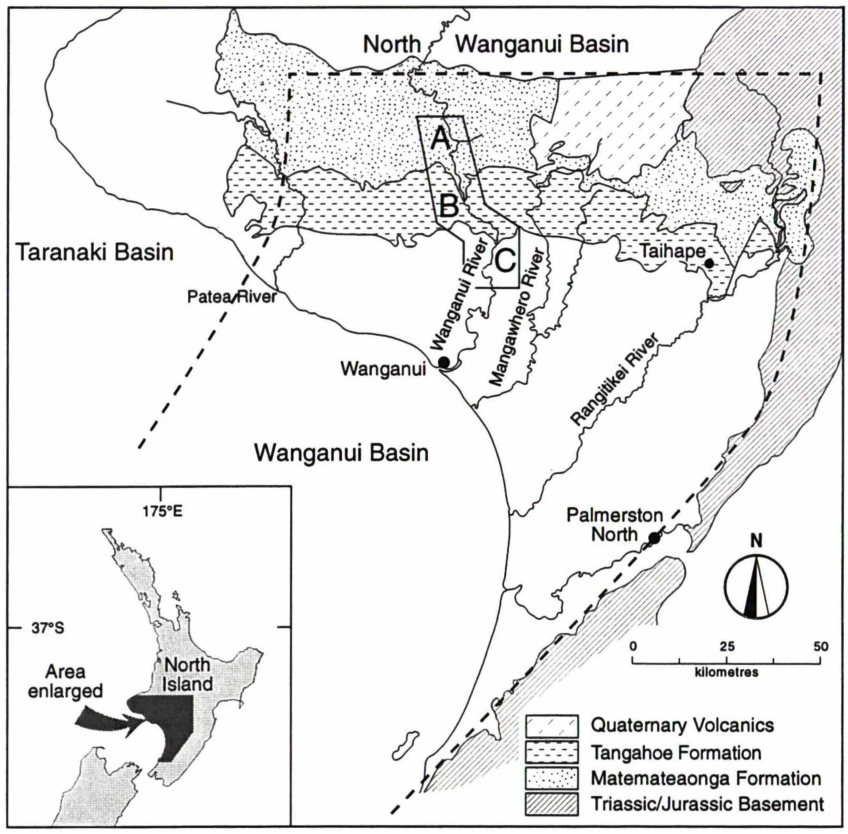

Figure 4:1. Distribution of the Tangahoe Formation (B) across the northern part of Wanganui Basin (after Hay, 1967; Katz and Leask, 1989; and Murphy *et al.*, 1994).

4:3 LITHOSTRATIGRAPHY

4:3:1 HISTORY

Siltstone and lesser amounts of locally prominent interbedded sandstone in the same stratigraphic position as the Tangahoe Formation have been given a variety of names in the past, the term Taihape Mudstone being used particularly in the eastern part of the Wanganui Basin. A summary of the formational nomenclature used by previous workers to describe late Miocene to late Pliocene strata in the western part of the basin is given in Figure 4:3. The Superior Oil Company Ltd report by Feldmeyer *et al.* (1943) is the earliest significant reference to the stratigraphy of the Wanganui River valley. They named the fine-grained lithology above the Reef-Bearing Sands as the Taihape Mudstone, the stratigraphic extent of which was described in the

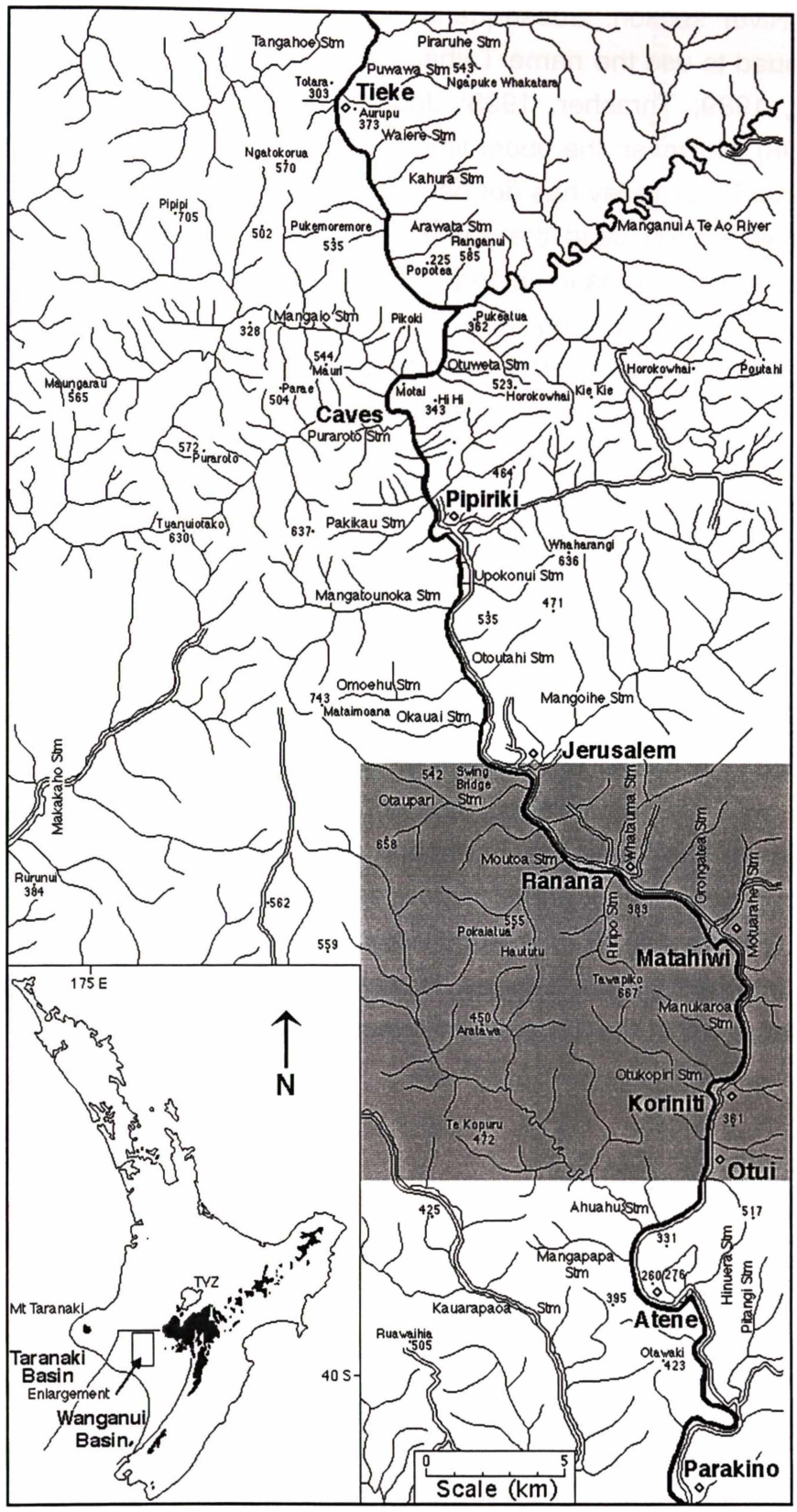

Figure 4:2. Locality map for the part of the Wanganui River valley considered in this study. The grey tone approximates the section of the river under study in this Chapter. Spot heights in metres. *Inset*: Location of the study area relative to the Wanganui Basin. Topography over 1000 m is blackened.

Rangitikei River section. Subsequent workers in eastern Wanganui Basin have continued to use the name Taihape Mudstone (e.g. Fleming, 1978; Katz and Leask, 1989; Thrasher, 1993; Journeaux *et al.*, 1996; Murrell, 1998; Oulton, 1998). However, the upper limit of the Taihape Mudstone equivalent in the Wanganui River valley has not been defined.

Arnold (1957) used the name Tangahoe Formation to describe the sandy mudstones exposed along the Tangahoe River in southeastern Taranaki. According to King and Thrasher (1996), the name Tangahoe Formation has been extensively used by oil company geologists to describe fine-grained sedimentary rocks of Pliocene age overlying the Matemateaonga Formation. Hay (1967), in Sheet 7 of the 1:250,000 geological map series of New Zealand, mapped these sediments as the Tangahoe Mudstone. However, the name Tangahoe Formation rather than Tangahoe Mudstone has persisted in the literature (e.g. Anderton, 1981; Murphy *et al.*, 1994; Thompson *et al.*, 1994), recognising that lithofacies other than mudstone do occur within the Tangahoe Formation.

Although the terminology of Feldmeyer *et al.* (1943) pre-dates that of Arnold (1957), Arnold's terminology is preferred as it simplifies regional correlation with the established nomenclature used in the neighbouring Taranaki Basin. The Tangahoe Formation as defined in this study differs from that used in previous work and incorporates a number of previously separated formations (Figure 4:3). Earlier subdivision has been on the basis of locally prominent interbedded sandstones. However, here these units are assigned member status within the Tangahoe Formation.

4:3:2 Reference Section

Feldmeyer *et al.* (1943) defined the Taihape Mudstone in the Rangitikei River. However, they were unable to correlate the upper boundary of the Taihape Mudstone, as described in the eastern part of Wanganui Basin, with the stratigraphy exposed in the Wanganui River. Arnold (1957) defined the type section for the Tangahoe Formation as the sandy mudstone exposed along the Tangahoe River in southeastern Taranaki. A reference section for the Tangahoe Formation in the Wanganui River Valley is proposed here, stretching from R21 847839 to S21 948667.

Age	Feldmeyer *et al.* (1943)	Fleming (1953)	Collen (1972)		Ker (1973)	Wilson (1993)		This Study
Wm	Mangaweka Formation	Mangaweka Mst		Pitangi Mst	Mangaweka Formation	Paparangi Group	Otawake Zst	Mangaweka Mudstone
	Atene Sands		Mangaweka Mst	Atene Sands	Atene Sst	Whenuakura Group	Atene Sst	Atene Formation
				Mangapapa Zst	Oxbow Zst		Oxbow Zst	Oxbow Siltstone Mbr
	Ahu Ahu Sands			Ahuahu Sands	Ahurangi Sst		Ahurangi Sst	Ahurangi Sandstone
				Raumati Mst	Otui Zst		Otui Zst	Tangahoe Formation
Wp	Koroniti Beds		Koroniti Sst		Koroniti Sst	Tangahoe Group	Koroniti Sst	Koroniti Sandstone Mbr
	Taihape Mst		Taihape Mst		?unnamed Zst		Raupirau Zst	
	Matahiwi Sands						Matahiwi Sst	Matahiwi Sandstone Mbr
							Ranana Mst	
uWo	Jerusalem Sands					Matemateaonga Group	Jerusalem Sst	Jerusalem Sandstone Mbr
lWo	Reef-Bearing Sands						Otuitahi Sst	Matemateaonga Formation
	Pipiriki Sands						Mangataunoka Zst	
uTk							Kahanui Mst	Various divisions
lTk							Popotea Sst	defined (see Chapter 3)
							Kabura Zst	
							Ramanui Sst	

NB: The upper Kapitean (uTk) - lower Opoitian (lWo) boundary approximates the Miocene-Pliocene boundary.

Figure 4:3. Historical lithostratigraphic nomenclature for the latest Miocene and Pliocene strata of the Wanganui River section and that proposed in this study. Dashed lines indicate approximate lowermost extent of study.

4:3:3 STRATIGRAPHY

Figure 4:4 summarises the exposed stratigraphy. However, the scale of this section is such that to accurately illustrate and record the detailed lithostratigraphy it has been necessary to subdivide the section into six map sections. Each of the six maps illustrates a detailed stratigraphic column, with pertinent sample information recorded on it (Maps 6-11). The lithostratigraphy of the Jerusalem, Matahiwi and Koroniti Sandstone Members is idealised on these maps and in Figure 4:4. Detailed columns for these sandstone members are given in Section 4:4.

4:3:4 LOWER AND UPPER BOUNDARIES

For the Wanganui River section the lower boundary of the Tangahoe Formation occurs at the base of the c. 1 m thick glauconitic siltstone above the uppermost shellbed of the Matemateaonga Formation. This glauconitic siltstone marks an abrupt change from sandstone to siltstone that characterises the Matemateaonga/Tangahoe Formation boundary. The lower boundary of the Tangahoe Formation is well exposed at road level, just south of the bridge over the unnamed stream at R21 847839 (at the time of study the bridge over the stream carried a label Otoutahi Stream; however, no name is used on either the 260 or 270 series maps). The boundary is also accessible, but poorly exposed, at river level along the western bank of the Wanganui River, with the glauconitic siltstone dipping below water level 200 m south of the Churton Farm swing bridge (private; R21 876815), approximately 1.5 km north of Jerusalem village. This glauconitic siltstone offered the only opportunity to obtain a numerical radiometric age. However, the occurrence of significant quantities of vermiculitic glauconite (≈20%) in the glauconite concentrate (see Appendix 1 for methodology) precludes the use of potassium/argon dating due to problems with inheritance from the parent micas (see papers within Odin, 1982).

Figure 4:4 (opposite page). Composite stratigraphic column for the Tangahoe Formation within the Wanganui River section showing the distribution of facies and extent of the maps (end of Chapter 2). The illustration of the Jerusalem, Matahiwi and Koroniti Sandstone Members is idealised; detailed columns for these units appear in Section 4:4. Age control is derived from information in Chapter 2. A.S. = Ahurangi Sandstone, M.F. = Matemateaonga Formation

Wanganui River Section, Wanganui Basin, New Zealand

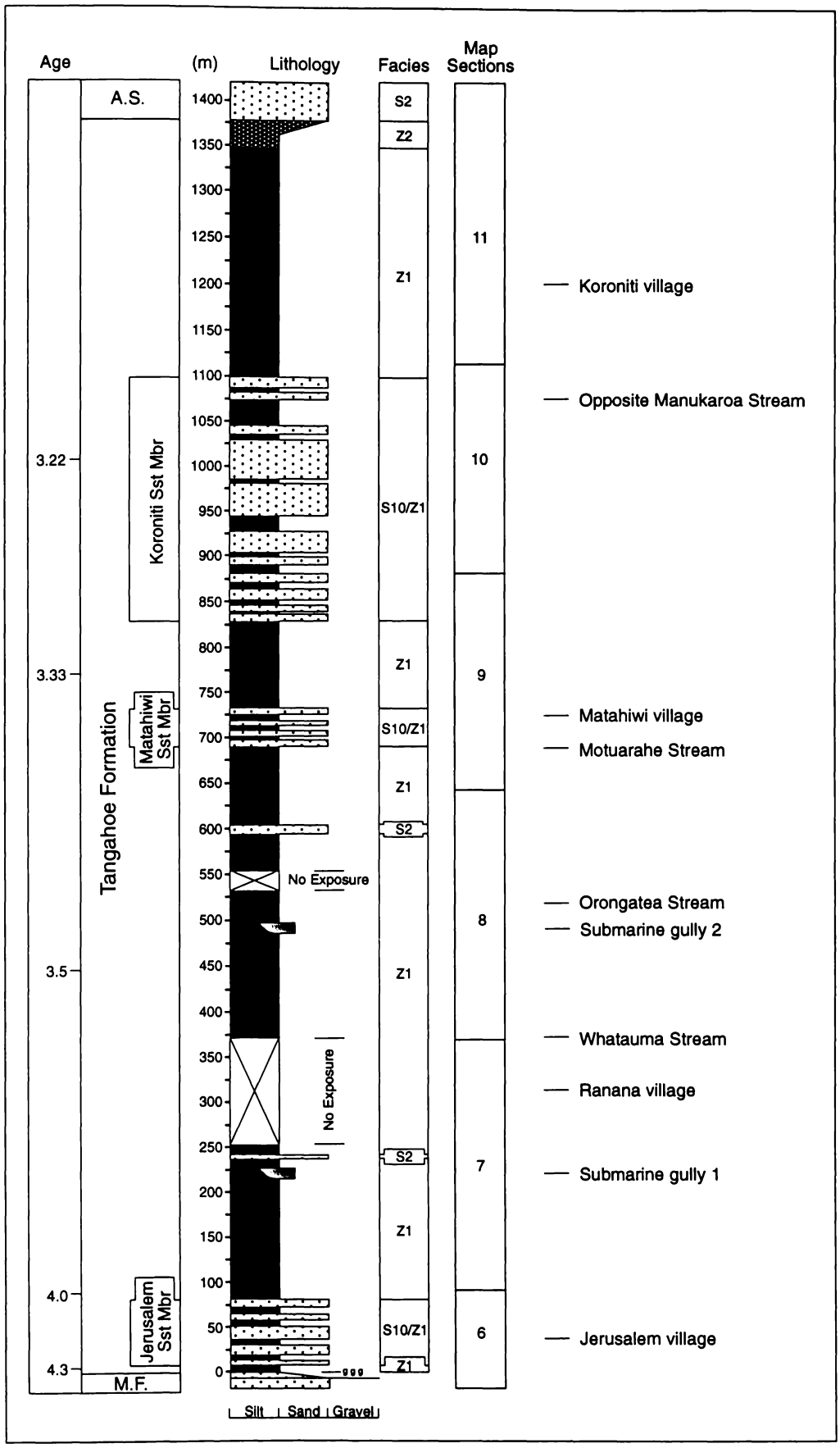

Feldmeyer *et al.* (1943) defined the upper boundary of the Taihape Mudstone in the Rangitikei River section as the boundary with the Utiku Sandstone (Utiku Group of Journeaux *et al.*, 1996). However, to the west of Rangitikei River valley the Utiku Sandstone pinches out and could not be identified in the Wanganui River section. Collen (1972), using the stratigraphy of Feldmeyer *et al.* (1943), placed the top of the Taihape Mudstone at the base of the Koroniti Sandstone, while Ker (1973) recorded an unnamed siltstone that is probably the equivalent of Tangahoe Formation at the base of the Koroniti Sandstone.

In this study the top of the Tangahoe Formation is defined by a transition (≈15 m) from siltstone to sandstone of the Ahurangi Sandstone. While it is unusual to place a major formational boundary at the base of a sandstone in what initially appears to be a succession of sandstone-mudstone dominated units, the difference in nature between the Tangahoe Formation sandstones and the Ahurangi Sandstone and the inferred change in depositional environment warrants it (Table 4:1). Unlike the Tangahoe Formation sandstones, the Ahurangi Sandstone is not composed of interbedded siltstone and sandstone, but solely of bedded sandstone. Microfaunal analyses of the siltstone beneath the Ahurangi Sandstone (sample W962475, data in Appendix 2, location shown on Map 12) indicates a significant shallowing from upper slope to mid/outer-shelf paleoenvironments, coinciding with the transition to sandstone.

The Tangahoe/Ahurangi boundary is equivalent to the Otui/Ahurangi boundary of Ker (1973) and Wilson (1993), and the Raumati/Ahuahu boundary of Collen (1972). The location of the boundary, as defined by Ker (1973) at R21 847839, is maintained. However, exposure of the succession leading up to this boundary is poor along the Wanganui River Road. More continuous sections can be obtained by working up one of the streams that flow into the Wanganui River in a zone that extends approximately 4 km north of the location of the boundary on the road. In this study, the Oporiki Stream and its tributaries (Map 11) were used.

Table 4:1. Summary of some of the differences between the sandstones of the Tangahoe Formation and the Ahurangi Sandstone.

Sandstones in the:-	Tangahoe Formation	Ahurangi Sandstone
Basal boundary	Sharp (mm)	Gradational (≈15 m)
Sedimentary structures	Flames and rip ups	dm bedding
Thickness	Up to a few 10s of m	≈195 m
Depositional environment	Upper slope (200-600 m)	Shelf (100-200 m)

4:3:5 THICKNESS

The total thickness of Tangahoe Formation in the Wanganui River section is c.1350 m (Figure 4:4). Feldmeyer *et al.* (1943) gave a thickness of c. 4800 feet (1450 m) for the same interval. Subsequent workers (e.g. Collen, 1972; Thompson *et al.*, 1994) mainly used thickness values obtained by Feldmeyer *et al.* (1943). The Parakino-1 well log of St John *et al.* (1964) was considered and, without detailed re-analysis, appears to give a thickness of 950 m for the Tangahoe Formation.

4:3:6 LITHOLOGY

The Tangahoe Formation is characterised by massive blue-grey siltstone in which rare macrofossils (bivalves, predominantly *Atrina* sp.) and a variety of concretions occur. Small random concretions tend to be spherical and up to 50 cm in diameter, while larger ones become elliptical with long axes up to 1 m and thicknesses up to 50 cm. Other concretions have formed along distinct layers, with the whole layer concreted or composed of numerous individual concretions up to 50 cm thick and 2 m long. The massiveness of this formation is probably a function of extensive bioturbation, as evidenced by occurrence of organic hieroglyphics.

So as to determine the correct grain-size terminology to be used for the Tangahoe Formation (i.e. mudstone versus siltstone) the grain-size of 218 fine-grained samples from the Tangahoe Formation was analysed using a Malvern Laser-sizer (Appendix 1 for methodology). While subsequently a problem due to the presence of mica was realised (Supplement 1 at the end of this chapter), the effect is unlikely to be significant because of the low mica content throughout the Tangahoe Formation samples. The average texture of these samples is shown in Figure 4:5, and indicates a dominance of silt-sized (4-8 ϕ, 63-4 μm) particles. A breakdown of the silt fraction shows that fine silt (6-7 ϕ, 16-8 μm) is the modal grain-size (Figure 4:6). To determine the appropriate classification of these silt-dominated samples, each analysis was plotted on a Folk sand-silt-clay triangular plot (Figure 4:7), using the Udden-Wentworth grain-size scale (i.e. where sand = <4 ϕ (>63 μm), silt = 4 to 8 ϕ (63-4 μm) and clay = >8 ϕ (<4 μm)). Figure 4:7 shows the samples group well, with the cluster straddling the siltstone-mudstone division. However, the bulk of the samples classify as siltstone, and thus siltstone is the appropriate terminology to use for the fine-grained sediments of the Tangahoe Formation. The minimal

spread of sample points in Figure 4:7 highlights how uniform the grain-size is for the siltstones of the Tangahoe Formation.

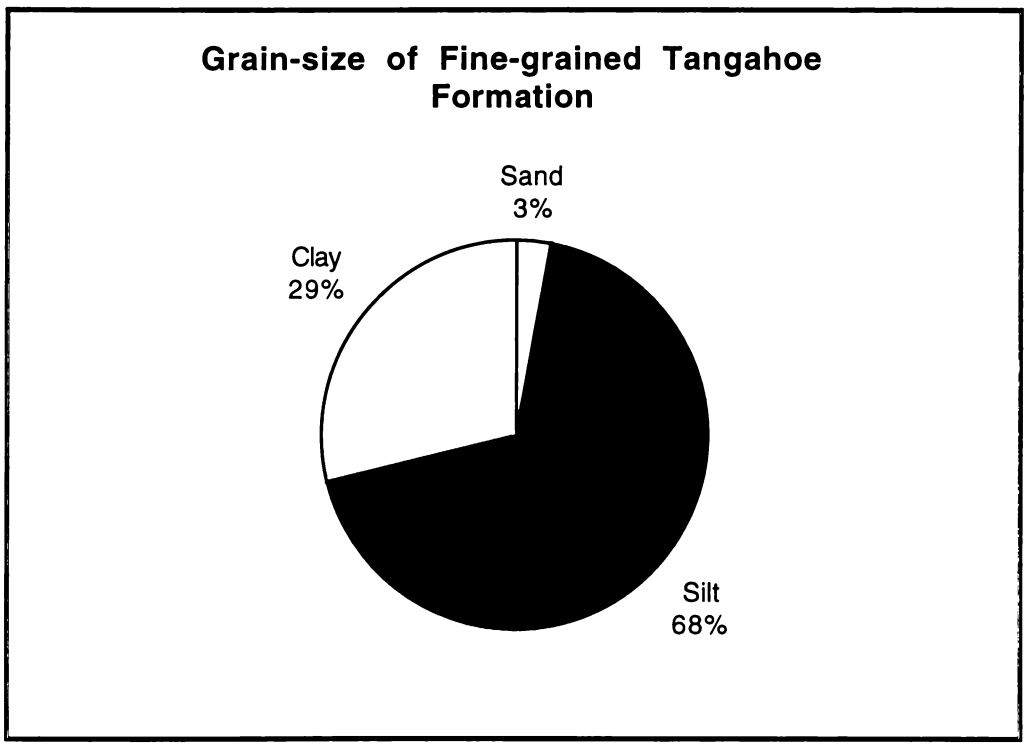

Figure 4:5. Average texture of the fine-grained deposits in the Tangahoe Formation. Raw data in Appendix 2: Particle size. (n=218)

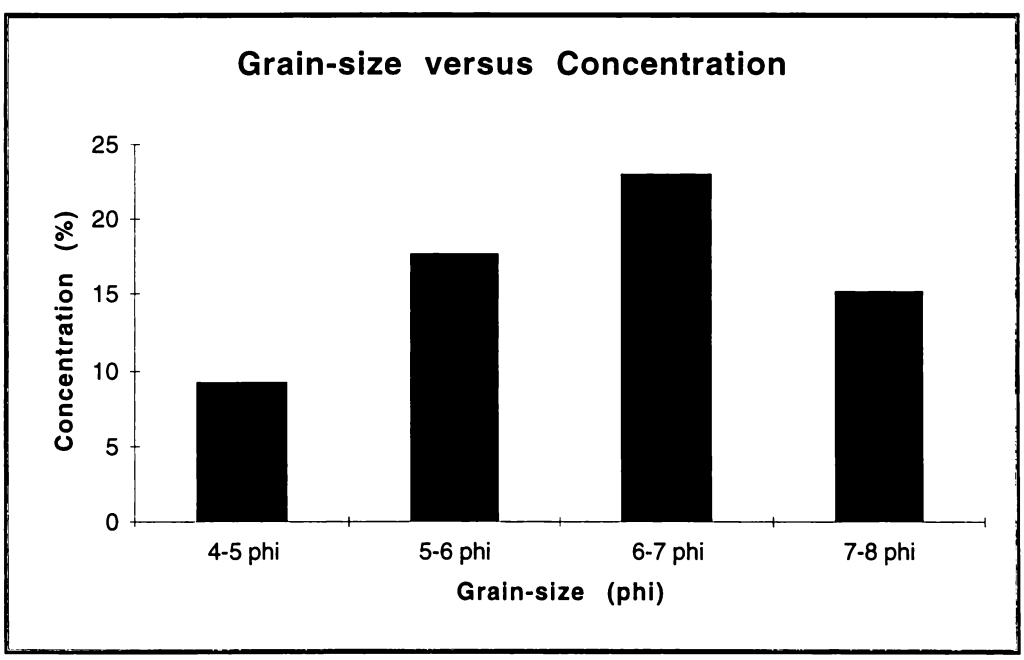

Figure 4:6. Average concentration of particles within each of the silt-size classes on the Udden-Wentworth scale for siltstone samples from the Tangahoe Formation. Coarse silt - 4-5 ϕ, medium silt - 5-6 ϕ, fine silt - 6-7 ϕ, and very fine silt - 7-8 ϕ. (n=218)

Konert and Vandenberghe (1997) undertook a comparative analysis of silt and clay sized materials using the classical pipette method and a laser particle sizer. While ground rock powder gave very similar results, the results from the laser sizer for platy clay particles show that the clay percentage was significantly underestimated by comparison with the pipette method. The correction for the laser sizer was determined as being an increase in the relative grain-size of the clay to the 8 μm level. If this "correction" was applied to the Tangahoe Formation samples, there would be a significant increase in the clay percentage (Figure 4:8) and a shift in sample classification to mainly mudstone (Figure 4:9). However, this "correction" was determined using samples of purely clay sized particles. As the fine-grained Tangahoe Formation is composed of a variety of particle sizes, the applicability of this "correction" is uncertain. The primary reason for this uncertainty is whether or not all of the very fine silt class is clay, or if it is a mixture of clay and silt. If the former is the case then the correction stands, but if the latter is the case, some form of scaled correction factor will need to be determined to give a true particle-size distribution. While there is some debate over the appropriateness of this "correction", raw results give mean values in the range expected from field observations. In terms of internal variability in particle-size distribution between samples, the "correction" can be ignored as the samples have been analysed using the same assumptions. Thus the raw results are adequate for the aims of this study.

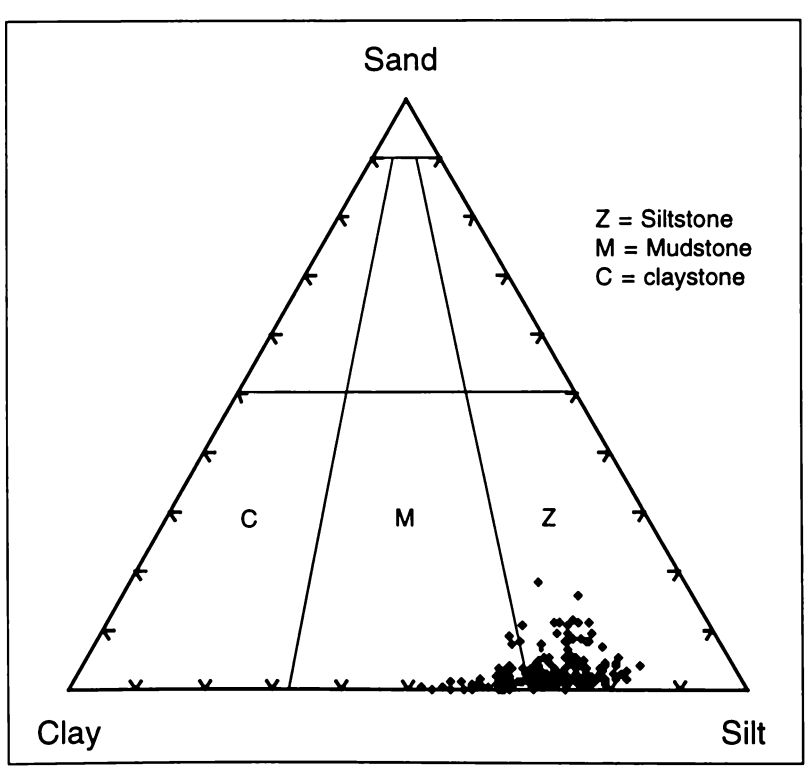

Figure 4:7. Folk textural classification tri-plot showing the distribution of fine-grained samples from the Tangahoe Formation. (n=218)

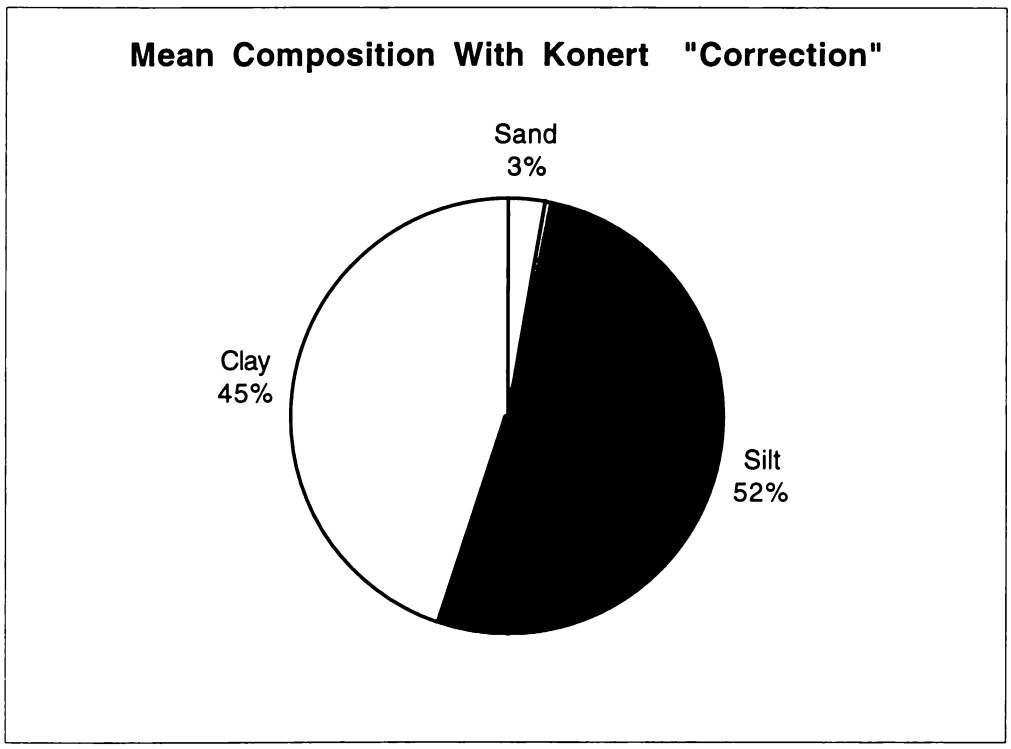

Figure 4:8. Average texture of the fine-grained Tangahoe Formation samples with the Konert "correction" (i.e. silt 4-7 ϕ, 63-8 μm) applied. (n=218)

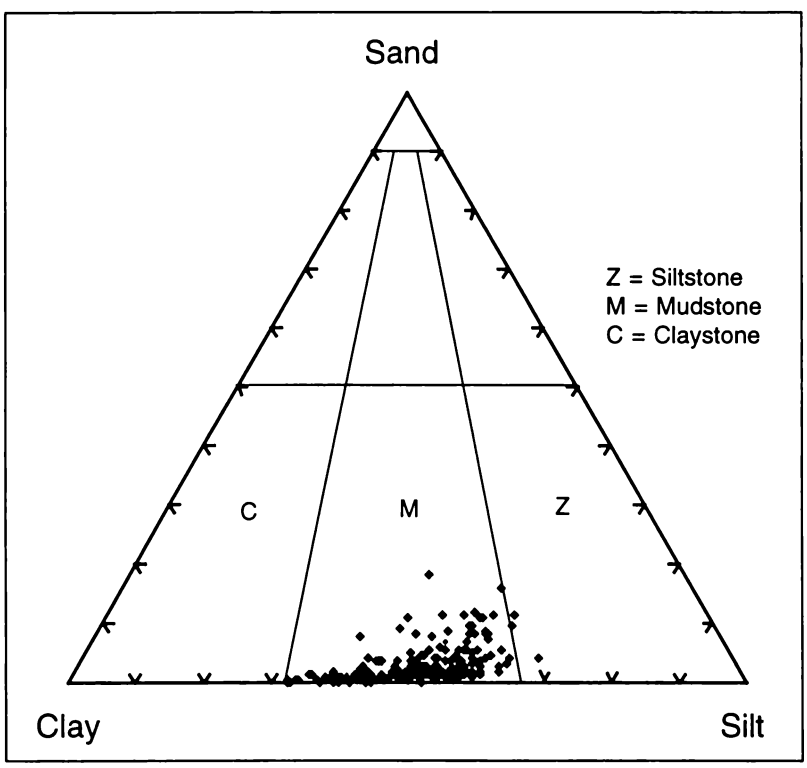

Figure 4:9. Folk textural classification tri-plot showing the distribution of fine-grained samples from the Tangahoe Formation with the Konert "correction" (i.e. silt 4-7 ϕ, 63-8 μm) applied. (n=218)

Within the Tangahoe Formation occur three prominent units, the Jerusalem, Matahiwi and Koroniti Sandstone Members (Figure 4:4). Each of the units is composed of multiple, sharply based, well sorted sandstones interbedded with typical Tangahoe Formation siltstone. These sandstones are later argued to be mass-emplaced deposits (Section 4:4).

4:3:7 FACIES TYPES

The diagnostic characteristics of the lithofacies are described according to their (a) physical description, and (b) paleontological content.

4:3:7:1 Siliciclastic Siltstone Lithotype

FACIES Z1 - (a) Barren to sparsely fossiliferous, massive, bioturbated, slightly micaceous (<1%), variably concretionary siltstone.

(b) Microfauna are dominantly benthic foraminifera, with planktic foraminifera commonly making up just over 10 % of the assemblage. Typically samples contain significant numbers of the following benthic foraminifera: *Anomalinoides parvumbilius*, *A. subnonionoides*, *Astrononion parki*, *Bolivinita* spp., *Bulimina* spp., *Cibicides deliquatus*, *C. molestus*, *Evolovocassidulina orientalis*, *Lenticulina* spp., *Notorotalia* spp., *Oridorsalis tenera*, *Pullenia bulloides*, *Uvigerina miozea* group, elongate Nodosariids, *Hauslerella parri*, *H. pliocenica* and *Karreriella cylindrica*.

FACIES Z2 - (a) Weakly lithified, blue-grey, massive, bioturbated, micaceous (<1%), fine sandy siltstone. Barren to sparsely fossiliferous and rarely concretionary.

(b) Microfauna are dominantly benthic foraminifera, with planktic foraminifera commonly making up about 10 % of the assemblage. Typically samples contain significant numbers of the following benthic foraminifera: *Astrononion parki*, *Bulimina* spp., *Cassidulina neocarinata*, *Elphidium charlottense*, *Evolvocassidulina orientalis*, *Hauslerellera parri*, *Notorotalia* spp., *Sphaeroidina bulloides,* and *Uvigerina miozea*.

4:3:7:2 Siliciclastic Sandstone Lithotype

FACIES S2 - (a) Soft, nonfossiliferous, moderately to well sorted, massive, micaceous (1-5%), variably concretionary, fine to medium sandstone.

FACIES S10 - (a) Loose, massive, micaceous (1-5%), fine to medium sandstone. Individual beds vary in thickness (few cm to 10s of metres), and

have sharp, wavy lower boundaries with flame and rip-up structures evident. The upper boundary is marked by a transition (<10 cm) from sandstone to siltstone. Burrowing down from the upper surface is common and typically consists of circular to ovoid, 1-2 cm diameter tubes, initially vertical but becoming horizontal with depth, and penetrating up to 30 cm (Plate 4:1).

(b) Microfaunal analysis was attempted on a number of samples from the sandstones beds (n=12), but all were found to be barren.

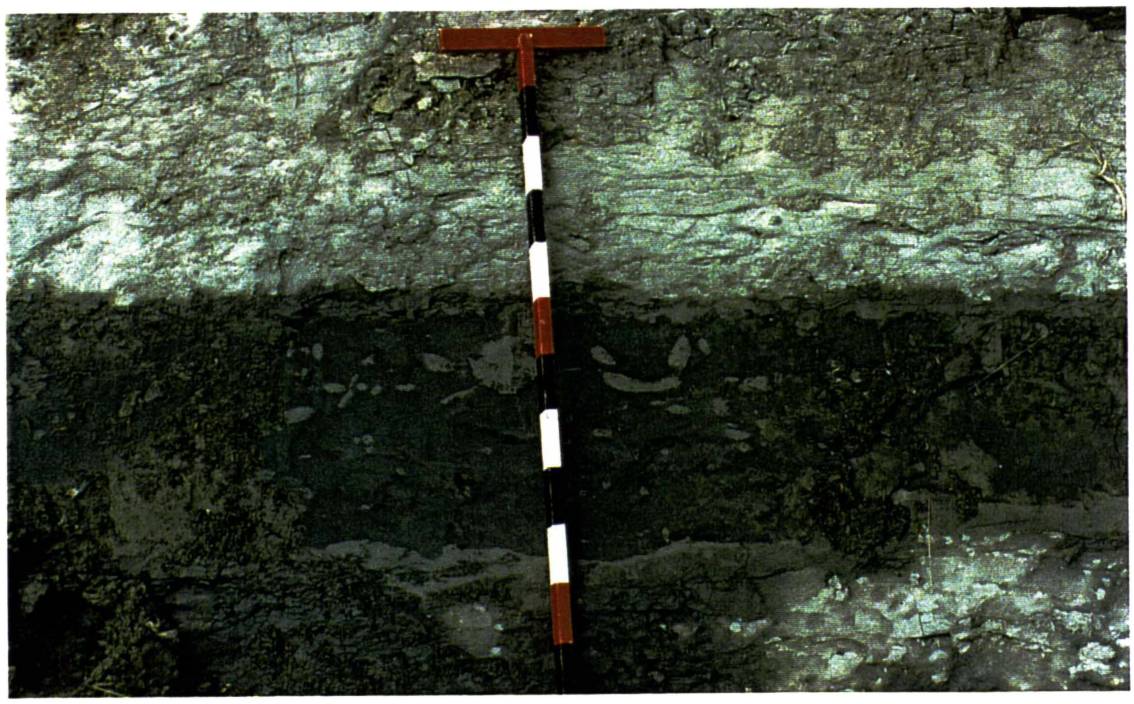

Plate 4:1. Sandstone bed showing extensive burrowing extending down from the upper contact. Also evident is the wavy relief on the sharp basal boundary. Jerusalem Sandstone Member, R21 890807, scale is in 10 cm segments.

4:3:8 Depositional Setting

While the dominant siltstone texture suggests a low-energy depositional regime, this could be any one of a number of environments. Microfaunal census analyses (Appendix 1 for methodology) were undertaken on siltstones throughout the Tangahoe Formation (n=44, sample locations are shown on Maps 6-11 at the end of Chapter 2), including siltstones from within the sandstone members, to help constrain the depositional environment. Comparison of the typical benthic foraminiferal listing of Facies Z1 (which forms the bulk of the Tangahoe Formation) with water-depth diagnostic foraminifera (Figure 4:10) indicates that the Tangahoe Formation was

deposited at upper-slope depths (200-600 m). Planktic foraminifera formed on average 12% of the census assemblages indicating a neritic environment (Hayward, 1986). This apparent incompatibility of determined paleoenvironments (i.e. deep-water and neritic) can be explained by having deposition occurring within a semi-enclosed deep-water (200-600 m) basin (i.e. development of the depocentre has probably occurred within a shallow continental sea-way, similar to Bass Strait, Australia). While hemipelagic fallout would have supplied some sediment, the shallowness of the depositional setting and the high sedimentation rates (Figure 2:6) support the occurrence of processes such as mud plumes where large amounts of material can be deposited very rapidly. The lack of sedimentary structures within the siltstones probably results from extensive bioturbation.

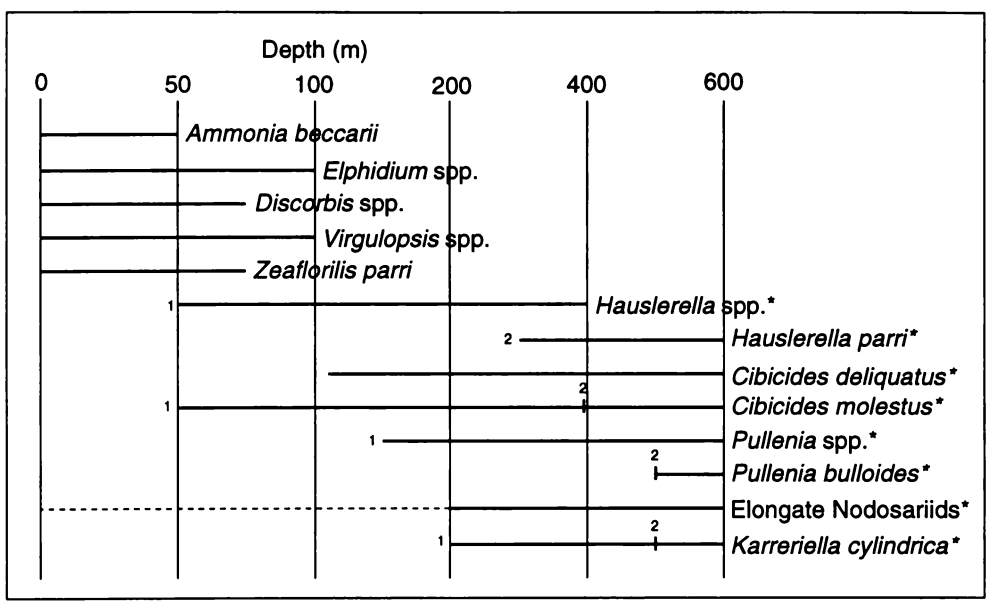

Figure 4:10. Depth range of some key benthic foraminifera used in determining paleo-water depths (after Hayward, 1986; Hornibrook *et al.*, 1989; Crundwell *et al.*, 1994; Hayward *et al.*, 1997). 1 = Hayward (1986), 2 = Crundwell *et al.* (1994), * = commonly observed in census samples from the Tangahoe Formation.

4:4 SANDSTONE MEMBERS WITHIN THE TANGAHOE FORMATION

4:4:1 INTRODUCTION

The Jerusalem, Matahiwi and Koroniti Sandstone Members are three distinctive sandstone dominated units within the massive, blue-grey siltstones of the Tangahoe Formation (Figure 4:4). The sharply interbedded

sandstone/siltstone alternations (Plate 4:2a) of these units have been commented on by others (e.g. Collen, 1972; Ker, 1973), especially in relation to the Koroniti Sandstone Member. However, no mechanism of emplacement or depositional regime has been suggested for the sandstones. In Section 4:3:8 the Tangahoe Formation, and by association the three sandstone members, were interpreted as having been deposited in a deep-water (200-600 m), semi-enclosed basin.

4:4:2 DESCRIPTION

Jerusalem, Matahiwi and Koroniti Sandstone Members are composed of many, micaceous (1-5%), fine to medium, sandstone beds interbedded with massive blue-grey siltstone (Figures 4:11). Individual sandstone beds are very similar in their characteristics and so are treated collectively. The details of these features are discussed below and summarised in Table 4:2.

The basal boundary of each sandstone bed is always sharp and may support some small scale relief (<30 cm), as well as flame structures, indicating an erosive surface (Plate 4:2b). Although the flame structures are typically in the few cm / dm range, they may be much larger (Plate 4:2c) and indicate flow direction to the north and northeast. Mud rip-ups occur mainly near the top of the sandstone beds, but occasionally within the body of the beds as well. The top of each sandstone bed appears to be very slightly undulating and may be extensively burrowed (Plate 4:2d). Distinction between rip-ups and burrows can in some cases be difficult. The burrows occur typically as 1-2 cm diameter (up to 10 cm observed) cross-sections of tubes that vary in aspect from horizontal to vertical and generally occur to depths of less than 30 cm into the sandstone bed (Plate 4d).

Plate 4:2 (opposite page). (**a**) The Koroniti Sandstone Member showing the repetitive sandstone-siltstone alternations that characterise the Tangahoe Formation sandstone members (S21 966733). (**b**) Flame structures within the sandstone beds of the Jerusalem Sandstone Member (R21 888804). Note also the sand filled burrows in the underlying siltstone. (**c**) Large flame structure in the upper part of the Koroniti Sandstone Member (S21 965713). Each segment on scale is 10 cm. (**d**) Burrows at the top of a sandstone bed within the Jerusalem Sandstone Member (S21 966733). (**e**) The variable thickness and pinching out of sandstone beds is clearly visible in the Jerusalem Sandstone Member (R21 888804).

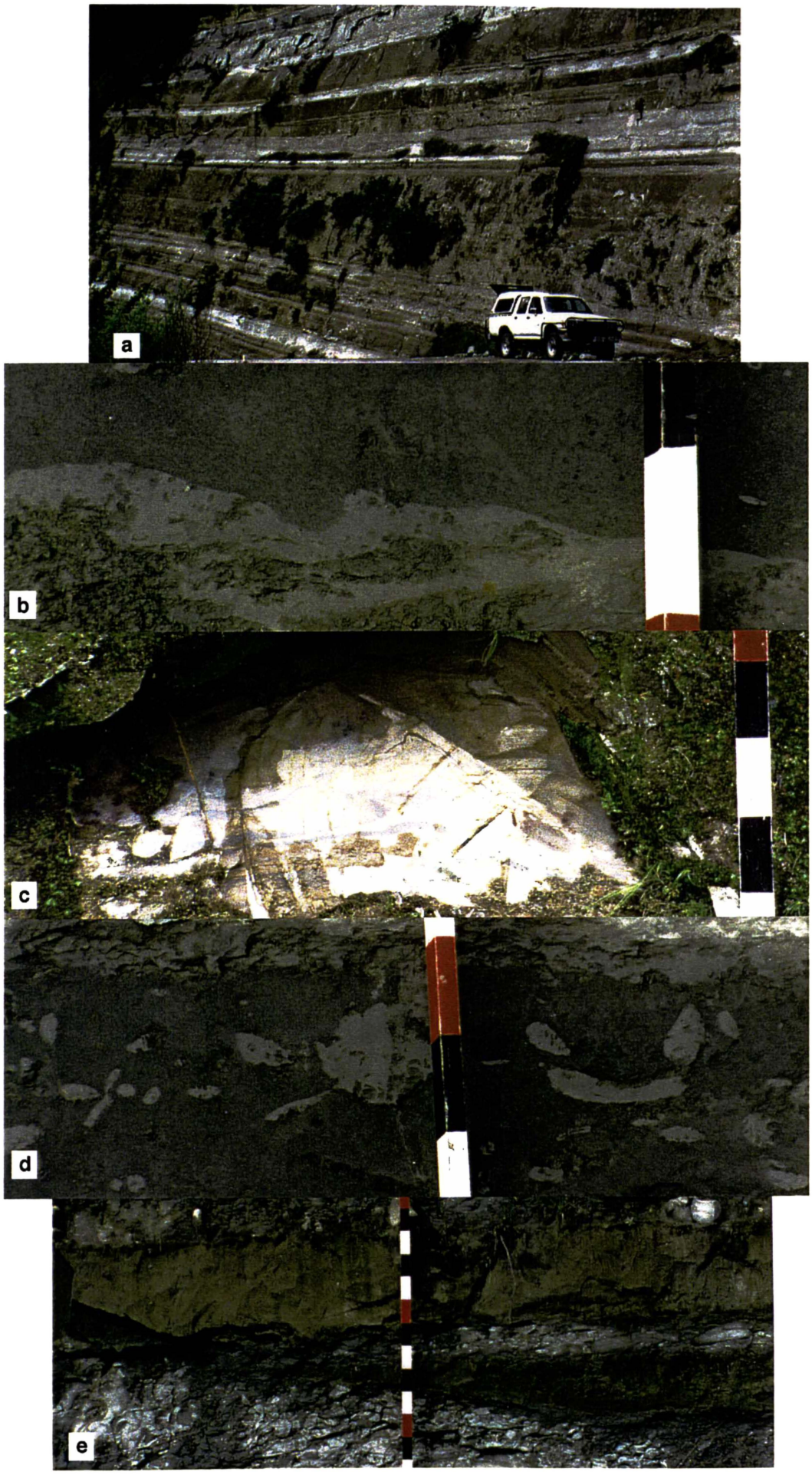
a
b
c
d
e

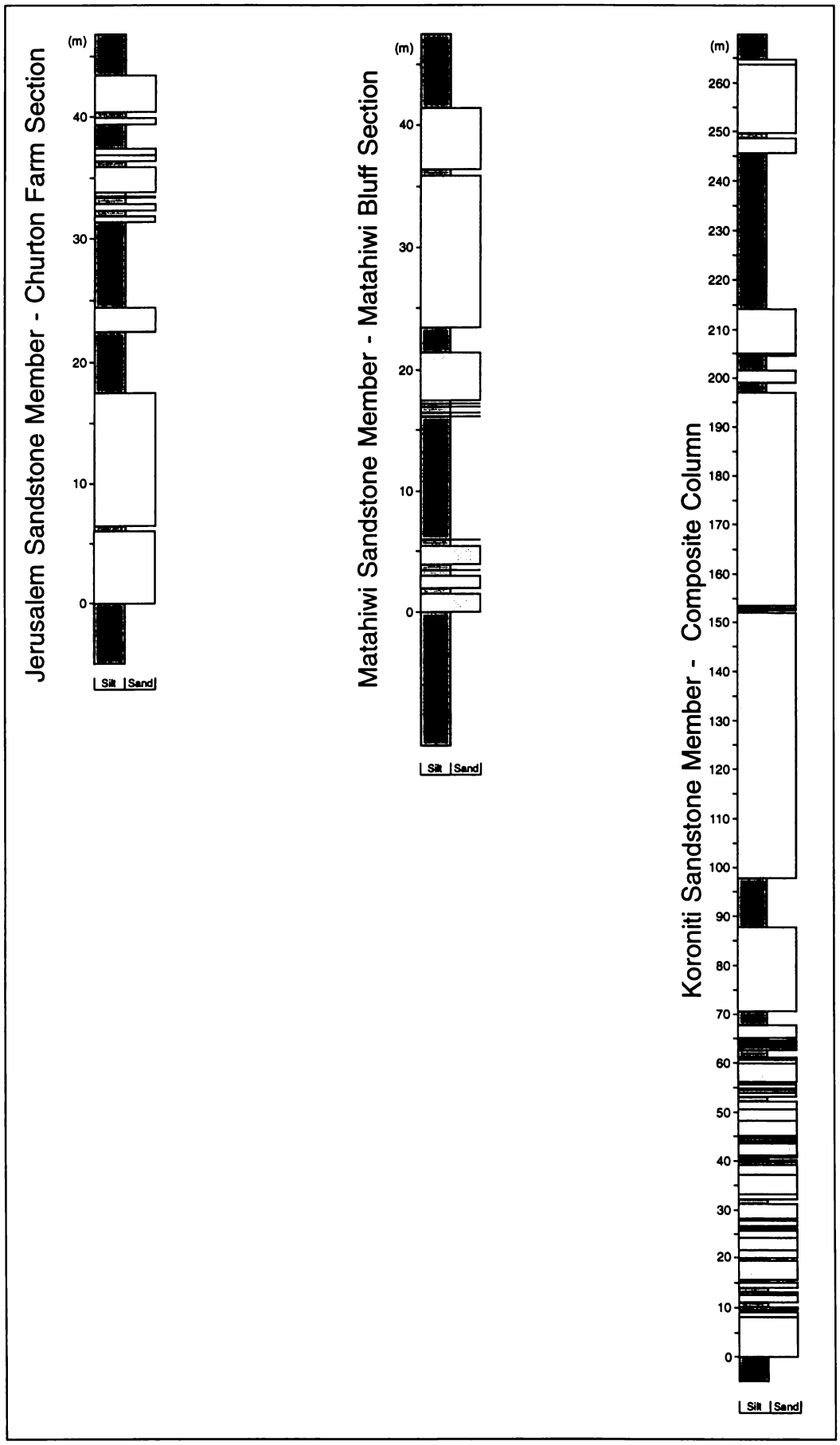
Jerusalem Sandstone Member - Churton Farm Section
(m)
40
30
20
10
0
Silt
Sand
Matahiwi Sandstone Member - Matahiwi Bluff Section
(m)
40
30
20
10
0
Silt
Sand
Koroniti Sandstone Member - Composite Column
(m)
260
250
240
230
220
210
200
190
180
170
160
150
140
130
120
110
100
90
80
70
60
50
40
30
20
10
0
Silt
Sand

Table 4:2. Summary of sedimentary structures in the sandstone beds of the Jerusalem, Matahiwi and Koroniti Sandstone Members.

Zone	Features
Lower Boundary	Erosional, wavy relief up to 30 cm, sharp siltstone to sandstone boundary
Erosional structures	Rip-up clasts
Grading	Restricted to the upper boundary
Upper boundary	Slightly undulating, rapid transition (<10 cm) from sandstone to siltstone
Post-depositional structures	Burrowing, typically restricted to top 30 cm

Apart from flame structures and occasional rip-up clasts, distinctive sedimentary structures, either depositional or post-depositional, are conspicuously absent within these sandstone beds. The only observed grading occurs at the top of each sandstone bed where there is a rapid transition, generally over <10 cm, into siltstone. Sand concentrations of 80-95% are typically obtained by sieve analysis for the sandstone beds, ignoring the graded top (Appendix 2: Particle size). While sieve data illustrate the dominance of > 63 μm particles in these units (80-95%), field observation confirms these results and indicates that the sands within the main body of the sandstone beds are very well sorted. Comparison of sieve and laser-sizer sand concentrations (Appendix 2: Particle size) shows that the laser-sizer consistently gives significantly lower sand percentages than sieve analysis. Subsequently this anomaly has been determined to result from the effect of mica on the grain-size distribution curve (see Supplement 1 at the end of this chapter). This is unfortunate as the detailed assessment of grain-size against various established parameters (e.g. sorting, sedimentation processes) can not be reliably undertaken using the laser particle size data. However data from low mica sediments (e.g. siltstones) has probably only been minimally affected by this problem.

Figure 4:11 (previous page). Stratigraphic columns for each of the three Tangahoe Formation sandstone members exposed within the Wanganui River valley. Jerusalem, R21 875815 - 885812 (Map 6); Matahiwi, S21 957758 (Map 9); Koroniti, S21 965738 - 964705 (Maps 9 & 10).

Commonly sandstone bed thickness is in the 30 cm to 1 m range (Figure 4:12). However, vertical and lateral dimensions of individual sandstone beds are highly variable (Plate 4:2e). An approximately 300 m along strike exposure of the upper part of the Jerusalem Sandstone Member (Figure 4:13), south of Jerusalem (R21 888804-887803), provides an excellent opportunity to record this variability. On a large scale, lateral variability in sandstone bed and intervening mudstone layer thickness has allowed the amalgamation of multiple small sandstone beds into one large unit and the subdivision of large sandstone beds into their component units. The complex interfingering that results from this amalgamating and splitting of sandstone beds is illustrated in the multiple columns that have been obtained for the Jerusalem and Matahiwi Sandstone Members (Figures 4:14 and 4:15 respectively). It is likely that most, if not all, of the thick sandstone beds shown in Figure 4:11 are composite in nature, given the amalgamation evident in Figures 4:14 and 4:15 and the occurrence of thin (< 5 cm) silty stringers within some of the thick sandstone beds that can occasionally be traced into a prominent siltstone layer.

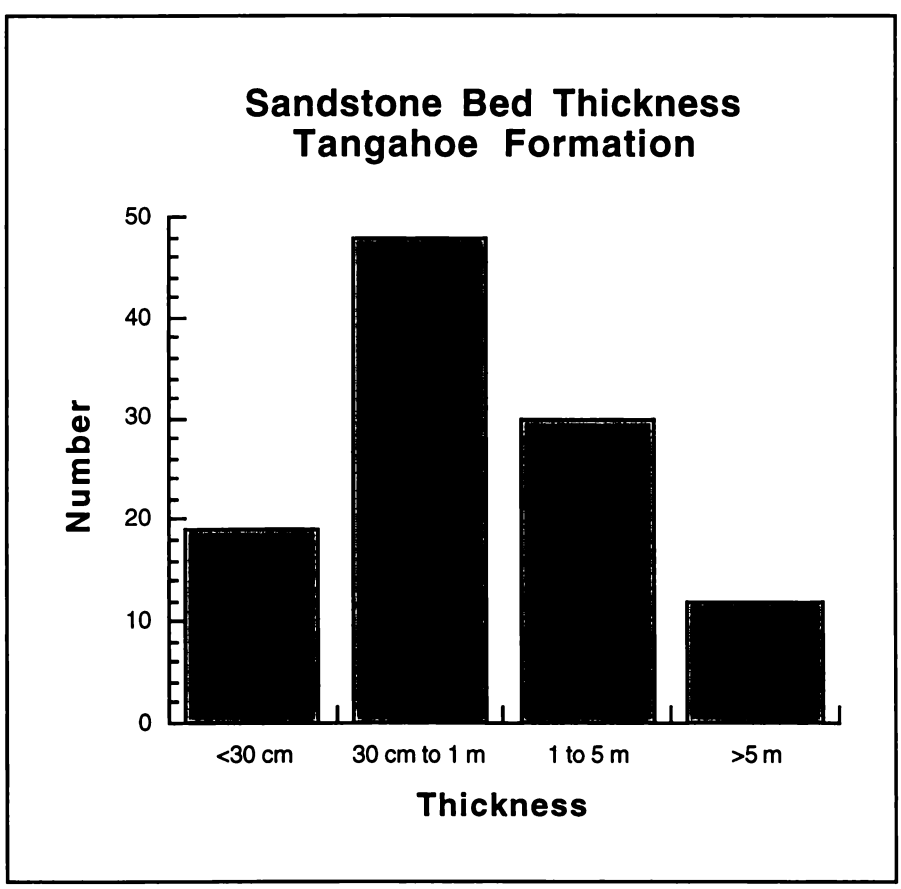

Figure 4:12. The number of beds within each of the sandstone bed thickness groupings for all of the sandstone beds within the Tangahoe Formation as exposed in the Wanganui River valley.

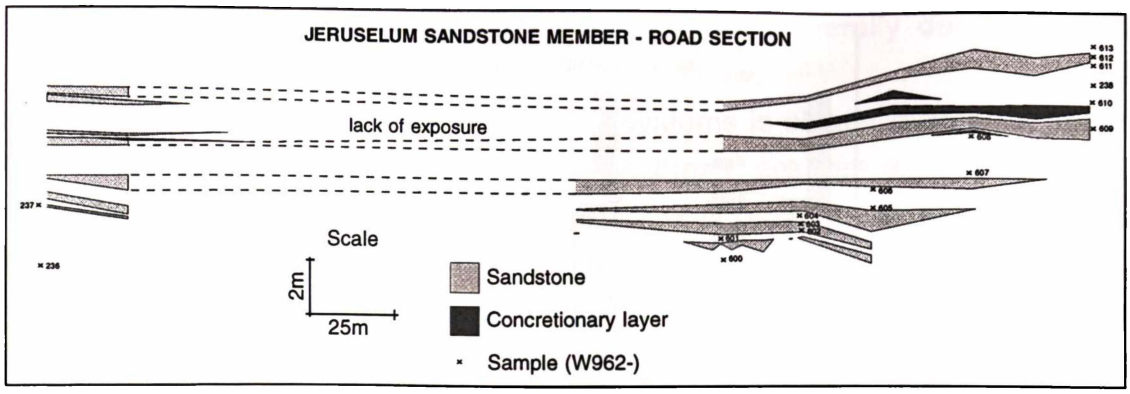

Figure 4:13. Along strike illustration of the Jerusalem Sandstone Member (R21 888804-887803), highlighting the lateral variability of the sandstone beds.

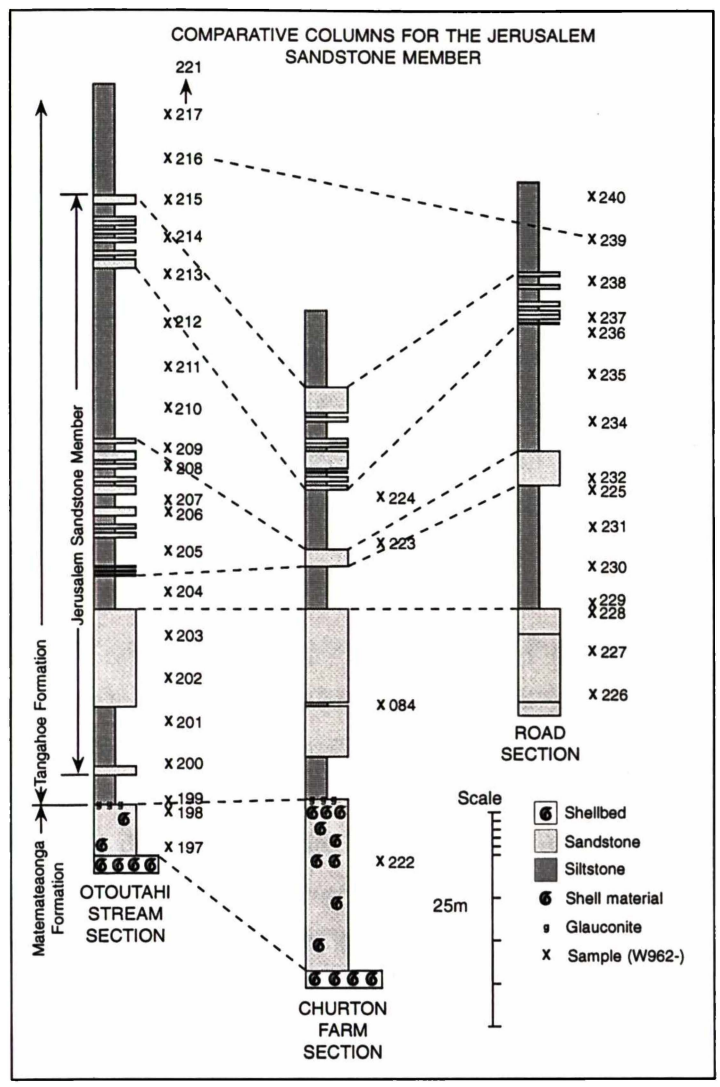

Figure 4:14. The three columns obtained for the Jerusalem Sandstone Member within the Wanganui River valley (Maps 6 & 7 give there locations) illustrate the complex amalgamation and subdivision of units that characterise these deposits. The dashed lines are the interpreted correlations between sections. Some of the correlations between the Churton Farm and Road Sections can be directly observed given the proximity of the sections.

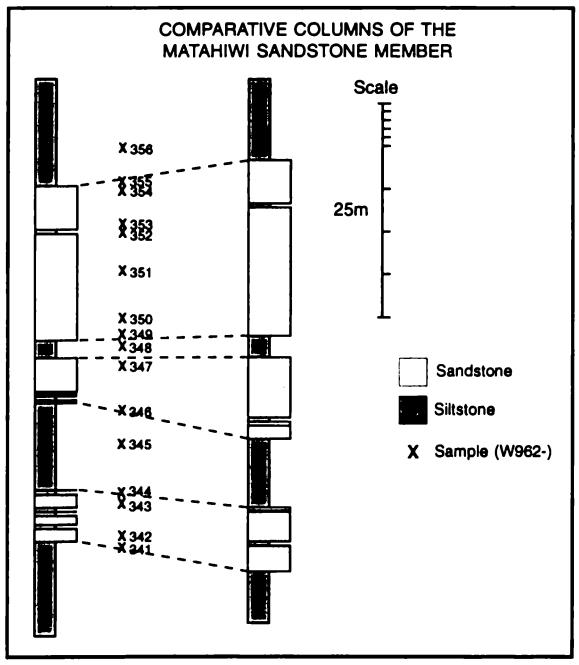

Figure 4:15. Two columns, approximately 200 m apart, through the Matahiwi Sandstone Member from the Matahiwi Bluff section (S21 957758; Map 9), showing the gross variability of the stratigraphy over even small distances. The dashed lines indicate boundaries that have been traced between the two columns.

4:4:3 INTERPRETATION

4:4:3:1 Deposit Type

The sharp basal boundary of the sandstone beds has all the characteristics of being erosional, with the occurrence of flame structures and rip-up clasts (Plates 4:2b-d) in the sandstone beds being particularly good evidence for the occurrence of shear stress and erosion (respectively) during the emplacement of the sandstone beds from mass flows. Such an interpretation is supported by the upper boundary, where there is rapid gradation back into "background" siltstone (over less than 10 cm). The extensive burrowing observed along the top surface of the sandstone beds.

The observed variability in bed thickness is thought to be a function of the interplay between a number of factors, including:

(a) Size of the flow - the larger the flow, the thicker and more extensive the deposit.

(b) Velocity and size of the flow relative to sea-floor topography will regulate whether or not the topography has any effect controlling the distribution of the flow, i.e. is the flow contained within the topography or does it overwhelm (and destroy ?) topographic features.

(c) Proximal-distal relationships - Bed thickness will generally decrease with increasing distance from the point source for the flow.
(d) Channel geometry - infilling of channel systems is clearly evident in some flows (Figure 4:13; Plate 4:2e). Whether these are pre-existing or flow generated features is debatable. However, there is probably an aspect of both processes in these deposits. Related overbank deposits will be present, although their finer-grained nature means that bioturbation may have destroyed much of the evidence for these features - the concretionary horizons shown in Figure 4:13 may be overbank deposits.
(e) Erosiveness of the flow - (i) on a small scale this forms the relief on the basal boundary of the sandstones; and (ii) on a large scale this is one of the major factors involved in the compounding of sandstone beds as it is the mechanism by which the intervening siltstones are removed.

The maximum water depths for the Tangahoe Formation, and consequently the Wanganui Basin floor during this time, are unknown. If the 200-600 m water depths obtained in this study represent depth to basin floor, then the mass-emplaced sandstones of the Jerusalem, Matahiwi and Koroniti Sandstone Members have been deposited on (a) the slope, and (b) across the basin floor. Thus these sandstones represent slope and basin floor fan deposits (relative to the depocentre), even though depth of deposition is somewhat less than is typically implied for basin floor fans.

4:4:3:2 Flow type

Lowe (1976a) and others have recognised that turbidity current theory does not readily explain the development of sandstone bodies lacking normal current structures (e.g. grading and laminations). While rapid sedimentation of coarse liquefied detritus would leave deposits of coarse-grained, relatively clay-free sand lacking normal current structures, water-escape structures are commonly observed (Lowe, 1976b). Thus fluidised and turbidite-type flows appear not to be important mechanisms for the emplacement of the Tangahoe Formation sandstones. This leaves the realm of plastic flows to explain the depositional regime responsible for these sandstones. The fully floated rip-up clasts indicate that intergranular dispersion has been an important aspect of the mechanisms by which the flow has been maintained, supporting a plastic flow categorisation. Within the plastic flow classification there are three general types of flow: grain flows, debris flows and mud flows (Boggs, 1987). Despite the existence of such a simple classification system, sand-rich plastic flows that result in structureless sandstone deposits have been variously labelled, including deposits of high-density turbidity currents or sandy debris

flows (e.g. Shanmugam *et al.*, 1995; Shanmugam, 1996; 1997). In this study the flow type is regarded simply as a grain flow as this best describes the sandstones in outcrop, namely well sorted, no grading, massive, flat top and erosionally based (Boggs, 1987).

4:4:3:3 Emplacement Of Sandstone Beds

Explanation of the development of thick structureless deep water sandstones has typically invoked mechanisms by which to achieve virtual instantaneous emplacement from large flows (e.g. Shanmugam *et al.*, 1994). Recently, Kneller and Branney (1995) have proposed another method of emplacement of sand bodies such as those found in the Jerusalem, Matahiwi and Koroniti Sandstone Members. In the Kneller model, rapid deposition occurs from a prolonged, quasi-steady state plastic flow (Figure 4:16), where stratification development is prevented by the absence of a sharp rheological interface (Figure 4:17) between the base of the flow and the just deposited material (Kneller and Branney, 1995). Steady state flow is defined as a succession of fluid particles through a point fixed in space having identical velocity vectors, the fluid remaining unchanged with time (Kneller, 1995). Rip-up clasts found within and at the top of the mass emplaced sand units probably delineate the unrecognisable depositional boundary that migrated upwards during sedimentation (Kneller and Branney, 1995).

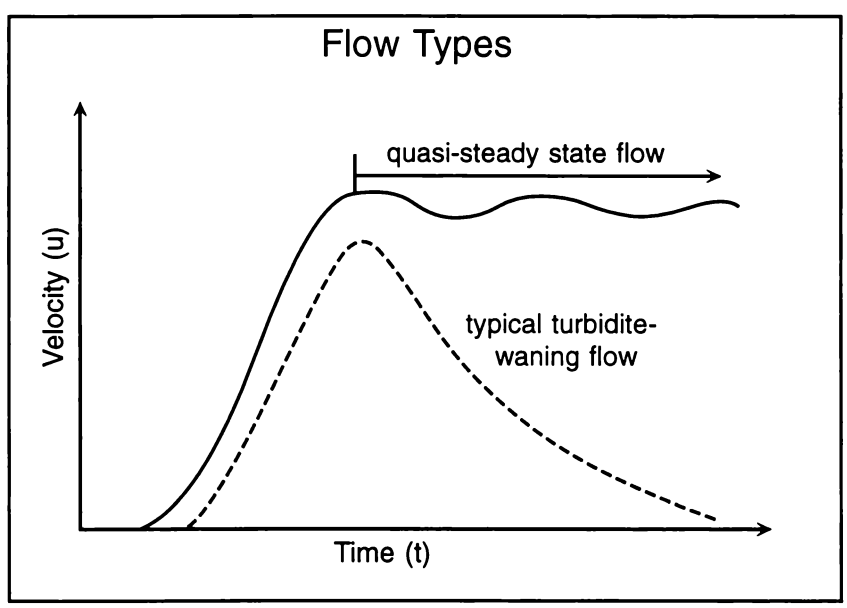

Figure 4:16. Comparison of flow types characteristic of turbidite and Kneller model flows (modified from Kneller, 1995; Kneller and Branney, 1995).

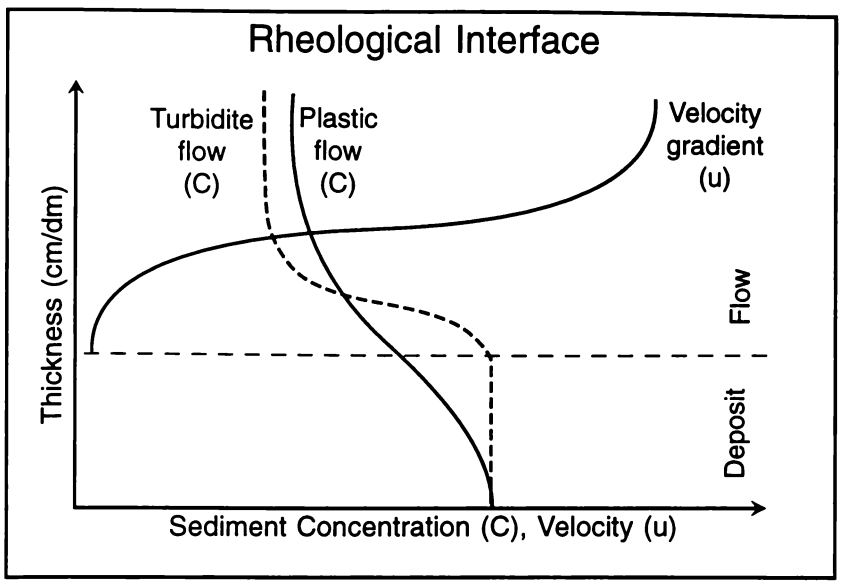

Figure 4:17. Comparison of across depositional boundary behaviour of turbidite and Kneller model flows (modified from Kneller, 1995; Kneller and Branney, 1995).

The Kneller and Branney (1995) model has distinctive advantages, especially when considering the larger units, as deposit thickness is dependent on rate of settling and duration of the flow rather than flow size. In comparison, traditional "freezing" models assume that the thickness of a deposit is directly related to the flow thickness. Another advantage of the Kneller model is that the fundamental concern of how to instantaneously "freeze" a large flow is avoided.

4:4:4 Other Features Relating To The Emplacement Of Mass-Emplaced Sandstones

Deep-water mass-emplaced sandstones are generally fed from the shelf and into the deep-water environment by way of submarine channel systems (Galloway *et al.*, 1991). Although the channel systems associated with the Jerusalem, Matahiwi and Koroniti Sandstone Members have not been observed, two submarine gully features have been noted within the Tangahoe Formation (Figure 4:4). In neither case is the complete channel cross-section observed; rather they are sections across the channel. Both channel sections are approximately 100 m wide, with channel sides sloping between 6-20° (Figure 4:18). Channel fill is not symmetrical, although sandstones define the edge of both channels. Initial deposits parallel the channel sides, however, later deposits infilling the centre of the channel appear to have been laid down approximately horizontally (Plate 4:3; some apparent dip visible).

4:4:5 Across Basin Nature of the Tangahoe Formation Sandstone Members

The earlier suggestion that the Jerusalem, Matahiwi and Koroniti Sandstone Members were better included as members within the Tangahoe Formation rather than as separate units subdividing the Tangahoe Formation is supported by an across basin analysis of the sandstones (Figure 4:19). Formational status implies that the units are continuous and mappable. The discontinuous nature of the sandstone units, in even near-by sections (e.g. Wanganui and Mangawhero in Figure 4:19; Figures 4:14 & 4:15) means that classification at formational status is not justified and highlights the importance of not using these units for correlation. The idealised 3-dimensional model illustrated in Figure 4:20 shows how the mass-emplaced sandstones are likely to be distributed more or less randomly within the Tangahoe Formation.

Plate 4:3. Two views of the northern edge of the second submarine channel at S21 929796. Deposits that approximately parallel the sides of the channel, as well as horizontal beds are present, and represent early and late phases of channel fill respectively.

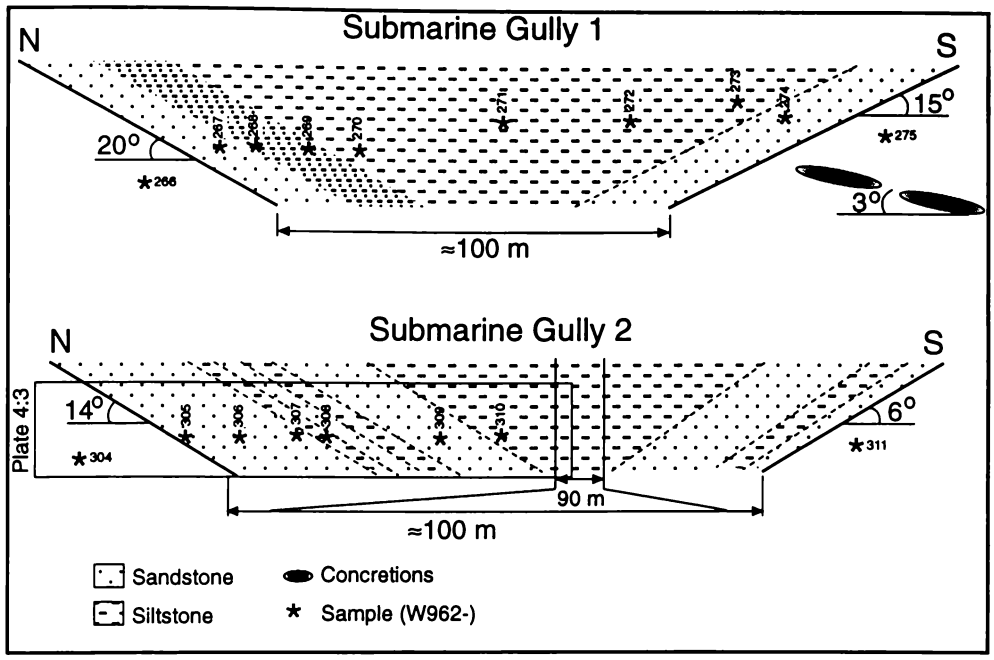

Figure 4:18. Illustration of the Tangahoe Formation submarine gullies seen within the Wanganui River valley. Submarine gully 1 at R21 897788 - 898787, submarine gully 2 at S21 929769 - 932769.

Comparison of lithostratigraphic columns from across the Wanganui Basin shows that the mass emplaced sandstones are concentrated in the central part of Wanganui Basin (Figure 4:19). This is coincident with the area of maximum thickness for the Tangahoe Formation as a whole and probably correlates to the area of maximum tectonic subsidence during the late Opoitian and into the Waipipian.

4:4:6 TIMING

4:4:6:1 Original Sequence Stratigraphic Model

Various papers (e.g. Vail *et al.*, 1977; 1991; Posamentier *et al.*, 1988; Posamentier and Vail, 1988; Van Wagoner *et al.*, 1988; Haq, 1991) have developed and highlighted the basic sequence stratigraphic model, where basin floor fan development has been tied into the lowstand systems tract. However, these models have been developed with the provisions that sea-floor subsidence is constant and increases basinward, a standard shelf-slope-basin physiography exists, and sediment supply is constant. These conditions have all too often been forgotten in the debate on sequence stratigraphy, a situation well highlighted in the Posamentier and James (1993, pg. 16) paper where they state "*The key to proper application of these concepts is to understand the first principles involved and then tailor the sequence*

stratigraphic model to account for local factors such as tectonics, sediment flux and physiography."

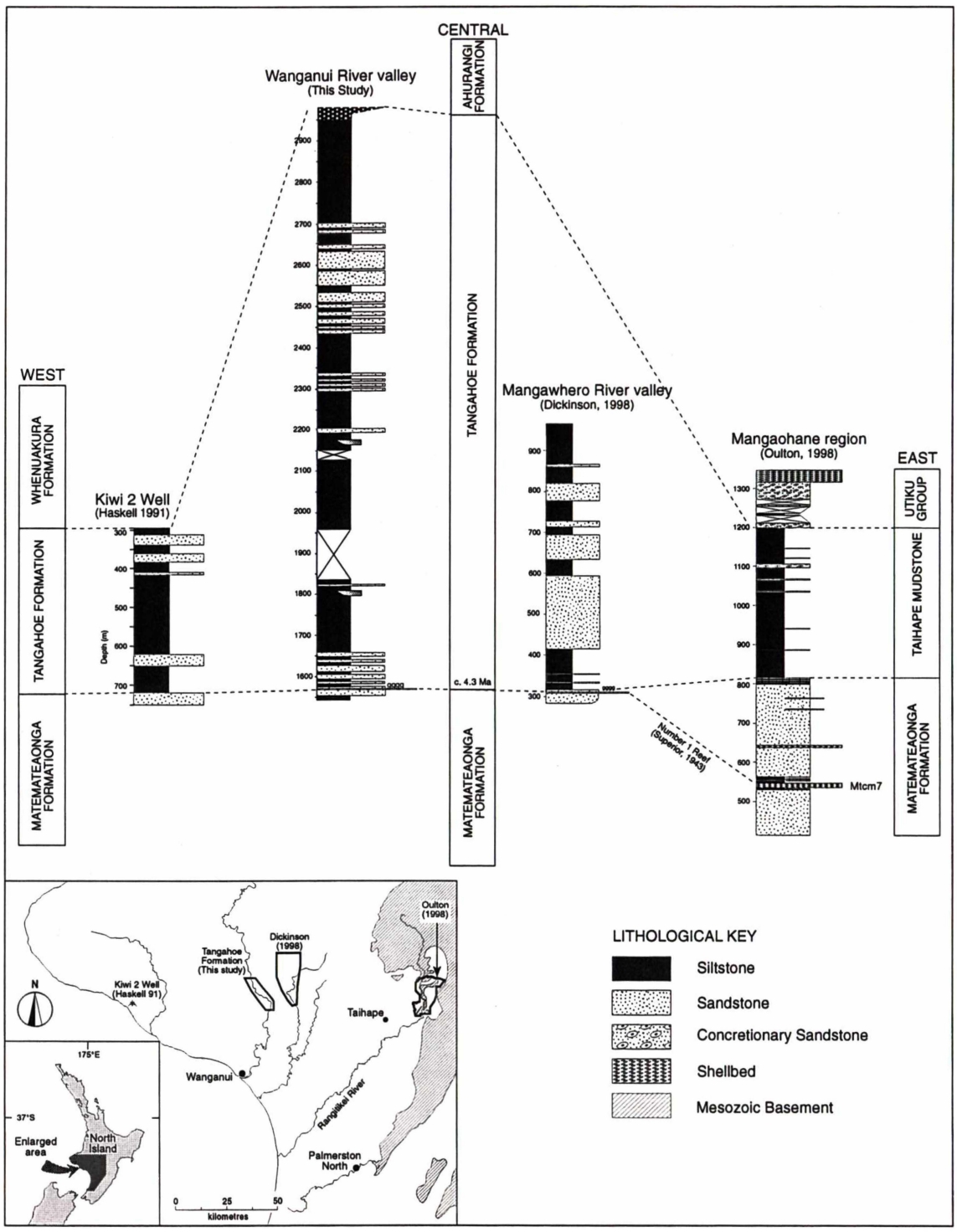

Figure 4:19. Comparison of the Tangahoe Formation and mass emplaced sandstones across the Wanganui Basin (information from Haskell, 1991; Dickinson, 1998; Oulton, 1998).

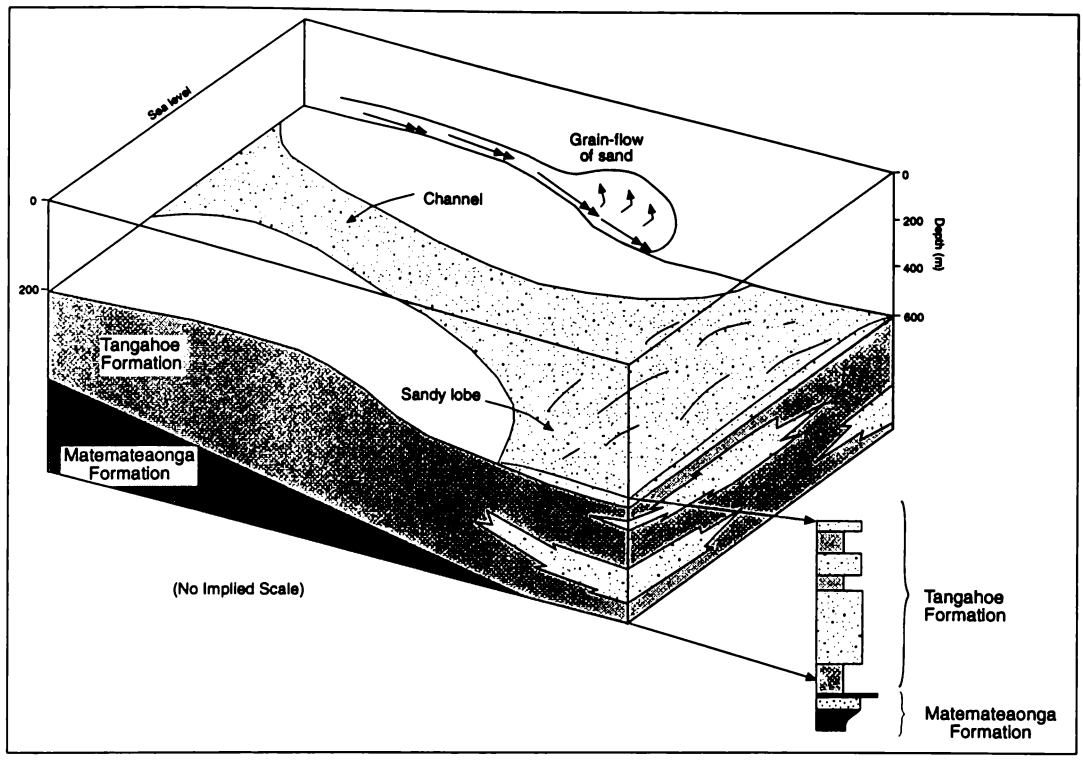

Figure 4:20. Idealised three-dimensional representation of the Tangahoe Formation during deposition (adapted from Pickering *et al.*, 1995).

4:4:6:2 Alternative Sequence Stratigraphic Models

"*In general, eustasy and sea-floor subsidence/uplift determine the timing of sequence bounding surfaces, whereas sediment flux and physiography are most effective in determining the stratal architecture between those bounding surfaces*" (Posamentier and Allen, 1993, pg. 91). There is a widespread realisation in the literature that the types of deposits formed during any particular phase of the relative sea-level curve can be highly variable as exemplified by papers within Macdonald (1991) and Posamentier *et al.* (1993), and by recent papers such as Chough *et al.* (1997) and Church and Gawthorpe (1997).

Within the deep-marine realm, sequence stratigraphic relationships are likely to be driven by sediment supply rather than accommodation, as space is readily available (Martinsen and Helland-Hansen, 1995). Various workers (e.g. Galloway *et al.*, 1991; Helland-Hansen and Gjelberg, 1994) have shown that an over-supply of sediment can cause development of basin floor mass-gravity deposition during all systems tracts. The development of basin-floor fans during the transgressive systems tract, a time of traditionally very low rates of offshore sedimentation, by (a) extension of submarine canyons to allow by-passing (Kolla and Perlmutter, 1993), (b) erosion of sand-rich shelf deposits during transgression (Rivenaes, 1997), or (c) an over-

supply of sediment leading to over-steepening and subsequent down-slope mass-gravity transport (Bruhn and Walker, 1997), highlights the variability in sequence architecture possible.

From the above discussion, it is apparent that emplacement of deep-water sandstones can occur at any stage of the relative sea-level curve, depending upon the interplay of sediment supply, tectonics and glacio-eustatic fluctuations. Some of the possible scenarios are shown in the idealised diagrams in Figures 4:21 & 4:22.

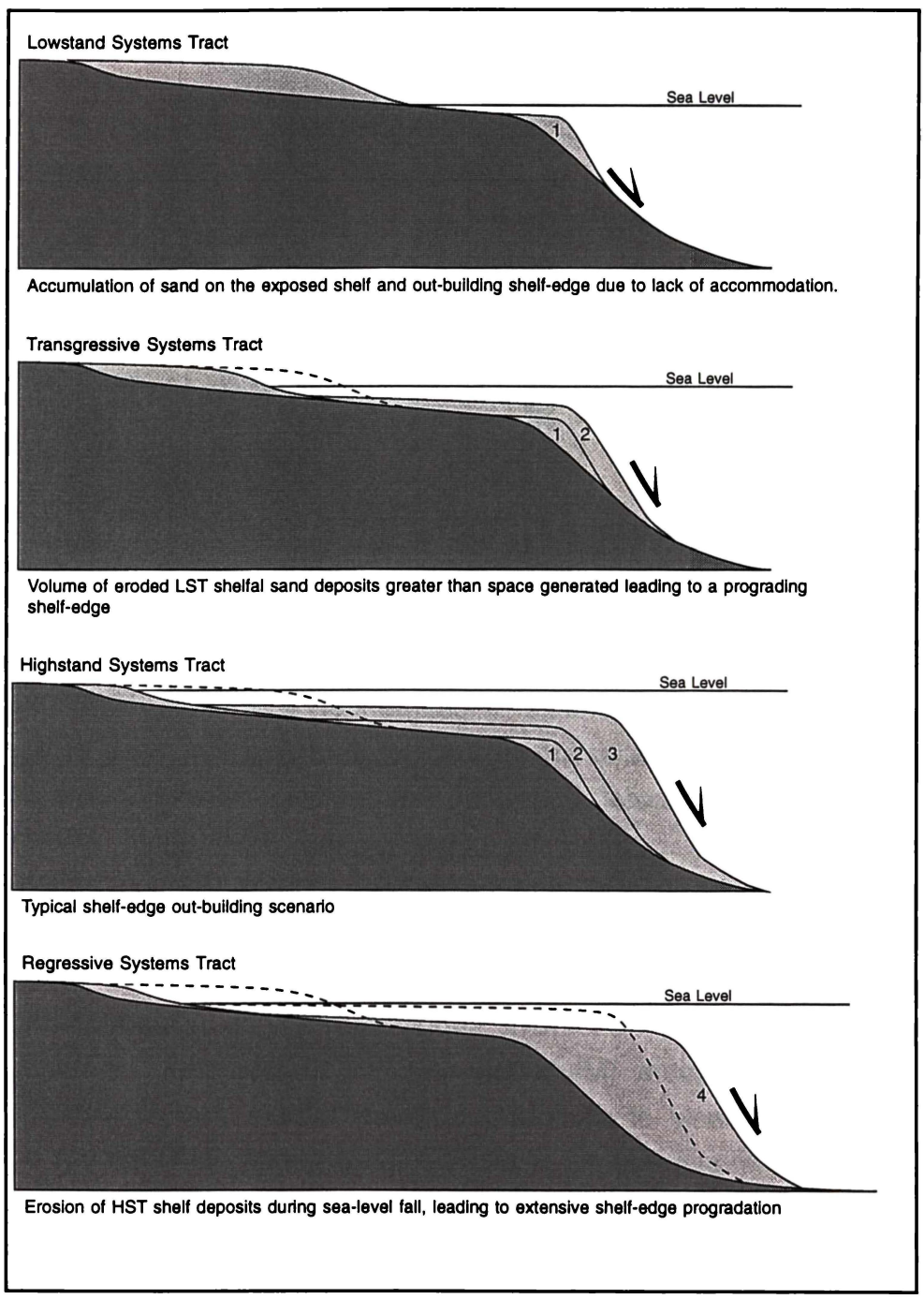

Figure 4:21. Idealised sequence of cross-sections for each of the systems tracts, showing ongoing shelf-edge over-steepening and mass flow deposition where tectonic subsidence in negligible and the sediment flux is high.

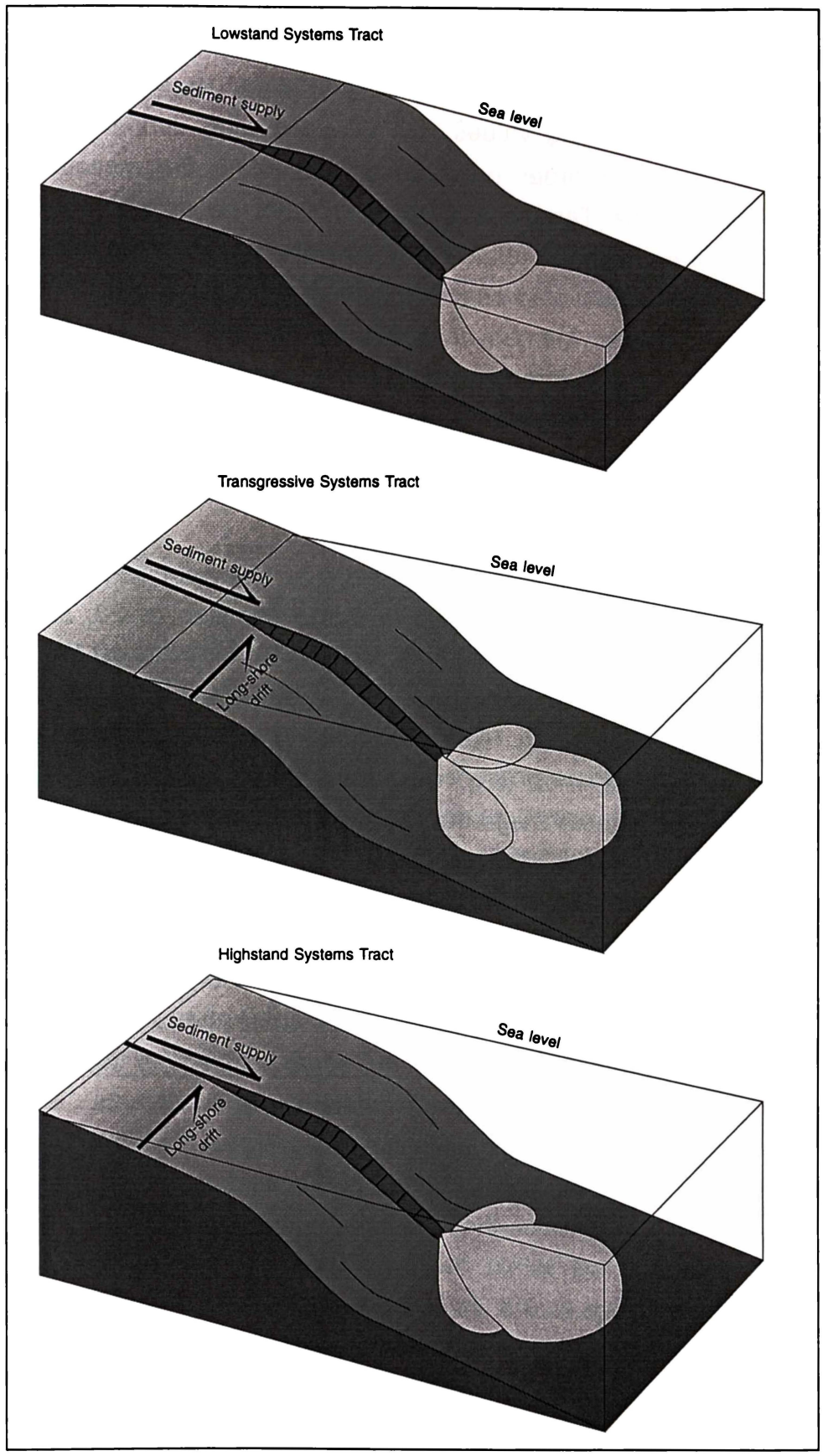

Figure 4:22. Idealised sequence of block diagrams showing sediment by-passing by a submarine canyon during various relative sea-levels.

4:4:6:3 Paleoenvironmental Interpretation Using Isotopes

Stable isotope analyses, especially $\delta^{18}O$, have been widely used to determine paleoclimatic fluctuations (e.g. Clemens and Tiedemann, 1997). Fluctuations in $\delta^{18}O‰$ are related to variations in global ice volume and water temperature, with increasing values of $\delta^{18}O‰$ occurring during ice buildup. Development of a short-order paleoclimatic curve for the mass-emplaced sandstone units of the Tangahoe Formation could determine whether the sandstone members might be related to a particular phase of the relative sea-level curve. To this end a comprehensive suite of siltstone samples from below the Matahiwi Sandstone Member to above the Koroniti Sandstone Member was picked for the benthic foraminifera *Uvigerina miozea* group and *Cibicides deliquatus*. These two foraminiferal species were used because they are common throughout the Tangahoe Formation and they have been used in other paleoclimatic studies (e.g. Tiedemann *et al.*, 1994; Shackleton *et al.*, 1995).

Prepared isotope samples (Appendix 1: Methods) were run on an Europa 20/20 mass spectrometer with replicate samples (n=28, standards) indicating a reproducibility of better than ±0.05‰ for $\delta^{13}C$ and ±0.1‰ for $\delta^{18}O$ (Appendix 2: Isotopes). These values are the same as achieved by other workers on this equipment (e.g. Hendy *et al.*, 1997) and the Waikato University Isotope Laboratory as a whole (e.g. Nelson and Smith, 1996).

The results for both *Uvigerina miozea* group and *Cibicides deliquatus* analysis are plotted on $\delta^{13}C‰$ versus $\delta^{18}O‰$ plots (Figures 4:23 & 4:24 respectively). Most samples cluster in a slightly positive $\delta^{13}C$ and $\delta^{18}O$ zone, but several trend away to moderately negative $\delta^{13}C$ and $\delta^{18}O$ values. Comparison of Figures 4:23 & 4:24 with the general isotope fields developed by Nelson and Smith (1996) (Figure 4:25) indicates that the clusters occur within the temperate marine field while the observed trend is towards values expected for carbonates produced in meteoric environments. The post-depositional alteration of biogenic tests in some samples is unfortunate but not totally unexpected given the porous nature of the sandstone beds interbedded within the siltstones from which these samples were obtained.

Samples that fell within the boundaries of the "acceptable" fields delineated in both Figure 4:23 & 4:24, the isotopic limits of which are given in Table 4:3, are plotted against the corresponding stratigraphy in Figure 4:26. Due to the loss of data with the removal of suspect samples (which occurred throughout the column), a rather patchy picture emerges in which no significant trends are apparent. However, there does appear to be a slight increase in $\delta^{18}O$ leading into some of the sandstones, which would support a degree of cooling leading up to the sandstones, although the fluctuations are

small (0.6). Such a lack of any distinct trends in the data may be due to a number of interacting factors including (a) timing of the sandstone members is independent of short-order sea-level fluctuation, and (b) alteration of the foraminiferal tests has been sufficient to destroy any paleoenvironmental signal.

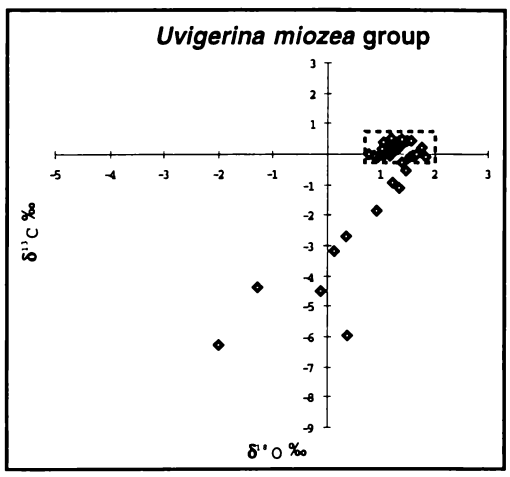

Figure 4:23. $\delta^{13}C‰$ versus $\delta^{18}O‰$ plot for *Uvigerina miozea* group, showing a distinct group at the head of a trend towards isotopically negative values.

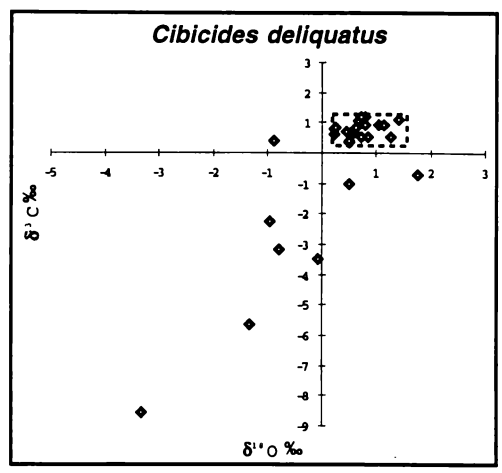

Figure 4:24. $\delta^{13}C‰$ versus $\delta^{18}O‰$ plot for *Cibicides deliquatus*, showing a distinct group at the head of a trend towards isotopically negative values.

Table 4:3. Limits used to determine the designated unaltered field. Samples had to be within both the $\delta^{13}C‰$ and $\delta^{18}O‰$ limits to be regarded as unaltered.

	$\delta^{13}C‰$		$\delta^{18}O‰$	
	Low	High	Low	High
Uvigerina miozea group	-0.25	0.75	0.75	2.00
Cibicides deliquatus	0.25	1.25	0.25	1.50

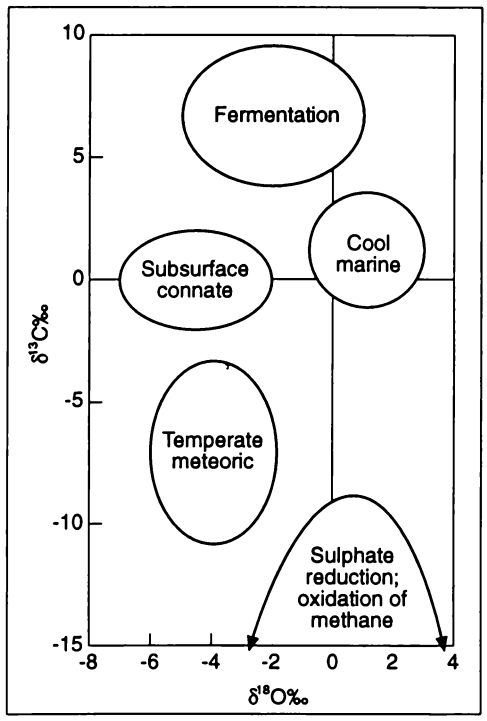

Figure 4:25. Generalised isotope fields and inferred environments for New Zealand carbonate precipitates (after Nelson and Smith, 1996).

4:5 SOURCE

Seismic lines show time transgressive onlapping of Plio-Pleistocene strata directly onto basement over much of the offshore Wanganui Basin (Anderton, 1981; Holt and Stern, 1994). The absence of a Cook Strait during the Pliocene (late Opoitian to Waipipian) would allow rivers draining the rapidly eroding South Island hinterland, via the now drowned, deeply incised valley system that extends north of the present Marlborough Sounds (Holt and Stern, 1994), to supply sediment directly to the Wanganui Basin. If the paleogeography of Anderton (1981) is plotted over the basement geology estimations of Mortimer *et al.* (1997) (Figure 4:27), then the abundance of mica (1-5%) found in the sandstones of the Tangahoe Formation and more generally could certainly have been supplied by the schist and granitic bodies that would have been subaerially exposed to the south. Hudson (1996) suggested the granitic bodies and high grade metamorphics of the South Island were the likely source of both muscovite and biotite. Flame structures wrenched up from the basal contact of the mass-emplaced sandstones pointing in a northerly to northeasterly direction support a southerly sediment source. Northern basement source areas are unlikely given the covering of pre-Pliocene Cenozoic strata that would have mantled these areas, while the eastern ranges were yet to be a factor in the paleogeography (Beu, 1995).

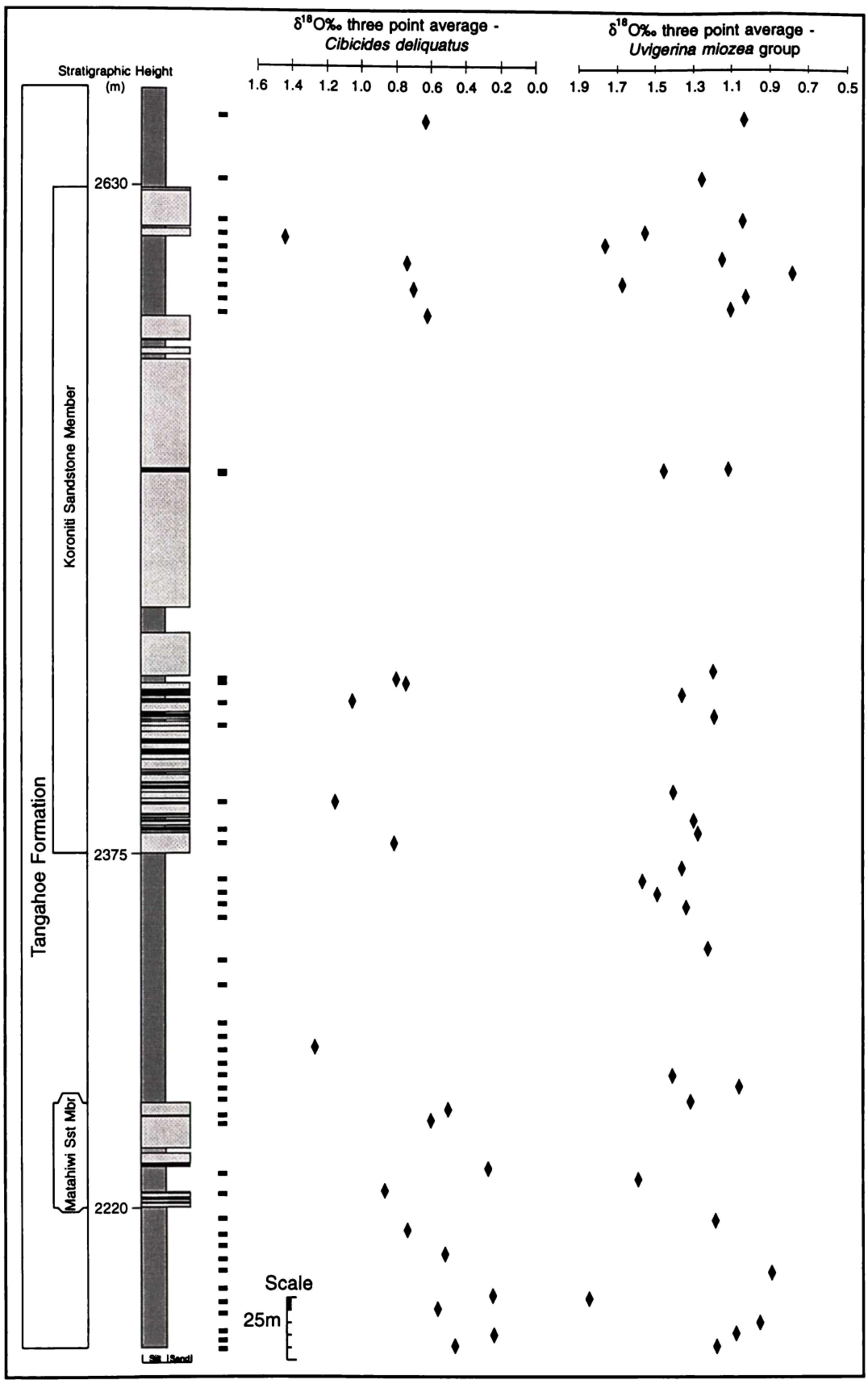

Figure 4:26. Isotope results plotted against the corresponding stratigraphy Sample locations are indicated immediately to the right of the stratigraphic column. Raw data is the Appendix 2: Isotopes.

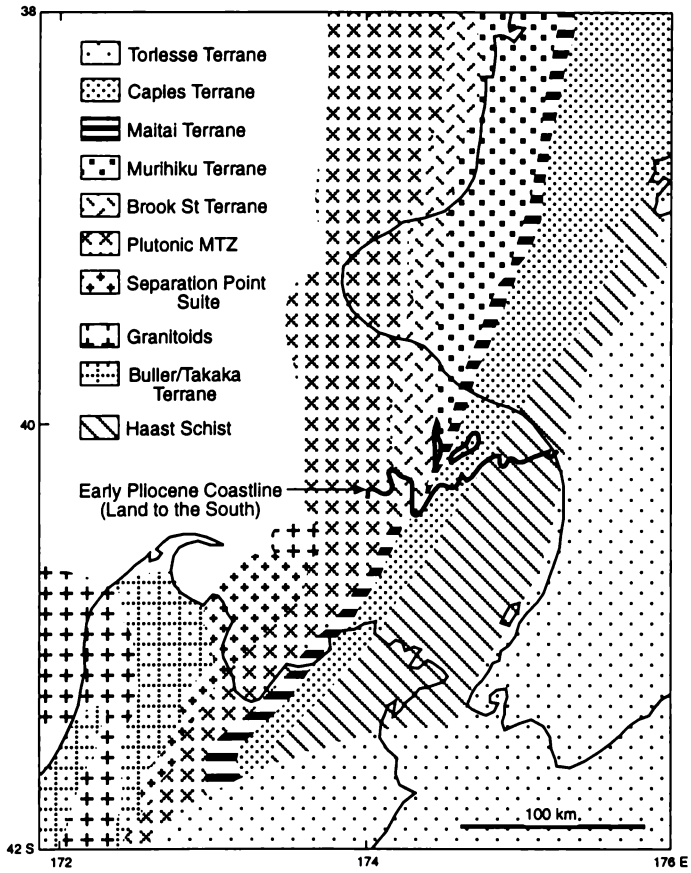

Figure 4:27. Basement geology estimates of Mortimer *et al.* (1997) showing possible sediment source rocks for the Tangahoe Formation. The early Pliocene coastline of Anderton (1981) highlights the absence of the Cook Strait and availability of mica-containing basement materials to the south of the Wanganui Basin.

Detailed analysis of source rocks for the Tangahoe Formation is beyond the scope of the current study. However, some bulk XRD analyses have been undertaken for the Tangahoe and underlying Matemateaonga Formation. The results are summarised in Table 4:4. While this provides no control on the composition of rock fragments, it does provide some control on the gross composition of the units. The Tangahoe Formation siltstones show an increased clay and decreased quartz and feldspar value reflecting the low energy environment. However, the quartz/feldspar ratio for the sandstones and siltstones of the Tangahoe Formation are identical, indicating that both the sandstones and siltstones are probably derived from the same principal sediment source. There appears to be some differences between the Matemateaonga and Tangahoe Formations. Provenance work by Hudson (1996) indicates that a southerly source was dominant in supplying the Matemateaonga Formation and that later units have an increasing greywacke derived sediment supply. Thus the only conclusion that can be drawn from the

comparison between formations is that the sediment source may have changed but only slightly.

Table 4:4. XRD determined weight percent of principal mineral components in the Matemateaonga and Tangahoe Formations. A breakdown of these results (and methodology) is given in Supplement 2 at the end of this chapter.

	Quartz	Plagioclase	Potash Feldspar	Qtz/Feldspar ratio	Clay
Matemateaonga Formation (n=6)	31 (15-61.5)	19 (14-22.5)	3 (0-6.5)	1.4	14
Tangahoe Formation Sst (n=4)	24 (21-26)	15 (5-26)	12 (0-29.5)	0.9	11
Tangahoe Formation Zst (n=3)	15 (14-16)	12 (11-13)	7 (6-9)	0.8	30 (27-36)

4:6 PALEOGEOGRAPHY

Consideration of sediment sources inevitably leads to contemplation of the paleogeography and depocentre development. The paleogeographic and depocentre interpretations of Anderton (1981) and Thompson *et al.* (1994) are constrained by offshore seismic and a few wells drilled close to the Wanganui coastline and along the margin with Taranaki Basin. Seismic data enabled Anderton (1981) to clearly establish the Opoitian paleocoastline as it progressively laps onto basement strata in the current Wanganui Bight. The Opoitian coastline as presented in Fig. 17 of Anderton (1981) is retained in this study.

Evidence from this study indicates that there was a significant change in the basin dynamics around 4.3 Ma (i.e. the Matemateaonga/Tangahoe Formation boundary). While undoubtedly the 5-3.5 Ma depocentre in the region of the Kupe field existed, as illustrated by Anderton (1981) and Stern and Davey (1989), across-basin analysis of the Tangahoe Formation in Section 4:4:5 indicates the possibility of a second depocentre in the area of the Wanganui and Mangawhero River valleys from 4.3-3.5 Ma (Figure 4:28). Determination of the dimensions and exact location of such a basin would require detailed seismic analysis, which unfortunately is not available for the northern part of the Wanganui Basin.

Katz (1968) suggested that the Patea-Tongaporutu basement high was emergent or at least very shallow during the lower Pliocene. Such a

northern submarine or island archipelago extension of the Patea High (Figure 4:28), which does not necessarily involve the exposure and erosion of basement rocks, would separate the two depocentres and help explain some of the features observed in the Tangahoe Formation, namely:

(a) The thinning of the Tangahoe Formation to the west (Figure 4:19).

(b) The northerly and northeasterly aspect in sandstone flow direction could be explained as a confining function of the high (Section 4:5).

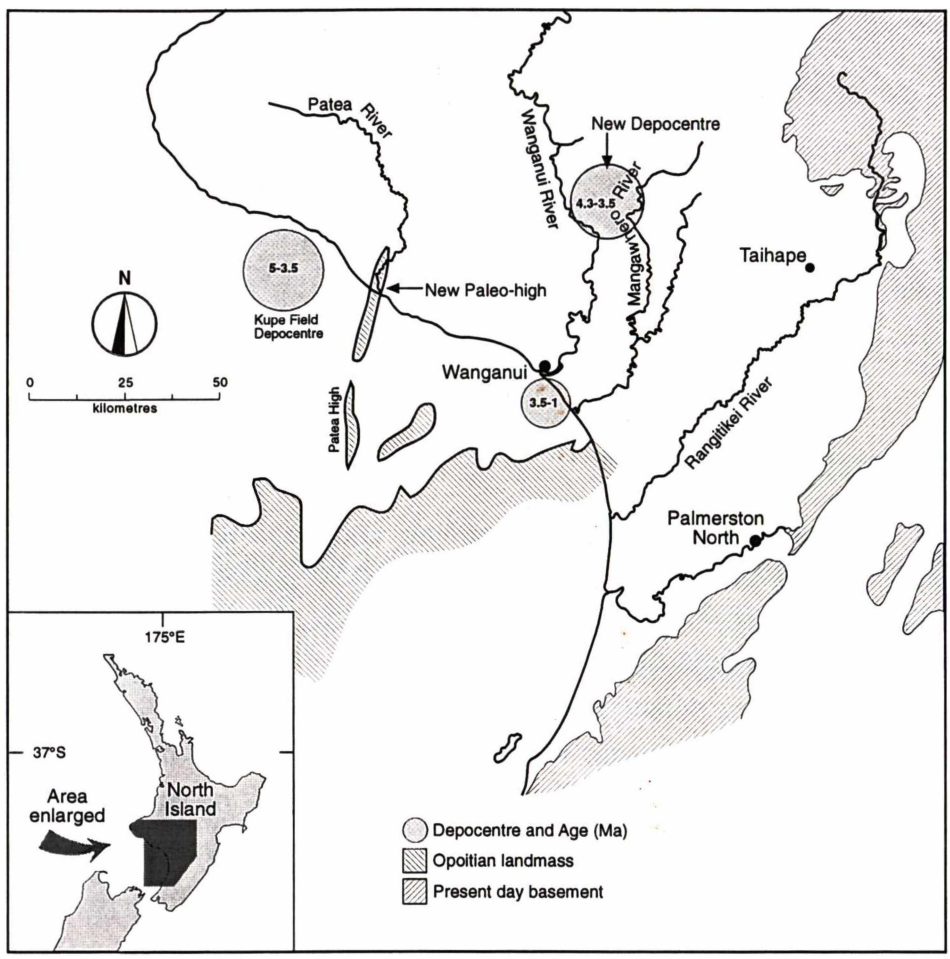

Figure 4:28. Opoitian coastline, showing the suggested new late Opoitian depocentre and the suggested extension of the Patea High (modified from Anderton, 1981).

Independent of these lines of evidence are the seismic interpretations of Haskell (1991) and Uruski (1998), which show the thickness of the Tangahoe Formation as being quite variable but with a distinct thinning to the west. Interpreted seismic lines in Uruski (1998) show the Tangahoe Formation pinching out against Matemateaonga Formation in the west (Figure 4:29).

For the reasons discussed above, movement along the western margin of the Wanganui Basin during the deposition of the Tangahoe Formation appears to be fairly certain. The "new" paleo-high illustrated in Figure 4:28 is a result of this movement, and while basement may not have

reached the surface, earlier sediments may have, although the degree to which they have been eroded is uncertain.

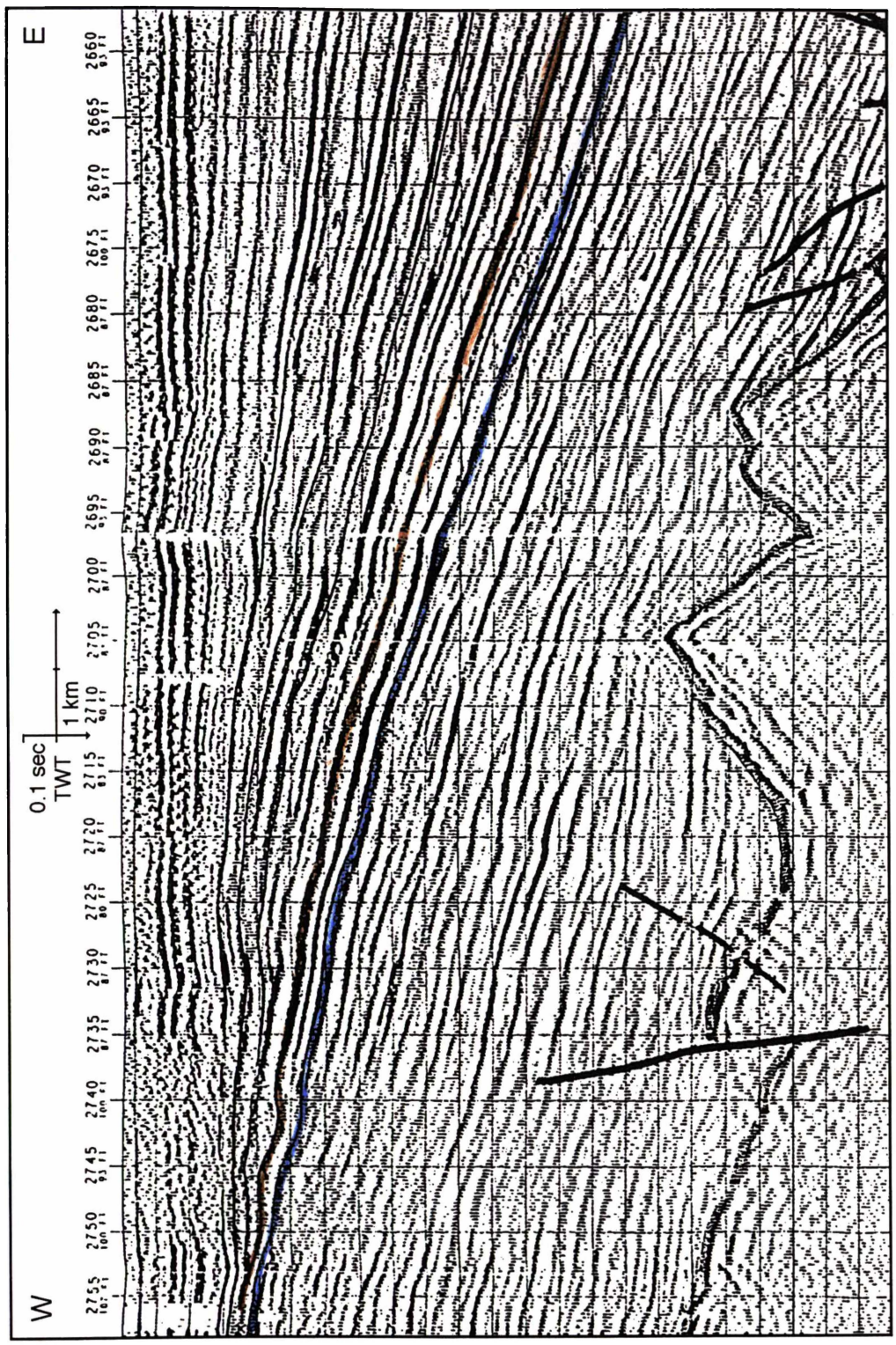

Figure 4:29. Seismic line EA-4 showing the wedging out of strata, against a western topographic high. The blue line has been interpreted by Uruski (1998) as being the base of the Tangahoe Formation. While the top of the Tangahoe Formation has not been clearly identified, it occurs below the brown line. Line EA-4 is located offshore, but parallels the coast, location shown in Figure 4:30. Each horizontal grid line equals 0.1 s two way travel time (From Uruski, 1998).

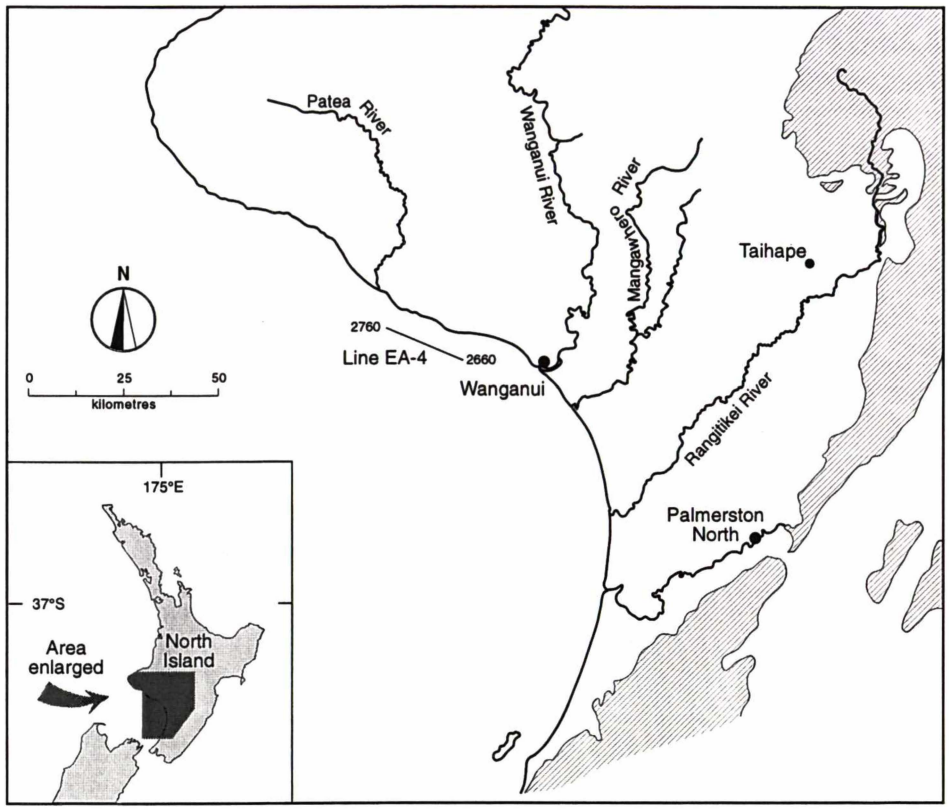

Figure 4:30. Location of the section of seismic line EA-4 shown in Figure 4:29.

CHAPTER 4: SUPPLEMENT 1

MICA EFFECT

Particle size can be determined by a number of methods, including in this study from field estimation, sand/mud ratio from sieve analysis, and laser particle size analysis. In general, field observations and sieve analyses are in agreement. However, the laser particle size analyser gave consistently lower sand percentages than were obtained by sieve analysis (Figure C4S1:1) and expected from field observations. This was unexpected as a large variety of different materials (including soils, various modern sediments and volcanic ash) have been run through the laser sizer, giving results that were consistent to within a few percent of those obtained by sieve analysis and well within expected field observation limits. However, the sediments analysed here differ from all of these other analyses in one important aspect, namely their obvious quantities of mica.

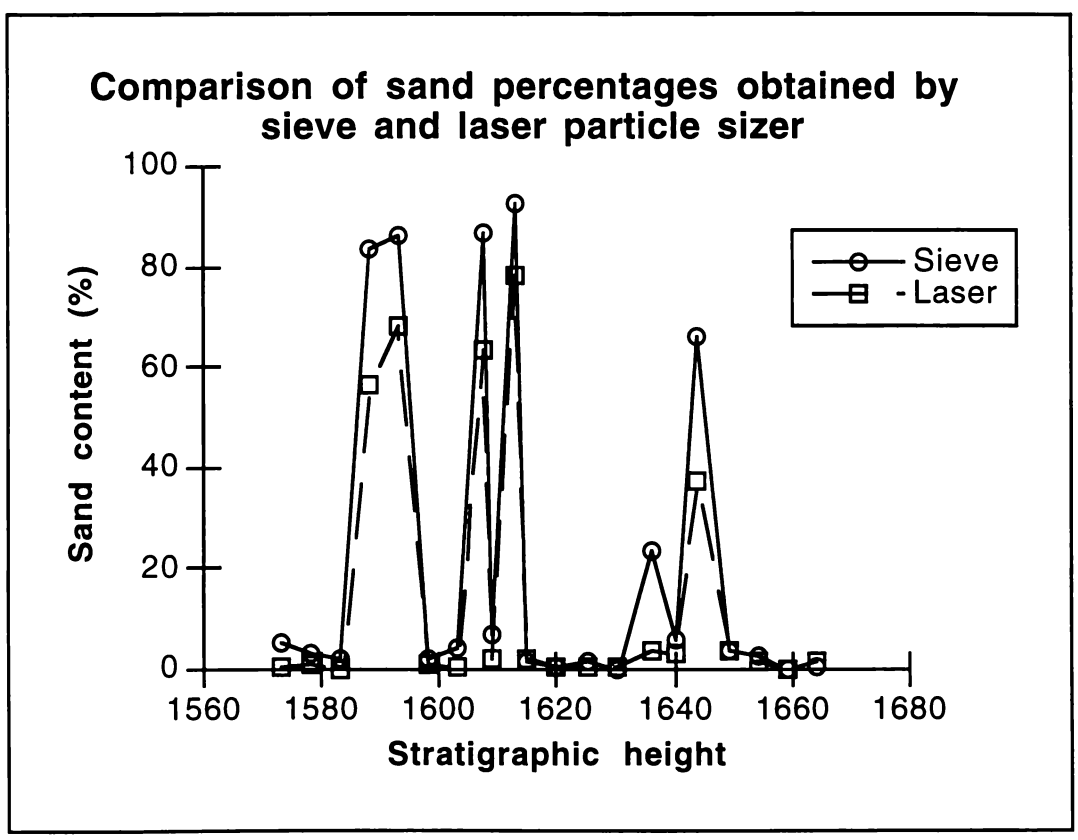

Figure C4S1:1. Comparison of sand percentages through part of a Pliocene section using wey sieving and laser particle size techniques. Data in Appendix 2: Particle size.

To try and understand the role, if any, of mica in the consistently lower sand percentage derived by the laser particle sizer compared to sieve and field estimations, a test series of analyses were undertaken. At this point it was thought that the platy nature of the mica was causing problems with preferential analysis of the edge of the mica, giving a bimodal result with a significantly reduced sand concentration.

In the test a known amount of clean, non-micaceous sand was run through the laser particle sizer, providing base-line results. Small known quantities of (2-4 ϕ, 250 - 63 μm; sieved) mica (mixture of muscovite and biotite) were progressively added to the particle sizer, and the analyses undertaken with each increase in mica concentration. As a final test run a 100% mica analysis was undertaken. The results of the test sequence are provided in Table C4S1:1 and plotted on Figure C4S1:2.

Table C4S1:1. Results of the mica test series where 2-4 ϕ (250 - 63 μm) sieved mica was progressively introduced into a clean beach sand.

% Mica	Grain-size (ϕ)								
	0 to 1	1 to 2	2 to 3	3 to 4	4 to 5	5 to 6	6 to 7	7 to 8	> 8
0	1.01	56.22	38.58	1.63	0.47	0.88	0.46	0.52	0.22
0.40	2.85	52.42	37.06	2.86	1.14	1.57	0.95	0.76	0.39
0.79	3.97	49.58	36.56	3.94	1.71	1.87	1.09	0.80	0.50
1.19	4.94	48.41	35.69	4.53	2.08	1.91	1.11	0.82	0.50
1.57	4.39	46.67	35.55	5.76	2.47	2.12	1.21	0.79	1.06
1.96	4.77	46.25	34.95	6.13	2.71	2.16	1.20	0.78	1.04
2.34	5.58	43.11	34.43	8.40	3.35	2.17	1.21	0.77	1.01
3.85	8.15	39.61	31.84	10.16	4.39	2.50	1.43	0.86	1.03
5.66	8.77	36.75	30.35	11.99	5.67	2.95	1.67	0.98	0.85
7.41	10.79	35.06	28.73	12.46	6.08	3.11	1.82	1.06	0.86
9.09	11.43	35.35	27.61	12.65	6.22	3.03	1.81	1.06	0.84
13.04	12.59	35.01	26.66	12.84	6.31	2.97	1.78	1.01	0.80
16.67	12.04	33.95	26.62	13.53	6.73	3.18	1.95	1.12	0.86
20.00	12.11	33.59	26.29	13.72	6.92	3.29	2.01	1.16	0.89
23.08	12.30	33.24	26.06	13.88	7.04	3.36	2.06	1.20	0.93
100.00	13.84	32.91	24.78	14.17	7.11	3.24	1.99	1.12	0.83

The effect of adding mica of an equivalent grain size range to the sand has not been to create a multi-modal distribution as expected, but to force the

grain size curve towards that of the pure mica at a rate far in excess of the total concentration of mica. Table C4S1:2 shows the percentage of change from the sand curve to the mica curve at each concentration step, while Figure C4S2:3 shows the percentage change for each mica concentration and highlights the very rapid shift towards the mica curve. This shift is so rapid that a sediment containing just 2.5% by weight of mica will give a predominantly mica grain size distribution rather than a mean sediment distribution.

Table C4S1:2. Percentage change from the sediment curve to the mica curve for each ϕ size at each mica concentration.

% Mica	Grain-size (ϕ)								
	0 to 1	1 to 2	2 to 3	3 to 4	4 to 5	5 to 6	6 to 7	7 to 8	> 8
0.40	14	16	11	10	10	29	32	40	28
0.79	23	28	15	18	19	42	41	47	46
1.19	31	34	21	23	24	44	42	50	46
1.57	26	41	22	33	30	53	49	45	138
1.96	29	43	26	36	34	54	48	43	134
2.34	36	56	30	54	43	55	49	42	130
3.85	56	71	49	68	59	69	63	57	133
5.66	60	84	60	83	78	88	79	77	103
7.41	76	91	71	86	84	94	89	90	105
9.09	81	90	79	88	87	91	88	89	102
13.04	90	91	86	89	88	89	86	82	95
16.67	86	96	87	95	94	97	97	100	105
20.00	87	97	89	96	97	102	101	107	110
23.08	88	99	91	98	99	105	105	113	116

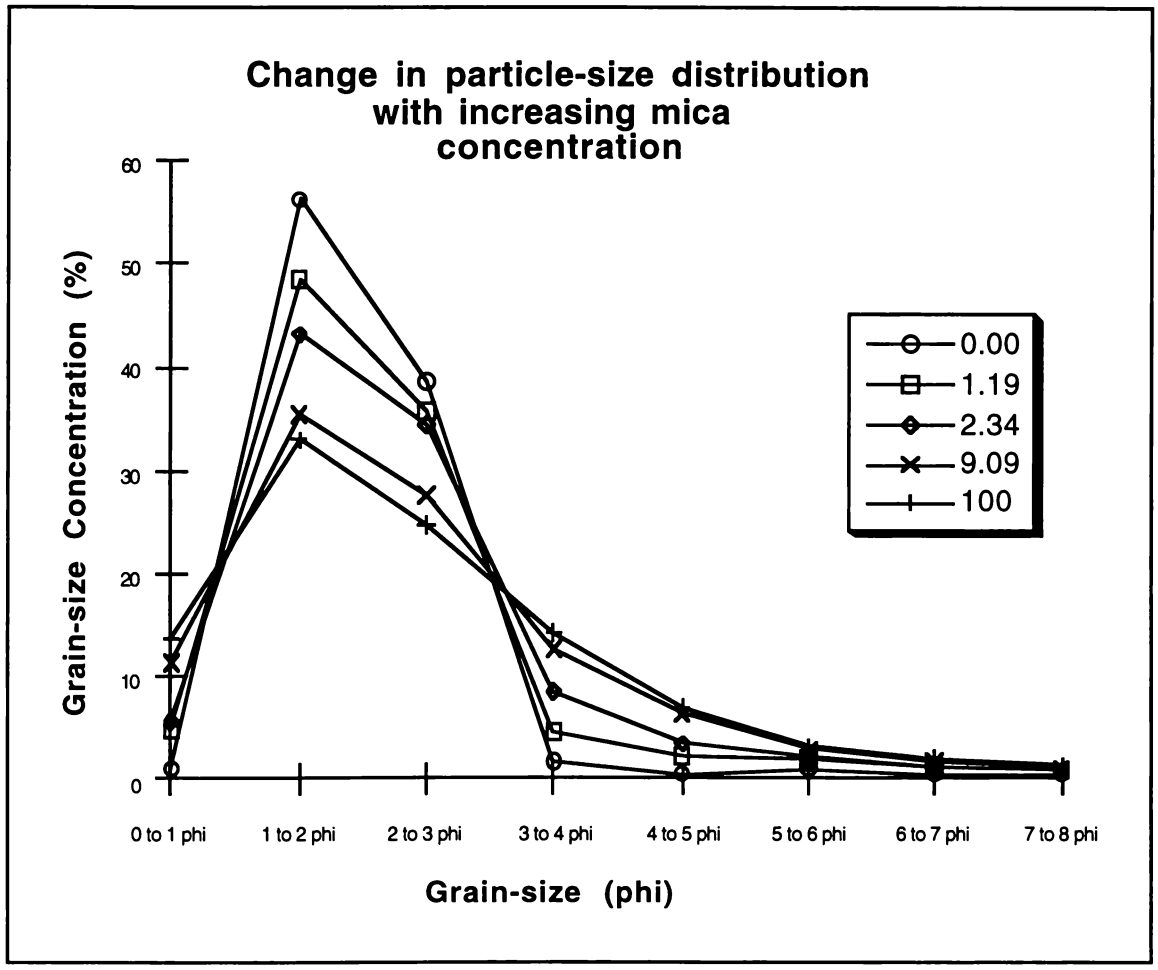

Figure C4S1:2. Particle-size curves for selected mica concentrations (0, 1.19, 2.34, 9.09 and 100%) showing the rapid forcing of the grain-size distribution to that of the mica.

The effect of this forcing towards the mica curve would be significantly more visible in samples where the mean mica size is different to the mean particle size. With this in mind the validity of using the laser particle size data is called in to question. To use these data requires the assumptions that mica concentration and effect are basically constant and are of such a low value that they have not significantly swamped the particle size distribution.

Any correction factor for the effect of mica would rely on knowing (1) the grain size distribution of the mica, (2) the concentration of mica within each grain size, and (3) the effect of the different mica grain-sizes on the sediment distribution curve. Given the complexity of the information required for any correction no attempt has been made in this project to develop such correction factors.

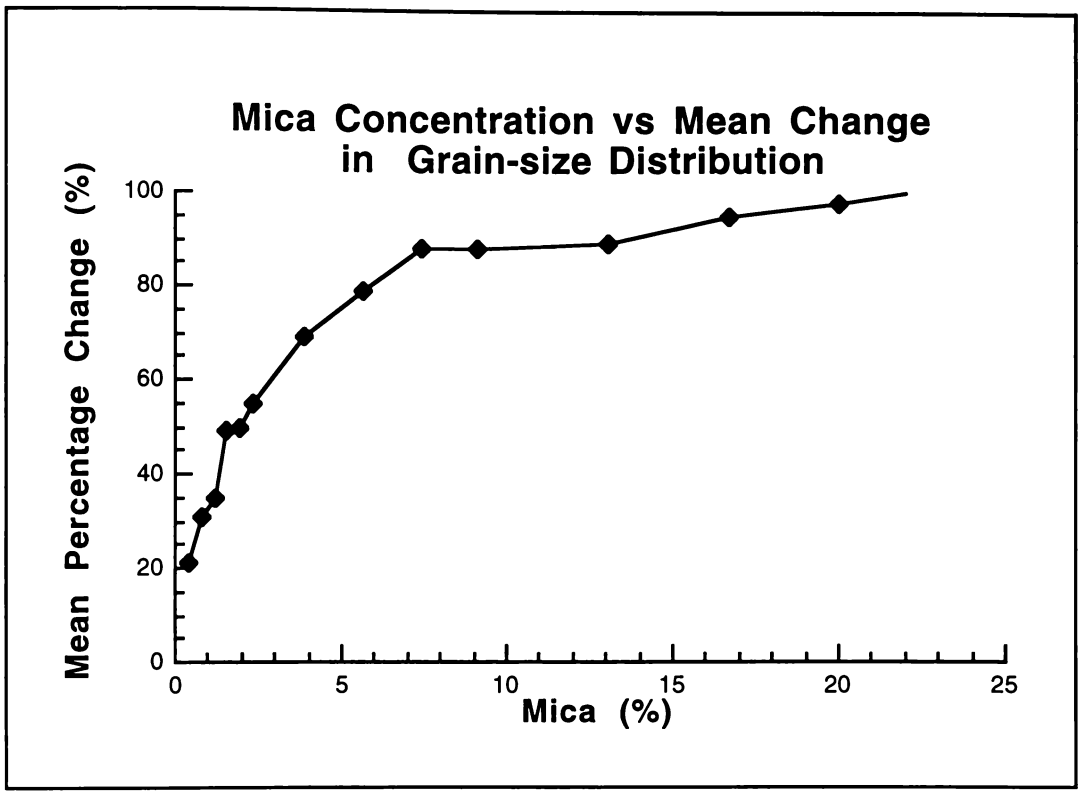

Figure C4S1:3. Percentage change towards the mica curve at each of the mica concentrations measured.

CHAPTER 4: SUPPLEMENT 2

XRD ANALYSES

X-ray diffraction is a rapid and relatively simple procedure for determining the semi-quantitative mineralogy of sedimentary materials. While it is recognised that problems such as peaks relating to minor components being hidden in peaks related to major components, it is still a powerful tool in helping to determine the principal mineral components of a sedimentary samples.

In this study, the bulk composition of the Tangahoe Formation sandstones and siltstones as well as Matemateaonga Formation sandstones were required. To this end a number of unorientated, hand powdered bulk samples from each formation were analysed on a Philips analytical x-ray diffractor with a PW 1729 x-ray generator and a PW 1840 diffractometer control at the following settings:

Voltage	34 kV
Current	26 mA
Range	2-45° 2∅
Speed	0.02° 2∅/s
Chart	10 mm/s
Range	5×10^3
T.C.	1.0
Slit	0.2

Peak heights for quartz, plagioclase, potash feldspar and clay at set degree 2∅ values (Table C4S2:1) were converted to semi-quantitative weight percentages using conversion correlations determined by Hume (1978). Peak height is the vertical distance between the peak apex and the background line and is expressed as the number of small grid units on the diffractometer trace to the nearest half unit. The background line is a straight line that was drawn on each diffraction trace between 18° and 32° 2∅. The results are summarised in Table C4S2:2. As a comparison, the results of Hume (1978) for the same formations (different locations and horizons) are summarised in Table C4S2:3.

Table C4S2:1. Degree 2∅ values used to determine key minerals present within the samples (after Hume, 1978).

Mineral		degrees 2∅	Å
Quartz		20.8	4.27
Plagioclase	A	28.0	3.19
	B	27.75	3.21
Potash Feldspar		27.5	3.24
Clay		19.9	4.46

Table C4S2:2. Peak height (PH), to the nearest half square, and corresponding weight percentage (C) for quartz, plagioclase, potash feldspar and clay minerals for samples from sandstones within the Matemateaonga and Tangahoe Formations.

Sample	Quartz		Plagioclase A		Plagioclase B		Potash Feldspar		Clay Minerals	
	PH	C	PH	C	PH	C	PH	C	PH	C
Matemateaonga Formation										
W962031	41	62	25.5	18	-	-	-	-	-	-
W962050	10	15	-	-	28	20	3.5	3	2.5	23
W962101	17	24	-	-	32	23	5	4	1	9
W962114	15	23	16.5	12	14	10	4	3	2.5	23
W962153	24	36	-	-	27.5	19	9	7	1	9
W962192	19	29	-	-	20	14	6	5	1	9
Tangahoe Formation Sst										
W962343	14	21	19	14	18	13	2	2	1.5	14
W962351	17.5	26	7.5	5	-	-	40	30	-	-
W962397	16.5	25	-	-	24.5	17	19.5	12	1.5	14
W962609	17	26	18	13	-	-	7	5	2	18
Tangahoe Formation Zst										
W962340	9	14	-	-	15.5	11	12	9	3	27
W962392	9	14	18.5	13	-	-	8	6	3	27
W962422	11	17	17	12	-	-	7.5	6	4	36

Table C4S2:3. Average results (weight percent) obtained by Hume (1978).

	Quartz	Plagioclase	Potash feldspar	Clay	Calcite
Matemateaonga (n=8)	28	31	4	43	2
Tangahoe (n=14)	26	27	3	42	2

CHAPTER 5

AHURANGI SANDSTONE, ATENE FORMATION AND MANGAWEKA MUDSTONE: STRATIGRAPHY AND SEDIMENTOLOGY

CHAPTER 5

AHURANGI SANDSTONE, ATENE FORMATION AND MANGAWEKA MUDSTONE: STRATIGRAPHY AND SEDIMENTOLOGY

5:1 INTRODUCTION

Overlying the deep-water (200-600 m) deposits of the Tangahoe Formation are sandstone dominated shelfal deposits of the Ahurangi Sandstone and Atene Formation. These are in turn over-topped by the fine-grained Mangaweka Mudstone. The Ahurangi Sandstone, Atene Formation and Mangaweka Mudstone form the uppermost part of the Wanganui River valley sedimentary succession considered in this study. Ahurangi Sandstone and Atene Formation do not appear to have direct lateral equivalents in the eastern part of the Wanganui Basin (e.g. Rangitikei River section), while the base of Mangaweka Mudstone appears to be time transgressive (i.e. comparison of ages from the Rangitikei and Wanganui River valleys). However, more locally these units form approximately east-west trending units that dip towards the south (Anderton, 1981). The north/south trend of the Wanganui River offers the opportunity to work up through a section that intersects this stratigraphy. Between Otui village and Pitangi Stream, north of Parakino (Figure 5:1), these three units form a 700 m-thick southward dipping terrigenous marine succession of late Pliocene age. The emphasis of this chapter is on a review of the lithostratigraphy, interpretation of lithofacies and depositional paleoenvironments of the lithostratigraphic units.

5:2 STRUCTURE OF THE AHURANGI, ATENE AND MANGAWEKA IN THE WANGANUI RIVER VALLEY

Late Pliocene sedimentary successions exposed in the study area between Otui village and Pitangi Stream (Figure 5:1) form part of an approximately east-west striking monocline that dips to the south. Structural information obtained in this study is shown on Maps 12-14 (Chapter 2). The regional strike is approximately 90° with a dip value of 4° S. The generally poor exposure in this section of the Wanganui River valley has limited the opportunities to obtain structural information.

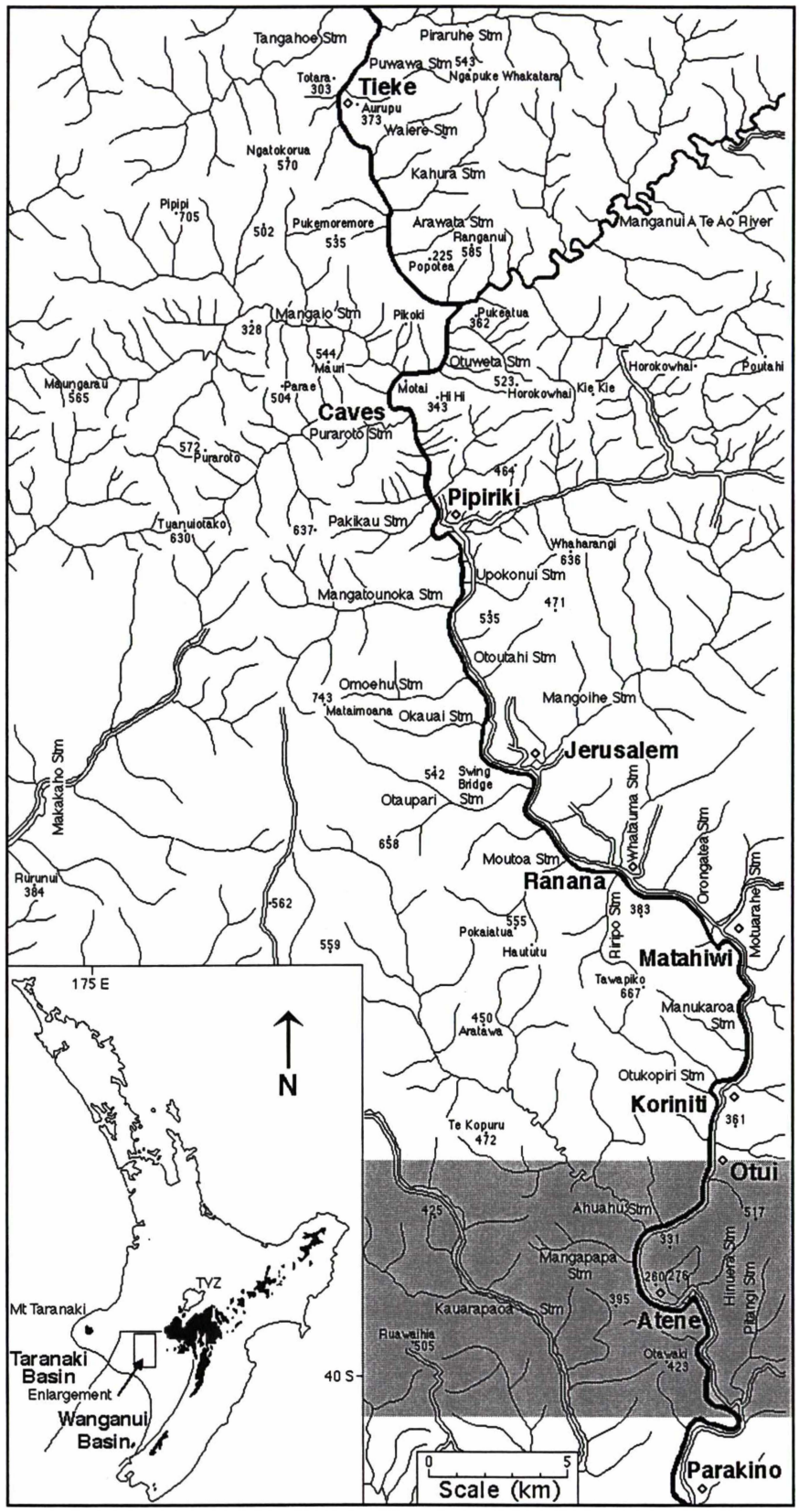

Figure 5:1. Locality map of the part of the Wanganui River valley considered in this study. The grey tone approximates the section of river under study in this Chapter Spot heights in metres. *Inset*: location of the study area relative to the Wanganui Basin. Topography over 1000 m is darkened. TVZ = Taupo Volcanic Zone.

5:3 LITHOSTRATIGRAPHY

5:3:1 HISTORY

Previously established stratigraphic nomenclature for the late Miocene to late Pliocene Wanganui River section is summarised in Figure 5:2. The stratigraphy between Otui and Parakino was initially established by Feldmeyer *et al.* (1943) with the recognition of two sandstone units (the Ahu Ahu and Atene Sands) within the Mangaweka Mudstone, the base of which was not defined. Subsequently, Collen (1972) subdivided the Mangaweka Mudstone into sandstone and mudstone members (Figure 5:2), with the Mangaweka Mudstone being defined as starting at the top of the Koroniti Sandstone and continuing to the base of the Wilkies Shellbed. Ker (1973) redefined the Mangaweka Formation, substantially limiting its stratigraphic extent to lie above the Atene Sands. The Atene and Ahurangi Sandstones, along with the intervening Oxbow Siltstone, were all defined by Ker (1973) and raised to formation status within the Whenuakura Group, the base of which Ker (1973) did not formalise.

In this study the Ahurangi Sandstone of Ker (1973) is maintained, while the Oxbow Siltstone (Ker, 1973; Wilson, 1993) (and equivalent Mangapapa Siltstone of Collen, 1972) is considered a member within the Atene Formation. The Mangaweka Mudstone as used here approximates the usage of Ker (1973).

5:3:2 STRATIGRAPHY

While Ker (1973) presented a stratigraphy for the succession exposed in the Wanganui River valley between Otui village and Pitangi Stream, this study presents for the first time a detailed lithostratigraphy and paleoenvironmental interpretation for this succession. Figure 5:3 summarises the stratigraphy. Separate stratigraphic columns have been prepared for each of the formations within this part of the Wanganui River section. Stratigraphic columns with sample location information, tied to appropriate map sections, are presented in Maps 11-14 at the end of Chapter 2.

5:3:3 AHURANGI SANDSTONE

5:3:3:1 History

Initially referred to as the Ahu Ahu Sands (Feldmeyer *et al.*, 1943), it was named the Ahurangi Sandstone and raised to formation status by Ker (1973). Collen (1972) used the name Ahuahu Sands, maintaining the nomenclature of Feldmeyer *et al.* (1943) but using the current spelling for the stream after which the unit is named. Given that Ker (1973) is the only one to formally define the unit as a formation, his terminology is continued within this study.

5:3:3:2 Reference Section

Ker (1973) cited the northern side of the hill upon which the upper boundary is located to be the type location for the Ahurangi Formation. This location, which is approximately 1 km north of the Ahuahu Stream / Wanganui River confluence at S21 926647, offers fantastic exposure of the upper part of the Ahurangi Formation. The rest of the formation is only poorly exposed, with slump material and modern river deposits being responsible for obscuring much of the potential exposure. The reference section in this study is defined as the exposure of this formation between the upper and lower boundaries at S21 933648 - 948667, respectively.

5:3:3:3 Stratigraphy

A stratigraphic column of the Ahurangi Sandstone is presented in Figure 5:4 and is tied to an appropriate map section in Maps 11-12. The Ahurangi Sandstone in its lower part is a massive tan coloured sandstone, which becomes bedded (10-20 cm sandstone to silty sandstone alternations) in its upper part (Figure 5:4), with coarser beds containing lensoidal, moderately cemented, concretions, which stand proud upon weathering of the exposure (Plate 5:1). The laser grain-size analyses available for this formation (Appendix 2: Particle size) record a lower than expected sand concentration (given field and sieve information). In this case it is probable that the mica effect (Chapter 4: Supplement 1) means that the silt component of samples from this formation has been overestimated in comparison with field observations and sieve data (Appendix 2: Particle size).

Age	Feldmeyer *et al.* (1943)	Fleming (1953)	Collen (1972)		Ker (1973)	Wilson (1993)		This Study
	Mangaweka Formation	Mangaweka Mst		Pitangi Mst	Mangaweka Formation	Paparangi Group	Otawake Zst	Mangaweka Mudstone
Wm	Atene Sands		Mangaweka Mst	Atene Sands	Atene Sst		Atene Sst	Atene Formation
				Mangapapa Zst	Oxbow Zst	Whenuakura Group	Oxbow Zst	Oxbow Siltstone Mbr
	Ahu Ahu Sands			Ahuahu Sands	Ahurangi Sst		Ahurangi Sst	Ahurangi Sandstone
				Raumati Mst	Otui Zst		Otui Zst	Tangahoe Formation
Wp	Koroniti Beds		Koroniti Sst		Koroniti Sst		Koroniti Sst	Koroniti Sandstone Mbr
	Taihape Mst		Taihape Mst		?unnamed Zst	Tangahoe Group	Raupirau Zst	
	Matahiwi Sands						Matahiwi Sst	Matahiwi Sandstone Mbr
							Ranana Mst	
uWo	Jerusalem Sands						Jerusalem Sst	Jerusalem Sandstone Mbr
lWo	Reef-Bearing Sands						Otuitahi Sst	Matemateaonga Formation
	Pipiriki Sands					Matemateaonga Group	Mangataunoka Zst	
uTk							Kahanui Mst	Various divisions
lTk							Popotea Sst	defined (see Chapter 3)
							Kabura Zst	
							Ramanui Sst	

NB: The upper Kapitean (uTk) - lower Opoitian (lWo) boundary approximates the Miocene-Pliocene boundary.

Figure 5:2. Historical lithostratigraphic nomenclature for the latest Miocene and Pliocene strata of the Wanganui River section and that proposed in this study. Dashed lines indicate approximate lowermost extent of study.

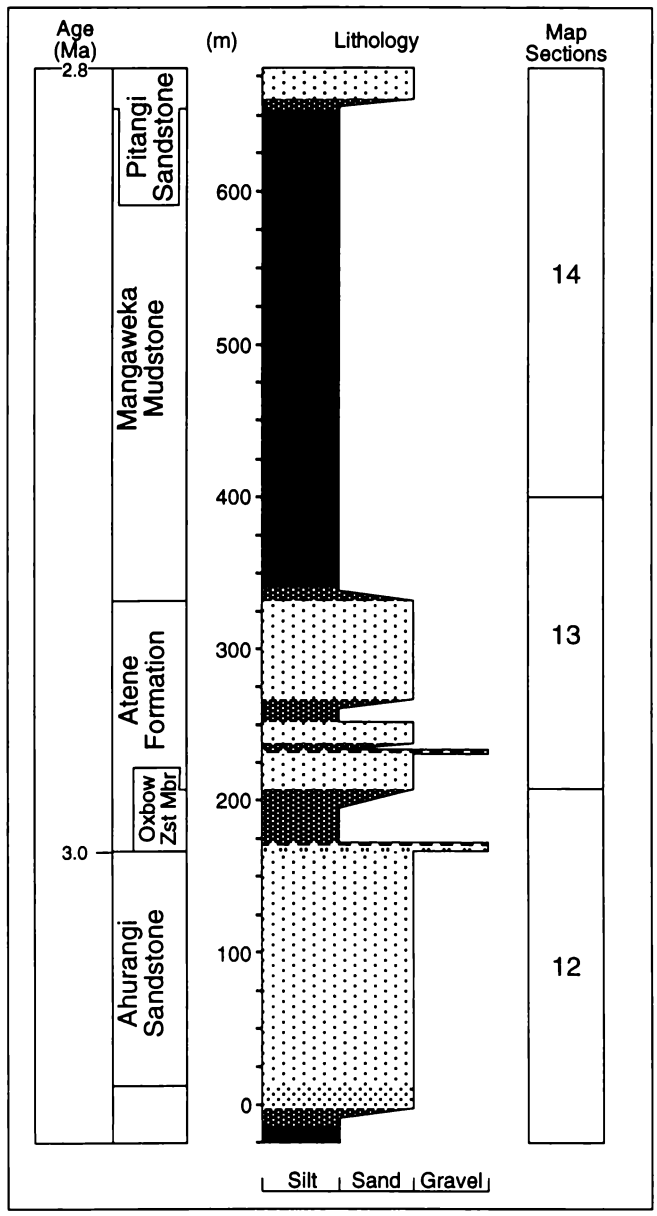

Figure 5:3. Composite stratigraphic column for the succession exposed in Wanganui River valley between Otui village and Pitangi Stream, showing distribution of formations and the stratigraphic extent of map sections. Age control is derived from data in Chapter 2. The unit Pitangi Sandstone is taken from McIntyre and Kamp (1998).

5:3:3:4 Lower and Upper Boundaries

The lower boundary is gradational with siltstones of the underlying Tangahoe Formation (over 10-15 m). This boundary is equivalent to the Otui/Ahurangi boundary of Ker (1973) and Wilson (1993), and the Raumati/Ahuahu boundary of Collen (1972). The equivalent boundary as defined by Ker (1973) at S21 950670-948667 is maintained. At this location a high road cutting (≈200 m long and extensively re-engineered during the time span of this study) exposes a sandy siltstone at its northern end and a

sandstone at the southern end, clearly showing the gradational nature of this boundary. The boundary between the Tangahoe Formation and Ahurangi Sandstone as drawn on Maps 11 and 12 are necessarily general. In this study the boundary is defined at the southern end of the exposure where the lithology is definitely a sandstone (Sample number W962480 - Appendix 2: Summary). However, exposure leading up to this boundary is poor along the Wanganui River Road. Much more continuous sections can be obtained by working up one of the streams that feed into the Wanganui River in a zone that extends approximately 4 km north of the road boundary location. In this study, the Operiki Stream and its tributaries (Map 11) were used.

The upper boundary of the Ahurangi Sandstone is delineated by a thin (c. 30 cm) poorly developed concretionary shellbed. Both the upper boundary and the poorly developed shellbed are exposed along the Wanganui River Road at the top of the hill (especially on the northern side), just north of the Wanganui River / Ahuahu Stream confluence at S21 926647. However, due to the poorly developed nature of the shellbed, it is not particularly obvious, with the best exposure on the northern side of the hill at S21 933648.

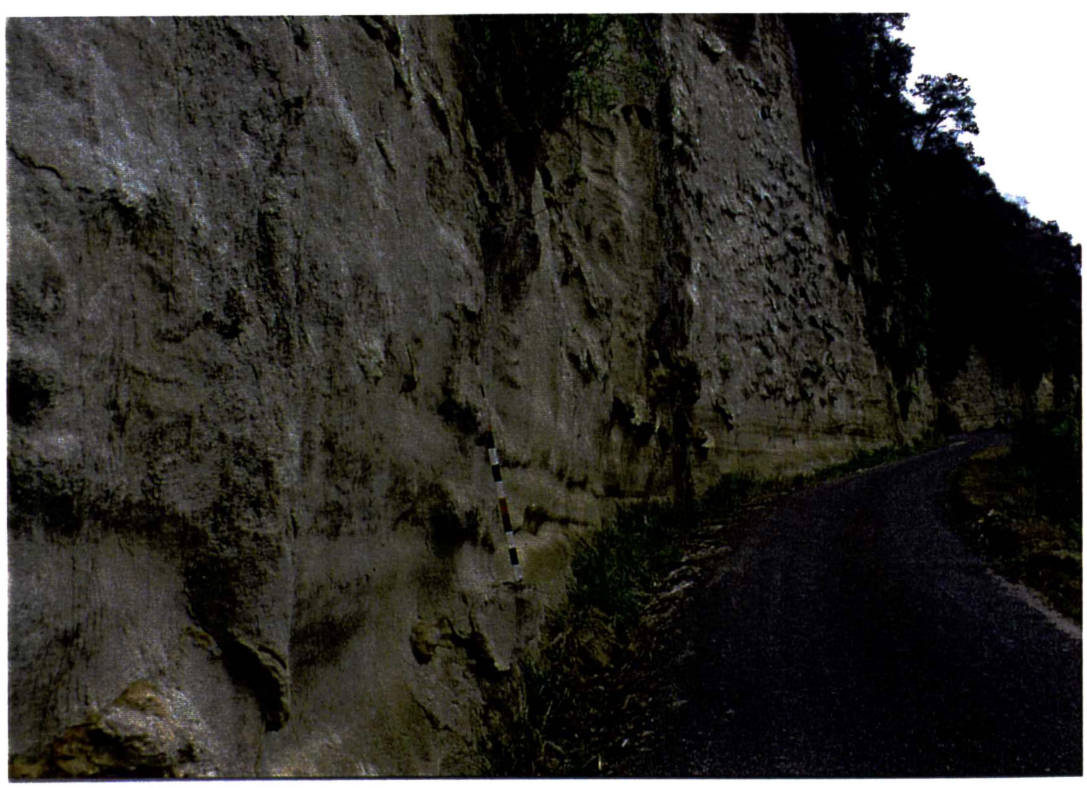

Plate 5:1. Concretionary, bedded sandstone near the top of the Ahurangi Sandstone (S21 936650).

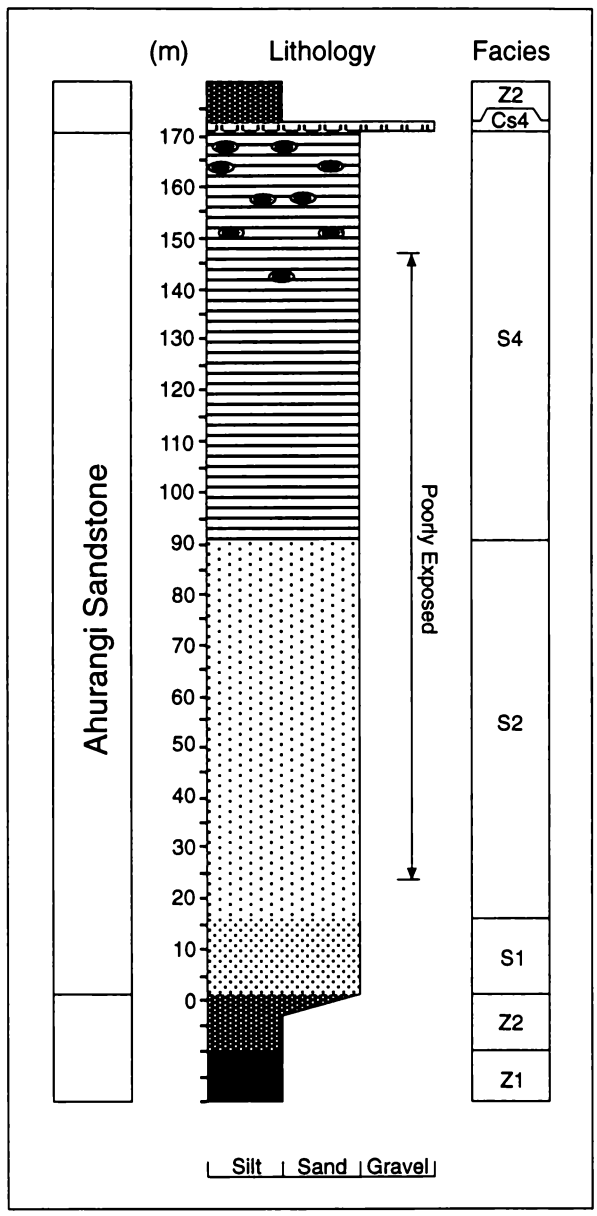

Figure 5:4. Composite stratigraphic column for the Ahurangi Sandstone within the Wanganui River valley, showing distribution of lithofacies.

5:3:3:5 Thickness

Ker (1973) measured the Ahurangi Sandstone as being 170 m thick, the same thickness obtained in this study (Figure 5:4).

5:3:4 Atene Formation

5:3:4:1 History

The name Atene Sand was first used by Feldmeyer *et al.* (1943) to define the sandstone at Atene. Subsequently this unit was redefined by Ker (1973) and named the Atene Sandstone with formational status. The variability in lithology within this unit means that a change in name from Atene

Sandstone to Atene Formation is recommended to recognise the occurrence of lithologies other than sandstone. In this study the Atene Formation encompasses both the Oxbow Siltstone and Atene Sandstone of Ker (1973), or equivalent units in other studies (Figure 5:2).

5:3:4:2 Reference Section

Ker (1973) defined the type locality for his Atene Sandstone as being the western cliff of the large oxbow (cut-off river bend) at Atene. This locality does have good exposure of the upper part of the Atene Formation. However, regeneration of scrub through much of this area means that previously clear areas are now very difficult to access. Elsewhere the Atene Formation is poorly exposed. The reference section in this study is defined as the exposure of this formation between the upper and lower boundaries at S21 937624 - 933648, respectively.

5:3:4:3 Stratigraphy

This study recognises the occurrence of three cyclothems within the Atene Formation, with the Oxbow Siltstone Member (Oxbow Siltstone Formation of Ker (1973) forming the lower half of the first of these cyclothems (Figure 5:5). The cyclothems reflect the return of shelfal environments to this part of the basin following infilling of the deep-water environments of the Tangahoe Formation (Chapter 4). For ease of referencing and discussion each of the cyclothems has been subdivided into lithological members using the alpha-numeric system of Naish and Kamp (1995) (Figure 5:5).

Two of the three Atene Formation cyclothems have basal shellbeds (Acm1 and Acm2) composed of weakly developed concentrations of shell material, which may be concretionary. Acm2 is distinctive, as it contains dispersed (over a thickness of approximately 50 cm), well-rounded, fine gravel (up to 5 mm in diameter) composed predominantly of greywacke and is tentatively correlated to the Mangapani Shell Conglomerate (McIntrye pers. comm. and personal observation). The majority of this formation is composed of sandstones and siltstones (Asm# and Azm# respectively), the particle size distributions of which are summarised in Figure 5:6. The sandstones are composed of tan coloured, micaceous (1-5%), massive, fine sand, while siltstones are composed of blue-grey, micaceous (<5%) sandy siltstones. Macro- and microfossils are restricted to finer-grained horizons within the formation.

The two weakly lithified sandstone beds near the top of the unit, which Ker (1973) described as being one of the few marker horizons available, are probably the most distinctive feature of the Atene Formation in the Wanganui

River valley. The silty sandstones (lithofacies S8) that occur under each of the weakly lithified sandstone horizons (Figure 5:5) were observed to contain numerous macrofossil moulds and flaser-like bedding structures. A stratigraphic column of the Atene Formation is presented in Figure 5:5 and is tied to appropriate map sections in Maps 12 and 13.

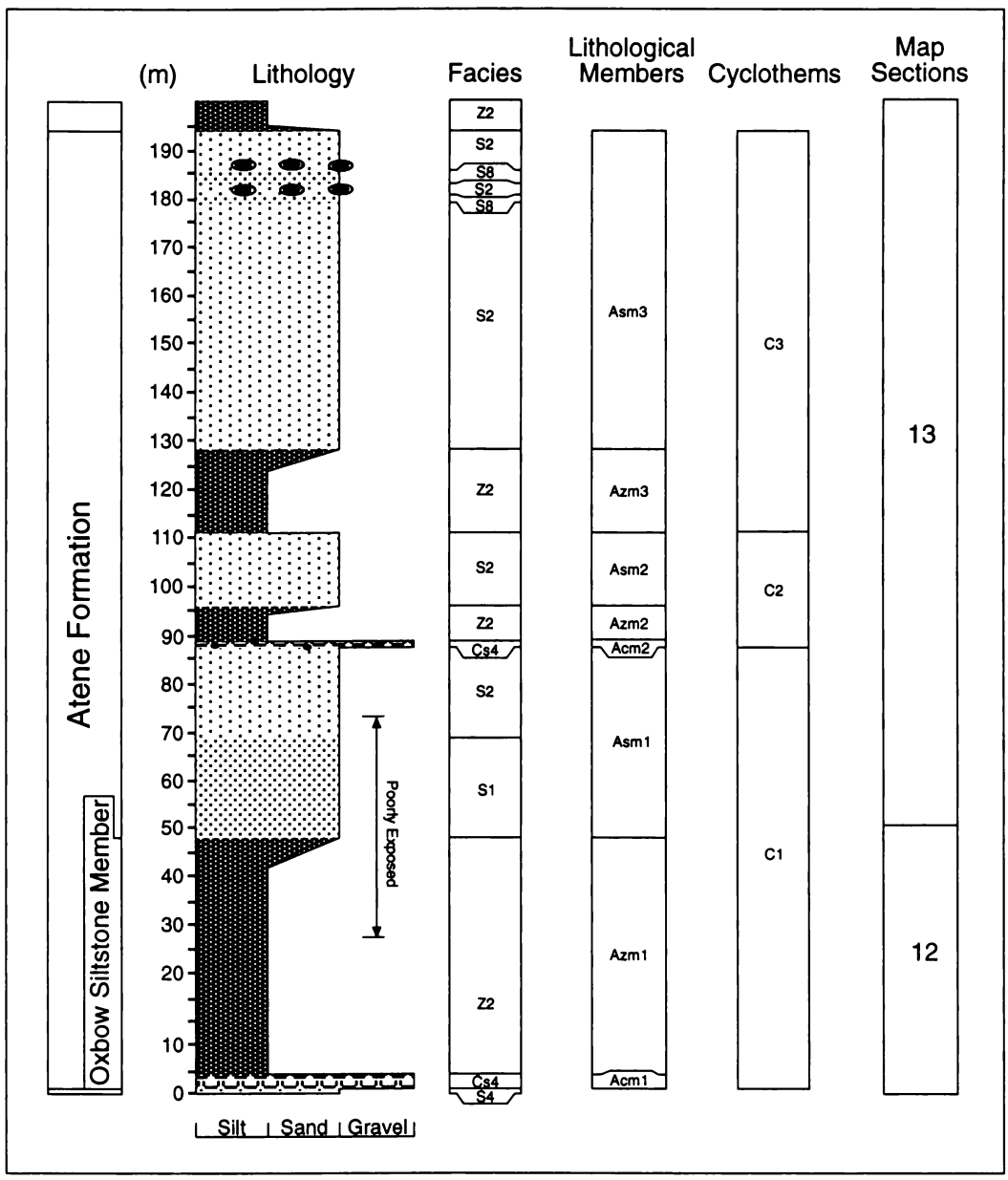

Figure 5:5. Composite column for the Atene Formation within the Wanganui River valley, showing distribution of lithofacies as well as lithological and cyclothemic subdivisions referred to in the text.

5:3:4:4 Lower and Upper Boundaries

The lower boundary of the Atene Formation is defined as being the base of the c. 30 cm thick concretionary, poorly developed shellbed that can be observed on the Wanganui River Road, at the top of the hill north of the

Wanganui River / Ahuahu Stream confluence at S21 926647. The shellbed is not particularly obvious, with the best exposure on the northern side of the hill (S21 933648). No lower boundary for the Oxbow Siltstone was defined by Ker (1973).

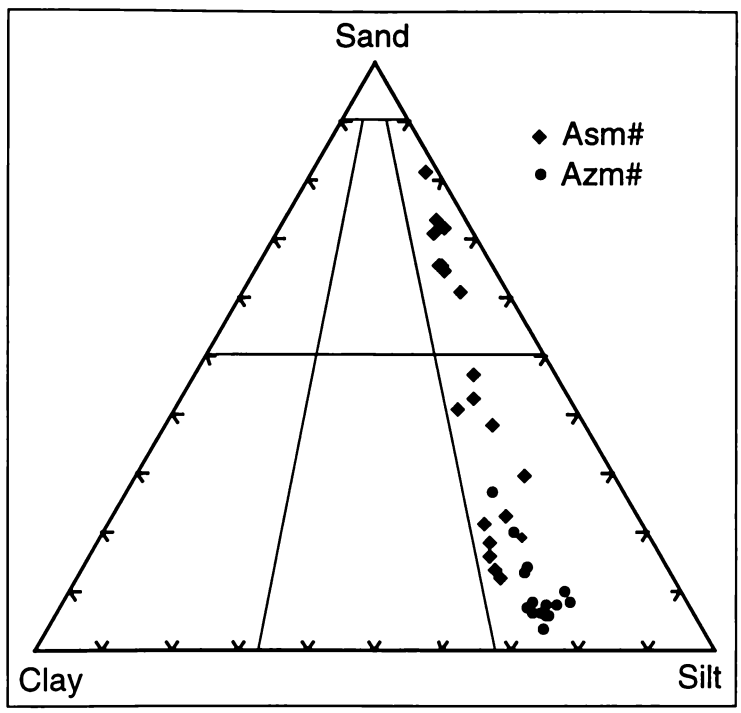

Figure 5:6. Folk plot of the sandstone (Asm#) and siltstone (Azm#) samples from the Atene Formation using laser particle size data. The classification into sandstone or siltstone is based on field observation; the differences in classification are probably due in large part to the effect of mica (Chapter 4: Supplement 1).

The upper boundary of the Atene Formation is delineated by a rapid sandstone/siltstone transition approximately 10 m above two prominent sandstone horizons within the cliffs of the oxbow at Atene. This transition is not clearly defined within the cliffs of the oxbow, being at best approximated by a break in slope. The most easily accessed location that cuts up through the upper part of the Atene Formation and the upper boundary is the small creek (S21 937624) behind the Atene Marae.

5:3:4:5 Thickness

In this study the Atene Formation has been calculated to be approximately 195 m thick (Figure 5:5). Ker (1973) found the equivalent stratigraphy to be 250 m. The differences in thickness obtained in these two studies revolves around thickness estimates for the Oxbow unit.

The Oxbow/Atene boundary of Ker (1973), within the oxbow at Atene, was re-examined in this study and found not to be the Oxbow, but the

uppermost siltstone within the Atene Formation (Figure 5:5). While the Oxbow/Atene boundary was not positively identified in an accessible location during the course of this study, the slump scarp at S21 948655 clearly shows both upper and lower bounds of the Oxbow Siltstone Member. Thickness estimates from this slump scarp have subsequently been used to define the thickness of the Oxbow Siltstone Member. A boundary that disappears into the river just south of the Mangapapa Stream confluence is thought to be the Oxbow/Atene boundary. Its location at this point is in agreement with the projected location using thickness estimates from the slump scarp mentioned above. Therefore this boundary is shown in Map 13.

5:3:5 MANGAWEKA MUDSTONE

5:3:5:1 History

The name Mangaweka Mudstone was first applied to the Wanganui River section by Feldmeyer *et al.* (1943) after being defined in the Rangitikei River section. However, at that time the base of the unit was not defined. Ker (1973) redefined the lower boundary of the Mangaweka Mudstone as occurring at the top of the upper prominent sandstone horizon within the Atene Formation, while the upper boundary was defined at the base of the Makokako Sandstone (after Fleming, 1953). More recently the Makokako Sandstone and overlying stratigraphy have been re-described (McIntyre and Kamp, 1998), with the sandstone unit immediately overlying the Mangaweka being renamed the Pitangi Sandstone. In this study the name Mangaweka Mudstone is retained given its common usage (e.g. Thrasher, 1993; Murphy *et al.*, 1994; Thompson *et al.*, 1994; Journeaux *et al.*, 1996).

5:3:5:2 Reference Section

Ker (1973) defined the type section for the Mangaweka Mudstone in the Wanganui River section as being the western cliff of the oxbow at Atene. However, this does not include the whole stratigraphic range of the unit and is currently totally covered in scrub. The Mangaweka Mudstone as a whole is poorly exposed, with only patches exposed along the road and up small streams draining the area. Thus the type section initially defined near Mangaweka, in the Rangitikei River by Feldmeyer *et al.* (1943) and subsequently by Journeaux *et al.* (1996), is the better section to use to describe the unit as it occurs more generally within the Wanganui Basin, even though its base may well be time transgressive across the basin.

5:3:5:3 Stratigraphy

The Mangaweka Mudstone consists of massive blue-grey siltstone, which is only rarely concretionary. The results of laser sizer grain-size analysis have been plotted on a Folk classification discrimination diagram (Figure 5:7), confirming a siltstone classification. Field observations indicate that the grain-size of the Mangaweka Mudstone is basically constant (confirmed by lab analysis; Appendix 2: Particle size), with the only significant variability occurring at the upper and lower contacts (Figure 5:8). This is quite a different scenario to the situation in the Rangitikei River area, where Journeaux *et al.* (1996) were able to determine distinct cyclicity in the texture of the formation. A stratigraphic column for the Mangaweka Mudstone is presented in Figure 5:8 and is tied to appropriate map sections in Maps 13-14.

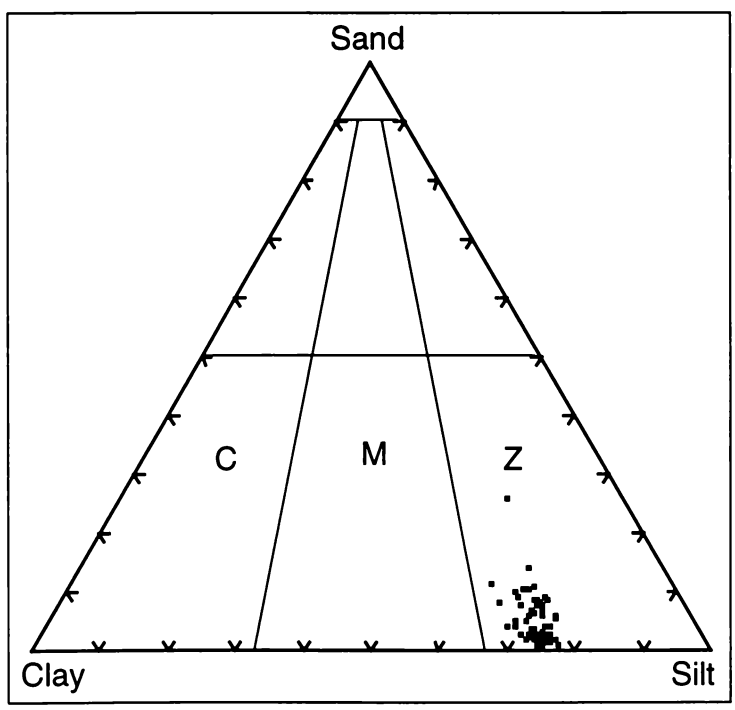

Figure 5:7. Folk classification tri-plot showing the distribution of siltstone samples from the Mangaweka Mudstone. Raw data in Appendix 2: Particle size. (n=66)

5:3:5:4 Lower and Upper Boundaries

Ker (1973) defined the base of the Mangaweka Mudstone as being at the top of the upper of two prominent weakly lithified sandstone beds that are clearly visible within the cliffs of the oxbow at Atene. However, in this study the rapid sandstone/siltstone transition that occurs approximately 10 m above these prominent marker horizons is the preferred lower boundary, as it recognises the significant change in lithology, recorded by the Mangaweka Mudstone. The lower boundary is not clearly defined within the walls of the oxbow, being

at best approximated by a break in slope. However, the small creek at S21 937624 behind the Atene Marae cuts up through the two prominent weakly lithified sandstone horizons (of the Atene Formation), the sandstone/siltstone transition zone and into the siltstones of the Mangaweka Mudstone.

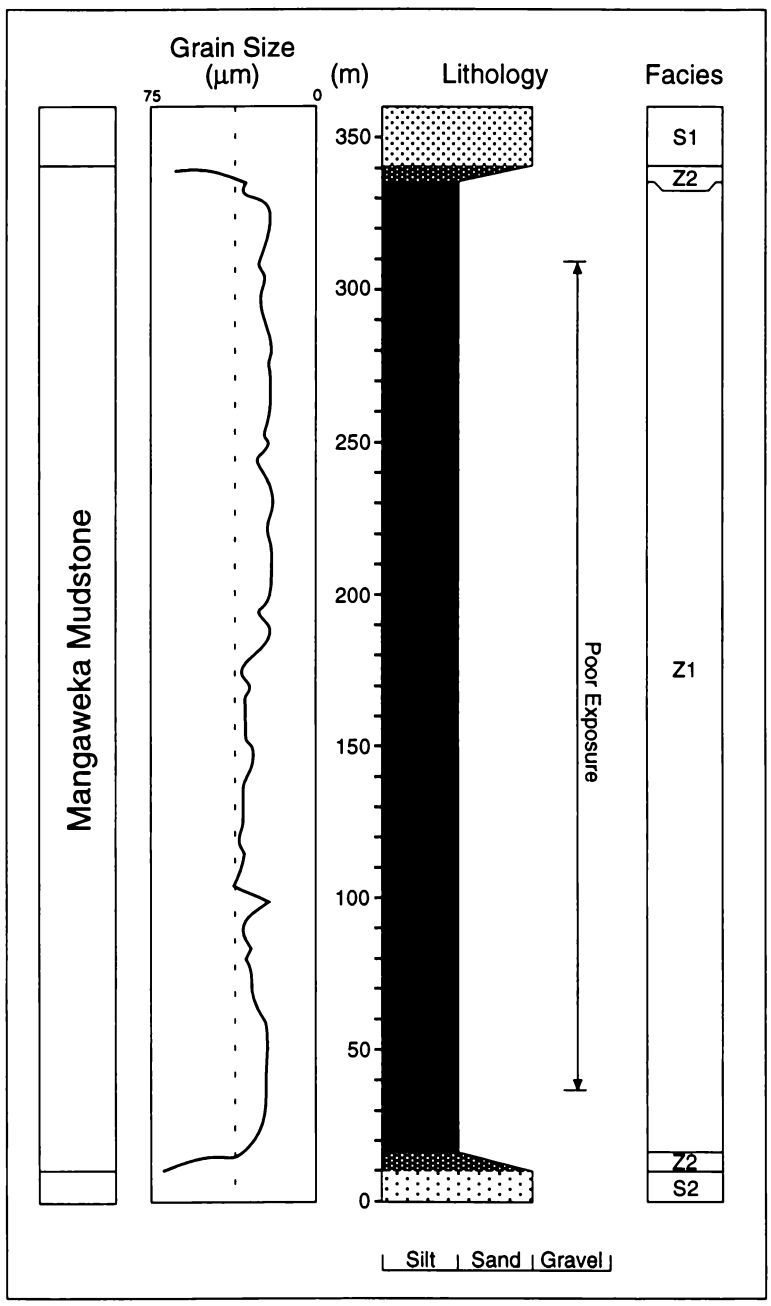

Figure 5:8. Composite stratigraphic column for the Mangaweka Mudstone within the Wanganui River valley showing the distribution of lithofacies. The massive nature of this unit is highlighted by the mean particle size curve as determined by laser particle sizer (Appendix 2: Particle-size; n=66).

The upper boundary of the Mangaweka Mudstone is characterised by a rapid siltstone/sandstone transition (Figure 5:8), the change to sandstone defining the top of the Mangaweka Mudstone and the beginning of the Pitangi Sandstone. This transition can be observed within Pitangi Stream (S22 958582) or up side gullies leading up from the road, such as the one at S21 950604. The boundary is only poorly seen on the road at S22 954584.

5:3:5:5 Thickness

The thickness determined in this study is approximately 330 m. A similar thickness was given by Ker (1973) and Collen (1972).

5:3:6 Facies Characteristics

Within the Ahurangi Sandstone, Atene Formation and Mangaweka Mudstone, seven lithofacies have been identified and grouped into three major lithotypes using sedimentological and faunal features. Lithotypes are named siltstone, sandstone and shellbed after the prominent lithology. The diagnostic characteristics of the lithofacies are described according to their (a) physical description, (b) paleontological content, and (c) an interpretation of depositional environment (summarised in Table 5:1). Analysis of the depositional paleoenvironments for all census samples (raw data in Appendix 2: Forams) is based on the identification of key ecologically restricted taxa (Figure 5:9) rather than statistical analysis as discussed in Appendix 1.

5:3:6:1 Siliciclastic siltstone lithotype

FACIES Z1 - (a) Barren to sparsely fossiliferous, massive, bioturbated, variably concretionary siltstone.

(b) Census analyses indicates the generalised occurrence of *Bulimina* spp., *Cassidulina neocarinata, Elphidium charlotense*[1], *Hauslerella* spp., *Notorotalia* spp., *Uvigerina miozea* group and *Virgulopsis wanganiensis* .

(c) Indicating a mid- to outer-shelf (≈100 m) depositional environment.

FACIES Z2 - (a) Weakly lithified, blue-grey, massive, bioturbated, micaceous (<2 %), fine sandy siltstone. Barren to sparsely fossiliferous and rarely concretionary.

(b) Census analysis indicates the generalised occurrence of *Cassidulina neocarinata, Elphidium charlottense*[1], *Nonionella flemingi, Notorotalia finlayi, Uvigerina rodelyi, Virgulopsis* spp..

(c) Indicating a mid-shelf (50-100 m) depositional environment.

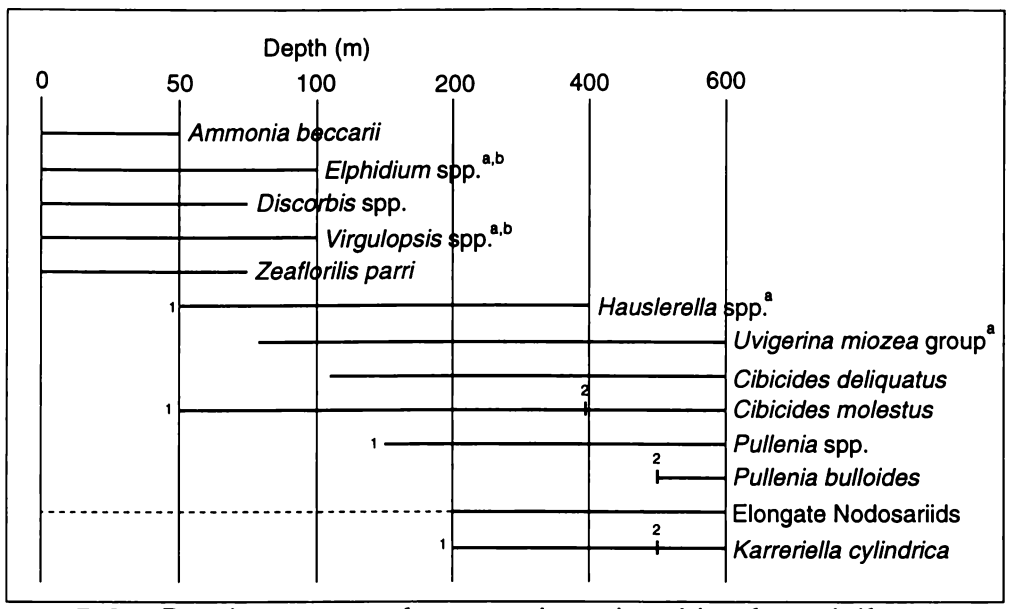

Figure 5:9. Depth range of some key benthic foraminifera used in determining paleowater depths (after Hayward, 1986; Hornibrook *et al.*, 1989; Crundwell *et al.*, 1994; Hayward *et al.*, 1997). 1 = (Hayward, 1986), 2 = (Crundwell *et al.*, 1994), a = commonly observed in facies Z1, b = commonly observed in facies Z2.

5:3:6:2 Siliciclastic sandstone lithotype

FACIES S1 - (a) Barren to sparsely fossiliferous, variably concretionary, massive, bioturbated, micaceous (1-5%), silty fine sandstone.

FACIES S2 - (a) Loose, barren, moderately to well sorted, massive, variably concretionary, bioturbated, fine micaceous(1-5%) sandstone.

FACIES S4 - (a) Barren, wavy to horizontally thinly bedded (approximately 5-20 cm), variably concretionary, micaceous (1-5%) fine sandstone.

(c) Such thinly bedded fine sandstones have been regarded as deposited in a mid- to outer-shelf environment (e.g. Driese *et al.*, 1991).

FACIES S8 - (a) Soft, bioturbated (commonly vertical tubes ≈1 cm in diameter), micaceous (1-5%), silty fine sandstone, with small siltstone lenses forming flaser-like bedding.

(b) Numerous macrofossil moulds.

[1] Commonly called *E. charlottensis*

5:3:6:3 Shellbed lithotype

FACIES Cs4 - (a) Bands, clumps and scattered shells that are commonly broken within massive fine silty sandstone to sandstone, matrix dominated and variably concretionary.

(c) The rarity of taxa and delicate nature of the shells suggests a lower energy inner- to mid-shelf depositional paleoenvironment (Beu and Maxwell, 1990; Gillespie and Nelson, 1996).

Table 5:1. Summary of sedimentary facies in late Pliocene sedimentary strata from the Wanganui River section.

Code	Description	Depositional environment	Example
Siliciclastic siltstone lithotypes			
Z1	Massive siltstone	Outer-shelf	Mangaweka Mudstone
Z2	Massive fine sandy siltstone	Mid to outer shelf	Atene Formation Azm1
Siliciclastic sandstone lithotypes			
S1	Massive, micaceous, silty fine sandstone	Inner to mid shelf	Base of Ahurangi Sandstone
S2	Massive, micaceous, medium to fine sandstone	Inner to mid shelf	Atene Sandstone Asm3
S4	Thinly bedded, micaceous, fine sandstone	Mid to outer shelf	Upper half Ahurangi Sandstone
S8	Flaser bedded, micaceous, silty fine sandstone	Intertidal to subtidal	Atene Formation Asm3
Shellbed lithotypes			
Cs4	Bands, clumps, and scattered shells in a fine sandstone matrix (matrix dominated)	Inner to mid-shelf	Atene Formation Acm1

5:4 DEPOSITIONAL PALEOENVIRONMENTS

5:4:1 AHURANGI SANDSTONE

As with Collen (1972), no microfauna were recovered from the sands of the Ahurangi Sandstone, making paleoenvironmental interpretations difficult. Census data from the siltstones below and above the Ahurangi Sandstone (W962475 (Chapter 3) and W962496 (Table 5:2) respectively) indicate outer (100-200) to mid-shelf (50-100 m) environments. This combined with the horizontal bedding (c. 10-20 cm) structures that occur in the upper half of the Ahurangi Sandstone and an absence of typically nearshore (0-25 m) bedding structures (i.e. cross-bedding) indicate that deposition of this unit is likely to have occurred in a predominantly mid-shelf (≈50 m) setting.

5:4:2 ATENE FORMATION

Siltstone-dominated units (Azm1 and Azm2) within the Atene Formation are interpreted from the foraminiferal census data as having mid-shelf (50-100 m) depositional environments (Section 5:3:6:1; Table 5:2). While sandstone bodies are likely to represent shallower conditions, the absence of microfaunal data or distinctive bedding structures means that quantifying this generalised statement is difficult. The occurrence of abundant macrofossil moulds and flaser-like bedding in the silty fine sandstones (Facies S8) under the weakly lithified sandstone horizons near the top of the unit, would indicate that nearshore conditions may have been achieved during the deposition of these units. Given that the three cyclothems within the ≈200 m thick Atene Formation (Figure 5:5) were deposited during a time of very high sedimentation rate (compacted sedimentation rate of 2.75 m/ky, Figure 2:6), these cyclothems represent high-order glacio-eustatically controlled sea-level fluctuations.

Table 5:2. Depositional water depth interpretations from microfaunal census analyses in the Wanganui River valley for samples taken between Otui village and Pitangi Stream. Interpretations are based on Crundwell *et al.* (1994) and Hayward (1986) with raw data presented in the Appendix 2: Forams.

Sample No. W962-	Stratigraphic Height (m)	Facies	Water Depth (m)
496	3105	Z2	50-100
510	3207.5	Z2	50-100
550	3395	Z1	≈100
559	3440	Z1	≈100

5:4:3 MANGAWEKA MUDSTONE

Despite the fine-grained nature of the Mangaweka Mudstone the foraminiferal content was extremely poor, with most samples being barren (Appendix 2: Summary), making microfaunal studies within this unit very difficult. This situation was also encountered by Collen (1972). However, foraminiferal data, summarised in Table 5:2, indicates that the Mangaweka Mudstone was deposited at mid- to outer-shelf depths (≈100 m). Extrapolation of sediment accumulation rates (Figure 2:6) indicates that emplacement of the Mangaweka Mudstone occurred very rapidly (rate of 2.75 m/ky), and helps to

explain the relative lack of foraminifera in samples collected from this unit as it would both reduce the rate of foraminiferal production (due to poor environmental conditions) and would dilute those that are present.

The depths of deposition and the evidently very high sedimentation rates, are reconciled in a model involving an out-building of clinoforms at the shelf-edge (at 100 m rather than the typical 200 m depth; Figure 5:10), analogous to the Giant Foresets Formation of Taranaki Basin (see King and Thrasher, 1996). Such an interpretation helps explain (a) the differences in the nature of the Mangaweka Mudstone between the Wanganui River section and the Rangitikei River section, where the formation has a much lower sedimentation rate (c. 0.9 m/ky) and has a more abundant microfaunal content (Journeaux *et al.*, 1996), and (b) how time equivalent deposits to the west have higher sand contents and display cyclicity (McIntyre pers. comm. and personal observation).

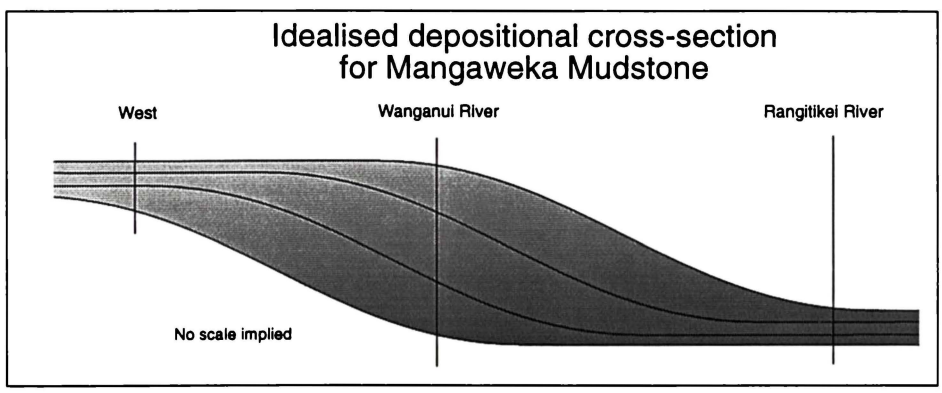

Figure 5:10. Idealised cross-sectional model showing clinoforms prograding from a shelf-edge (≈100 m), with the relative location of the Wanganui and Rangitikei River sections shown.

5:5 SUMMARY

The three key lithostratigraphic units in the 700 m-thick mid to late Pliocene, terrigenous marine succession between Otui village and Pitangi Stream in the Wanganui River valley, represent a variety of paleoenvironments.

(a) The ≈170 m-thick massive Ahurangi Sandstone records the transition from deep-water (200-600 m) environments of the underlying Tangahoe Formation to the mid-shelf, cyclothemic deposits of the Atene Formation.

(b) The ≈195 m-thick weakly cyclothemic Atene Formation reflects the return of shelfal environments to this part of the basin.

(c) The depositional environment of the ≈330 m-thick massive Mangaweka Mudstone has been reconciled to a prograding shelf-edge clinoform situation.

CHAPTER 6

GEOLOGICAL SYNTHESIS

CHAPTER 6

GEOLOGICAL SYNTHESIS

6:1 INTRODUCTION

Between Taranaki Basin and the central ranges of the North Island, New Zealand, lies the broadly elliptical, back-arc Wanganui Basin. This basin covers an area of some 22,000 km^2, approximately half of which is offshore and contains a Plio-Pleistocene sedimentary succession some 4 km thick. On-going south- to southeast-ward migration of the basin depocentre has resulted in progressive onlap of younger strata onto basement rocks. This, combined with thermally driven uplift to the north, has resulted in the development of broad east-west trending stratal belts that young and dip to the south and southeast. The Wanganui River intersects these stratal belts and offers the potential to examine the entire late Miocene (lower Kapitean) to late Pliocene (Mangapanian) succession in the western half of Wanganui Basin. The remoteness and severe difficulties in accessing much of the area, together with poor exposure in the more accessible areas, have meant there are few recent publications concerning the geology of the Wanganui River section. This thesis addresses the limited knowledge of the stratigraphy and depositional paleoenvironments of the sedimentary succession, enabling a better understanding of the development of the Wanganui Basin as a whole. Some of the main conclusions from this study are mentioned below, followed by a discussion of the geological evolution of the Wanganui River succession.

6:1:1 Biostratigraphy and Chronology

Foraminiferal analysis has allowed, the identification of five planktic foraminiferal biozones (*Globorotalia conomiozea* zone, *G. punticulata* zone, *G. inflata* zone, combined dextral *G. crassaformis* and *Cibicides molestus* zone, and dextral *G. crassaformis* zone), and implied the location of another one (*G. sphericomiozea* zone), see Figure 2:3. This is the first time that the Wanganui River section has been divided into predominantly planktic foraminiferal biozones that are linked to the New Zealand stage classification system (Figure 6:1). The absolute ages of these foraminiferal datums have allowed the magnetostratigraphy to be correlated with the global geomagnetic polarity time-scale. The resulting biostratigraphic and magnetostratigraphic age data have then been combined to form an age framework for the sedimentary

succession exposed in the Wanganui River valley between Tieke and Parakino (Figure 2:5). An important development of this work has been the recognition that the base of the major dextral coiling zone of *Globorotalia crassaformis* and the last appearance datum of *Cibicides molestus*, which have been previously tied to the boundary between the Mangapanian and Waipipian stages, are in fact significantly diachronous. While the last appearance datum of *Cibicides molestus* appears to approximate the original definition of this boundary (i.e. the base of the Mangapani Shell Conglomerate), the base of the major dextral coiling zone of *Globorotalia crassaformis* occurs significantly earlier (by about 200 ky).

Pliocene	Mangapanian		Dextral *Globorotalia crassaformis*
	Waipipian	?upper	Combined dextral *G. crassaformis* and *Cibicides molestus*
			Globorotalia inflata
	Opoitian	upper	
		lower	*Globorotalia punticulata*
Miocene	Kapitean	upper	*Globorotalia sphericomiozea* (inferred)
		lower	*Globorotalia conomiozea*

Figure 6:1. Wanganui River section biozones and corresponding New Zealand stages. The upper part of the Kapitean Stage was not located, thus its location in the stratigraphy has been inferred (Figure 2:3).

6:1:2 MATEMATEAONGA FORMATION

For the first time the lithostratigraphy of the strongly cyclothemic, limestone-bearing, sandstone-dominated Matemateaonga Formation, between Tieke and Jerusalem in the Wanganui River valley, has been analysed (the base of this formation was not located). This approximately 1570 m thick, late Miocene (lower Kapitean) to Pliocene (mid Opoitian) aged succession is composed of 31 cyclothems (Figure 3:5). Within the Matemateaonga Formation three lithotypes (siltstone, sandstone and shellbed, named after the dominant lithology recorded in the field) and thirteen constituent lithofacies have been identified. These lithofacies are representative of a wide range environments from the outer-shelf to the nearshore, as determined from their sedimentary structures and benthic foraminiferal characteristics (Table 3:1). While the detailed nature of the cyclothems is variable, in general they display a coarsening upward trend, with the basal boundary of each cyclothem typically being delineated by a shellbed(s). In terms of depositional environments the basal shellbeds are indicative of moderate to high energy nearshore to inner-shelf locations, with

the overlying silty lithofacies representing the deepest environments (mid- to outer-shelf) recognised within the cyclothems. The coarsening upward trend in each cyclothem represents a progressive shallowing, probably to inner-shelf environments.

Comparison of the Matemateaonga Formation cyclothems with the Naish and Kamp (1997) sequence stratigraphic model for 6th-order late Plio-Pleistocene glacio-eustatically controlled shelf cycles, shows up both many similarities and some differences. While the basal boundaries of some cyclothems are obviously erosional or conformable, many others are marked by a planar surface. Such a surface may be erosional, however, processes such as diagenetic cementation fronts can also explain their development, thus their interpretation is problematic. Three transgressive systems tract motifs are recognised (Table 6:1 and Figure 6:2). An important difference recognised in this study is that the backlap shellbed is not always overtopped by facies representative of the highstand systems tract. There may be an intervening massive fine to medium sandstone. This is thought to represent a short-lived regressive parasequence at the base of the highstand systems tract (HST; Section 3:4:1:2). The highstand and regressive systems tracts are

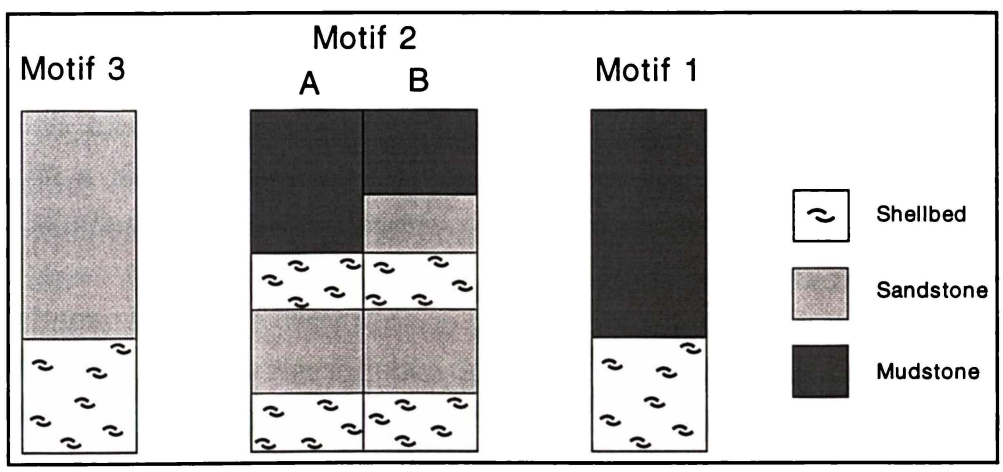

Figure 6:2. Transgressive systems tract motifs, descriptions are given in Table 6:1.

Table 6:1. Transgressive systems tract motifs.

	Description
Motif 1	Compound shellbed, overtopped by silty lithologies
Motif 2	Onlap and backlap shellbeds are separated by a massive fine to medium sandstone of the nearshore siliciclastic wedge. May be overtopped directly by silty lithologies or there may be an intervening massive sandstone
Motif 3	Onlap shellbed, overtopped by massive fine to medium sandstone, which is overlain by silty lithologies, no backlap shellbed

represented by a coarsening upward succession. Extrapolation of compacted sediment accumulation rates suggests internal architecture of the cyclothems has commonly been controlled by high-order (6th) glacio-eustatic fluctuations (Section 3:5). However, these extrapolations also show that some of the cyclothems are derived from much longer-term controls, of probably tectonic origin.

6:1:3 TANGAHOE FORMATION

The Wanganui River valley between Jerusalem and Otui exposes the 1350 m thick, predominantly fine-grained, upper Opoitian and Waipipian aged Tangahoe Formation. Extensive grain-size determinations using a laser particle sizer has determined that this succession is predominantly a siltstone. The abrupt change from the underlying sandstone-dominated Matemateaonga Formation to the siltstone-dominated Tangahoe Formation is marked by an approximately 1 m thick glauconitic siltstone. Analysis of benthic foraminifera within these structureless, blue-grey siltstones consistently indicates paleodepths in the 200-600 m range, while the low abundance of planktic foraminifera (average 12%) suggests a neritic environment. This apparent inconsistency in paleoenvironments (i.e. deep-water and neritic) is explained by the Tangahoe depocentre occupying a semi-enclosed situation, i.e. development of the depocentre has probably occurred within a shallow, continental sea-way. Basin development within Bass Strait, Australia, is a modern situation with some similarities.

Within the Tangahoe Formation occur three distinctive sandstone-dominated units, the Jerusalem, Matahiwi and Koroniti Sandstone Members (Figure 4:4). These sandstone members are composed of multiple, mass-emplaced, well-sorted, micaceous, fine sandstones interbedded with typical Tangahoe Formation siltstone. The basal boundary of the sandstone beds is erosional (flame structures), while the top surface is gradational (over about 10 cm) and extensively burrowed. Commonly sandstone bed thickness is in the 30 cm to 1 m range. However, vertical and lateral dimensions of individual beds are highly variable and on a large scale show amalgamation into, and subdivision of, large sandstone beds. It is likely that most, if not all, of the thick sandstone beds are composite in nature. The sandstones are interpreted as being depocentre (cf traditional continental margin) slope and basin floor fan deposits derived from quasi-steady state grain-flows. An attempt to confine the timing of the sandstone members in relation to glacio-eustatic fluctuations using isotopic analysis of foraminiferal tests through the Matahiwi and Koroniti

Sandstone Members proved to be inconclusive due primarily to diagenetic overprinting of the foraminiferal tests.

Across basin analysis of the Tangahoe Formation has highlighted the unsuitability of using the sandstone members for correlation as these mass-emplaced units are likely to be more or less randomly placed within the succession. Paleogeographic considerations of this across basin work has resulted in: (a) possible identification of a previously unknown depocentre during the upper Opoitian; (b) recognition of the need to extend the highs along the western margin of the basin; and (c) the realisation that sediment was supplied into the Wanganui Basin directly from the South Island via the now submerged river system that extended north of the current Marlborough Sounds.

6:1:4 Ahurangi Sandstone, Atene Formation and Mangaweka Mudstone

The Ahurangi Sandstone, Atene Formation and Mangaweka Mudstone form the upper-most part of the Wanganui River valley succession considered in this study. These three units form a 700 m thick terrigenous marine succession of Waipipian and Mangapanian age. The transition from the siltstone-dominated Tangahoe Formation into the overlying sandstone-dominated Ahurangi Sandstone occurs over approximately 15 m. This transition reflects the progressive infilling, due to decreased subsidence, of the slope-depth depocentre responsible for the development of the Tangahoe Formation. The Ahurangi Sandstone is initially massive, but becomes bedded (10-20 cm) in its upper half, with moderately cemented, lensoidal concretions forming along the coarser beds in the upper third of the bedded section.

A poorly developed concretionary shellbed marks the return of cyclothemic shelf deposits and the beginning of the Atene Formation. This formation recognises the return of high-order glacio-eustatic fluctuations as the dominant control on relative sea-levels and thus deposition within the shelf environment. The poorly developed concentration of shell material and scattered greywacke gravel (<5 mm in size) at the base of the second cyclothem within the Atene Formation (Acm2) has been tentatively correlated to the Mangapani Shell Conglomerate.

The uppermost unit in this study, the Mangaweka Mudstone, records a deepening to mid-shelf depths (about 100 m). sediment supply has been sufficient to maintain very high compacted sedimentation rates (2.75 m/ky) despite the change to a siltstone-dominated lithology. In this study, in the

Wanganui River section, the Mangaweka Mudstone is interpreted as being deposited in a "giant-foreset" type of prograding clinoform environment. From the age control available it appears that the base of the Mangaweka Mudstone is time transgressive across the basin, the LAD of *Cibicides molestus* occurring well within the formation in the Rangitikei River section (Journeaux, 1995) but well below the base of the Mangaweka Mudstone in the Wanganui River valley.

6:2 GEOLOGICAL EVOLUTION

The Wanganui Basin developed in a series of discrete steps as the basin depocentre migrated south and southeast since at least the late Pliocene (Figure 4:28). The interplay of depocentre migration and global sea-level fluctuations has resulted in the development of a complex lithostratigraphic succession. Whereas Chapters 3, 4 and 5 considered the details of the exposed succession, this section appraises the overall development of the Wanganui River succession.

Consideration of a complete composite stratigraphic column for the Wanganui River valley between Tieke and Pitangi Stream (north of Parakino) highlights six major periods of geological development, named in Figure 6:3. The variability in the extent and duration of each of these phases is probably related to the size, duration and proximity of the developing depocentre. The closer the stratigraphic succession is to the corresponding depocentre, the greater the accommodation space generated and the thicker the resulting deposits (Figure 6:4). Figure 6:5 (foldout on page 195) summarises much of the information concerning the nature of the phases, using paleogeographic maps and facies cross sections. The paleogeographic maps provide an indication of the location of the depocentre relative to the paleoshoreline and how it has varied over time. These maps also highlight the semi-enclosed nature of the resultant basins. Idealised facies cross sections, have the phases located on them and show how the nature of the phase varies depending upon both the location of the phase on the profile and the loci of the depocentre. Alongside each phase location is a series of numbers, these numbers relate to the box's located under each profile. Each box represents a key paleoenvironment and provides a summary of the information available on that environment. By its very nature such a diagram is a simplification of the true situation and is rather idealised. One possibly confusing feature in Figure 6:5 is the location of multiple phases on one cross-section. This does not imply that they occur at the same time, but rather that they can be represented on the

same facies cross section and are derived from similar paleogeographies. Each of the six identified phases are discussed below.

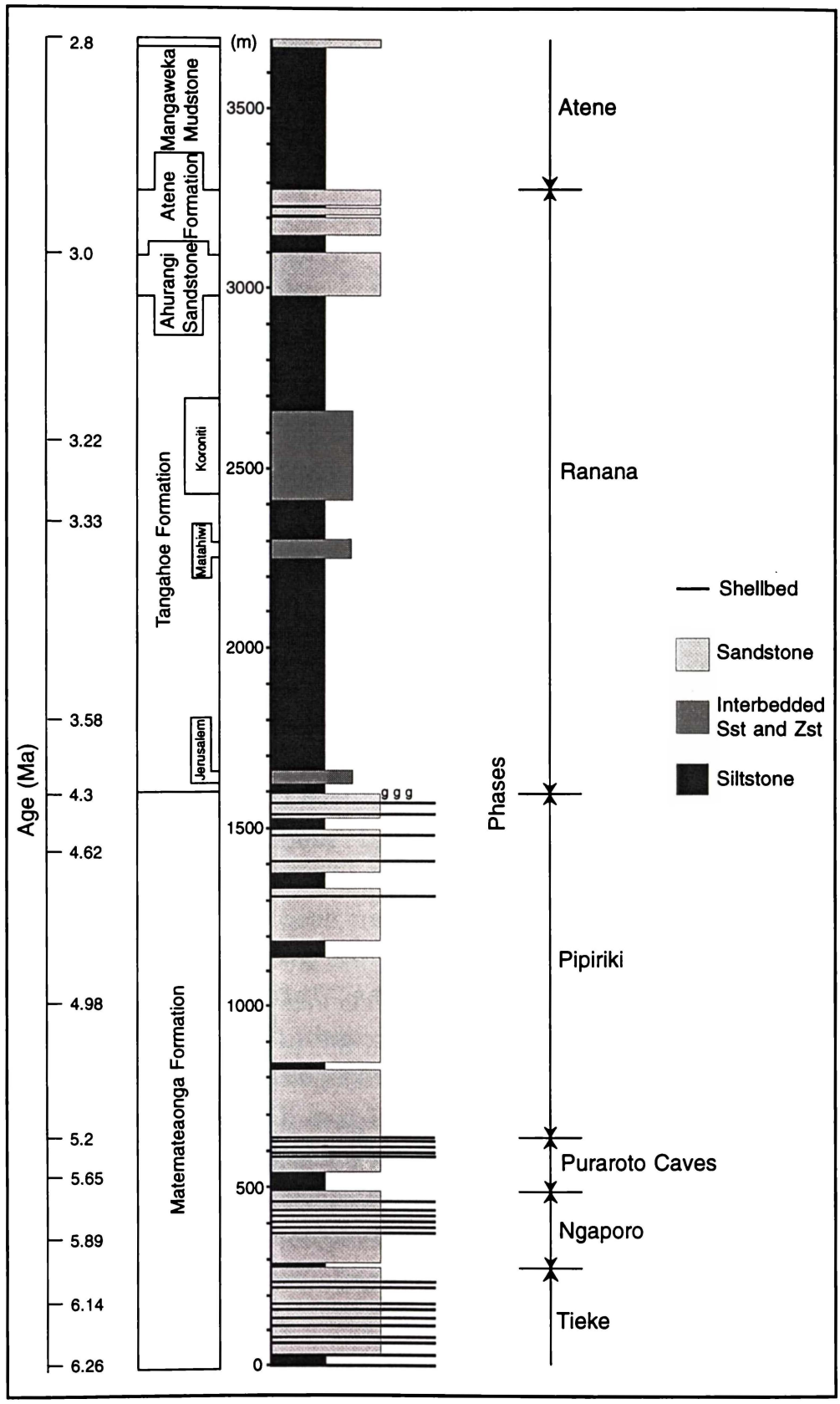

Figure 6:3. Composite stratigraphic column for the late Miocene to late Pliocene Wanganui River section, showing the six phases of development.

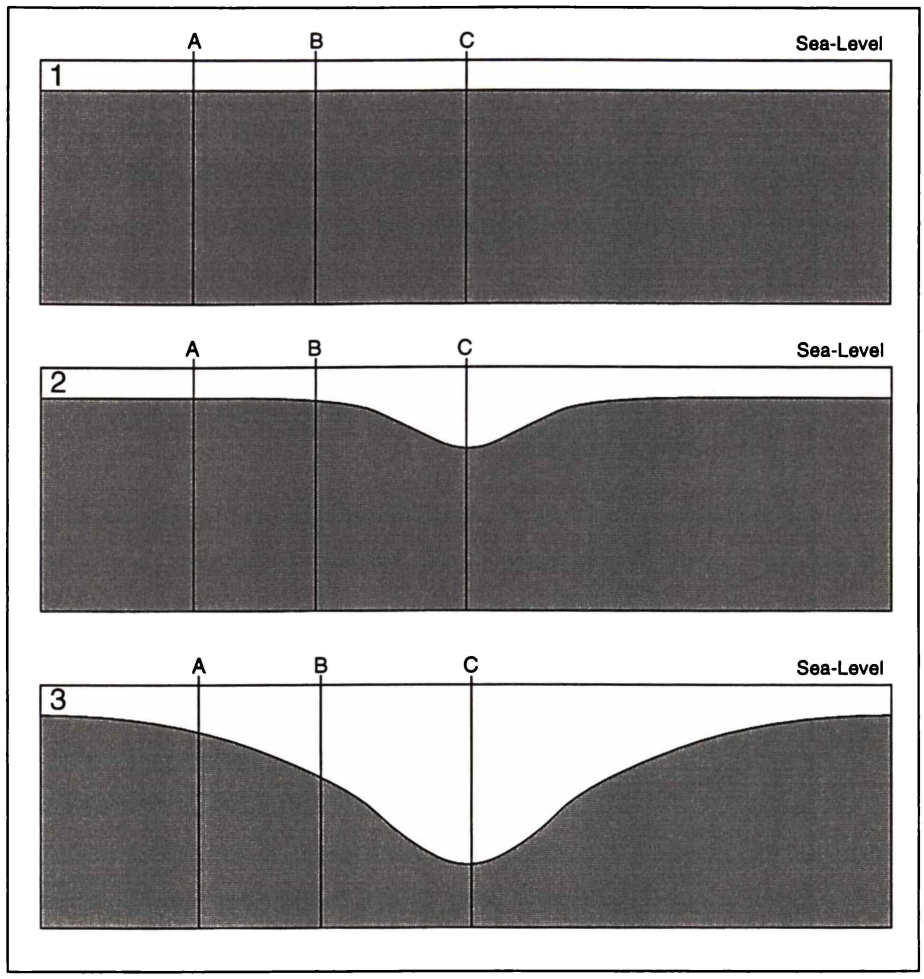

Figure 6:4. Idealised cross-section of basin development by pull down, showing the differences in accommodation space generated depending upon proximity to the loci of the depocentre.

6:2:1 TIEKE PHASE

The Tieke phase comprises the first 10 cyclothems in the Matemateaonga Formation (Figure 6:3); each characterised by a basal shellbed(s) and a coarsening upward, terrigenous succession (Figure 3:5). With an average cyclothem thickness of 27.5 m (Chapter 3) and compacted sedimentation rate of 1.5 m/ky (Figure 2:6), these cyclothems are deposits resulting from high order glacio-eustatically driven sea-level fluctuations. In this situation, tectonic stability and gradual regional subsidence has allowed the development and preservation of the cyclic succession (Figure 6:5, cross section A-B).

6:2:2 NGAPORO PHASE

The 250 m thick Ngaporo phase is defined as starting at the base of cyclothem 11 and ending at the top of cyclothem 18a (Figures 6:3 and 3:5). The 20 m thick siltstone at the base of cyclothem 11 is suggested to be the result of a tectonically driven regional deepening. The seven cyclothems at the top of the Ngaporo phase (cyclothems 12 - 18a), each typically characterised by basal shellbed(s) and a coarsening upward, terrigenous succession, represent the re-establishment of the high-order glacio-eustatic signal as the dominant control on relative sea-level (c. 40 ky 6th order; average 18 m thick and compacted sedimentation rate of 0.66 m/ky (Figure 2:6)). The sandstone that forms the bulk of the lower half of this phase (Mtsm19, approximately 85 m thick) is thought to be related to the infilling of accommodation space until conditions were such that global glacio-eustatic fluctuations were not being repressed at this location by local basin development controls on relative sea-level (Figure 6:5; cross section CD). This repression of the glacio-eustatic signal is probably due to ongoing tectonically driven transgression related to the depocentre development, with the slump deposits within Mtsm19 (Cyclothem 11) being associated with this ongoing tectonic activity.

6:2:3 PURAROTO CAVES PHASE

This condensed phase begins with the siltstone at the base of cyclothem 18b and ends at the eroded top of cyclothem 22. An unknown amount of material has been removed during the development of the unconformity between this and the overlying Pipiriki phase. A surprisingly low sedimentation rate (0.24 m/ky; Figure 2.6) has been calculated for this phase. Given that the cyclothems at the top of this phase (cyclothems 19 - 22) are expected to be of a similar magnitude to those of the lower zones (i.e. c. 40 ky cyclicity) and have an average thickness of 11.5 m, the calculated sedimentation rate appears to be realistic. However, there is no independent way of assessing the correctness of this sedimentation rate against the lower two thirds of this phase, so an assessment of the amount of material lost in the unconformity is not currently possible. As with the Ngaporo phase, the siltstone at the base of this phase is thought to be related to a tectonically controlled deepening, with the overlying sandstone representing the transition from local tectonic to global glacio-eustatic controls on relative sea-level (Figure 6:5; cross section CD).

6:2:4 Pipiriki Phase

The Pipiriki phase extends from the base of cyclothem 23 to the top of cyclothem 30. This phase is different to the two previous ones because the 8 m thick shellbed (Mtcm28) at the base of this phase represents the physical transgression of the sea over the land surface, resulting from a tectonically driven deepening event (Figure 6:5, cross section E-F). Slumping and siltstone based cyclothems (24 and 25) are regarded as being the results of tectonic activity related to ongoing deepening. Thus tectonically driven subsidence related to the development of the depocentre occurred over a significant period of time (c. 350 ky). The top 250 m of the Pipiriki phase contains five 40 ky 6^{th}-order glacio-eustatically produced cyclothems. Individual cyclothems are much thicker than previously observed, which is probably a function of the space generated during the deepening being utilised by the high-order cyclicity. The much greater thickness of this phase, approximately 900 m, suggests that the active depocentre was much closer than was the case in previous phases.

6:2:5 Ranana Phase

This phase extends from the base of the Tangahoe Formation to the top of the Atene Formation. The very low sedimentation rates for the lower part of the zone are consistent with sediment starvation during transgression brought on by a major tectonically controlled deepening. Sediment starvation is emphasised by the presence of a glauconitic siltstone at the base of this phase. Subsequent ongoing subsidence has been able to maintain depositional depths despite very high compacted sedimentation rates (2.24 m/ky) throughout the (approximately 1350 m thick) Tangahoe Formation. The Ahurangi Sandstone expresses the reduction in sea-level due to diminished basin subsidence and associated basin infilling; note that sedimentation rates have not changed significantly (Figure 2:6). The cyclothemic Atene Formation denotes the return of glacio-eustatic fluctuations as the dominant control on relative sea-level. The very prominent mass-emplaced sandstones of the Tangahoe Formation probably represent slope/basin floor (in the relation to the depocentre rather than a continental margin) fan deposits. The apparent cyclicity of these deposits is probably in fact a function of randomness, where the deposits have been derived from a migrating point source (Figure 6:6). The thickness (1600 m) of this phase in comparison to the other phases suggests a central depocentre location (Figure 6:5, cross section E-F).

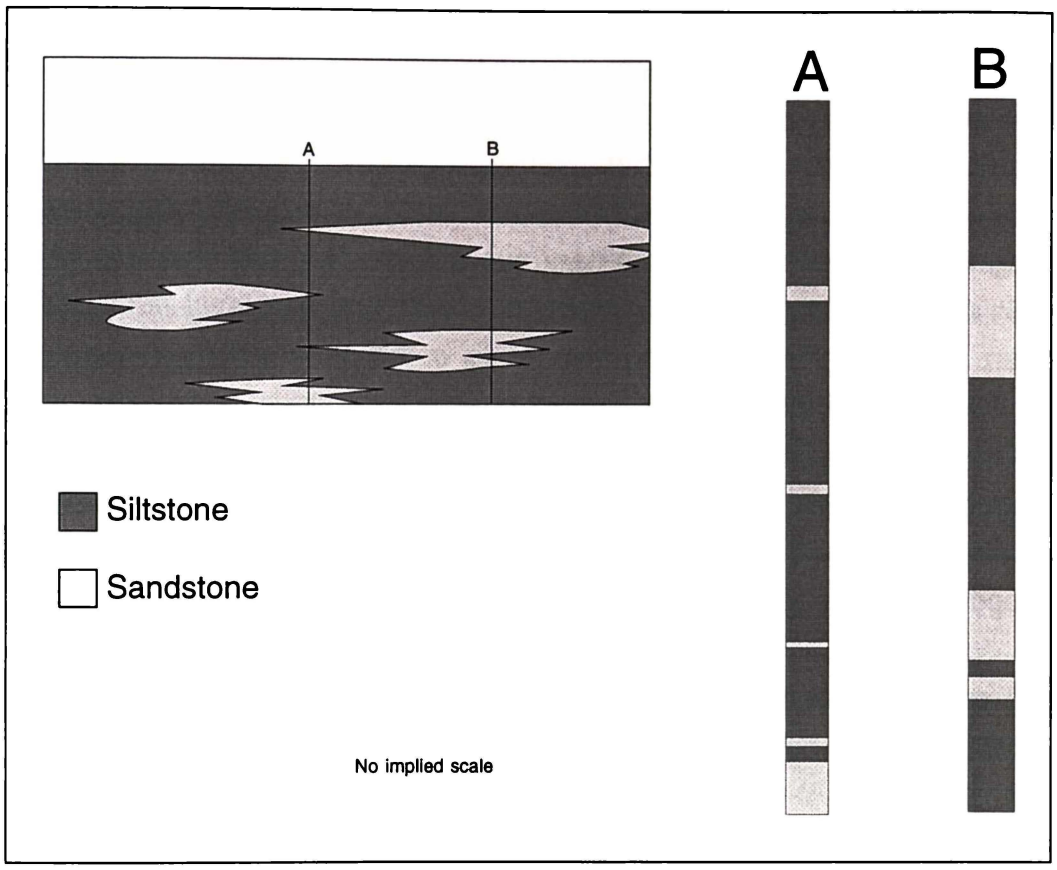

Figure 6:6. Idealised cross-section of mass-emplaced units deposited from a migrating point source system and two possible stratigraphic columns showing a degree of cyclicity that is in fact related to randomness.

6:2:6 Atene Phase

Only the base of this phase, the Mangaweka Mudstone, is part of this study; the Pitangi Sandstone and overlying units of McIntyre and Kamp (1998) represent the upper part. As with the Ngaporo, Puraroto and Ranana phases, the mudstone is thought to be related to tectonically driven deepening. The very high compacted sedimentation rates (2.75 m/ky, Figure 2:6) are likely to have prevented the development of a condensed section (cf. Ranana and Pipiriki phases). This zone, as with the Pipiriki phase, is probably proximal to, but not centrally located within (cf. Ranana phase), the depocentre.

6:2:7 Discussion

The Wanganui River succession records a generalised ongoing subsidence that is punctuated by localised deepening events, the effects of which vary across the basin depending on proximity of the loci of deepening

(Figure 6:6). The extraordinarily high compacted sedimentation rates achieved through this succession (over 50% of the succession has rates in excess of 1.5 m/ky with values reaching 2.75 m/ky; Figure 2:6) indicate that sediment supply to this basin has been extremely high. However, it has been the relative sea-level and associated accommodation space that has played a key role in controlling the nature of the sedimentary succession. Primarily this has been of tectonic origin, while global glacio-eustatic controlled sea-level fluctuations have been important for controlling the nature of the sedimentary succession during quiescent periods between stages of active depocentre development. Although the Pipiriki, Ranana and Atene phases appear to be the result of distinctive depocentres, the more distal Ngaporo and Puraroto deepenings may be related to different depocentres or multiple deepening events within a single depocentre.

6: 3 POSTSCRIPT

While mapping of individual cyclothems within the Matemateaonga Formation is unlikely to be a feasible option across the Wanganui Basin, the phases of development recognised here do offer the possibility of being able to be correlated basinwide. This is possible as the deepenings related to depocentre development are likely to be notable across the basin and the phases are of sufficient duration for current dating methods (i.e. biostratigraphy and paleomagnetism) to be able to resolve one phase from another.

The relationships between the units above the Matemateaonga Formation need to be considered on a basinwide scale. Currently there is two sets of terminology and stratigraphy, one for the eastern part of the basin and one for the western part. While this may be appropriate, their regional relationships need to be considered. This is one of many topics currently being addressed as part of the Public Good Science Foundation (PGSF) funded Wanganui Basin Project within the Department of Earth Sciences, at The University of Waikato.

Work on the nature, definition and boundaries of the Tangahoe Formation is required so that the lateral relationships between the Tangahoe Formation at the type section, the coastal section and the Wanganui River section can be determined. The topic is currently being reviewed in another study.

Detailed analysis of the source of the sediments in the Wanganui Basin succession, especially in relation to any change over time, is definitely required. This analysis would also help to determine the importance of the Marlborough-Wanganui Shield, relative to the Southern Alps, in supplying sediment to the Wanganui Basin, and the way in which sediment arrived at the basin (i.e. longshore drift cf. directly via rivers). These problems are deserving of a major separate study.

The relationship of dextral *Globorotalia crassaformis*, *Cibicides molestus* and the Mangapani Shell Conglomerate needs to be established. Independent age constraints are also required so that comparisons with other studies can be made. This project is currently underway.

Further work in tying down more precisely the relationships between the biostratigraphy and magnetostratigraphy identified in this study. This section I believe offers the potential to become one of New Zealand's key sections relating stage boundaries and the global paleomagnetic timescale.

A feature that has come clear to me in this study is that the Patea-Tongaporutu High (western high shown in Figure 6:3) has been far more active and important than previously thought. While it may not have been emergent it has, as a submarine high or island archipelago, played a major role in the development of the sedimentary succession in the Wanganui Basin and in affecting the oceanicity of the basin.

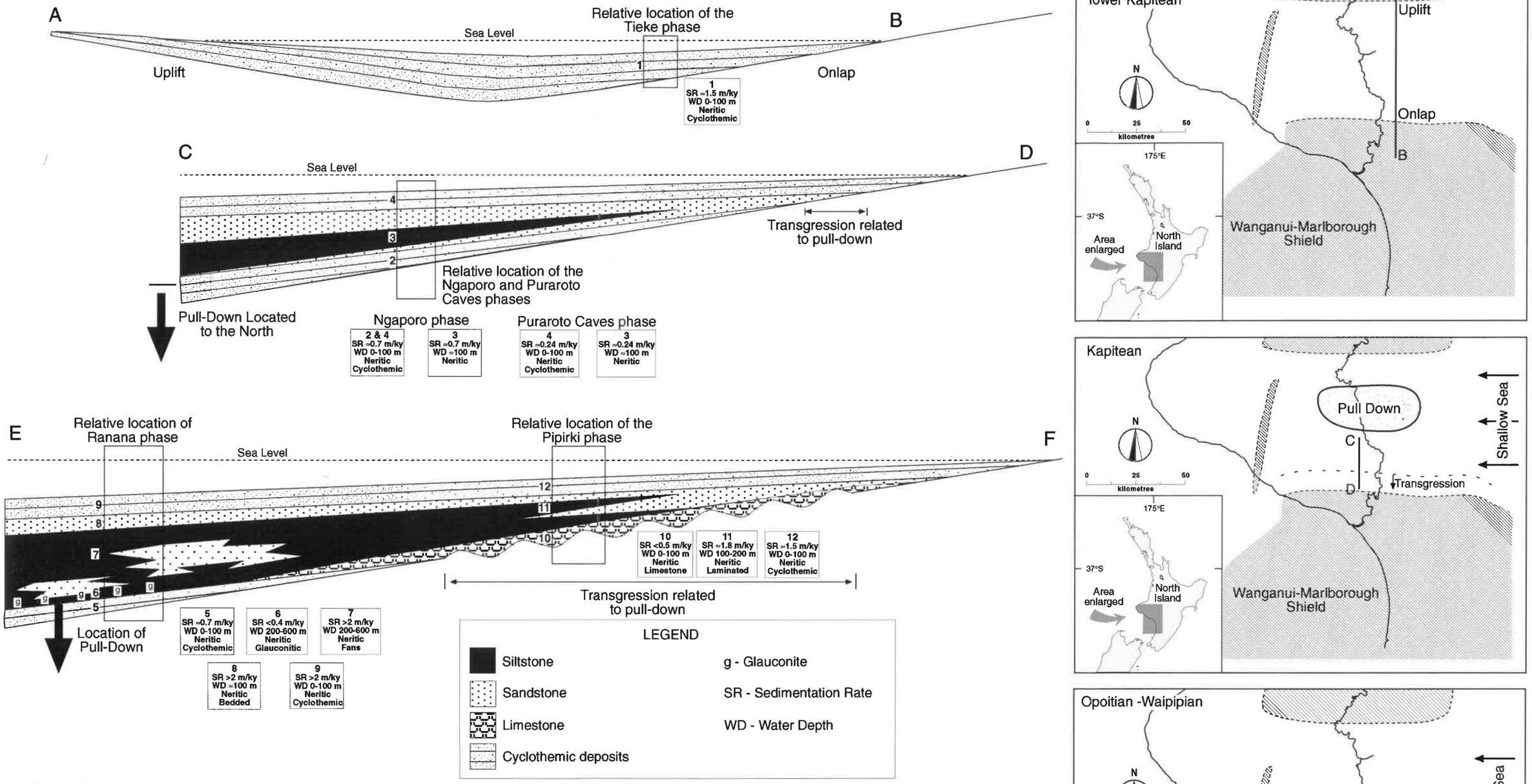

Figure 6:5. Schematic diagrams linking the phases of development discussed in the text to north-south facies cross sections and idealised paleogeographic maps. The maps illustrate the semi-enclosed nature of the depocentres and the approximate loci of pull down relative to the cross sections and paleoshoreline. Cross section A-B illustrates a stable situation where glacio-eustatic fluctuations are developing extensive cyclothemic deposits across a broad shallow sea, while land masses are subsiding to the south and emerging to the north. Cross section B-C represents both the Ngaporo and Puraroto Caves phases, where depocentre development is well to the north of the outcrop location and shoreline. Consequently there is minimal shoreline transgression and deepening. Cross section E-F illustrates the situation when depocentre development is located near the shoreline and outcrop location. Both the Pipiriki and Ranana phases are representative of this situation, although they represent different locations along the cross section. In this case the transgression is much more extensive, with the consequent development of condensed deposits. As the phases represent locations close to the loci of depocentre development, the deepening is much more significant, generating large amounts of accommodation space and supporting much higher sedimentation rates. The representation of two phases on cross sections C-D and E-F has been done to simplify the diagram; in reality each phase occupies a separate time frame with the phases stacked upon one another (see Figure 6:3). Boxes 1-12 contain information on the nature of the depositional environment during different parts of each phase. The box number relates to the number located alongside each phase location panel.

REFERENCES

REFERENCES

Abbott, S. T., and R. M. Carter, 1994: The sequence architecture of mid-Pleistocene (c. 1.1 - 0.4 Ma) cyclothems from New Zealand: facies development during a period of orbital control on sea level cyclicity, *in* P. L. de Boer, and D. G. Smith, eds., Orbital forcing and cyclic sequences: International association of sedimentology; Special publication 19, p. 367-394.

Anderton, P. W., 1981: Structure and evolution of the South Wanganui Basin, New Zealand: New Zealand journal of geology and geophysics; v. 24, p. 39-63.

Arnold, H. C., 1957: The Pliocene stratigraphy of South Taranaki: Shell BP and Todd oil services limited, Geological report 11; Unpublished open-flie petroleum report 414A.

Berggren, W. A., F. J. Hilgen, C. G. Langereis, D. V. Kent, J. D. Obradovich, I. Raffi, M. E. Raymo, and N. J. Shackleton, 1995a: Late Neogene chronology: New perspectives in high-resolution stratigraphy: Geological society of America bulletin; v. 107, p. 1272-1287.

Berggren, W. A., D. V. Kent, C. C. I. Swisher, and M-P. Aubry, 1995b: A revised Cenozoic geochronology and chronostratigraphy, *in* W. A. Berrgren, D. V. Kent, M.-P. Aubry, and J. Hardenbol, eds., Geochronology time scales and global stratigraphic correlation: Society for sedimentary geology; Special publication 54, p. 129-212.

Beu, A. G., 1995: Pliocene limestones and their scallops. Lithostratigraphy, Pectinid biostratigraphy and paleogeography of eastern North Island late Neogene limestone: Institute of geological and nuclear sciences, Monograph 10 (New Zealand geological survey paleontological bulletin 68).

Beu, A. G., and A. R. Edwards, 1984: New Zealand Pleistocene and late Pliocene glacio-eustatic cycles: Palaeogeography, palaeoclimatology, palaeoecology; v.46, p.119-142.

Beu, A. G., and P. A. Maxwell, 1990: Cenozoic Mollusca of New Zealand: New Zealand geological survey, Department of scientific and industrial research, Paleontological bulletin 58.

Boggs, S., 1987: Principles of sedimentology and stratigraphy: Ohio, Merrill Publishing Company; 784 p.

Bornhold, B. D., and P. Giresse, 1985: Glauconitic sediments on the continental shelf off Vancouver Island, British Columbia, Canada: Journal of sedimentary petrology; v. 55, p. 653-664.

Bromley, R. G., 1996: Trace fossils: biology, taphonomy and applications: London, Chapman and Hall; 361 p.

Bruhn, C. H. L., and R. G. Walker, 1997: Internal architecture and sedimentary evolution of coarse-grained, turbidite channel-levee complexes, early Eocene Regencia Canyon, Espírito Santo Basin, Brazil: Sedimentology; v. 44, p. 17-46.

Carter, R. M., S. T. Abbott, C. S. Fulthorpe, D. W. Haywick, and R. A. Henderson, 1991: Application of global sea-level and sequence-stratigraphic models in Southern Hemisphere Neogene strata from New Zealand, *in* D. I. M. MacDonald, ed., Sedimentation, ectonics and eustatasy: International association sedimentary geologists; Special publication 12, p. 41-65.

Chough, S. K., S. H. Yoon, and S. J. Park, 1997: Stratal patterns in the southwestern margin of the Ulleung Basin off southeast Korea: sequence architecture controlled by back-arc tectonism: Geo-marine letters; v. 17, p. 207-212.

Church, K. D., and R. L. Gawthorpe, 1997: Sediment supply as a control on the variability of sequences: an example from the late Namurian of northern England: Journal of the geological society, London; v. 154, p. 55-60.

Clemens, S. C., and R. Tiedemann, 1997: Eccentricity forcing of Pliocene-early Pleistocene climate revealed in a marine oxygen-isotope record: Nature; v. 385, p. 801-804.

Clifton, H. E., R. E. Hunter, J. V. Gardner, 1988: Analysis of eustatic and sedimentological influences on transgressive and regressive cycles in the upper Cenozoic Merced Formation, San Francisco, California, *in* K. L. Kleinspehn, C. Paola, eds., New Perspectives in basin analysis: New York, Springer-Verlag; p. 109-128.

Collen, J. D., 1972: Studies in the Wanganui Series: Pliocene foraminifera from Wanganui Basin: Ph.D thesis, Victoria University, Wellington.

Compton, S. M., 1989: Morphology & geochemistry of glauconite from the Te Kuiti Group, South Auckland Region, New Zealand: MSc thesis, Waikato University, Hamilton; 193 p.

Cope, R. N., 1966: The hydrocarbon prospects of the Wanganui Basin, New Zealand: Shell BP and Todd Oil Services, Unpublished open-file exploration report 64.

Crundwell, M. P., G. H. Scott, and G. P. Thrasher, 1994: Calibration of paleobathymetry indicators by integrated seismic and paleontological analysis of foreset sequences, Taranaki Basin, New Zealand: 1994 New Zealand Petroleum conference proceedings; p. 169-178.

Davies, G. F., 1981: Regional compensation of subducted lithosphere: effects of geoid, gravity and topography from a perliminary model: Earth planetary science letters; v. 54, p. 431-441.

Dickinson, J. A., 1998: Stratigraphy and sedimentology of early Pliocene strata, Mangawhero valley, and subsurface correlations, central Wanganui Basin: MSc thesis, University of Waikato, Hamilton; 121 p.

Dodd, R. J., R. J. Stanton Jr, 1991: Cyclic sedimentation in three Neogene basins in California, *in* D. I. M. MacDonald, ed., Sedimentation, tectonics and eustasy: International association of sedimentary geologists; Special publication 12, p. 201-215.

Driese, S. G., M. W. Fischer, K. A. Easthouse, G. T. Marks, A. R. Gogola, and A. E. Schoner, 1991: Model for genesis of shoreface and shelf sandstone sequences, southern Appalachians: paleoenvironmental reconstruction of an early Silurian shelf system, *in* D. J. P. Swift, G. F.

Oertel, R. W. Tillman, and J. A. Thorne, eds., Shelf sand and sandstone bodies: geometry, facies and sequence stratigraphy: Blackwell scientific publications; p. 309-338.

Edwards, A. R., 1987: An integrated biostratigraphy, magnetostratigraphy and oxygen isotope stratigraphy for the late Neogene of New Zealand: New Zealand geological survey, Record 23.

Feldmeyer, A. E., B. C. Jones, C. W. Firth, and J. Knight, 1943: Geology of the Palmerston-Wanganui Basin, "West Side", North Island, New Zealand: Superior Oil Company of NZ.

Finlay, H. J., and J. Marwick, 1947: New divisions of the New Zealand upper Cretaceous and Tertiary: New Zealand journal of science and technology, section B; v. 24, p. 228-236.

Fleming, C. A., 1953: The geology of Wanganui Subdivision: New Zealand geological survey bulletin 52.

Fleming, C. A., 1959: Fascicule 4, New Zealand, *in* C. A. Fleming, ed., Lexique stratigraphique international, Paris, Centre National de la Recherche Scientifique; p. 527.

Fleming, C. A., 1978: Wanganui-Manawatu, *in* R. P. Suggate, G. R. Stevens, and M. T. Te Punga, eds., The geology of New Zealand: Wellington, Government Printer; p. 460-465.

Galloway, W. E., W. F. Dingus, and R. E. Paige, 1991: Seismic and depositional facies of Paleocene-Eocene Wilcox Group submarine canyon fills, Northwest Gulf Coast, U.S.A., *in* P. Weimer, and M. H. Link, eds., Seismic facies and sedimentary processes of submarine fans and turbidite systems: Frontiers in sedimentary geology: Springer-Verlag; p. 247-272.

Gillespie, J. L., and C. S. Nelson, 1996: Distribution and control of mixed terrigenous-carbonate surficial sediment facies, Wanganui shelf, New Zealand: New Zealand journal of geology and geophysics; v. 39, p. 533-549.

Gillespie, J. L., C. S. Nelson, and S. D. Nodder, In press: Post-glacial sea-level control and sequence stratigraphy of carbonate-terrigenous sediments, Wanganui Shelf, New Zealand: Sedimentary geology.

Haq, B. U., 1991: Sequence stratigraphy, sea-level change, and significance for the deep sea, *in* D. I. M. MacDonald, ed,. Sedimentation, tectonics and eustasy: International association of sedimentary geologists; Special publication 12, p. 3-39.

Haskell, T. R., 1991: Kiwi Co-operative dairies company Kiwi - 2 well completion report: Haskell exploration services, report 57.

Hay, R. F., 1967: Sheet 7 Taranaki (1:250,000): Department of scientific and industrial research.

Hayward, B. W., 1986: A guide to paleoenvironmental assessment using New Zealand Cenozoic foraminiferal faunas: New Zealand geological survey - Paleontology Group, Report Pal109.

Hayward, B. W., H. Grenfell, and C. Reid, 1997: Foraminiferal associations in Wanganui Bight and Queen Charlotte Sound, New Zealand: New Zealand journal of marine and freshwater research; v. 31, p. 337-365.

Haywick, D. W., R. M. Carter, and R. A. Henderson, 1992: Sedimentology of 40 000 year Milankovitch-controlled cyclotherms from central Hawke's Bay, New Zealand: Sedimentology; v. 39, p. 675-696.

Helland-Hansen, W., and J. G. Gjelberg, 1994: Conceptual basis and variability in sequence stratigraphy: a different perspective: Sedimentary geology; v. 92, p. 31-52.

Hendy, C., S. Prosser, S. Cooke, P. Cooke, and C. van der Veen, 1997: CAPS a new automated isotopic analysis system for carbonates: Sixth Australian-New Zealand environmental isotope conference; p. 19-20.

Holt, W. E., and T. A. Stern, 1994: Subduction, platform subsidence, and foreland thrust folding: The late Tertiary development of Taranaki Basin, New Zealand: Tectonics; v. 13, p. 1068-1092.

Hornibrook, N. de. B., 1981: Globorotalia (planktic Foraminiferida) in the late Pliocene and early Pleistocene of New Zealand: New Zealand journal of geology and geophysics; v. 24, p. 263-292.

Hornibrook, N. de. B., 1982: Late Miocene to Pleistocene Globorotalia (Foraminiferida) from DSDP leg 29, site 284, southwest Pacific: New Zealand journal of geology and geophysics; v. 25, p. 83-99.

Hornibrook, N. de. B., R. C. Brazier, and C. P. Strong, 1989: Manual of New Zealand Permian to Pleistocene foraminiferal biostratigraphy: New Zealand geological survey; paleontological bulletin 56.

Hudson, D. S., 1996: Provenance of Miocene to Recent sands and sandstones of the Taranaki - Wanganui Region, New Zealand: MSc thesis, University of Waikato, Hamilton; 143 p.

Hughes, A. D., and D. Whitehead, 1987: Glauconitization of detrital silica substrates in the Barton Formation (upper Eocene) of the Hampshire Basin, southern England: Sedimentology; v. 34, p. 825-835.

Hume, T. M., 1978: Clay petrology of Mesozoic to Recent sediments of Central Western North Island, New Zealand: DPhil thesis, University of Waikato, Hamilton; 410 p.

Hunt, T. M., 1980: Basement structure of the Wanganui Basin, onshore, interpreted from gravity data: New Zealand journal of geology and geophysics; v. 23, p. 1-16.

Ito, M., 1992: High-frequency depositional sequences of the upper part of the Kazusa Group, a middle Pleistocene forearc basin fill in Boso Peninsula, Japan: Sedimentary geology; v. 76, p. 155-175.

Journeaux, T. D., 1995: Lithostratigraphy, foraminiferal paleoecology, and sequence stratigraphy of middle Pliocene strata, Wanganui Basin: MSc thesis, University of Waikato, Hamilton; 150 p.

Journeaux, T. D., P. J. J. Kamp, and T. Naish, 1996: Middle Pliocene cyclothems, Mangaweka region, Wanganui Basin, New Zealand: a lithostratigraphic framework: New Zealand journal of geology and geophysics; v. 39, p. 135-149.

Kamp, P. J. J., and G. M. Turner, 1990: Pleistocene unconformity-bounded shelf sequences (Wanganui Basin, New Zealand) correlated with global isotope record: Sedimentary geology; v. 68, p. 155-161.

Katz, H. R., 1968: Potential oil formations in New Zealand, and their stratigraphic position as related to basin evolution: New Zealand journal of geology and geophysics; v. 11, p. 1077-1133.

Katz, H. R., 1988: Wanganui and East Coast Basins - two of New Zealand's little explored sedimentary basins: Energy, exploration and exploitation; v. 6, p. 281-297.

Katz, R., and B. L. Leask, 1989: The South Wanganui Basin - A neglected hydrocarbom prospect: 1989 New Zealand oil exploration conference proceedings; p. 71-80.

Ker, D. S., 1973: Stratigraphy and engineering geology of the lower Wanganui Valley, Koriniti to Parakino: New Zealand journal of geology and geophysics; v. 16, p. 189-208.

Ker, D. S., 1991: Provisional geological map of 1:50 000 sheet T21AC (Hautapu): New Zealnd geological survey.

Kidwell, S. M., 1991: Condensed deposits in siliciclastic sequences: expected and observed features, *in* G. Einsele, W. Ricken, and A. Seilacher, eds., Cycles and events in stratigraphy, Springer-Verlag; p. 682-695.

King, P. R., and G. P. Thrasher, 1996: Creatceous-Cenozoic geology of petroleum systems of the Taranaki Basin, New Zealand: Institute of geological and nuclear sciences, monograph 13.

Kneller, B., 1995: Beyond the turbidite paradigm: physical models for deposition of turbidites and their implications for reservoir prediction, *in* A. Hartley, and D. J. Prosser, eds., Characterization of deep marine clastic systems: Geological society; p. 31-49.

Kneller, B. C., and M. J. Branney, 1995: Sustained high-density turbidity currents and the deposition of thick massive sands: Sedimentology; v. 42, p. 607-616.

Kolla, V., and M. A. Perlmutter, 1993: Timing of turbidite sedimentation on the Mississippi Fan: The American association of petroleum geologists bulletin; v. 77, p. 1129-1141.

Konert, M., and J. Vandenberghe, 1997: Comparison of laser grain size analysis with pipette and sieve analysis: a solution for the underestimation of the clay fraction: Sedimentology; v. 44, p. 523-535.

Lewis, D. W., 1984: Practical Sedimentology: Pennsylvania, Hutchinson Ross Publishing Company; 229 p.

Li, Q., B. McGowran, N. P. James, and Y. Bone, 1996: Foraminiferal biofacies on the mid-latitude Lincoln Shelf, South Australia: oceanographic and sedimentological implications: Marine geology; v. 129, p. 285-312.

Lindholm, R. C., 1987: A practical approach to sedimentology: London, Allen & Unwin; 276 p.

Loman, W. H., 1986: Calcareous nannoplankton biostratigraphy of the southern Coral Sea, Tasman Sea and southwestern Pacific Ocean, deep sea drilling project leg 90: Neogene and Quaternary, *in* J. P. Kennett, and C. C. Von den Borch, eds., Initial reports of the deep sea drilling project 90: Washington (U.S. Government printers); p. 763-794.

Lowe, D. R., 1976a: Grain flow and grain flow deposits: Journal of sedimentary petrology; v. 46, p. 188-199.

Lowe, D. R., 1976b: Subaqueous liquefied and fluidized sediment flows and their deposits: Sedimentology; v. 23, p. 285-308.

Macdonald, D. I. M., (editor), 1991: Sedimentation, tectonics, and eustasy: International association of sedimentary geologists; Special publication 12, 518 p.

Martinsen, O. J., and W. Helland-Hansen, 1995: Strike variability of clastic depositional systems: Does it matter for sequence-stratigraphic analysis?: Geology; v. 23, p. 439-442.

McConchie, D. M., and D. W. Lewis, 1978: Authigenic, perigenic, and allogenic glauconites from the Castle Hill Basin, North Canterbury, New Zealand: New Zealand journal of geology and geophysics; v. 21, p. 199-214.

McIntyre, A. P., and P. J. J. Kamp, 1998: Late Pliocene (2.8-2.4 Ma) cyclothemic shelf deposits, Parikino, Wanganui Basin, New Zealand: lithostratigraphy and correlation of cycles: New Zealand journal of geology and geophysics; v. 41, p. 69-84.

McQuillan, H., 1977: Hydrocarbon potential of the North Wanganui Basin, New Zealand: The Australian petroleum exploration association journal; v. 1, p. 94-104.

Morgans, H. E. G., G. H. Scott, A. G. Beu, I. J. Graham, T. C. Mumme, W. St George, and C. P. Strong, 1996: New Zealand Cenozoic time scale (1996): Institute of geological and nuclear sciences ltd, Science report 96/38.

Morris, B. D., 1994: The geology of the Matemateaonga Formation, central Taranaki, New Zealand: DPhil thesis, Victoria, Wellington; 133 p.

Mortimer, N., A. J. Tulloch, and T. R. Ireland, 1997: Basement geology of Taranaki and Wanganui Basins, New Zealand: New Zealand journal of geology and geophysics; v. 40, p. 223-236.

Murphy, L. S., W. L. Leask, and J. D. Collen, 1994: Source rock potential of the Wanganui Basin: 1994 New Zealand petroleum conference proceedings; p. 95-107.

Murrell, G. R., 1998: Lithostratigraphy and sequence stratigraphy of Matemateaonga Formation (early Pliocene), Moawhango valley eastern Wanganui Basin: MSc thesis, University of Waikato, Hamilton; 171 p.

Naish, T., and P. J. J. Kamp, 1995: Pliocene-Pleistocene marine cyclothems, Wanganui Basin, New Zealand: a lithostratigraphic framework: New Zealand journal of geology and geophysics; v. 38, p. 223-243.

Naish, T., and P. J. J. Kamp, 1997: Sequence stratigraphy of sixth-order (41k.y.) Pliocene-Pleistocene cyclothems, Wanganui Basin, New Zealand: A case for the regressive systems tract: Geological society of America bulletin; v. 109, p. 978-999.

Naish, T., P. J. J. Kamp, B. V. Alloway, B. Pillans, G. S. Wilson, and J. A. Westgate, 1996: Integrated tephrochronology and magnetostratigraphy for cyclothemic marine strata, Wanganui Basin: implications for the Pliocene-Pleistocene boundary in New Zealand: Quaternary international; v. 34-36, p. 29-48.

Naish, T. R., R. M. Carter, and G. Saul, 1997: High resolution integrated chronology for the Plio-Pleistocene, Wanganui Basin, New Zealand: Townsville, Australia, School of Earth Sciences, James Cook University.

Nelson, C. S., and A. M. Smith, 1996: Stable oxygen and carbon isotope compositional fields for skeletal and diagenetic components in New Zealand Cenozoic nontropical carbonate sediments and limestones: a synthesis and review: New Zealand journal of geology and geophysics; v. 39, p. 93-107.

Nummendal, D., and D. J. P. Swift, 1987: Transgeressive stratigraphy at sequence-bounding unconformities: Some principals derived from Holocene and Cretaceous examples, *in* D. Nummedal, O. H. Pilky, and J. D. Howard, eds., Sea-level fluctuation and coastal evolution: Society of paleontologists and mineralogists; p. 241-259.

Odin, G. S., (editor), 1982: Numerical dating in stratigraphy: Chiechester, England, John Wiley and Sons Ltd, 1040 p.

Oulton, D. M., 1998: Stratigraphy and sedimentology of the Pliocene succession, Mangaohane Region, eastern Wanganui Basin: MSc thesis, University of Waikato, Hamilton; 157 p.

Pasquier, J-B., and A. Strasser, 1997: Platform-to-basin correlation by high-resolution sequence stratigraphy and cyclostratigraphy (Berriasian, Switzerland and France): Sedimentology; v. 44, p. 1071-1092.

Pickering, K. T., R. N. Hiscott, N. H. Kenyon, F. Ricci Lucchi, and R. D. A. Smith, 1995: Atlas of deep water environments: Architectural style in turbidite systems, Conoco and Chapman & Hall; 333 p.

Posamentier, H. W., and P. R. Vail, 1988: Eustatic controls on clastic deposition 11 - sequence and systems tract models, *in* C. K. Wilgus, B. S. Hastings, C. G. S. C. Kendall, H. W. Posamentier, C. A. Ross, and J. C. Van Wagnor, eds., Sea-level changes: an integrated approach: Society of economic paleontologists and mineralogists; Special publication 42, p. 125-154.

Posamentier, H. W., and G. P. Allen, 1993: Variablility of the sequence stratigraphic model: effects of local basin factors: Sedimentary geology; v. 86, p. 91-109.

Posamentier, H. W., and D. P. James, 1993: An overview of sequence-stratigraphic concepts: uses and abuses, *in* Posamentier, H. W., C. P. Summerhayes, B. U. Haq, and G. P. Allen, eds., Sequece stratigraphy and facies associations: International association of sedimentologists; Special publication 18, p. 3-18.

Posamentier, H. W., M. T. Jervey, and P. R. Vail, 1988: Eustatic controls on clastic deposition 1 - conceptual framework, *in* C. K. Wilgus, B. S. Hastings, C. G. S. C. Kendall, H. W. Posalentier, C. A. Ross and J. C. Van Wagnor, eds., Sea-level changes - an integrated approach: The society of economic paleontologists and mineralogists; Special publication 42, p. 109-124.

Posamentier, H. W., C. P. Summerhayes, B. U. Haq, and G. P. Allen, (editors), 1993: Sequece stratigraphy and facies associations: International association of sedimentologists; Special publication 18, 644 p.

Postma, G., A. R. Fortuin, and W. A. Van Wamel, 1993: Basin fill patterns controlled by tectonics and climate: the Neogene 'fore-arc' basins of eastern Crete as a case history, *in* L. E. Frostick, and R. J. Steel, eds.,

Tectonic controls and signatures in sedimentary successions: Blackwell scientific publications; p. 335-362.

Rivenaes, J. C., 1997: Impact of sediment transport efficiency on large-scale sequence architecture: results from stratigraphic computer simulation: Basin research; v. 9, p. 91-105.

Roberts, A. P., G. M. Turner, and P. P. Vella, 1994: Magnetostratigraphic chronology of late Miocene to early Pliocene biostratigraphy and oceanographic events in New Zealand: Geological society of America Bulletin; v. 106, p. 665-683.

Sarg, J. F., 1988: Carbonate sequence stratigraphy, *in* C. K. Wilgus, B. S. Hastings, C. G. S. C. Kendall, H. W. Posamentier, C. A. Ross, and J. C. Van Wagnor, eds., Sea-level changes: an integrated approach: Society of economic paleontologists and mineralogists; Special publication 42, p. 155-181.

Schlager, W., 1993: Accommodation and supply - a dual control on stratigraphic sequences: Sedimentary geology; v. 86, p. 111-136.

Scott, G. H., 1982: Review of Kapitean stratotype and boundary with Opoitian Stage (upper Neogene, New Zealand): New Zealand journal of geology and geophysics; v. 25, p. 475-485.

Seward, D., D. A. Christoffel, and B. Lienert, 1986: Magnetic polarity stratigraphy of a Plio-Pleistocene marine sequence of North Island, New Zealand: Earth and planetary science letters; v. 80, p. 353-360.

Shackleton, N. J., M. A. Hall, and D. Pate, 1995: 15. Pliocene stable isotope stratigraphy of site 846: Proceedings of the ocean drilling program, scientific results; v. 138, p. 337-353.

Shanmugam, G., 1996: High-density turbidity currents: are they sandy debris flows?: Journal of sedimentary research; v. 66, p. 2-10.

Shanmugam, G., 1997: The Bouma sequence and the turbidite mind set: Earth-science reviews; v. 42, p. 201-229.

Shanmugam, G., L. R. Lehtonen, T. Straume, S. E. Syvertsen, R. J. Hodgkinson, and M. Skibeli, 1994: Slump and debris-flow dominated upper slope facies in the Cretaceous of the Norwegian and northern North Seas (61-67N): Implications for sand distribution: The American association of petroleum geologists bulletin; v. 78, p. 910-937.

Shanmugam, G., R. B. Bloch, S. M. Mitchell, G. W. J. Beamish, R. J. Hodgkinson, J. E. Damuth, T. Straume, S. E. Syvertsen, and K. E. Sheilds, 1995: Basin-floor fan in the North Sea: sequence stratigraphic models vs. sedimentary facies: The American association of petroleum geologists bulletin; v. 79, p. 477-512.

St John, D. H., R. N. Cope, and G. W. Gibson, 1964: Parikino-1 exploration well resume: Shell BP Todd Oil Services Ltd, Unpublished open-file petroleum report 452.

Stern, T. A., and F. J. Davey, 1989: Crustal structure and origin of basins formed behind the Hikurangi subduction zone, New Zealand, *in* R. A. Price, ed., Origin and evolution of sedimentary basins and their energy and mineral resources: International union of geodesy and geophysics; Geophysical monograph 48, p. 73-85.

Stern, T. A., and F. J. Davey, 1990: Deep seismic expression of a foreland basin: Taranaki Basin, New Zealand: Geology; v. 18, p. 979-982.

Stern, T. A., G. M. Quinlan, and W. E. Holt, 1992: Basin formation behind an active subduction zone: three-dimensional flexural modelling of Wanganui Basin, New Zealand: Basin research; v. 4, p. 197-214.

Thompson, T. L., W. L. Leask, and B. T. May, 1994: Petroleun potential of the South Wanganui Basin: 1994 New Zealand petroleum conference proceedings; p. 108-127.

Thrasher, G., 1993: The South Wanganui Basin, *in* A. T. Crampton, R. C. Cregg, and V. Killops, eds., An introduction to the petroleum geology of New Zealand: Wellington, Publicity unit, crown minerals operations group, Energy and resources division, Ministry of Commerce; p. 46-53.

Tiedemann, R., M. Sarnthein, and N. J. Shackleton, 1994: Astronomic timescale for the Pliocene Atlantic $\delta^{18}O$ and dust flux records of Ocean Drilling Program site 659: Paleoceanography; v. 9, p. 619-638.

Uruski, C. I., 1998: Wanganui Basin seismic maps: Institute of geological and nuclear sciences, Client Report 54767A.12.

Vail, P. R., R. M. Mitchum Jr, R. G. Todd, J. M. Widmier, S. r. Thompson, J. B. Sangree, J. N. Budd, and W. G. Hatlelid, 1977: Seismic Stratigraphy and global changes in sea level, *in* C. E. Payton, ed., Seismic stratigraphy - applications to hydrocarbon exploration: American association of petroleum geologists; Memoir 26, p. 49-212.

Vail, P. R., F. Audemard, S. A. Bowman, P. N. Eisner, and C. Perez-Cruz, 1991: The stratigraphic signitures of tectonics, eustacy and sedimentology - an overview, *in* G. Einsele, W. Ricken, and A. Seilacher, eds., Cycles and events in stratigraphy: Springer-Verlag; p. 617-659.

Van Wagoner, J. C., H. W. Posamentier, R. M. Mitchum, P. R. Vail, J. F. Sarg, T. S. Loutit, and J. Hardenbol, 1988: An overview of the fundamentals of sequence stratigraphy and key definitions, *in* C. K. Wilgus, B. S. Hastings, C. G. S. C. Kendall, H. W. Posalentier, C. A. Ross and J. C. Van Wagnor, eds., Sea-level changes - an integrated approach: The society of economic paleontologists and mineralogists; Special publication 42, p. 39-45.

Walker, R. G., 1992: Facies, facies models and modern stratigraphic concepts, *in* R. G. Walker, and N. P. James, eds., Facies models - response to sea level change: Geological association of Canada; p. 1-14.

Walker, R. G., and T. R. Wiseman, 1995: Lowestand shorefaces, transgressive incised shorefaces, and forced regressions: examples from the Viking Formation, Joarcam Area, Alberta: Journal of sedimentary research; v. B65, p. 132-141.

Wilson, G. S., 1993: Ice induced sea level change in the late Neogene: PhD thesis, Victoria University, Wellington.

APPENDIX 1

METHODS

APPENDIX 1: METHODS

(1) PARTICLE SIZE ANALYSIS

Particle size is an important and standard component of studies involving sedimentary materials. In this study, grain-size was determined both in the field and in the lab. Laboratory based grain-size determinations provide an important check of these field determinations. The development of technologies such as the Malvern laser particle size analyser allows detailed grain-size analysis of hundreds of samples to be a realistic aspect of studies such as this one. However, the new technology required the development of sample preparation procedures.

SAMPLE PREPARATION FOR THE LASER PARTICLE SIZER

This section provides information on sample preparation for the Malvern laser particle size analyser and sample presentation unit setup in the Department of Earth Sciences, The University of Waikato, and may or may-not be suitable for dissimilar systems. For operating procedures see the appropriate user manuals. Although the disaggregation of partially lithified samples is a standard procedure with well documented methodologies (e.g. Lewis, 1984; Lindholm, 1987), the use of the laser particle sizer presented a new series of problems. Experimentation showed that sample weights of between 0.25g (mud) and 2.5g (sand) of material are required to obtain the required obscuration values in the Melvern Particle Sizer. The usage of such small sample sizes means that there is (i) a concern that the sub-sample is representative of the sample as a whole, and (ii) any material loss will have a major effect on the grain-size distribution. To minimise these difficulties aggregates[1] were used in the sub-sample rather than loose material, and sample preparation procedures where undertaken in a single vial. Also a large number of analyses were undertaken to obtain as complete a picture as possible of the grain-size distribution of any particular unit.

Design of the disaggregation methodology required a number of features to be taken into account: (1) total sample preparation in a single container to minimise the risk of material loss, (2) the use of the complete sub-sample to prevent preferential separation, (3) a methodology sufficiently robust to

[1] Aggregates refer to small chips or lumps of material as obtained from the outcrop.

disaggregate a wide range of partially lithified sediment types, yet gentle enough so as not to destroy the original texture, (4) the use of established procedures so as to prevent the development of sample preparation artefacts in the particle size distribution, and (5) a procedure sufficiently simple so that sample preparation was standardised and mass analysis was feasible. The procedure that resulted after a significant amount of experimentation is outlined below.

1) Air dry a portion of fresh, unweathered sample.

2) A suitable weight of material, varying from 0.25 to 2.5g depending upon the concentration of mud in the sample (the greater the concentration of mud the less sample required), in aggregate form is weighed into a 30 ml vial. Several samples at different weights may be required to obtain the right concentration at time of analysis.

3) 10 ml of 10% hydrogen peroxide (H_2O_2) is added to each vial. Once the obvious reaction has ceased, seal the vials and place on a shaker table at a moderate speed (≈160 rpm) for one hour.

4) Uncap the vials, wash material from the sides of the vial using distilled water into the sample container, place into an oven and heat until simmering, upon simmering turn off the heat and allow the samples to settle. This removes any surplus hydrogen peroxide.

5) Once the sample is fully settled, the clear fluid is carefully pipetted off. Ten ml of 10% Calgon (sodium hexametaphosphate buffered in sodium carbonate) is added to the vial before being resealed.

6) Return the sample to the shaker table for one hour at a moderate speed (≈160 rpm) followed by 5 minutes in an ultrasonic bath.

7) Allow the sample to stand overnight before repeating point 6.

8) Visual inspection of the material (via the base of the vial) should show that the material is fully disaggregated. If not, it will be necessary to repeat the procedure with a fresh sample.

SAMPLE PREPARATION FOR SAND:MUD RATIO BY SIEVE ANALYSIS

For a variety of reasons a large number of samples underwent bulk sand separation procedures. To maximise the information obtained the sand/mud concentrations were calculated and recorded as part of the particle size data base. The washing procedure and sand percentage calculations were constant and are summarised below.

1) A sample of approximately 200 g is placed into a numbered 600-800 ml beaker. The sample should be hand broken into gravel (10-20 mm diameter) sized aggregates.

2) Place beakers and sample in a warm (60°C) oven overnight.

3) Allow beakers to cool and weigh (beaker + sample).

4) Add sufficient 10% hydrogen peroxide to cover the sample, stir with a glass rod. Care is required as muddy samples will foam up and the sample can easily be lost over the side of the beaker. To combat this, continue to stir and/or add one or two drops of caprylalcohol.

5) Once the sample is completely disaggregated pour into a large 63 μm sieve, and wash residues from the beaker into the sieve. Wash the sample with water over a bucket, gentle stirring will assist the washing procedure. Once the water draining from the sieve is clear, sieving is complete. Wash the greater than 63 μm fraction back into the beaker from which it came. Finer than 63 μm samples can be obtained from the bucket as required.

6) Place beaker in warm (60°C) oven, once dry, allow to cool and weigh (sand + beaker). The sand is then placed into a suitable container for storage until required. The empty beaker is then reweighed (beaker).

7) Sand percentage is determined with the following equation

(((sand + beaker)-(beaker))/((sample + beaker)-(beaker)))*100

(2) Foraminiferal Census Analysis

Foraminiferal census analysis is used particularly in the determination of paleoenvironments, where the relative abundance of several species may provide clues as to the nature of, or changes in paleoconditions. Such determinations are repeatable as the splits are true unbiased divisions of the sample, and at each step, the entire split has been picked. The procedure below describes how the census analyses were undertaken.

1) The sand fraction (>63μm) is separated from an approximately 250 gram bulk sample as described in the "Sample preparation for sand:mud ratio by sieve analysis".

2) The greater than 63 μm sample fraction is sieved at 125 μm.

3) The >125 μm fraction is split using a Sepor sediment splitter with 3.1 mm veins, sufficient times such that the sample has about 200 foraminiferal specimens. In reality this involved splitting a sample about 10X and then picking successively larger splits until the desired number of specimens was obtained.

4) Starting with the smallest split, sufficient (or all) of the split is sprinkled onto a picking tray such that there is a light covering of material. All foraminifera observed are picked from the sample and stuck onto a census tray according to their species. This process is repeated until the entire split has been picked.

5) Ideally 200 specimens were picked from each sample, although 150 is sufficient.

6) Progressively larger splits are completely picked until the required number of specimens are obtained. Occasionally the target was not achieved, because either the entire sample had been picked, or foraminifera were so rare that continued picking was not justified. This difficulty was mainly restricted to the sandy lithologies of the Matemateaonga Formation.

7) Once picked, identification of all specimens is checked and counts made of each species or grouping used.

8) To determine the required paleoenvironmental information, the results are compared to prepared tables from other studies (e.g. Hayward, 1986; Hornibrook *et al.*, 1989; Crundwell *et al.*, 1994).

Interpretation of depositional paleoenvironments depends upon the identification of key benthic foraminifera. The principle problem with cluster analysis and similar statistical procedures is that rarely occurring non-key species can have a major influence on the nature of the cluster. Thus it is necessary to define the parameters of the analysis so that key species define the groupings. Rather than trying to define these parameters, the key taxa have been identified by hand in each sample. The relative occurrence of these key benthic foraminifera in anyone sample defined the depositional environment of that sample.

(3) Glauconite Separation

The techniques used to separate out glauconite for investigation are varied (e.g. McConchie and Lewis, 1978; Bornhold and Giresse, 1985; Hughes and Whitehead, 1987) with no apparent standard methodology commonly used. Therefore a robust methodology, described below, has been developed to concentrate glauconite from samples of partially lithified siltstone, previous studies have been used as a guide.

(1) Disaggregation of the sample was achieved by reacting the sample with 10% hydrogen peroxide. Washing the resulting slurry on a 63μm sieve separated out the sand sized fraction. Once washed the washed, sand sample was dried in a warm oven (maximum of 40°C).

(2) The dried sample was then resieved to obtain <125 μm, 125 - 250 μm & >250 μm fractions

(3) Magnetic separation of the 125 - 250 μm & >250 μm size fractions was undertaken using a Isodynamic Frantz. It appears that a twin run scenario has been used with good results by Hughes and Whitehead (1987) and Compton (1989) and is adopted here. The Frantz displacement settings remained constant, at a forward tilt of 15°, side tilt of 30° and magnet displacement of 5° at the front and 7° at the back for both runs. After several trial attempts, it was found that an initial separation at 0.5 amps, followed by a second run at 0.4 amps gave the best results.

(4) Compton (1989) found that the use of dilute HCl (1M recommended) can be used to wash calcite cement off glauconite without adversely affecting the nature of the glauconite provided the glauconite was in contact with the HCl for only short periods of time (<5 minutes). As the glauconite recovered in step 3 had calcite over-growths, on observation under a stereo microscope, dilute hydrochloric acid was used to remove the overgrowths. In this study it was found that 0.1 M HCl for 2 minutes was sufficient to remove the overgrowths and stay well inside the guidelines established by Compton (1989). Once reacted with the HCl the sample was well rinsed with water over the corresponding minimum sized sieve.

The result of this process is a sample in which glauconite has been separated and concentrated from the original siltstone and cleaned of adhering calcite.

From this point further preparation will depend upon the nature of the glauconites and the type of the analysis being undertaken. In this study preparation to this level is all that was required as the different morphotypes present could be distinguished.

(4) Isotope Sample Preparation

This appendix is based on the preparation of the samples ready for analysis. For procedures regarding the use of the mass spectrometer, consult the appropriate user manual as procedures will vary depending upon the type of mass-spectrometer used and the sample presentation mechanism. In this study *Cibicides deliquatus* and *Uvigerina miozea* group were determined as being the best foraminifera for isotope analysis. The sample preparation procedures used are set out below and follow well established methodologies.

1) The washed, greater than 63 μm sand fraction were separated over a 150 μm sieve.

2) The required foraminifera were picked from the greater than 150 μm fraction, choosing the most pristine specimens.

3) Ideally 30 specimens, that showed no sign of dissolution, infilling or encrusting were separated. In reality many samples had only 10-15 specimens from the entire sample that appeared to be of sufficient quality.

4) The specimens were washed in methanol and treated in an ultrasound bath for about 1 minute to remove any particles that were adhering to the tests.

5) Once dry (evaporated) the foraminifera were rechecked before being placed in a roasting vial and roasted at 400 oC for 1.5 hours in a vacuum, which was maintained while the sample cooled.

The samples were then ready to be run through the mass spectrometer.

(5) PALAEOMAGNETIC SAMPLE ANALYSIS

(Based on a report to P.J.J. Kamp by G. Turner, Victoria University, July 1998)

Natural Remnant Magnetisation and Magnetic Susceptibility

Firstly the natural remnant magnetisation (NRM) and low field magnetic susceptibility of each specimen was measured.

Susceptibility is a measure of the concentration of magnetisable materials in a sample. It is dominated by the contribution of ferrimagnetic minerals (such as titanomagnetite). NRM is the vector resultant of all the different components of magnetisation in a specimen, which are usually acquired at different stages in the rock's history.

The range of susceptibility values, and within site standard deviations are very small compared with those for NRM intensities. Susceptibility ranges from 0.16 to 0.22 x 10^{-3} SI units, with as overall mean of 0.19 x 10^{-3} SI units, while NRM intensity ranges from 0.03 to 0.53 x 10^{-3} A/m, with an overall mean of 0.14 x 10^{-3} A/m.

There appears to be no direct relationship between intensity of the NRM vector and magnetic susceptibility and this suggests that the variability in NRM is not due primarily to variations in the concentration of ferrimagnetic material, but to factors that influence the magnetic recording process. These factors may include:

- the original depositional environment,
- the spectrum of magnetic relaxation times or blocking temperatures within the ferrimagnetic grains,
- the post-depositional history of the rocks.

Consideration of these factors will be important in the interpretation of various components of magnetisation in the specimens.

The average intensity of magnetisation is sufficiently weak that only a cryogenic magnetometer can be used for detailed demagnetisation procedures. The SCT cryogenic magnetometer at Victoria University Wellington (VUW) measures reliability at about 0.005 mA/m in each component, or about 0.01 mA/m overall (for 10 ml specimens).

Progressive Demagnetisation

(a) Pilot studies

The initial procedure was to demagnetise one specimen from each site thermally, and one by AF demagnetisation, then to devise a system for as many of the remaining specimens as practical.

Thermal demagnetisation was carried out at temperatures of 100, 150, 200, 250, 280, 300, 320 and 340 °C. After each step the Remnant magnetisation and magnetic susceptibility were measured. Sediments such as these almost invariably show a marked rise in susceptibility around 300 °C, when thermally induced chemical changes lead to the formation of new ferrimagnetic minerals. When this occurs any remaining primary magnetisation is obliterated, precluding further attempts to isolate it. Susceptibility is therefore closely monitored, and as soon as any significant change is seen, thermal demagnetisation is stopped.

Stepwise alternating field demagnetisation was concluded using 5 mT increments of peak field, until no more useful information was obtained. This method of demagnetisation involves no heating, so the possibility of chemical changes to the mineralogy is avoided. However AF demagnetisation selects grains according to their coercivities rather than blocking temperatures. According to classical single domain theory, blocking temperature and relaxation time (at a particular temperature) are uniquely and monotonically related, however, coercivity and relaxation time are not. So stepwise AF demagnetisation does not systematically work through the grain spectrum from shortest to longest relaxation time (least to most stable in a temporal or thermal sense).

(b) Procedure

The routine procedure adopted for the remaining samples was

(1) to thermally demagnetise at 100, 150, 200, 240, 280 and 300 °C, or until susceptibility begins to change, or until the magnetisation is reduced below 0.01 mA/m for two successive steps, whichever occurs first.

(2) If sufficient magnetisation remains, then to proceed with AF demagnetisation at 5 mT increments of peak field, until no more useful data is obtained.

Preliminary Discussion of Data

All specimens show a strong thermoviscous component of magnetisation (TVRM), acquired during the Brunches normal polarity chron, which is removed by thermal demagnetisation up to 150 °C. In terms of the magnitude of the NRM vector, the TVRM ranges from 30% to 228%. It is more instructive to compare the magnitudes of the low and high blocking temperature components: the TVRM/HT ratio, since both are, more or less unidirectional, single components of magnetisation and so can be considered proxies for the proportion of grains in the least and most stable parts of the grain spectrum (NRM is the vector resultant of a number of components of magnetisation, which may be in different directions, so NRM intensity does not mirror the grain spectrum). TVRM/HT varies from 0.28 to 4.49, with a mean of 1.8 - reflecting a huge variation in the blocking temperature spectra of specimens from different sites.

Site by Site Analysis and Interpretation

Analysis of the data for each specimen involves either

- the determination of an endpoint direction, interpreted as the direction of the primary magnetisation, or

- the determination of a trend, seen as a great circle on a stereographic plot, as the secondary overprint is progressively removed and the primary is approached, but not reached.

The endpoints and great circles of all specimens from a site are then combined to give the best estimate primary direction, and an angle of 95% confidence.

(6) XRD ANALYSES

X-ray diffraction is a rapid and relatively simple procedure for determining the semi-quantitative mineralogy of sedimentary materials. While it is recognised that problems such as peaks relating to minor components being hidden in peaks related to major components, it is still a powerful tool in helping to determine the principal mineral components of a sedimentary samples.

In this study, the bulk composition of the Tangahoe Formation sandstones and siltstones as well as Matemateaonga Formation sandstones were required. To this end a number of unorientated, hand powdered bulk samples from each formation were analysed on a Philips analytical x-ray diffractor with a PW 1729 x-ray generator and a PW 1840 diffractometer control at the following settings:

Voltage	34 kV
Current	26 mA
Range	2-45° 2∅
Speed	0.02° 2∅/s
Chart	10 mm/s
Range	5×10^3
T.C.	1.0
Slit	0.2

Peak heights for quartz, plagioclase, potash feldspar and clay at set degree 2∅ values (Table next page) were converted to semi-quantitative weight percentages using conversion correlations determined by Hume (1978). Peak height is the vertical distance between the peak apex and the background line and is expressed as the number of small grid units on the diffractometer trace to the nearest half unit. The background line is a straight line that was drawn on each diffraction trace between 18° and 32° 2∅.

Degree 2∅ values used to determine key minerals present within the samples (after Hume, 1978).

Mineral		degrees 2∅	Å
Quartz		20.8	4.27
Plagioclase	A	28.0	3.19
	B	27.75	3.21
Potash Feldspar		27.5	3.24
Clay		19.9	4.46

(7) FIELDWORK

Fieldwork was begun in the middle of 1995 and continued off and on for the duration of the study which concluded in mid 1998. Fieldtrips of between 5 and 14 days duration were undertaken during this time, using primarily the Department of Conservation Wanganui Park Headquarters at Pipiriki as a base. Total time spent in the field is in excess of 150 days.

The first 18 moths or so - fieldtrips were based on the analysis and collection of samples along the Wanganui River Road south of Pipiriki. During the summer of 1995/6 I had the assistance of Mr S. Flint (BSc (Tech) student). Other fieldwork was undertaken subsequent to this time-frame to (a) undertake paleomagnetic sampling for which I had the assistance of Technical Officer Mr L. , (b) check relationships, interpretations, and (c) obtain further samples were they were required.

The summers of 96/7 and 97/8 involved the analysis of outcrops and collection of samples in the Wanganui River valley, north of Pipiriki, using a local jet boat operator (Baldy (Paul) Haitana) as the Wanganui River Road stops at Pipiriki. During this work I had the assistance of my supervisor - Associate Professor P.J.J. Kamp and Technical Officer Mr L. Gaylor.

APPENDIX 2

DATA

APPENDIX 2: DATA

(1) SUMMARY

Summary of available data:

(A) sample numbers:

University No.,

Sample No.;

(B) stratigraphic heights (m);

CFS = Churton Farm Section

JRS = Jerusalem - Road Section

SG1 = Submarine Gully 1

SG2 = Submarine Gully 2

JRXS = Jerualem - Road Cross Section

(C) grid references (NZMS 260);

(D) particle size:

mean (laser particle sizer, μm),

sand concentration (sieve, %);

(E) foraminiferal information:

B = Barren,

C = Census data available,

IGNS = Institute of geological and nuclear sciences examined,

biostratigraphic information available (IGNS sample numbers),

I = Isotope data available

This information is also viewable on and down loadable from the accompanying CD ROM

Appendix 2: Summary

				Particle Size		
University No.	Sample No.	Strat. Height	Grid Ref	Laser Sizer	Sieve Analysis	Forams
		(m)	NZMS 260	Mean (μm)	SAND%	
Matemateaonga Formation						
W962000	312	0	R20 816057	32.31	38.16	
W962001	313	6	R20 817055			
W962002	314	8	R20 817055		14.48	C/IGNS(A15 & SH#314)
W962003	315	24	R20 818051	20.68		
W962004	316	30	R20 818050	27.04	17.48	
W962005	317	35	R20 818049	182.78	91.49	
W962006	318	36	R20 818049			
W962007	319	40	R20 818049	25.1	9.45	B
W962008	320	61	R20 819044			
W962009	321	69	R20 819044	51.13		
W962010	322	100	R20 819043	27.42	32.03	
W962011	323	117	R20 820043	28.42		
W962012	324	123	R20 822041	60.23		
W962013	325	137	R20 854039	45.45		
W962014	326	140	R20 854039	78.84		
W962015	327	146	R20 826038	18.65	6.91	B
W962016	328	160	R20 828033	82.59		
W962017	329	166	R20 828032	44.02		
W962018	330	171	R20 828029	36.59		
W962019	331	176	R20 829026	35		
W962020	332	182	R20 830025	37.88		
W962021	333	186	R20 831026			
W962022	334	191	R20 832022	66.9		
W962023	335	198	R20 833020	16.84	29.17	C/IGNS(SH#335)
W962024	336	221	R20 835013			
W962025	337	229	R20 835006			
W962026	338	231	R20 835006	56.23		
W962027	339	241	R20 835004	36.71	62.67	
W962028	340	285	R20 838995	22.71	31.32	C/IGNS(A6 & SH#340)
W962029	341	325	R20 848985	37.29	39.99	
W962030	342	367	R20 861980	64.92	82.47	
W962031	343	390	R20 857971	105.13	88.53	
W962032	344	391	R20 857971			
W962033	345	393	R20 857971	17.65	34.05	
W962034	346	399	R20 857969	28.81		
W962035	347	402	R20 857969	77.41		
W962036	348	423	R20 856966	44.5		
W962037	349	429	R20 857962			
W962038	350	437	R20 856960	25.3		IGNS(A5)
W962039	351	460	R20 854957	27.54		
W962040	352	463	R20 854957	52.57		
W962041	353	464	R20 854957	25.31	45.72	C/IGNS(SH#353)
W962042	354	467	R20 854957	43.54		
W962043	356	472	R20 850957	47.45		
W962044A	355	474	R20 850957	37.64		
W962044B	357	479	R20 844957	68.44		
W962045	358	485	R20 838956	13.74		
W962046	359	492	R20 837954	16.25		IGNS(A4)
W962047	360	521	R20 836951	33.3	49.16	
W962048	361	532	R20 835949	25.06		IGNS(A3)
W962049	362	543	R20 835949	24.81		
W962050	363	563	R20 837945	48.93	57.93	B
W962051	364	575	R20 843943	109.23		
W962052	365	579	R20 844942	102.97		
W962053	366	584	R20 844942	156.87		
W962054	367	585	R20 844942			
W962055	368	587	R20 844942	27.68		
W962056	369	593	R20 844939	94.37		
W962057	371	626	R20 845936	99.81		
W962058	370	634	R20 846934			
W962059	372	638	R20 846934	37.28	37.64	IGNS(A2)
W962060	373	647	R20 845932	51.27		
W962061	374	641	R20 845932	47.69		
W962062	375	681	R20 847928	30.55	48.12	C/IGNS(A1)
W962063	376	753	R20 850921	27.51		
W962064	377	800	R20 849915	37.33	53.17	
W962065	378	815	R20 849912	25.9		
W962066	379	828	R20 852910	21.57	38.02	C/IGNS(A13)
W962068	302	851	R20 854909	36.57		
W962069	303	856	R20 854909	28.84		
W962070	304	861	R20 854908	24.03		
W962071	305	866	R20 854907	22.9		
W962072	306	871	R20 854907	24.97	25.35	

Wanganui River Section, Wanganui Basin, New Zealand

				Particle Size		
University No.	Sample No.	Strat. Height	Grid Ref	Laser Sizer	Sieve Analysis	Forams
		(m)	NZMS 260	Mean (μm)	SAND%	
W962073	307	876	R20 854906	28.94		
W962074	308	881	R20 854905	33.11		
W962075	309	886	R20 854904	22.69		
W962076	310	891	R20 854903	36.33		
W962077	311	896	R20 854901	31.36		
W962078	380	903	R21 858896	19.1		
W962079	384	911	R21 858898	18.89		
W962080	383	918	R21 858898	17.52		
W962081A	382	921	R21 858898	19.29	11.16	C
W962081B	385	926	R21 858898	24.76		
W962082	386	958	R21 863888	25.66		
W962083	387	963	R21 863888	32.54	51.9	
W962085	284	1009	R21 863891	29.83		
W962086	285	1014	R21 863891	37.44		
W962087	286	1019	R21 863890	33.57		
W962088	287	1024	R21 863890	36.65	45.25	C
W962089	288	1029	R21 863890	40.78		
W962090	289	1034	R21 863889	36.22		
W962091	290	1039	R21 863889	36.51		
W962092	415	1078	R21 867882	49.56	65.28	
W962093	414	1083	R21 868883	47.32		
W962094	413	1088	R21 868882	53.26		
W962095	301	1093	R21 869882	38.52	2.69	
W962096	300	1098	R21 869883	39.57		
W962097	299	1103	R21 869883	41.97		
W962098	298	1108	R21 870883	48.78		
W962099	297	1113	R21 870883	39.81		
W962100	296	1118	R21 871883	49.92		
W962101	295	1123	R21 872883	56.02	69.87	
W962102	294	1128	R21 873883	53.82		
W962103	293	1133	R21 873883	55.93		
W962104	292	1138	R21 873882	50.78		
W962105	291	1143	R21 873882	46.41	65.37	
W962106	250	1148	R21 873882	26.04	27	C
W962107	251	1155	R21 873882	16.92		
W962108	252	1161	R21 873882	18.73		C
W962109	253	1166	R21 873882	19.29		C
W962110	254	1171	R21 873882	18.61		
W962111	255	1176	R21 873882	21.68	9.19	C/IGNS(SH#255)
W962112	256	1181	R21 873882	21.21	15.13	
W962113	257	1186	R21 874881	29.11	35.59	
W962114	258	1191	R21 874881	58.37	73.94	
W962115	259	1197	R21 874881	23.41	20.58	
W962116	260	1202	R21 874881	80.18	83.87	
W962117	261	1207	R21 874881	32.27	32.12	
W962118	262	1214	R21 875880	32.29	37.11	
W962119	263	1219	R21 875880	85.92	66.36	
W962120	264	1226	R21 875880	40.01	74.03	
W962121	265	1234	R21 875880		56.74	
W962122	266	1239	R21 875880	67.82	60.62	
W962123	267	1244	R21 875880	60.34	45.95	
W962124	268	1249	R21 875880	29.7	54.94	
W962125	269	1264	R21 875879		20.48	
W962126	270	1272	R21 875879	37.14		
W962127	271	1275	R21 875879	44.45		
W962128	272	1276	R21 875879			
W962129	273	1279	R21 875879	50.75		
W962130	274	1284	R21 875879	51.69		
W962131	275	1299	R21 876879	43.74		
W962132	276	1307	R21 876879	74.95	77.8	
W962133	277	1312	R21 876879			
W962134	278	1315	R21 876879			
W962135	279	1321	R21 876878			
W962136	280	1326	R21 876878	41.41		
W962137	281	1332	R21 876878	47.3	68.95	
W962138	282	1337	R21 876878	21.78	14.29	
W962139	246	1341	R21 865856	20.41	11.49	C
W962140	283	1343	R21 876878	23.99		
W962141	245	1346	R21 865856	16.76	6.51	
W962142	242	1351	R21 865856	20.94	18.21	B
W962143	243	1356	R21 865856	26.44	26.44	
W962144	244	1361	R21 865856	19.74	15.59	
W962145	241	1375	R21 866853	46.35	35.3	
W962146	240	1380	R21 866853	77.5	67.75	

Appendix 2: Summary

				Particle Size		
University No.	Sample No.	Strat. Height	Grid Ref	Laser Sizer	Sieve Analysis	Forams
		(m)	NZMS 260	Mean (μm)	SAND%	
W962147	239	1385	R21 867852	52.7	55.76	
W962148	238	1390	R21 867852	73.97	67.76	
W962149	236	1395	R21 866851	89.32	80.99	
W962150	235	1400	R21 866851	68.06	70.15	
W962151	234	1404	R21 867850	79.12	72.05	
W962152	233	1408	R21 867850	85.33	75.7	
W962153	232	1412	R21 867850	112.27	84.58	
W962154	231	1414	R21 868850			
W962155	230	1415	R21 868850			
W962156	229	1416	R21 868850			
W962157	228	1418	R21 868850	88.27	76.82	
W962158	237	1422	R21 868850			
W962159	227	1426	R21 869849	73.77	70.2	
W962160	226	1431	R21 869848	72.21	78.34	
W962161	225	1436	R21 869848	89.99	80.7	
W962162	224	1441	R21 869848	45.67	61.57	
W962163	223	1446	R21 870847	41.61	45.91	
W962164	222	1451	R21 870847	27.91	38.18	
W962165	221	1454	R21 871847	54.93	59.43	
W962166	220	1459	R21 871847	52.14	54.18	C
W962167	219	1464	R21 872846	93.44	79.19	
W962168	218	1469	R21 872846	130.47	92.24	
W962169	217	1474	R21 871846		89.75	
W962170	216	1479	R21 872845	135.5	92.12	
W962171	215	1484	R21 872844	21.33	12.3	
W962172	214	1489	R21 872844	145.93	88.31	
W962173	213	1494	R21 872844	27.95	24.49	
W962174	212	1499	R21 873844	23.44	16.92	IGNS(A12)
W962175	211	1504	R21 873844	23.18	21.75	
W962176	210	1509	R21 874844	26.52	21.77	
W962177	209	1511	R21 874844	25.38	27.91	C
W962178	208	1514	R21 874843	40.7	29.63	
W962179	207	1519	R21 874843	42.16	35.56	
W962180	206	1524	R21 874842	27.99	18.53	C
W962181	205	1528	R21 874842	71.45	57.95	
W962182	204	1534	R21 874841	72.98	78.54	
W962183	203	1535	R21 874841			
W962184	202	1538	R21 874841			
W962185	201	1539	R21 874841			
W962186	200	1540	R21 874841	41.51	51.93	C
W962187	199	1544	R21 874841	28.91	11.63	
W962188	198	1549	R21 875840		27.48	
W962189	197	1553	R21 875840	49.82	66.28	
W962190	196	1556	R21 875839	42.85	59.68	
W962191	195	1559	R21 875839	49.27	62.41	B
W962192	194	1563	R21 875839	80.77	77.91	
W962193	193	1565	R21 875839			
W962194	192	1565	R21 875839			
W962195	191	1566	R21 875839			
W962196	190	1566	R21 875839			
W962197	163	1567	R21 875839	85.6	80.94	B
W962198	164	1571	R21 875839	39.32	60.95	C
Tangahoe Formation						
W962199	165	1573	R21 875839	7.97	5.32	C/IGNS(A10)
W962200	166	1578	R21 875839	9.35	2.97	C/IGNS(SH#166)
W962201	167	1583	R21 875839	8.48	1.91	C
W962202	168	1588	R21 875839	105.29	83.36	B
W962203	169	1593	R21 875839	129.86	86.08	
W962204	170	1598	R21 875839	9.97	2.38	C
W962205	171	1603	R21 876839	9.46	4.12	C
W962206	172	1607.5	R21 877839	102.55	86.66	B
W962207	173	1609	R21 877839	12.3	6.95	B
W962208	174	1613	R21 877839	155.08	92.66	
W962209	175	1615	R21 877839	12.12	1.63	
W962210	176	1620	R21 877839	8.93	0.64	C
W962211	177	1625	R21 877839	9.51	1.39	
W962212	178	1630	R21 878839	9.63	0.11	
W962213	179	1636	R21 878839	14.86	23.22	C
W962214	180	1640	R21 878839	14.42	5.66	B
W962215	181	1644	R21 878839	61.89	66.22	
W962216	182	1649	R21 879839	14.46	3.77	C
W962217	183	1654	R21 879840	9.65	2.44	C
W962218	184	1659	R21 879840	7.35	0.25	
W962219	185	1664	R21 879840	12.55	0.54	C

Wanganui River Section, Wanganui Basin, New Zealand

University No.	Sample No.	Strat. Height (m)	Grid Ref NZMS 260	Particle Size Laser Sizer Mean (μm)	Sieve Analysis SAND%	Forams
W962220	186	1669	R21 879840	12.68	0.38	
W962221	187	1674	R21 879840	12.08	0.45	C
W962222	381	CFS	R21 875815		75.57	B
W962084	388	CFS	R21 875815	9.16	1.78	
W962223	389	CFS	R21 878813	10.04	0.85	C
W962224	390	CFS	R21 878813	10.88	1.14	C
W962226	189	JRS	R21 890815	112.32	87.83	
W962227	188	JRS	R21 890814	108.42	88.65	
W962228	20	JRS	R21 891813	140.64	89.53	B
W962229	19	JRS	R21 891813	8.7	0.33	
W962230	62	JRS	R21 891812	10.35	73.82	
W962231	63	JRS	R21 891812	10.44	43.63	
W962225	391	JRS	R21 892812	9.77	1.2	C
W962232	392	JRS	R21 892812	122.74	91.56	
W962234	64	JRS	R21 890807	10.33	1.54	B
W962235	65	JRS	R21 890807	9.84	0.63	
W962236	66	JRS	R21 890807	14.34	20.32	
W962237	67	JRS	R21 890806	100.16	84.78	
W962238	68	JRS	R21 889805	11.54	20.64	
W962239	69	1649	R21 888803	11.98	1.07	
W962240	70	1654	R21 887802	13.19	28.44	
W962241	106	1659	R21 886801	14	18.01	
W962242	71	1664	R21 886800	13.88		
W962243	107	1669	R21 887799	12.98	0.54	
W962244	72	1674	R21 887799	18.15	2.38	
W962246	109	1680	R21 888798	15.76	3.52	B
W962247	108	1683	R21 888798	19.32	12.63	
W962248	110	1688	R21 888798	18.22	12.56	
W962249	73	1694	R21 889797	23.33		
W962250	111	1699	R21 889796	15.53	3.99	B
W962251	112	1704	R21 890796	14.51	22.51	
W962252	113	1709	R21 891796	13.09	14.31	B
W962253	114	1714	R21 891796	12.89	15.4	
W962254	116	1720	R21 892796	13.86	11.3	
W962255	115	1724	R21 892795	14.03	1.62	
W962256	74	1729	R21 893795	16.81		
W962257	75	1734	R21 894794	14.94		
W962258	76	1739	R21 894794	14.82		
W962259	77	1744	R21 884794	19.48		
W962260	78	1749	R21 895792	13.33		
W962261	79	1754	R21 896792	14.81		
W962262	80	1759	R21 896791	14.49		
W962263	81	1764	R21 896790	13.04		
W962264	82	1769	R21 897790	15.59		
W962265	83	1774	R21 897789	18.88	8.73	C
W962266	84	1779	R21 897788	28.87		
W962267	85	SG1	R21 897788	126.88		
W962268	86	SG1	R21 897788	61.05		
W962269	87	SG1	R21 897788	28.25		
W962270	88	SG1	R21 897788	16.38		
W962271	89	SG1	R21 897788	12.98		
W962272	90	SG1	R21 897788	15.1		
W962273	91	SG1	R21 898787	14.68		
W962274	92	SG1	R21 898787	37.7		
W962275	93	1790	R21 899786	14.62		
W962276	94	1795	R21 900786	12.01		
W962277A	95	1800	S21 900785	12.41		
W962277B	12	1804	S21 901785	11.1	1.98	
W962277C	11	1804.5	S21 901785	32.34	28.63	
W962277D	10	1805	S21 901785	19.05		
W962278	96	1806	S21 901785	16.76	8.07	
W962279	97	1810	S21 902784	16.66	25.51	
W962280	98	1815	S21 903783	10.1	1.35	C
W962281	99	1935	S21 919779	15.05	1.93	C
W962282	100	1940	S21 919779	13.41	10.29	
W962283	118	1945	S21 919779	13.74	12.3	
W962284	119	1950	S21 919778	13.7	9.23	
W962285	101	1955	S21 920778	13.72	18.26	
W962286	120	1959	S21 921778	15.25	12.16	
W962287	121	1964	S21 921777	15.58	58.03	
W962288	122	1974	S21 922777	17.29	5.06	B
W962289	102	1979	S21 922777	13.58	0.94	
W962290	123	1985	S21 922776	14.43	2.65	
W962291	124	1990	S21 923776	12.06	0.77	

Appendix 2: Summary

University No.	Sample No.	Strat. Height (m)	Grid Ref NZMS 260	Particle Size Laser Sizer Mean (μm)	Sieve Analysis SAND%	Forams
W962292	103	1994	S21 923776	13.89	43.08	
W962293	125	2000	S21 923775	14.45	0.5	C/IGNS(SH#125)
W962294	126	2005	S21 923775	15.07	3.23	
W962295	104	2009	S21 924774	18.49	6.73	
W962296	105	2014	S21 924773	15.66		
W962297	127	2017	S21 924772	16.62	1.89	
W962298	128	2020	S21 924772	17.14	0.74	
W962299	129	2024	S21 924772	15.03	1.24	
W962300	130	2038	S21 927770	20.71	5.23	
W962301	131	2041	S21 927770	22.6	5.22	
W962302	132	2053	S21 928770	12.92	0.65	C
W962303	133	2057	S21 928769	14.57	0.43	
W962304	134	2061	S21 929769	12.9	0.49	
W962305	135	SG2	S21 929769	129.08	74.08	
W962306	136	SG2	S21 930769	158.51	91.45	
W962307	137	SG2	S21 931769	126.14	87.59	
W962308	138	SG2	S21 931769	14.02	11.91	
W962309	139	SG2	S21 931769	137.41	91.71	
W962310	140	SG2	S21 931769	12.11	2.23	
W962311	141	SG2	S21 932769	11.39	0.5	
W962312	142	2082	S21 933769	19.94	3.9	C
W962313	143	2088	S21 933769	14.05	0.99	C
W962314	144	2093	S21 934769	17.91	4.64	
W962315	145	2095	S21 934769	14.73	0.39	
W962316	146	2120	S21 938769	13.84	0.78	
W962317	147	2125	S21 939769	16.88	5.3	C
W962318	148	2135	S21 940769	14.27	2.34	
W962319	149	2140	S21 940768	17.74	2.69	
W962320	150	2145	S21 941768	15.66	1.28	
W962321	151	2150	S21 941768	16.41	1.78	
W962322	152	2155	S21 942768	15.75	3.61	
W962323	153	2160	S21 942768	18.16	6.06	
W962324	154	2165	S21 943767	17.06	4.74	
W962325	155	2170	S21 944767	15.07	3.06	
W962326	156	2179	S21 945766	12.27	0.64	C
W962327	157	2184	S21 945766	16.75	3.15	
W962328	158	2190	S21 947765	14.44	1.01	
W962329	159	2195	S21 947765	13.55	1.71	
W962330	160	2200	S21 948764	17.07	6.84	
W962332	420	2396	S21 948762	13.45	0.47	
W962333	419	2204	S21 948762	14.54	1.53	I
W962334	418	2208	S21 948762	16.87	4.6	I
W962335	417	2213	S21 948762	15.17	4.64	I
W962336	416	2223	S21 948762	12.93	2.43	C/I
W962337	162	2228	S21 949762	10.76	1.88	I
W962338	161	2233	S21 949763	10.92	0.69	I
W962339A	412	2240	S21 954757	12.47	1.23	C/I
W962339B	411	2244	S21 954757	11.83	1.16	I
W962340	61	2249	S21 957758	9.57	1.69	C/I
W962341	5	2253.5	S21 957758	19.63	0.67	C/I
W962342	4	2255	S21 957758	115.68	78.9	B
W962343	60	2259	S21 957758	98.22	90.68	B
W962344	59	2260	S21 957758	14.16	9.18	C/I
W962345	58B	2264	S21 957758	13.96	0.76	
W962346	58	2269	S21 957758	15.07	1.07	C/IGNS(SH#58)/I
W962347	57	2274	S21 957758	62.62	86.35	B
W962348	3	2277.5	S21 957758	12.84	0.69	C/I
W962349	2	2278	S21 957758	69.01	86.54	B
W962350	56	2280	S21 957758	52.39	61.81	B
W962351	55	2285	S21 957758	75.61	88.05	B
W962352	54	2289	S21 957758	19.04	3.82	B
W962353	53	2290	S21 957758	77.85	80	B
W962354	52	2294	S21 957758	116.12	81.59	B
W962355	51	2296	S21 957758	13.17	1.6	C/I
W962356	50	2300	S21 957758		0.27	C/I
W962358A	410	2306	S21 957757	8.1	0.2	I
W962358B	409	2310	S21 957757	10.94	1.01	I
W962358C	393	2315	S21 964751	7.7	0.13	C/I
W962359	394	2320	S21 964751	7.67	0.42	I
W962360	395	2325	S21 964751	7.74	0.56	I
W962361	396	2330	S21 964751	8.89	0.41	C/I
W962362	397	2335	S21 964751	7.6	0.96	I
W962363	398	2345	S21 964751	8.26	0.25	
W962364	399	2350	S21 964751	9.54	0.18	I

Wanganui River Section, Wanganui Basin, New Zealand

				Particle Size		
University No.	Sample No.	Strat. Height	Grid Ref	Laser Sizer	Sieve Analysis	Forams
		(m)	NZMS 260	Mean (μm)	SAND%	
W962365	400	2355	S21 964751	9.67	0.31	
W962366	401	2360	S21 964751	10.97	20.36	C/I
W962367	402	2365	S21 964751	11.54	0.39	
W962368	403	2370	S21 964751	8.65	0.2	
W962369	404	2376	S21 964751	10.96	0.59	I
W962370	405	2381	S21 964751	12.52	0.75	I
W962371	406	2386	S21 964751	11.91	0.43	I
W962372	407	2391	S21 964751	10.79	0.38	I
W962373	408	2394	S21 964751	10.48	0.32	C/IGNS(SH#408)
W962375A		2395	S21 965738			IGNS(A30)
W962375	435	2396	S21 965738	61.42	75.07	
W962376	436	2404	S21 966737	100.69	85.23	
W962377	437	2404.5	S21 966737	13.03	10.48	I
W962378	438	2405	S21 966737	94.36	91.87	
W962379	439	2406	S21 966737	9.26		
W962380	440	2410	S21 966735	9.4	6.3	C
W962381	441	2411	S21 966735	104.21	88.14	
W962382	442	2414	S21 966735	107.79	94.39	
W962383	443	2416	S21 966735	9.94	11.9	
W962384	444	2420.5	S21 966734	9.32	2.23	I
W962385	445	2426	S21 966733	11.89		
W962386	446	2425	S21 966733	12.36	1.65	B
W962387	447	2429	S21 966733	120.09	89.81	
W962388	448	2432	S21 966733	118.01	94.5	
W962389	449	2437	S21 966732	14.05	11.79	
W962390	450	2441	S21 965732	104.55	90.93	
W962391	451	2445	S21 965732	25.08	23.12	
W962392	452	2450	S21 965732	12.39	2.77	I
W962393	453	2459	S21 965732	12.53	4.72	Biostrat/I
W962394	454	2466	S21 965732	14.69	2.69	I
W962395	455	2468	S21 965732	12.9	1.29	C/I
W962396	456	2469	S21 965732	99.64	88.41	
W962397	457	2544	S21 965724	125.46	89.25	
W962398	458	2547	S21 965724	12.45	2.77	C/I
W962399	459	2548	S21 965724	17.89	6.62	I
W962400	460	2559	S21 965724	116.07	92.59	
W962401	491	2589	S21 965718	86.68	81.31	
W962402	490	2593	S21 965718	14.71	2.71	B
W962403	489	2596	S21 965718	143.7	93.66	
W962404	461	2599	S21 965718	21.34	23.5	
W962405	462	2606	S21 965718	64.75	55.03	
W962406	463	2610	S21 965718	13.93	2.57	C/IGNS(A31)/I
W962407	540	2615	S21 965717	14.9	5.88	I
W962408	541	2620	S21 965716	14.33	2	I
W962409	542	2625	S21 965715	26.04	7.37	C/I
W962410	543	2630	S21 965714	14.51	2.51	I
W962411	544	2635	S21 965714	14.34	3.15	I
W962412	464	2640	S21 965713	10.19	0.94	C/I
W962413	588	2643	S21 965713	144.52		
W962414	465	2645	S21 965713	14.64	5.72	I
W962415	589	2647	S21 965713	140.38		
W962416	496	2658.5	S21 964705	148.21	95.29	
W962417	495	2659	S21 964705	23.3	58.21	
W962418	494	2660	S21 964705	110.84	88.91	
W962419	493	2661	S21 964705	21.44	36.01	I
W962420	492	2667	S21 964705	9.52	0.66	C/IGNS(SH#492)
W962421	545	2670	S21 965706	12.39		
W962422	466	2675	S21 964705	12.95	0.53	
W962423	546	2680	S21 965706	12.77		
W962424	547	2685	S21 965706	9.39		I
W962425	548	2690	S21 965706	10.21		
W962426	549	2695	S21 965706	13.26		
W962427	550	2700	S21 965706	14.04	0.73	
W962428	551	2705	S21 965706	13.69		
W962429	467	2710	S21 961700	13.81		
W962430	563	2715	S21 961700	15.06		
W962431	564	2720	S21 961699	14.01		
W962432	565	2725	S21 961699	12.98	0.31	C
W962433	566	2730	S21 961699	12.91		
W962434	567	2735	S21 961699	11.94		
W962435	568	2740	S21 962698	12.24		
W962436	569	2745	S21 963698	14.1		
W962437	570	2750	S21 964697	13.22	2.51	
W962438	571	2755	S21 963697	13.87		

Appendix 2: Summary

University No.	Sample No.	Strat. Height (m)	Grid Ref NZMS 260	Particle Size Laser Sizer Mean (μm)	Sieve Analysis SAND%	Forams
W962439	572	2760	S21 964697	12.44		
W962440	573	2765	S21 965697	13.62		
W962441	552	2770	S21 965696	23.18		
W962442	553	2775	S21 965696	11.9	1.16	C/IGNS(SH#553)
W962443A	554	2779	S21 965696	13.34		
W962443B	468	2780	S21 953691	17.5		
W962444	555	2785	S21 965696			
W962445	556	2790	S21 965696	16.57		
W962446	557	2795	S21 965696	19.73		
W962447	558	2800	S21 965696	25.08	11.75	
W962448	559	2805	S21 965696	15.75	3.53	
W962449A	560	2810	S21 965696	13.69		
W962449B	469	2810	S21 951689	19.65	7.43	C
W962450	561	2815	S21 965696	15.4		
W962451	562	2820	S21 965696	19.62		
W962452	574	2825	S21 965695	20.12	4.74	B
W962453	575	2830	S21 965695	18.23		
W962454	576	2835	S21 965695	22.96		
W962455	577	2840	S21 965695	21.09		
W962456	578	2845	S21 965695	28.27		
W962457	579	2850	S21 965695	36.32	25.19	B
W962458	470	2850	S21 950681	38.08		B
W962459	580	2855	S21 965695	21.76		
W962460	581	2860	S21 965694	22.71		
W962461	582	2865	S21 965694	23.72		
W962462	583	2870	S21 965694	24.35		
W962463	584	2875	S21 965694	26.56	6.9	B
W962464	585	2880	S21 965694	28.43		
W962465	586	2885	S21 965694	32.35		
W962466	587	2890	S21 965694	23.5		
W962467	652	2895	S21 965694	68.36		
W962468	653	2900	S21 965694	20.48	8.44	
W962469	654	2905	S21 965694	24.54		
W962470	655	2910	S21 965694	19.6		
W962471	656	2915	S21 965693	22.94		
W962472	657	2920	S21 965693	26.43		
W962473	658	2926	S21 965693	19.03	5.33	
W962474	659	2931	S21 965693	25.47		
W962476	660	2936	S21 965693	21.15	5.22	
W962479	661	2937.5	S21 965693	32.12	12.97	
W962475	471	2939	S21 950670	32.68	43.91	C/IGNS(471)
W962481	662	2939	S21 965693	31.31	45.04	
W962477	472	2941	S21 949668	46.02		
W962478	473	2943	S21 948667	47.4		
Ahurangi Sandstone						
W962480	474	2946	S21 948667	56.28	57.73	
W962482	475	2952	S21 948667	79.52	76.3	
W962483	497	2990	S21 948661	43.97		
W962484	476	3005	S21 948658	37.19	55.26	B
W962485	477	3035	S21 946655	46.57		B
W962486	478	3035.5	S21 946655	35.81		B
W962487	590	3070	S21 936650	43.84		
W962488	479	3075	S21 936650	40.45		
W962489	591	3080	S21 935649	38.94		
W962490	592	3085	S21 934649	43.92		
W962491	593	3090	S21 933648	37.27		
W962492	498	3095	S21 933649	32.47		
W962493	488	3101	S21 932648	85.72	72.17	
Oxbow Siltstone						
W962494	499	3105	S21 932648		79.12	
W962495	500	3105	S21 932648			
W962496	480	3105	S21 932648	23.44	32.75	C/IGNS(A36 & SH#480)
W962497	487	3112	S21 932648	22.47		
W962498	481	3120	S21 932648	25.26		
W962499	482	3125	S21 932648	26.77	9.53	
W962500	483	3130	S21 932648	22.99		
W962501	484	3136	S21 932648	17.05		
W962502	485	3140	S21 932648	21.05		
W962503	486	3145	S21 932648	21.18	5.97	
Atene Sandstone						
W962504	521	3173	S21 938639	42.4	54.44	
W962505	598	3187	S21 923633	71.17		
W962506	597	3193	S21 923632	112.56	81.9	
W962507	596	3198	S21 923632	71.93		

Wanganui River Section, Wanganui Basin, New Zealand

University No.	Sample No.	Strat. Height (m)	Grid Ref NZMS 260	Particle Size Laser Sizer Mean (μm)	Sieve Analysis SAND%	Forams
W962508	595	3198	S21 923632	124.3		
W962509	501	3199	S21 923632		60.68	
W962510	594	3200	S21 923632	24.74	43.14	C/IGNS(SH#594)
W962511	502	3202	S21 923632	27.65	33.03	IGNS(Foram)
W962512	503	3207	S21 923632	37.4	58.14	
W962513	599	3218	S21 923633	32.2	57.37	
W962514	519	3225	S21 931631	38.13	37.81	
W962515	518	3228	S21 931631	22.84	9.84	
W962516	520	3232	S21 931631	20.91	8.1	
W962517	539	3238	S21 926630	20.5	16.16	
W962518	515	3238	S21 931631	20.98	10.61	
W962519	538	3239	S21 926630	29.59	35.48	
W962520	537	3240	S21 926630	31.37	24.75	
W962521	516	3242	S21 931631	39.74	39.66	
W962522	517	3245	S21 931631	83.01	82.44	
W962523	504	3270	S21 929622	136.8	96.99	
W962524	505	3275	S21 929622	38.37	79.33	
W962525	506	3277	S21 929622	124.6	89.18	
W962526	513	3285	S21 934628	120.18	87.12	
W962527	600	3290	S21 937623	113.04		
W962528	514	3295	S21 933628	57.54	43.22	B
W962529	601	3296.5	S21 937623	138.75	93.95	
W962530	602	3299	S21 937623	66.88		
W962531	603	3301.5	S21 937623	169.02		
W962532	604	3306	S21 937623	51.34		
W962533	510	3310	S21 937624	33.96	48.21	
Mangaweka Mudstone						
W962534	511	3312	S21 937624	24.14	17.88	
W962535	512	3315	S21 937624	20.21	16.83	B
W962536	507	3320	S21 936620	17.55	3.09	
W962537	508	3327	S21 936620	16.88	2.57	
W962538	509	3333	S21 936620	16.77	3.47	
W962539	643	3340	S21 931630	15.4	1.09	P
W962540	644	3345	S21 931630	15.55		
W962541	645	3350	S21 931630	15.15		
W962542	646	3355	S21 931630	17.3		
W962543	647	3360	S21 931630	19.1		
W962544	648	3365	S21 931630	21.09	7.62	B
W962545	649	3370	S21 931630	20.05		
W962546	650	3375	S21 931630	22.19		
W962547	651	3380	S21 931630	21.4		
W962548	605	3383	S21 950610	22.67		
W962549	523	3390	S21 950610	22.56	10.1	
W962550	606	3395	S21 950610	14.72	11.08	C
W962551	607	3400	S21 950609	26.61		
W962552	608	3405	S21 950608	24.1		
W962553	610	3410	S21 950608	21.98		
W962554	611	3415	S21 950608	23.75		
W962555	609	3420	S21 949606	22.76	5.38	
W962556	524	3427	S21 949606	23.31	9.4	
W962557	612	3430	S21 948606	23.23		
W962558	613	3435	S21 947606	23.23		
W962559	525	3440	S21 946605	20.56	5.97	C
W962560	631	3445	S21 946605	20.89	2.55	
W962561	632	3450	S21 946605	22.46		
W962562	614	3455	S21 949606	22.03		
W962563	615	3460	S21 949606	22.13		
W962564	616	3465	S21 949606	20.96	8.73	
W962565	617	3470	S21 949606	23.98		
W962566	618	3475	S21 949606	20.25		
W962567	619	3480	S21 949606	15.78		
W962568	620	3485	S21 949606	14.71		
W962569	621	3490	S21 949606	18.07	1.64	B
W962570	622	3495	S21 949606	14.74		
W962571	623	3505	S21 949605	13.56		
W962572	624	3510	S21 949605	13.85		
W962573	625	3515	S21 949605	15.64	0.14	
W962574	626	3520	S21 949605	15.04		
W962575	627	3525	S21 949605	13.95		
W962576	628	3530	S21 949605	15.72		
W962577	629	3535	S21 949605	16.27		
W962578	630	3540	S21 949605	18.42	0.54	
W962579	536	3545	S21 952604	15.04	2.97	
W962580	642	3550	S21 952604	16.48		

Appendix 2: Summary

				Particle Size		
University No.	Sample No.	Strat. Height	Grid Ref	Laser Sizer	Sieve Analysis	Forams
		(m)	NZMS 260	Mean (μm)	SAND%	
W962581	535	3555	S21 952604	14.94	1.15	
W962582	641	3560	S21 952604	14.11		
W962583	640	3565	S21 952604	14.32	0.22	
W962584	534	3570	S21 952604	15.18	0.25	
W962585	639	3575	S21 952604	14.83		
W962586	533	3580	S21 952604	14.69	0.22	
W962587	638	3585	S21 952604	16.81	0.23	B
W962588	532	3595	S21 952604	18.08	1.98	
W962589	637	3600	S21 952604	16.4		
W962590	531	3605	S21 952604	17.88		
W962591	636	3610	S21 952604	16.37		
W962592	530	3615	S21 952604	15.82	1.56	
W962593	635	3620	S21 952604	15.06		
W962594	634	3625	S21 952604	16.93		
W962595	529	3628	S21 952604	23.2	2.51	B
W962596	633	3630	S21 952604	21.49		
W962597	528	3633	S21 952604	25.25	33.67	
W962598	527	3635	S21 952604	29.36	24.48	
W962599	526	3636	S21 952604	46.24	43.06	
W962600	421	JRXS	R21 888804	22.81	23.89	
W962601	422	JRXS	R21 888804	15.51	2.59	
W962602	423	JRXS	R21 888804	94.56	88.34	
W962603	424	JRXS	R21 888804	105.99	90.29	
W962604	425	JRXS	R21 888804	12.26	5.02	
W962605	426	JRXS	R21 888804	14.39	12.07	
W962606	427	JRXS	R21 888804	12.13	4.41	
W962607	428	JRXS	R21 887803	12.01	9.19	
W962608	429	JRXS	R21 887803	12.01	4.37	
W962609	430	JRXS	R21 887803	106.69	89.17	
W962610	431	JRXS	R21 887803	13.26	9.43	
W962611	432	JRXS	R21 887803	11.98	4.12	
W962612	433	JRXS	R21 887803	24.9	39.3	
W962613	434	JRXS	R21 887803	29.24	35.47	

(2) FORAMS

This section contains both census data and biostratigraphic data. This information is also available in electronic form (viewable and down loadable) from the CD ROM in the back of this thesis

Census information:

This is shown as raw numbers

Biostratigraphic information:

The occurrence of forams is shown by the presence of an astrix.

Where other biostratigraphic information is relevant, e.g. coiling ratios, this information occurs between asterix.

E.g. 3*26S:1D* = 3 specimens in census sample; 27 specimens in biostrat sample (IGNS) - 26 sinistrally coiled and 1 dextrally coiled.

Waikato Univ. No.	W962002	W962023	W962028	W962038	W962041	W962046	W962048	W962059	W962062	W962066
Sample No.	314	335	340	350	353	359	361	372	375	379
Stratigraphic height (m)	8	198	285	437	464	492	521	638	681	828
BENTHICS										
Alabamina sp.										
Ammonia beccarii										
Ammonia sp.										
Amphicoryna cf *bortonica*										
Amphicoryna hirsuta	*				*		*	*	*	
Amphicoryna aff *hirsuta*										
Amphicoryna cf *hirsuta*			*			*			1	*
Amphicoryna scalaris										
Amphicoryna sp.	13	12	4						3	
Anomalina spherica	*		*							
Anomalinoides alazanensis										
Anomalinoides parvumbilius	47	5	30		*	*			4	
Anomalinoides cf *parvumbilius*										
Anomalinoides sp.										
Anomalinoides sphericus	14	6	2							
Anomalinoides subnonionoides										
Astrononion kickinskii	1					*	*		*	
Astrononion neefi										
Astrononion cf *neefi*										
Astrononion novozealandicum										
Astrononion cf *novozealandicum*										
Astrononion parki	84	30	11	*	5	*	*	*	26	86
Astrononion sp.										
Bolivina affiliata	*	1							*	
Bolivina aff *affiliata*										
Bolivina cf *affiliata*										1
Bolivina albatrossi										
Bolivina aff *albatrossi*										
Bolivina lapsus										
Bolivina numerosa	9	10	1		2					
Bolivina spathulata	*?*		*				*			
Bolivina sp.									1	1
Bolivina watti		2								
Bolivina zigzag										
Bolivinita finlayi	23	*	*						6	34
Bolivinita aff *finlayi*		16	3							
Bolivinita cf *finlayi*	*									
Bolivinita pliobliqua										
Bolivinita pliozea										
Bolivinita pohana										
Bolivinita pseudocompressa										
Bolivinita aff *pseudocompressa*										

Waikato Univ. No.	W962002	W962023	W962028	W962038	W962041	W962046	W962048	W962059	W962062	W962066
Sample No.	314	335	340	350	353	359	361	372	375	379
Stratigraphic height (m)	8	198	285	437	464	492	521	638	681	828
Bolivinita quadrilatera										
Bulimina aculeata		3								
Bulimina aff *aculeata* (reduced spines)	*	7								
Bulimina cf *aculeata*	*		4			*				
Bulimina elongata										
Bulimina *cf* elongata										
Bulimina marginata										
Bulimina aff *marginata*										
Bulimina cf *marginata*										
Bulimina sp.										
Bulimina striata										
Bulimina cf *striata*									1	
Bulimina cf *vella*		*								
Cassidulina neocarinata	13	1	1		1				9	46
Ceratocancris sp.										
Chilostomella ovoidea							*			
Chrysalogonium verticale								*		
Cibicides amoenus										
Cibicides deliquatus	*		*	*	2	*	*	*	*	*
Cibicides cf *deliquatus*										
Cibicides finlayi										
Cibicides aff *finlayi*										
Cibicides cf *finlayi*										
Cibicides molestus	*		*			*		*	*	*
Cibicides aff *molestus*										
Cibicides neoperforatus										
Cibicides cf *notocenicus*										
Cibicides novozealandicus										
Cibicides spp.		5	1		1	*			14	2
Cibicides subhaidingeri										
Dentalina obliquecostata										
Dentalina sp.		*				*				1
Dentalina soluta							*?*			
Dentalina substrigata										
Discorbinella bertheloti		2								
Discorbinella cf *bertheloti*										
Discorbinella sp.									1	
Discorbis dimidiatus										
Discorbis sp.										
Dyocibicides primitiva										
Dyocibicides sp.		1	*				*		*	
Elphidium advenum										
Elphidium charlottensis	*	6	3		1	*		*	4	1

Waikato Univ. No.	W962002	W962023	W962028	W962038	W962041	W962046	W962048	W962059	W962062	W962066
Sample No.	314	335	340	350	353	359	361	372	375	379
Stratigraphic height (m)	8	198	285	437	464	492	521	638	681	828
Elphidium cf *charlottensis*										
Elphidium simplex aoteanum									2	
Elphidium sp.						*				
Epistomella sp.			?1							
Evolvocassidulina orientalis	22	30	17		3	*	*	*	55	8
Evolvocassidulina cf *orientalis*										*
Evolvocassidulina cf *orientalis* (carinate var)										
Fissurina sp.		*								1
Gavelinopsis hamatus		?3			*	*	*	*	9	
Gavelinopsis cf *hamatus*										
Gavelinopsis sp.			*						1	
Globocassidulina laevigata										
Globocassidulina subglobosa					*			*	1	
Gyroidina danvillensis	1	1							*	
Gyroidina sp.										
Gyroidinoides sp.										
Gyroidinoides zelandicus								*	*	
Hoeglundina elegans										*
Lagena sp.	*	1				*				*
Lagena striata	*					*?*	*	*	*	
Lagena aff *striata*			*					*		
Lagena cf *striata*										*
Laticarinina pauperata										
Lenticulina calcar	20	*	*	*?*	*	*	*	*	*	
Lenticulina aff *calcar*										
Lenticulina cf *calcar*										*
Lenticulina costatus										
Lenticulina gyroscalpra										
Lenticulina loculosus			*				*?*			
Lenticulina mamilligera										
Lenticulina orbicularis			*							
Lenticulina spp.	*	3					*	*		1
Marginulina sp.										
Margmulina subbullata										
Mucronina sinalata										
Mucronina sp.										
Mucronina multicostales										
Mucronina sinalata										
Nodosaria longiscata								*		
Nodosaria sp.										
Nodosaria substrigata	*?*						*?*			
Nonionella flemingi	1	2	4	*		*		*	16	8
Notorotalia depressa grp										37

Waikato Univ. No.	W962002	W962023	W962028	W962038	W962041	W962046	W962048	W962059	W962062	W962066
Sample No.	314	335	340	350	353	359	361	372	375	379
Stratigraphic height (m)	8	198	285	437	464	492	521	638	681	828
Notorotalia cf *depressa*										
Notorotalia finlayi										
Notorotalia cf *finlayi*									10	
Notorotalia finlayi grp										
Notorotalia finlayi/hurupiensis										
Notorotalia hurupiensis	8	17	9	*		*	*	*	*	*
Notorotalia cf *hurupiensis*										
Notorotalia hurupiensis/depressa					20					
Notorotalia macinnesi					*	*				
Notorotalia pliozea							*	*	*	
Notorotalia aff *pliozea*										
Notorotalia spp.										
Notorotalia taranakia										
Notorotalia aff *taranakia*										
Notorotalia cf *taranakia*										
Oolina hexagona	*		1					*	2	
Oolina sp.										
Oolina squamosa		*						*	1	*
Oridorsalis tenera	*							*		*
Parafissurina sp.					*					
Patellinella inconspicua								*		
Pileolina sp.										
Plectofrondicularia pellucida								*	1	*
Plectofrondicularia cf *pellucida*										
Plectofrondicularia pohana									*	
Proxifrons advena										
Pseudonodosaria sp.										
Pullenia bulloides	*							*		
Pullenia quinqueloba										
Pullenia cf *quinqueloba*										
Pullenia sp.							*			
Pullenia subcarinata										
Rectobolivina striatula	*	1	*						*	
Rectouvigerina striatula						*				
Rosalina bradyi										
Rotalia sp.										
Saracenaria italica							*	*		
Saracenaria cf *italica*										
Saracenaria latifrons										1
Saracenaria sp.										
Sigmoilopsis sp.										
Sigmoilopsis zeaserus										
Sigmomorphina sp.									*	

Waikato Univ. No.	W962002	W962023	W962028	W962038	W962041	W962046	W962048	W962059	W962062	W962066
Sample No.	314	335	340	350	353	359	361	372	375	379
Stratigraphic height (m)	8	198	285	437	464	492	521	638	681	828
Siphonia australis										
Siphotextularia wairoana										
Siphouvigerina belluda										
Siphouvigerina canariensis										*
Siphouvigerina eketahuna										
Siphouvigerina cf *eketahuna*										
Siphouvigerina sp.										
Sphaeroidina bulloides	3	1	1		2		*	*		1
Spheroidinellopsis seminulina										
Spheroidinellopsis sp.	8									
Spiroloculina kennetti										
Stainforthia concava					1					
Stilostomella hochstetteri										
Stilostomella lepidula										
Stilostomella sp.	*	?2	*?*		*			*	4	3
Trifarina bradyi									1	
Trifarina sp.	1									
Uvigerina (*Euuvigerina*) *miozea* grp	5		1		*		*	*	*	10
Uvigerina (*Siphouvigerina*) sp.										
Uvigerina cf *pliozea* (*miozea* grp)										
Uvigerina cf *poroporoensis* (*miozea* grp)										
Uvigerina rodleyi						*				
Vagulina elegans										
Vaginulina sp.	*									
Vaginulina vagina							*			
Virgulopsis parri	*									
Virgulopsis patiae	1	1			*					*
Virgulopsis pustulata									1	
Virgulopsis sp.										
Virgulopsis subspinescens										
Virgulopsis *aff* subspinescens										
Virgulopsis turris									2	
Virgulopsis wanganuiensis									2	1
Virgulopsis aff *wanganuiensis*										
Virgulopsis cf *wanganuiensis*										
Zeaflorilis parri										
PLANKTICS										
Globigerina bulloides								*		
Globigerina falconensis									*	
Globigerina quinqueloba	*									
Globigerina aff *quinqueloba*										

Waikato Univ. No.	W962002	W962023	W962028	W962038	W962041	W962046	W962048	W962059	W962062	W962066
Sample No.	314	335	340	350	353	359	361	372	375	379
Stratigraphic height (m)	8	198	285	437	464	492	521	638	681	828
Globigerina cf *quinqueloba*										
Globigerina spp.	10	18	*		1	*	*	*	7	*
Globogirina (*Zeaglobigerina*) *apertura*										
Globogerina (*Zeaglobigerina*) sp.	*	*	*					*		*
Globogerina (*Zeaglobigerina*) *woodi*		1						*	*	
Globogerina (*Zeaglobigerina*) cf *woodi*										
Globigerinita glutinata										
Globigerinita cf *glutinata*										
Globigerinita sp.										
Globigerinoides ruber								*	*	
Globigerinoides sp.										
Globigerinoides trilobus										
Globorotalia conomiozea	3*26S:1D*	1 *6S*	*6S*	*5S:1D*		*94S:2D*				
Globorotalia crassaconica										
Globorotalia aff *crassaconica* (unkeeled)										
Globorotalia cf *crassaconica*										
Globorotalia crassaformis								*52S*	*15S*	*8S*
Globorotalia inflata		?1								
Globorotalia inflata triangula										
Globorotalia miotumida	*3S*									
Globorotalia pliozea								*2S:12D*	?1 *2s:10D*	*15S*
Globorotalia puncticulata								*38S*	*6S*	*5S*
Globorotalia aff *puncticulata*										
Globorotalia cf *puncticulata*										
Globorotalia puncticuloides										
Globorotalia scitula	1 *2D*								*1D*	
Globorotalia sp.	1	*2S:1D*								1
Globorotalia cf *subconomiozea*										
Globorotalia truncatulinoides tosaensis										
Globorotalia tumida										
Globorotaloides punticuloides										
Neogloboquadrina pachyderma	2 *3S:2D*	*4S*						*	*1S*	1
Neogloboquadrina cf pachyderma										
Neogloboquadrina sp.										
Orbulina bilobata									*	
Orbulina universa	*	*				*		*	*	*
AGGLUTINATED										
Bathysiphon sp.								*		
Haeuslerella finlayi										
Haeuslerella cf *finlayi*										
Haeuslerella morgani	*		*	*	*	*	*		*	*

Waikato Univ. No.	W962002	W962023	W962028	W962038	W962041	W962046	W962048	W962059	W962062	W962066
Sample No.	314	335	340	350	353	359	361	372	375	379
Stratigraphic height (m)	8	198	285	437	464	492	521	638	681	828
Haeuslerella parri	39		?7					*		
Haeuslerella aff *parri*										
Haeuslerella *cf* parri	*	3								
Haeuslerella pliocenica										
Haeuslerella sp.										10
Karreriella cylindrica								*		
Karreriella bradyi										
Martinotiella sp.										
Martinottiella communis							*	*	*	
Sigmoilopsis zeaserus										
Siphonaperta macbeathi										
Siphonaperta aff *macbeathi*										
Texturlria kapitea	*									
Textularia lythostrota										
Texturlria cf *mestayeri*										
Thalmannammina sp.								*		
RADIOLARIANS										
Total										

Waikato Univ. No.	W962081A	W962088	W962106	W962108	W962109	W962111	W962139	W962166	W962174	W962177
Sample No.	382	287	250	252	253	255	246	220	212	209
Stratigraphic height (m)	921	1024	1148	1161	1166	1176	1341	1459	1499	1511
BENTHICS										
Alabamina sp.										
Ammonia beccarii				1					*	8
Ammonia sp.										
Amphicoryna cf *bortonica*										
Amphicoryna hirsuta										
Amphicoryna aff *hirsuta*										
Amphicoryna cf *hirsuta*			7							
Amphicoryna scalaris										
Amphicoryna sp.	3		1		1	*		1		
Anomalina spherica										
Anomalinoides alazanensis										
Anomalinoides parvumbilius	2									
Anomalinoides cf *parvumbilius*										
Anomalinoides sp.									*	
Anomalinoides sphericus										
Anomalinoides subnonionoides										2
Astrononion kickinskii										
Astrononion neefi										
Astrononion cf *neefi*										
Astrononion novozealandicum										
Astrononion cf *novozealandicum*	1									
Astrononion parki	45	34			4	*	5	4	*	
Astrononion sp.										
Bolivina affiliata	3					*				
Bolivina aff *affiliata*										
Bolivina cf *affiliata*				2						
Bolivina albatrossi										
Bolivina aff *albatrossi*										
Bolivina lapsus						*				
Bolivina numerosa							2			
Bolivina spathulata										
Bolivina sp.	13		1	2	1			14		
Bolivina watti										
Bolivina zigzag										
Bolivinita finlayi		3	2	5					*	
Bolivinita aff *finlayi*										
Bolivinita cf *finlayi*							1			
Bolivinita pliobliqua										
Bolivinita pliozea										
Bolivinita pohana										
Bolivinita pseudocompressa										
Bolivinita aff *pseudocompressa*										

Waikato Univ. No.	W962081A	W962088	W962106	W962108	W962109	W962111	W962139	W962166	W962174	W962177
Sample No.	382	287	250	252	253	255	246	220	212	209
Stratigraphic height (m)	921	1024	1148	1161	1166	1176	1341	1459	1499	1511
Bolivinita quadrilatera										
Bulimina aculeata								4		
Bulimina aff *aculeata* (reduced spines)							1			
Bulimina cf *aculeata*										
Bulimina elongata	4									
Bulimina *cf* elongata										
Bulimina marginata										
Bulimina aff *marginata*										
Bulimina cf *marginata*										
Bulimina sp.										
Bulimina striata										
Bulimina cf *striata*		1								
Bulimina cf *vella*										
Cassidulina neocarinata	12	10			2	*	26	9		4
Ceratocancris sp.										
Chilostomella ovoidea										
Chrysalogonium verticale										
Cibicides amoenus										
Cibicides deliquatus										
Cibicides cf *deliquatus*	1									
Cibicides finlayi										
Cibicides aff *finlayi*										
Cibicides cf *finlayi*										
Cibicides molestus								?1		2
Cibicides aff *molestus*										
Cibicides neoperforatus										
Cibicides cf *notocenicus*										
Cibicides novozealandicus										
Cibicides spp.	7		2		3	*	3	10	*	5
Cibicides subhaidingeri										
Dentalina obliquecostata										
Dentalina sp.			?1							
Dentalina soluta										
Dentalina substrigata										
Discorbinella bertheloti	7		1							
Discorbinella cf *bertheloti*										
Discorbinella sp.										
Discorbis dimidiatus										
Discorbis sp.										
Dyocibicides primitiva										3
Dyocibicides sp.										
Elphidium advenum										
Elphidium charlottensis	7			4	3	8	6	41	*	18

Waikato Univ. No.	W962081A	W962088	W962106	W962108	W962109	W962111	W962139	W962166	W962174	W962177
Sample No.	382	287	250	252	253	255	246	220	212	209
Stratigraphic height (m)	921	1024	1148	1161	1166	1176	1341	1459	1499	1511
Elphidium cf *charlottensis*										
Elphidium simplex aoteanum						2		1	*?*	
Elphidium sp.							2	2		
Epistomella sp.										
Evolvocassidulina orientalis	18	14	1		3	1	1	76	*	1
Evolvocassidulina cf *orientalis*										
Evolvocassidulina cf *orientalis* (carinate var)										
Fissurina sp.	1									1
Gavelinopsis hamatus	2	1				?*			*?*	
Gavelinopsis cf *hamatus*								4		
Gavelinopsis sp.					1			8		8
Globocassidulina laevigata										
Globocassidulina subglobosa	4					*				
Gyroidina danvillensis						*				
Gyroidina sp.										
Gyroidinoides sp.										
Gyroidinoides zelandicus										
Hoeglundina elegans										
Lagena sp.										
Lagena striata									*	
Lagena aff *striata*										
Lagena cf *striata*										
Laticarinina pauperata										
Lenticulina calcar										
Lenticulina aff *calcar*										
Lenticulina cf *calcar*										
Lenticulina costatus										
Lenticulina gyroscalpra										
Lenticulina loculosus										
Lenticulina marnilligera										
Lenticulina orbicularis										
Lenticulina spp.		1		2						1
Marginulina sp.										
Margmulina subbullata										
Mucronina sinalata										
Mucronina sp.										
Mucronina multicostales										
Mucronina sinalata										
Nodosaria longiscata										
Nodosaria sp.				1						
Nodosaria substrigata										
Nonionella flemingi		40		65	106	6	7	7	*	1
Notorotalia depressa grp	45	87						47		

Waikato Univ. No.	W962081A	W962088	W962106	W962108	W962109	W962111	W962139	W962166	W962174	W962177
Sample No.	382	287	250	252	253	255	246	220	212	209
Stratigraphic height (m)	921	1024	1148	1161	1166	1176	1341	1459	1499	1511
Notorotalia cf *depressa*				?2						
Notorotalia finlayi										
Notorotalia cf *finlayi*			1							5
Notorotalia finlayi grp										
Notorotalia finlayi/hurupiensis										
Notorotalia hurupiensis						*			*	
Notorotalia cf *hurupiensis*										
Notorotalia hurupiensis/depressa										
Notorotalia macinnesi										
Notorotalia pliozea										
Notorotalia aff *pliozea*										
Notorotalia spp.							5			
Notorotalia taranakia										
Notorotalia aff *taranakia*										
Notorotalia cf *taranakia*										
Oolina hexagona	2					*		1	*	
Oolina sp.										
Oolina squamosa	2								*	
Oridorsalis tenera						*				
Parafissurina sp.										
Patellinella inconspicua										
Pileolina sp.										
Plectofrondicularia pellucida								1		
Plectofrondicularia cf *pellucida*										
Plectofrondicularia pohana										
Proxifrons advena										
Pseudonodosaria sp.										
Pullenia bulloides										
Pullenia quinqueloba										
Pullenia cf *quinqueloba*										
Pullenia sp.										
Pullenia subcarinata										
Rectobolivina striatula						*				
Rectouvigerina striatula										
Rosalina bradyi										
Rotalia sp.										
Saracenaria italica										
Saracenaria cf *italica*										
Saracenaria latifrons										
Saracenaria sp.										
Sigmoilopsis sp.										
Sigmoilopsis zeaserus										
Sigmomorphina sp.										

Waikato Univ. No.	W962081A	W962088	W962106	W962108	W962109	W962111	W962139	W962166	W962174	W962177
Sample No.	382	287	250	252	253	255	246	220	212	209
Stratigraphic height (m)	921	1024	1148	1161	1166	1176	1341	1459	1499	1511
Siphonia australis										
Siphotextularia wairoana										
Siphouvigerina belluda										
Siphouvigerina canariensis										
Siphouvigerina eketahuna										
Siphouvigerina cf *eketahuna*										
Siphouvigerina sp.										
Sphaeroidina bulloides	1								*	
Spheroidinellopsis seminulina										
Spheroidinellopsis sp.										
Spiroloculina kennetti										
Stainforthia concava										
Stilostomella hochstetteri										
Stilostomella lepidula										
Stilostomella sp.	2	1								1
Trifarina bradyi										
Trifarina sp.	1							1		
Uvigerina (*Euuvigerina*) *miozea* grp	3			1			1	1		1
Uvigerina (*Siphouvigerina*) sp.										
Uvigerina cf *pliozea* (*miozea* grp)										
Uvigerina cf *poroporoensis* (*miozea* grp)										
Uvigerina rodleyi										
Vagulina elegans										
Vaginulina sp.										
Vaginulina vagina										
Virgulopsis parri										
Virgulopsis patiae										
Virgulopsis pustulata	6							1		
Virgulopsis sp.						*				
Virgulopsis subspinescens										
Virgulopsis *aff* subspinescens										
Virgulopsis turris							3			
Virgulopsis wanganuiensis							1	6		10
Virgulopsis aff *wanganuiensis*										
Virgulopsis cf *wanganuiensis*						?1				
Zeaflorilis parri						*		1	*	2
PLANKTICS										
Globigerina bulloides										
Globigerina falconensis										
Globigerina quinqueloba						1				
Globigerina aff *quinqueloba*										

Waikato Univ. No.	W962081A	W962088	W962106	W962108	W962109	W962111	W962139	W962166	W962174	W962177
Sample No.	382	287	250	252	253	255	246	220	212	209
Stratigraphic height (m)	921	1024	1148	1161	1166	1176	1341	1459	1499	1511
Globigerina cf *quinqueloba*										
Globigerina spp.	2	2		2	6	1	10	12	*	2
Globogirina (*Zeaglobigerina*) *apertura*										
Globogerina (*Zeaglobigerina*) sp.						*			*	
Globogerina (*Zeaglobigerina*) *woodi*										
Globogerina (*Zeaglobigerina*) cf *woodi*										
Globigerinita glutinata										
Globigerinita cf *glutinata*										
Globigerinita sp.										
Globigerinoides ruber										
Globigerinoides sp.										
Globigerinoides trilobus										
Globorotalia conomiozea										
Globorotalia crassaconica										
Globorotalia aff *crassaconica* (unkeeled)										
Globorotalia cf *crassaconica*										
Globorotalia crassaformis									*	
Globorotalia inflata										
Globorotalia inflata triangula										
Globorotalia miotumida										
Globorotalia pliozea									*	
Globorotalia puncticulata						2S			*	
Globorotalia aff *puncticulata*										
Globorotalia cf *puncticulata*								1		
Globorotalia puncticuloides										
Globorotalia scitula										
Globorotalia sp.										
Globorotalia cf *subconomiozea*										
Globorotalia truncatulinoides tosaensis										
Globorotalia tumida										
Globorotaloides punticuloides										
Neogloboquadrina pachyderma										?1
Neogloboquadrina cf pachyderma										
Neogloboquadrina sp.										
Orbulina bilobata										
Orbulina universa									*	
AGGLUTINATED										
Bathysiphon sp.										
Haeuslerella finlayi										
Haeuslerella cf *finlayi*										
Haeuslerella morgani										

Waikato Univ. No.	W962081A	W962088	W962106	W962108	W962109	W962111	W962139	W962166	W962174	W962177
Sample No.	382	287	250	252	253	255	246	220	212	209
Stratigraphic height (m)	921	1024	1148	1161	1166	1176	1341	1459	1499	1511
Haeuslerella parri										
Haeuslerella aff *parri*										
Haeuslerella *cf* parri										
Haeuslerella pliocenica										
Haeuslerella sp.										
Karreriella cylindrica										
Karreriella bradyi										
Martinotiella sp.										
Martinottiella communis										
Sigmollopsis zeaserus										
Siphonaperta macbeathi										
Siphonaperta aff *macbeathi*										
Textulria kapitea										
Textularia lythostrota										
Textulria cf *mestayeri*										
Thalmannammina sp.										
RADIOLARIANS										
Total										

Waikato Univ. No.	W962180	W962186	W962198	W962199	W962200	W962201	W962204	W962205	W962210	W962213
Sample No.	206	200	164	165	166	167	170	171	176	179
Stratigraphic height (m)	1524	1540	1571	1573	1578	1583	1598	1603	1620	1636
BENTHICS										
Alabamina sp.										
Ammonia beccarii	2									?1
Ammonia sp.		?2								
Amphicoryna cf *bortonica*					*					
Amphicoryna hirsuta			4	*	3				2	6
Amphicoryna aff *hirsuta*										
Amphicoryna cf *hirsuta*										
Amphicoryna scalaris				?1	*		1			
Amphicoryna sp.						10		1		1
Anomalina spherica										
Anomalinoides alazanensis				*						
Anomalinoides parvumbilius			1		3	2		1	5	5
Anomalinoides cf *parvumbilius*					1					
Anomalinoides sp.										
Anomalinoides sphericus										
Anomalinoides subnonionoides					1					
Astrononion kickinskii										
Astrononion neefi				?1		1				
Astrononion cf *neefi*										
Astrononion novozealandicum										
Astrononion cf *novozealandicum*										
Astrononion parki			?1		3			3		44
Astrononion sp.		4								
Bolivina affiliata			4	2	*	5		1	1	1
Bolivina aff *affiliata*	1									
Bolivina cf *affiliata*										
Bolivina albatrossi				*	*			1		2
Bolivina aff *albatrossi*				2						
Bolivina lapsus										
Bolivina numerosa										
Bolivina spathulata										
Bolivina sp.		1								
Bolivina watti										
Bolivina zigzag										
Bolivinita finlayi			1							
Bolivinita aff *finlayi*										
Bolivinita cf *finlayi*										
Bolivinita pliobliqua										2
Bolivinita pliozea										18
Bolivinita pohana										
Bolivinita pseudocompressa					2				2	3
Bolivinita aff *pseudocompressa*										

Waikato Univ. No.	W962180	W962186	W962198	W962199	W962200	W962201	W962204	W962205	W962210	W962213
Sample No.	206	200	164	165	166	167	170	171	176	179
Stratigraphic height (m)	1524	1540	1571	1573	1578	1583	1598	1603	1620	1636
Bolivinita quadrilatera										
Bulimina aculeata		4	10					2	1	
Bulimina aff *aculeata* (reduced spines)				17						8
Bulimina cf *aculeata*										
Bulimina elongata										
Bulimina *cf* elongata										
Bulimina marginata										
Bulimina aff *marginata*										
Bulimina cf *marginata*								1		
Bulimina sp.							?1			
Bulimina striata										
Bulimina cf *striata*		2	3	1	4	3	2		44	29
Bulimina cf *vella*										
Cassidulina neocarinata	4	29	1	1	1		2	8		
Ceratocancris sp.										
Chilostomella ovoidea										
Chrysalogonium verticale				*?*	2					
Cibicides amoenus				2						
Cibicides deliquatus			7	11	2	6	5	5	14	12
Cibicides cf *deliquatus*				44		15				17
Cibicides finlayi										
Cibicides aff *finlayi*				3						
Cibicides cf *finlayi*							1			
Cibicides molestus			23	12	8	9	4	18	7	7
Cibicides aff *molestus*										
Cibicides neoperforatus				*			?1			
Cibicides cf *notocenicus*										
Cibicides novozealandicus				1						
Cibicides spp.	6	5	57		7		6	18	5	
Cibicides subhaldingeri				*						
Dentalina obliquecostata				*	*					
Dentalina sp.					1	1	1	1	3	1
Dentalina soluta										
Dentalina substrigata										
Discorbinella bertheloti		5								
Discorbinella cf *bertheloti*										
Discorbinella sp.			1							
Discorbis dimidiatus										
Discorbis sp.										
Dyocibicides primitiva										
Dyocibicides sp.		1								
Elphidium advenum					?*					
Elphidium charlottensis	18	61								

Waikato Univ. No.	W962180	W962186	W962198	W962199	W962200	W962201	W962204	W962205	W962210	W962213
Sample No.	206	200	164	165	166	167	170	171	176	179
Stratigraphic height (m)	1524	1540	1571	1573	1578	1583	1598	1603	1620	1636
Elphidium cf *charlottensis*							1			
Elphidium simplex aoteanum										
Elphidium sp.										
Epistomella sp.										
Evolvocassidulina orientalis	1	19			1					
Evolvocassidulina cf *orientalis*										
Evolvocassidulina cf *orientalis* (carinate var)										
Fissurina sp.	1				*	1	1			1
Gavelinopsis hamatus										
Gavelinopsis cf *hamatus*										
Gavelinopsis sp.	9	1	3							
Globocassidulina laevigata										
Globocassidulina subglobosa			2	2	1	1		1	6	2
Gyroidina danvillensis			1						2	4
Gyroidina sp.					*					
Gyroidinoides sp.							1			
Gyroidinoides zelandicus	2								1	
Hoeglundina elegans										1
Lagena sp.									1	
Lagena striata					*					
Lagena aff *striata*										
Lagena cf *striata*					*					
Laticarinina pauperata			2	3	*	6	2	1	2	
Lenticulina calcar				?1	3					
Lenticulina aff *calcar*										
Lenticulina cf *calcar*										
Lenticulina costatus										
Lenticulina gyroscalpra										
Lenticulina loculosus										
Lenticulina mamilligera				*						
Lenticulina orbicularis										
Lenticulina spp.		1	5	6	*	3	7	6	8	13
Marginulina sp.										
Margmulina subbullata				*?*						
Mucronina sinalata					*					
Mucronina sp.									2	
Mucronina multicostales										
Mucronina sinalata				*						
Nodosaria longiscata			1	*	1				6	
Nodosaria sp.				*	1			1		
Nodosaria substrigata										
Nonionella flemingi	2	13								
Notorotalia depressa grp		25								

Waikato Univ. No.	W962180	W962186	W962198	W962199	W962200	W962201	W962204	W962205	W962210	W962213
Sample No.	206	200	164	165	166	167	170	171	176	179
Stratigraphic height (m)	1524	1540	1571	1573	1578	1583	1598	1603	1620	1636
Notorotalia cf *depressa*										
Notorotalia finlayi										
Notorotalia cf *finlayi*	2									
Notorotalia finlayi grp										
Notorotalia finlayi/hurupiensis										
Notorotalia hurupiensis				6						
Notorotalia cf *hurupiensis*			1			7	14	4	4	8
Notorotalia hurupiensis/depressa										
Notorotalia macinnesi										
Notorotalia pliozea										
Notorotalia aff *pliozea*										
Notorotalia spp.	1	1	5							
Notorotalia taranakia				1						
Notorotalia aff *taranakia*										
Notorotalia cf *taranakia*					9					
Oolina hexagona		2								
Oolina sp.	1									
Oolina squamosa		1								
Oridorsalis tenera			3		1	4	4	5	2	5
Parafissurina sp.									?1	
Patellinella inconspicua										
Pileolina sp.										
Plectofrondicularia pellucida				*	*		36	2		
Plectofrondicularia cf *pellucida*									1	
Plectofrondicularia pohana										
Proxifrons advena				1			1			
Pseudonodosaria sp.		1								
Pullenia bulloides				7	8	9	2	4	7	9
Pullenia quinqueloba					*			1		
Pullenia cf *quinqueloba*										
Pullenia sp.						1				
Pullenia subcarinata										
Rectobolivina striatula										
Rectouvigerina striatula		1								
Rosalina bradyi										
Rotalia sp.				*						
Saracenaria italica				1						
Saracenaria cf *italica*										
Saracenaria latifrons										
Saracenaria sp.										
Sigmoilopsis sp.										
Sigmoilopsis zeaserus				*?*						
Sigmomorphina sp.										

Waikato Univ. No.	W962180	W962186	W962198	W962199	W962200	W962201	W962204	W962205	W962210	W962213
Sample No.	206	200	164	165	166	167	170	171	176	179
Stratigraphic height (m)	1524	1540	1571	1573	1578	1583	1598	1603	1620	1636
Siphonia australis				*						
Siphotextularia wairoana										
Siphouvigerina belluda				?28	4					
Siphouvigerina canariensis					1					
Siphouvigerina eketahuna				*		?8				
Siphouvigerina cf *eketahuna*				3						
Siphouvigerina sp.			3						2	1
Sphaeroidina bulloides			1	*	1	1		1		
Spheroidinellopsis seminulina				*						
Spheroidinellopsis sp.				?1						
Spiroloculina kennetti							?1			
Stainforthia concava										
Stilostomella hochstetteri						1				
Stilostomella lepidula										
Stilostomella sp.		1			1					1
Trifarina bradyi			1							
Trifarina sp.		1								
Uvigerina (*Euuvigerina*) *miozea* grp	1	1	9	10		17	6	13	14	4
Uvigerina (*Siphouvigerina*) sp.										
Uvigerina cf *pliozea* (*miozea* grp)										
Uvigerina cf *poroporoensis* (*miozea* grp)					10					
Uvigerina rodleyi				*?*						
Vagulina elegans					*					
Vaginulina sp.									1	3
Vaginulina vagina										
Virgulopsis parri										
Virgulopsis patiae										
Virgulopsis pustulata		3								1
Virgulopsis sp.										
Virgulopsis subspinescens										
Virgulopsis *aff* subspinescens										
Virgulopsis turris										
Virgulopsis wanganuiensis	7									
Virgulopsis aff *wanganuiensis*										
Virgulopsis cf *wanganuiensis*										
Zeaflorilis parri		?2								
PLANKTICS										
Globigerina bulloides				3	1	4				2
Globigerina falconensis					*					
Globigerina quinqueloba					2	3			9	
Globigerina aff *quinqueloba*										

Waikato Univ. No.	W962180	W962186	W962198	W962199	W962200	W962201	W962204	W962205	W962210	W962213
Sample No.	206	200	164	165	166	167	170	171	176	179
Stratigraphic height (m)	1524	1540	1571	1573	1578	1583	1598	1603	1620	1636
Globigerina cf *quinqueloba*										
Globigerina spp.		3	21	41	22	32	170	26	49	16
Globogirina (*Zeaglobigerina*) *apertura*					2					
Globogerina (*Zeaglobigerina*) sp.				*	6					
Globogerina (*Zeaglobigerina*) *woodi*				7	2				1	
Globogerina (*Zeaglobigerina*) cf *woodi*										
Globigerinita glutinata				4	5			?1	1	
Globigerinita cf *glutinata*										
Globigerinita sp.						3				
Globigerinoides ruber				*?*		1			2	
Globigerinoides sp.										
Globigerinoides trilobus										
Globorotalia conomiozea										
Globorotalia crassaconica			2		*2D*		4			
Globorotalia aff *crassaconica* (unkeeled)										
Globorotalia cf *crassaconica*										
Globorotalia crassaformis				?2 *44S*	*9S:3D*					
Globorotalia inflata	1		?1	*S*	28 S>>D	13	41	3	2	5
Globorotalia inflata triangula										
Globorotalia miotumida										
Globorotalia pliozea										
Globorotalia puncticulata				29 *S*	8 *8S*	4				
Globorotalia aff *puncticulata*			2					6		
Globorotalia cf *puncticulata*										2
Globorotalia puncticuloides										
Globorotalia scitula				1						1
Globorotalia sp.									1	
Globorotalia cf *subconomiozea*										
Globorotalia truncatulinoides tosaensis										
Globorotalia tumida										
Globorotaloides punticuloides							?2			
Neogloboquadrina pachyderma				*3D*	19D	4	3		2	
Neogloboquadrina cf pachyderma										6
Neogloboquadrina sp.				1			10			
Orbulina bilobata										
Orbulina universa				*	*					
AGGLUTINATED										
Bathysiphon sp.										
Haeuslerella finlayi				*						
Haeuslerella cf *finlayi*							7			
Haeuslerella morgani				1		2				

Waikato Univ. No.	W962180	W962186	W962198	W962199	W962200	W962201	W962204	W962205	W962210	W962213
Sample No.	206	200	164	165	166	167	170	171	176	179
Stratigraphic height (m)	1524	1540	1571	1573	1578	1583	1598	1603	1620	1636
Haeuslerella parri				1						24
Haeuslerella aff *parri*										
Haeuslerella *cf* parri										
Haeuslerella pliocenica			3	2	2	?3	?3	2	7	4
Haeuslerella sp.										
Karreriella cylindrica				*	4	3	5	1	5	
Karreriella bradyi				*						
Martinotiella sp.					*					
Martinottiella communis			6	6						
Sigmoilopsis zeaserus										
Siphonaperta macbeathi										
Siphonaperta aff *macbeathi*					1					
Texturlria kapitea										
Textularia lythostrota				*?*						
Texturlria cf *mestayeri*		1								
Thalmannammina sp.										
RADIOLARIANS										
Total										

Waikato Univ. No.	W962216	W962217	W962219	W962221	W962225	W96223	W962224	W962265	W962280	W962281
Sample No.	182	183	185	187	391	389	390	83	98	99
Stratigraphic height (m)	1649	1654	1664	1674	JRS	CFS	CFS	1774	1815	1935
BENTHICS										
Alabamina sp.										
Ammonia beccarii										
Ammonia sp.										
Amphicoryna cf *bortonica*										
Amphicoryna hirsuta			9			2			9	
Amphicoryna aff *hirsuta*										
Amphicoryna cf *hirsuta*	2						1			
Amphicoryna scalaris										
Amphicoryna sp.		6	10	3	1	2	1	2		
Anomalina spherica										
Anomalinoides alazanensis										
Anomalinoides parvumbilius	16	1	1	16	1	7	1	4	3	1
Anomalinoides cf *parvumbilius*										
Anomalinoides sp.							1			
Anomalinoides sphericus		1								
Anomalinoides subnonionoides										
Astrononion kickinskii										
Astrononion neefi										
Astrononion cf *neefi*						1				
Astrononion novozealandicum										
Astrononion cf *novozealandicum*										
Astrononion parki	1							7	1	13
Astrononion sp.		1					1			
Bolivina affillata	8	10	1	2	3		3			
Bolivina aff *affiliata*		2								
Bolivina cf *affiliata*										
Bolivina albatrossi	5						1			
Bolivina aff *albatrossi*						3				
Bolivina lapsus										
Bolivina numerosa										
Bolivina spathulata										
Bolivina sp.								3		
Bolivina watti										
Bolivina zigzag										
Bolivinita finlayi										
Bolivinita aff *finlayi*										
Bolivinita cf *finlayi*										
Bolivinita pliobliqua								3		
Bolivinita pliozea	11		7	7					3	
Bolivinita pohana										
Bolivinita pseudocompressa	2					4				
Bolivinita aff *pseudocompressa*										

Waikato Univ. No.	W962216	W962217	W962219	W962221	W962225	W96223	W962224	W962265	W962280	W962281
Sample No.	182	183	185	187	391	389	390	83	98	99
Stratigraphic height (m)	1649	1654	1664	1674	JRS	CFS	CFS	1774	1815	1935
Bolivinita quadrilatera										
Bulimina aculeata		15	5							
Bulimina aff *aculeata* (reduced spines)								1	2	2
Bulimina cf *aculeata*										
Bulimina elongata										
Bulimina *cf* elongata										
Bulimina marginata		8								
Bulimina aff *marginata*										
Bulimina cf *marginata*										
Bulimina sp.										
Bulimina striata										
Bulimina cf *striata*	8	4	7	122	5	5	3		1	1
Bulimina cf *vella*										
Cassidulina neocarinata	1		2		3	2	3		3	
Ceratocancris sp.										
Chilostomella ovoidea										
Chrysalogonium verticale								1		1
Cibicides amoenus										
Cibicides deliquatus	5	5	8	4	6	5	3	10	1	8
Cibicides cf *deliquatus*	10		31	27			4	9	8	25
Cibicides finlayi										
Cibicides aff *finlayi*										
Cibicides cf *finlayi*										
Cibicides molestus	1	11		2		9	5	40	5	5
Cibicides aff *molestus*			1							
Cibicides neoperforatus										
Cibicides cf *notocenicus*										
Cibicides novozealandicus										
Cibicides spp.		29			1	10				2
Cibicides subhaidingeri										
Dentalina obliquecostata										
Dentalina sp.	1	1	6	1	2	1		6	4	2
Dentalina soluta										
Dentalina substrigata										
Discorbinella bertheloti										
Discorbinella cf *bertheloti*										
Discorbinella sp.										
Discorbis dimidiatus										
Discorbis sp.										
Dyocibicides primitiva										
Dyocibicides sp.										
Elphidium advenum										
Elphidium charlottensis						1				

Waikato Univ. No.	W962216	W962217	W962219	W962221	W962225	W96223	W962224	W962265	W962280	W962281
Sample No.	182	183	185	187	391	389	390	83	98	99
Stratigraphic height (m)	1649	1654	1664	1674	JRS	CFS	CFS	1774	1815	1935
Elphidium cf *charlottensis*										
Elphidium simplex aoteanum										
Elphidium sp.										
Epistomella sp.										
Evolvocassidulina orientalis	1				1	1	4	5	29	
Evolvocassidulina cf *orientalis*										
Evolvocassidulina cf *orientalis* (carinate var)										
Fissurina sp.			1			1			2	
Gavelinopsis hamatus										
Gavelinopsis cf *hamatus*										
Gavelinopsis sp.										
Globocassidulina laevigata	?1									
Globocassidulina subglobosa	3	1	1	20	5	6	5			
Gyroidina danvillensis										
Gyroidina sp.							2			
Gyroidinoides sp.										
Gyroidinoides zelandicus					1		1			
Hoeglundina elegans						1		6	1	
Lagena sp.			1	2		1			4	
Lagena striata										
Lagena aff *striata*										
Lagena cf *striata*										
Laticarinina pauperata						1	1			
Lenticulina calcar				1				?11	1	4
Lenticulina aff *calcar*										
Lenticulina cf *calcar*										
Lenticulina costatus										
Lenticulina gyroscalpra										
Lenticulina loculosus										
Lenticulina mamilligera										
Lenticulina orbicularis										
Lenticulina spp.	8	4	7	3	5	9	12		2	1
Marginulina sp.										
Margmulina subbullata										
Mucronina sinalata										
Mucronina sp.										
Mucronina multicostales										
Mucronina sinalata										
Nodosaria longiscata										
Nodosaria sp.							1			
Nodosaria substrigata										
Nonionella flemingi										
Notorotalia depressa grp										

Waikato Univ. No.	W962216	W962217	W962219	W962221	W962225	W96223	W962224	W962265	W962280	W962281
Sample No.	182	183	185	187	391	389	390	83	98	99
Stratigraphic height (m)	1649	1654	1664	1674	JRS	CFS	CFS	1774	1815	1935
Notorotalia cf *depressa*										
Notorotalia finlayi								2	?22	4
Notorotalia cf *finlayi*										
Notorotalia finlayi grp										
Notorotalia finlayi/hurupiensis										
Notorotalia hurupiensis				?2					?9	
Notorotalia cf *hurupiensis*	10	6	2		6	5	7			
Notorotalia hurupiensis/depressa										
Notorotalia macinnesi										
Notorotalia pliozea										
Notorotalia aff *pliozea*										
Notorotalia spp.										
Notorotalia taranakia										
Notorotalia aff *taranakia*									3	
Notorotalia cf *taranakia*										
Oolina hexagona										
Oolina sp.		3								
Oolina squamosa										
Oridorsalis tenera	13	3	2	6	1	2	3	?1	21	10
Parafissurina sp.										
Patellinella inconspicua										
Pileolina sp.										
Plectofrondicularia pellucida			1	3	1	6	1			
Plectofrondicularia cf *pellucida*										
Plectofrondicularia pohana										
Proxifrons advena						1				
Pseudonodosaria sp.										
Pullenia bulloides	11	4	4	12	3	7	5			
Pullenia quinqueloba										
Pullenia cf *quinqueloba*										
Pullenia sp.						2				
Pullenia subcarinata				?1						
Rectobolivina striatula										
Rectouvigerina striatula										
Rosalina bradyi										
Rotalia sp.										
Saracenaria itallica			1			1				
Saracenaria cf *itallica*				1						
Saracenaria latifrons						1				
Saracenaria sp.			1							
Sigmoilopsis sp.										
Sigmoilopsis zeaserus										
Sigmomorphina sp.										

Waikato Univ. No.	W962216	W962217	W962219	W962221	W962225	W96223	W962224	W962265	W962280	W962281
Sample No.	182	183	185	187	391	389	390	83	98	99
Stratigraphic height (m)	1649	1654	1664	1674	JRS	CFS	CFS	1774	1815	1935
Siphonia australis					1					
Siphotextularia wairoana										
Siphouvigerina belluda										
Siphouvigerina canariensis										
Siphouvigerina eketahuna					1					
Siphouvigerina cf *eketahuna*										
Siphouvigerina sp.						1	2			
Sphaeroidina bulloides		3		4	1	4			5	
Spheroidinellopsis seminulina										
Spheroidinellopsis sp.										
Spiroloculina kennetti										
Stainforthia concava										
Stilostomella hochstetteri										
Stilostomella lepidula										
Stilostomella sp.			6		1	6				
Trifarina bradyi	1			1						
Trifarina sp.										
Uvigerina (*Euuvigerina*) *miozea* grp	27	51	30	7	11	17	14	2	36	13
Uvigerina (*Siphouvigerina*) sp.										
Uvigerina cf *pliozea* (*miozea* grp)										
Uvigerina cf *poroporoensis* (*miozea* grp)										
Uvigerina rodleyi			1							
Vagulina elegans										
Vaginulina sp.	?3			4	2	1	1			
Vaginulina vagina										
Virgulopsis parri										
Virgulopsis patiae										
Virgulopsis pustulata										
Virgulopsis sp.										
Virgulopsis subspinescens										
Virgulopsis *aff* subspinescens										
Virgulopsis turris										
Virgulopsis wanganuiensis	1									
Virgulopsis aff *wanganuiensis*										
Virgulopsis cf *wanganuiensis*										
Zeaflorilis parri										
PLANKTICS										
Globigerina bulloides									1	
Globigerina falconensis										
Globigerina quinqueloba					1		7		3	
Globigerina aff *quinqueloba*										

Waikato Univ. No.	W962216	W962217	W962219	W962221	W962225	W96223	W962224	W962265	W962280	W962281
Sample No.	182	183	185	187	391	389	390	83	98	99
Stratigraphic height (m)	1649	1654	1664	1674	JRS	CFS	CFS	1774	1815	1935
Globigerina cf *quinqueloba*										
Globigerina spp.	14	9	11	12	54	146	32		13	3
Globogirina (*Zeaglobigerina*) *apertura*										
Globogerina (*Zeaglobigerina*) sp.										
Globogerina (*Zeaglobigerina*) *woodi*				9						
Globogerina (*Zeaglobigerina*) cf *woodi*							2			
Globigerinita glutinata				3	22				1	
Globigerinita cf *glutinata*										
Globigerinita sp.							24			
Globigerinoides ruber										
Globigerinoides sp.										
Globigerinoides trilobus							1			
Globorotalia conomiozea										
Globorotalia crassaconica	?4									
Globorotalia aff *crassaconica* (unkeeled)										
Globorotalia cf *crassaconica*										
Globorotalia crassaformis				2		3	2			
Globorotalia inflata	2		7	2	4	12	18		6	1
Globorotalia inflata triangula										
Globorotalia miotumida										
Globorotalia pliozea										
Globorotalia puncticulata					1	3	1	1	4	
Globorotalia aff *puncticulata*										
Globorotalia cf *puncticulata*										
Globorotalia puncticuloides	1									
Globorotalia scitula										
Globorotalia sp.										
Globorotalia cf *subconomiozea*					?2	6				
Globorotalia truncatulinoides tosaensis										
Globorotalia tumida										
Globorotaloides punticuloides										
Neogloboquadrina pachyderma	1		1	2	4		3		11	
Neogloboquadrina cf pachyderma										
Neogloboquadrina sp.										
Orbulina bilobata										
Orbulina universa	1	?2				2				
AGGLUTINATED										
Bathysiphon sp.										
Haeuslerella finlayi			?6							
Haeuslerella cf *finlayi*										
Haeuslerella morgani				3		18				

Waikato Univ. No.	W962216	W962217	W962219	W962221	W962225	W96223	W962224	W962265	W962280	W962281
Sample No.	182	183	185	187	391	389	390	83	98	99
Stratigraphic height (m)	1649	1654	1664	1674	JRS	CFS	CFS	1774	1815	1935
Haeuslerella parri	14			11				11	58	18
Haeuslerella aff *parri*										
Haeuslerella *cf* parri										
Haeuslerella pliocenica	7	?4	8	2		21	9			2
Haeuslerella sp.		29			3					
Karreriella cylindrica	1	16		2	5	4	2			1
Karreriella bradyi										
Martinotiella sp.		1				1				
Martinottiella communis				2						
Sigmollopsis zeaserus										1
Siphonaperta macbeathi										
Siphonaperta aff *macbeathi*										
Textularia kapitea										
Textularia lythostrota										
Textularia cf *mestayeri*										
Thalmannammina sp.										
RADIOLARIANS										
Total										

Waikato Univ. No.	W962293	W962302	W962312	W962313	W962317	W962326	W2336	W962339A	W962340	W962341
Sample No.	125	132	142	143	147	156	416	412	61	5
Stratigraphic height (m)	2000	2053	2082	2088	2125	2179	2223	2240	2249	2253.5
BENTHICS										
Alabamina sp.			2							
Ammonia beccarii										
Ammonia sp.										
Amphicoryna cf *bortonica*										
Amphicoryna hirsuta	2	3			3	1	5			3
Amphicoryna aff *hirsuta*										
Amphicoryna cf *hirsuta*										
Amphicoryna scalaris										
Amphicoryna sp.	1	1	3		3	5	3	2		
Anomalina spherica					1					
Anomalinoides alazanensis										
Anomalinoides parvumbilius	1	1	1		10		4	3	4	
Anomalinoides cf *parvumbilius*										
Anomalinoides sp.										
Anomalinoides sphericus										
Anomalinoides subnonionoides	1	2			2		7	32	2	
Astrononion kickinskii					1					
Astrononion neefi										
Astrononion cf *neefi*										
Astrononion novozealandicum										
Astrononion cf *novozealandicum*										
Astrononion parki	3	15	1		9				1	10
Astrononion sp.										
Bolivina affiliata			2		1		1			
Bolivina aff *affiliata*										
Bolivina cf *affiliata*										
Bolivina albatrossi	1		1	2						
Bolivina aff *albatrossi*										
Bolivina lapsus										
Bolivina numerosa										
Bolivina spathulata										
Bolivina sp.										
Bolivina watti			?1							
Bolivina zigzag										
Bolivinita finlayi										
Bolivinita aff *finlayi*										
Bolivinita cf *finlayi*										
Bolivinita pliobliqua			6				1			
Bolivinita pliozea	*				2			5	12	
Bolivinita pohana		1								
Bolivinita pseudocompressa					8					
Bolivinita aff *pseudocompressa*										

Waikato Univ. No.	W962293	W962302	W962312	W962313	W962317	W962326	W2336	W962339A	W962340	W962341
Sample No.	125	132	142	143	147	156	416	412	61	5
Stratigraphic height (m)	2000	2053	2082	2088	2125	2179	2223	2240	2249	2253.5
Bolivinita quadrilatera										
Bulimina aculeata	*			1						
Bulimina aff *aculeata* (reduced spines)	15	3	24		2	1	16	10		
Bulimina cf *aculeata*										
Bulimina elongata										
Bulimina *cf* elongata										
Bulimina marginata										
Bulimina aff *marginata*										
Bulimina cf *marginata*										
Bulimina sp.										
Bulimina striata								25		
Bulimina cf *striata*	75	15	1	6	2	3			6	
Bulimina cf *vella*										
Cassidulina neocarinata		2	1		31		40			1
Ceratocancris sp.										
Chilostomella ovoidea										
Chrysalogonium verticale						?1				1
Cibicides amoenus										
Cibicides deliquatus	32	3	3		5	9	2		19	7
Cibicides cf *deliquatus*		16	12	13	20	24	25	23		15
Cibicides finlayi	*	3								
Cibicides aff *finlayi*										
Cibicides cf *finlayi*										
Cibicides molestus	4	9	1	2	12		21	1		
Cibicides aff *molestus*										
Cibicides neoperforatus										
Cibicides cf *notocenicus*										
Cibicides novozealandicus										
Cibicides spp.										2
Cibicides subhaidingeri										
Dentalina obliquecostata										
Dentalina sp.	4	2	3	?1	4	1	1	6	?6	?2
Dentalina soluta										
Dentalina substrigata										
Discorbinella bertheloti										
Discorbinella cf *bertheloti*										
Discorbinella sp.										
Discorbis dimidiatus										
Discorbis sp.										
Dyocibicides primitiva										
Dyocibicides sp.										
Elphidium advenum										
Elphidium charlottensis			?1		6					

Waikato Univ. No.	W962293	W962302	W962312	W962313	W962317	W962326	W2336	W962339A	W962340	W962341
Sample No.	125	132	142	143	147	156	416	412	61	5
Stratigraphic height (m)	2000	2053	2082	2088	2125	2179	2223	2240	2249	2253.5
Elphidium cf *charlottensis*										
Elphidium simplex aoteanum										
Elphidium sp.										
Epistomella sp.	*									
Evolvocassidulina orientalis	*	1		1	8		229	2	8	5
Evolvocassidulina cf *orientalis*										
Evolvocassidulina cf *orientalis* (carinate var)										
Fissurina sp.	*			1	2					
Gavelinopsis hamatus										
Gavelinopsis cf *hamatus*										
Gavelinopsis sp.										
Globocassidulina laevigata										
Globocassidulina subglobosa	4	3		3						
Gyroidina danvillensis	1	2	4		3		8	1		
Gyroidina sp.										
Gyroidinoides sp.										
Gyroidinoides zelandicus	*	1	3		4	1		1		
Hoeglundina elegans		4	3							1
Lagena sp.	*									
Lagena striata					1			1		
Lagena aff *striata*										
Lagena cf *striata*					1					
Laticarinina pauperata										
Lenticulina calcar	5	3	7	1	4	10				
Lenticulina aff *calcar*							14			3
Lenticulina cf *calcar*										
Lenticulina costatus										
Lenticulina gyroscalpra										
Lenticulina loculosus										
Lenticulina mamilligera										
Lenticulina orbicularis										
Lenticulina spp.	8	3	6	6	8	3		1	1	2
Marginulina sp.										
Margmulina subbullata	*									
Mucronina sinalata										
Mucronina sp.										
Mucronina multicostales										
Mucronina sinalata										
Nodosaria longiscata	*									
Nodosaria sp.	*									
Nodosaria substrigata										
Nonionella flemingi					1					
Notorotalia depressa grp										

Waikato Univ. No.	W962293	W962302	W962312	W962313	W962317	W962326	W2336	W962339A	W962340	W962341
Sample No.	125	132	142	143	147	156	416	412	61	5
Stratigraphic height (m)	2000	2053	2082	2088	2125	2179	2223	2240	2249	2253.5
Notorotalia cf *depressa*										
Notorotalia finlayi							10	13		?17
Notorotalia cf *finlayi*										
Notorotalia finlayi grp										
Notorotalia finlayi/hurupiensis										
Notorotalia hurupiensis	*	10	?16		?24	?13				
Notorotalia cf *hurupiensis*				11						
Notorotalia hurupiensis/depressa										
Notorotalia macinnesi										
Notorotalia pliozea									?15	
Notorotalia aff *pliozea*										
Notorotalia spp.										
Notorotalia taranakia										
Notorotalia aff *taranakia*										
Notorotalia cf *taranakia*										
Oolina hexagona										
Oolina sp.										
Oolina squamosa										
Oridorsalis tenera	10	2	3	3	15	6	5	7		3
Parafissurina sp.										
Patellinella inconspicua										
Pileolina sp.										
Plectofrondicularia pellucida	1	2	58	28	2		19			
Plectofrondicularia cf *pellucida*										
Plectofrondicularia pohana										
Proxifrons advena										
Pseudonodosaria sp.										
Pullenia bulloides		1	1	1	2	11	8	1		
Pullenia quinqueloba										
Pullenia cf *quinqueloba*										1
Pullenia sp.										
Pullenia subcarinata										
Rectobolivina striatula	?*		1							
Rectouvigerina striatula										
Rosalina bradyi										
Rotalia sp.										
Saracenaria italica	2									
Saracenaria cf *italica*										
Saracenaria latifrons			1							
Saracenaria sp.										
Sigmoilopsis sp.										
Sigmoilopsis zeaserus										
Sigmomorphina sp.										

Waikato Univ. No.	W962293	W962302	W962312	W962313	W962317	W962326	W2336	W962339A	W962340	W962341
Sample No.	125	132	142	143	147	156	416	412	61	5
Stratigraphic height (m)	2000	2053	2082	2088	2125	2179	2223	2240	2249	2253.5
Siphonia australis										
Siphotextularia wairoana										
Siphouvigerina belluda										
Siphouvigerina canariensis										
Siphouvigerina eketahuna										
Siphouvigerina cf *eketahuna*										
Siphouvigerina sp.										
Sphaeroidina bulloides	3				3	9	1		1	2
Spheroidinellopsis seminulina										
Spheroidinellopsis sp.										
Spiroloculina kennetti										
Stainforthia concava										
Stilostomella hochstetteri										
Stilostomella lepidula										
Stilostomella sp.	*			?1	1	2	4			
Trifarina bradyi										
Trifarina sp.										
Uvigerina (*Euuvigerina*) *miozea* grp		27	29	5	30	52	25	44	75	98
Uvigerina (*Siphouvigerina*) sp.										
Uvigerina cf *pliozea* (*miozea* grp)										
Uvigerina cf *poroporoensis* (*miozea* grp)	52									
Uvigerina rodleyi	1									
Vagulina elegans										
Vaginulina sp.				?1						
Vaginulina vagina										
Virgulopsis parri										
Virgulopsis patiae										
Virgulopsis pustulata										
Virgulopsis sp.	*									
Virgulopsis subspinescens										
Virgulopsis *aff* subspinescens										
Virgulopsis turris					5					
Virgulopsis wanganuiensis										
Virgulopsis aff *wanganuiensis*										
Virgulopsis cf *wanganuiensis*										
Zeaflorilis parri					1					
PLANKTICS										
Globigerina bulloides										
Globigerina falconensis			1							
Globigerina quinqueloba			2		2		9			
Globigerina aff *quinqueloba*										

Waikato Univ. No.	W962293	W962302	W962312	W962313	W962317	W962326	W2336	W962339A	W962340	W962341
Sample No.	125	132	142	143	147	156	416	412	61	5
Stratigraphic height (m)	2000	2053	2082	2088	2125	2179	2223	2240	2249	2253.5
Globigerina cf *quinqueloba*										
Globigerina spp.	*	5	1	1	8	7	4			
Globogirina (*Zeaglobigerina*) *apertura*										
Globogerina (*Zeaglobigerina*) sp.										
Globogerina (*Zeaglobigerina*) *woodi*			1		1	3				3
Globogerina (*Zeaglobigerina*) cf *woodi*										
Globigerinita glutinata		1	1		10		2			
Globigerinita cf *glutinata*	*									
Globigerinita sp.										
Globigerinoides ruber										
Globigerinoides sp.						?1				
Globigerinoides trilobus	*									
Globorotalia conomiozea										
Globorotalia crassaconica							?1			
Globorotalia aff *crassaconica* (unkeeled)										
Globorotalia cf *crassaconica*										
Globorotalia crassaformis	*1S*									
Globorotalia inflata	1S *2S*	4		1	4					
Globorotalia inflata triangula										
Globorotalia miotumida										
Globorotalia pliozea										
Globorotalia puncticulata	2S *1S*	7	2		?1	1	3			
Globorotalia aff *puncticulata*										
Globorotalia cf *puncticulata*										
Globorotalia puncticuloides				1						
Globorotalia scitula										
Globorotalia sp.										
Globorotalia cf *subconomiozea*										
Globorotalia truncatulinoides tosaensis										
Globorotalia tumida										
Globorotaloides punticuloides										
Neogloboquadrina pachyderma	1S *4S*		?1	1	6					
Neogloboquadrina cf pachyderma										
Neogloboquadrina sp.			1							
Orbulina bilobata										
Orbulina universa										
AGGLUTINATED										
Bathysiphon sp.										
Haeuslerella finlayi										
Haeuslerella cf *finlayi*										
Haeuslerella morgani										

Waikato Univ. No.	W962293	W962302	W962312	W962313	W962317	W962326	W2336	W962339A	W962340	W962341
Sample No.	125	132	142	143	147	156	416	412	61	5
Stratigraphic height (m)	2000	2053	2082	2088	2125	2179	2223	2240	2249	2253.5
Haeuslerella parri		21	15		18		22			2
Haeuslerella aff *parri*										
Haeuslerella *cf* parri										
Haeuslerella pliocenica		1	1		3					
Haeuslerella sp.										
Karreriella cylindrica	*		1						3	3
Karreriella bradyi										
Martinotiella sp.										
Martinottiella communis					1				2	
Sigmoilopsis zeaserus										
Siphonaperta macbeathi										
Siphonaperta aff *macbeathi*										
Texturlria kapitea										
Textularia lythostrota										
Texturlria cf *mestayeri*										
Thalmannammina sp.										
RADIOLARIANS										
Total			4		12		1	14		

Waikato Univ. No.	W962344	W962346	W962348	W962355	W962356	W962358C	W962361	W962366	W962373	W962375A
Sample No.	59	58	3	51	50	393	396	401	408	
Stratigraphic height (m)	2260	2269	2277.5	2296	2300	2315	2330	2360	2394	2395
BENTHICS										
Alabamina sp.										
Ammonia beccarii										
Ammonia sp.										
Amphicoryna cf *bortonica*										
Amphicoryna hirsuta								7		*
Amphicoryna aff *hirsuta*										
Amphicoryna cf *hirsuta*									*	
Amphicoryna scalaris										
Amphicoryna sp.		*		1		2	6	5	5	
Anomalina spherica										*
Anomalinoides alazanensis										
Anomalinoides parvumbilius	2	1	2	4	6	1				*
Anomalinoides cf *parvumbilius*										
Anomalinoides sp.										
Anomalinoides sphericus		*								
Anomalinoides subnonionoides		*							1	*
Astrononion kickinskii										
Astrononion neefi										
Astrononion cf *neefi*										
Astrononion novozealandicum										
Astrononion cf *novozealandicum*										
Astrononion parki	28	4	1	2		45		44	2	*
Astrononion sp.					2					
Bolivina affiliata									*	
Bolivina aff *affiliata*										
Bolivina cf *affiliata*										
Bolivina albatrossi										
Bolivina aff *albatrossi*										
Bolivina lapsus										
Bolivina numerosa										
Bolivina spathulata										
Bolivina sp.									*	
Bolivina watti										
Bolivina zigzag										
Bolivinita finlayi										
Bolivinita aff *finlayi*										
Bolivinita cf *finlayi*										
Bolivinita pliobliqua			3							
Bolivinita pliozea		1	1	4	5	12	1	3	27	*
Bolivinita pohana										
Bolivinita pseudocompressa										
Bolivinita aff *pseudocompressa*										

Waikato Univ. No.	W962344	W962346	W962348	W962355	W962356	W962358C	W962361	W962366	W962373	W962375A
Sample No.	59	58	3	51	50	393	396	401	408	
Stratigraphic height (m)	2260	2269	2277.5	2296	2300	2315	2330	2360	2394	2395
Bolivinita quadrilatera										
Bulimina aculeata					12			4		
Bulimina aff *aculeata* (reduced spines)		1	2	8		6			3	
Bulimina cf *aculeata*										*
Bulimina elongata										
Bulimina *cf* elongata						9				
Bulimina marginata										
Bulimina aff *marginata*										
Bulimina cf *marginata*										
Bulimina sp.										
Bulimina striata				3						
Bulimina cf *striata*	1	*	1		1			1	1	
Bulimina cf *vella*										
Cassidulina neocarinata	2	*				1	9	1		
Ceratocancris sp.										
Chilostomella ovoidea										
Chrysalogonium verticale										
Cibicides amoenus										
Cibicides deliquatus	6	23	4	15	6	3		1	5	*
Cibicides cf *deliquatus*	11		10	7		15	2	3		
Cibicides finlayi					2					
Cibicides aff *finlayi*										
Cibicides cf *finlayi*										
Cibicides molestus	7							1	9	*
Cibicides aff *molestus*										
Cibicides neoperforatus										
Cibicides cf *notocenicus*			1				1			
Cibicides novozealandicus										
Cibicides spp.	3		2	24						
Cibicides subhaidingeri										
Dentalina obliquecostata										
Dentalina sp.	1				?2	11	1	2	?4	
Dentalina soluta										
Dentalina substrigata										
Discorbinella bertheloti										
Discorbinella cf *bertheloti*										
Discorbinella sp.										
Discorbis dimidiatus										
Discorbis sp.										
Dyocibicides primitiva										
Dyocibicides sp.										
Elphidium advenum										
Elphidium charlottensis									*	

Waikato Univ. No.	W962344	W962346	W962348	W962355	W962356	W962358C	W962361	W962366	W962373	W962375A
Sample No.	59	58	3	51	50	393	396	401	408	
Stratigraphic height (m)	2260	2269	2277.5	2296	2300	2315	2330	2360	2394	2395
Elphidium cf *charlottensis*										
Elphidium simplex aoteanum										
Elphidium sp.										
Epistomella sp.										
Evolvocassidulina orientalis	6	4	20	16	4	4	14	31	14	
Evolvocassidulina cf *orientalis*										*
Evolvocassidulina cf *orientalis* (carinate var)										
Fissurina sp.		*				2				
Gavelinopsis hamatus										
Gavelinopsis cf *hamatus*										
Gavelinopsis sp.										
Globocassidulina laevigata										
Globocassidulina subglobosa	1								*	
Gyroidina danvillensis			1							
Gyroidina sp.										
Gyroidinoides sp.										
Gyroidinoides zelandicus										*
Hoeglundina elegans	6				1		5	1		*
Lagena sp.				1					*	
Lagena striata				2	1					
Lagena aff *striata*										
Lagena cf *striata*										
Laticarinina pauperata										
Lenticulina calcar		*							*	*
Lenticulina aff *calcar*	2	4		3		2				
Lenticulina cf *calcar*			8							
Lenticulina costatus										*
Lenticulina gyroscalpra										
Lenticulina loculosus										
Lenticulina mamilligera										
Lenticulina orbicularis										
Lenticulina spp.				2	9	1		3	2	*
Marginulina sp.										
Margmulina subbullata										
Mucronina sinalata										
Mucronina sp.										
Mucronina multicostales										
Mucronina sinalata										
Nodosaria longiscata									*	*
Nodosaria sp.	1	1			2	1				*
Nodosaria substrigata										
Nonionella flemingi										
Notorotalia depressa grp										

Waikato Univ. No.	W962344	W962346	W962348	W962355	W962356	W962358C	W962361	W962366	W962373	W962375A
Sample No.	59	58	3	51	50	393	396	401	408	
Stratigraphic height (m)	2260	2269	2277.5	2296	2300	2315	2330	2360	2394	2395
Notorotalia cf *depressa*										
Notorotalia finlayi				29		34	17			
Notorotalia cf *finlayi*										
Notorotalia finlayi grp										
Notorotalia finlayi/hurupiensis										
Notorotalia hurupiensis		15	23						7	*
Notorotalia cf *hurupiensis*										
Notorotalia hurupiensis/depressa										
Notorotalia macinnesi										
Notorotalia pliozea										
Notorotalia aff *pliozea*										
Notorotalia spp.	24				37					
Notorotalia taranakia										
Notorotalia aff *taranakia*										
Notorotalia cf *taranakia*								27		
Oolina hexagona										
Oolina sp.							1			
Oolina squamosa										*
Oridorsalis tenera	1	12	15	18	8	15	3	8	2	*
Parafissurina sp.										
Patellinella inconspicua										
Pileolina sp.										
Plectofrondicularia pellucida	2	1		5	2			1	*	
Plectofrondicularia cf *pellucida*				1						
Plectofrondicularia pohana										
Proxifrons advena										
Pseudonodosaria sp.										
Pullenia bulloides		*		1	5			1	2	*
Pullenia quinqueloba									*	
Pullenia cf *quinqueloba*	1									
Pullenia sp.										
Pullenia subcarinata										
Rectobolivina striatula										
Rectouvigerina striatula										
Rosalina bradyi										
Rotalia sp.										
Saracenaria italica										*
Saracenaria cf *italica*										
Saracenaria latifrons		1								
Saracenaria sp.										
Sigmoilopsis sp.										
Sigmoilopsis zeaserus										
Sigmomorphina sp.										

Waikato Univ. No.	W962344	W962346	W962348	W962355	W962356	W962358C	W962361	W962366	W962373	W962375A
Sample No.	59	58	3	51	50	393	396	401	408	
Stratigraphic height (m)	2260	2269	2277.5	2296	2300	2315	2330	2360	2394	2395
Siphonia australis										
Siphotextularia wairoana										
Siphouvigerina belluda										
Siphouvigerina canariensis									1	
Siphouvigerina eketahuna										
Siphouvigerina cf *eketahuna*										
Siphouvigerina sp.										
Sphaeroidina bulloides	3	2		1	2	3	1		1	
Spheroidinellopsis seminulina										
Spheroidinellopsis sp.										
Spiroloculina kennetti										
Stainforthia concava										
Stilostomella hochstetteri										
Stilostomella lepidula										
Stilostomella sp.										
Trifarina bradyi										
Trifarina sp.										
Uvigerina (*Euuvigerina*) *miozea* grp	68		1	7	20	31		70		*
Uvigerina (*Siphouvigerina*) sp.										
Uvigerina cf *pliozea* (*miozea* grp)		27								
Uvigerina cf *poroporoensis* (*miozea* grp)									91	
Uvigerina rodleyi										
Vagulina elegans										
Vaginulina sp.								?1	*	
Vaginulina vagina										
Virgulopsis parri										
Virgulopsis patiae										
Virgulopsis pustulata										
Virgulopsis sp.			1							
Virgulopsis subspinescens		3								
Virgulopsis *aff* subspinescens										
Virgulopsis turris										
Virgulopsis wanganuiensis										
Virgulopsis aff *wanganuiensis*										
Virgulopsis cf *wanganuiensis*										
Zeaflorilis parri										*
PLANKTICS										
Globigerina bulloides		*				1				*
Globigerina falconensis		*								*
Globigerina quinqueloba		1	4	2			7			
Globigerina aff *quinqueloba*										

Waikato Univ. No.	W962344	W962346	W962348	W962355	W962356	W962358C	W962361	W962366	W962373	W962375A
Sample No.	59	58	3	51	50	393	396	401	408	
Stratigraphic height (m)	2260	2269	2277.5	2296	2300	2315	2330	2360	2394	2395
Globigerina cf *quinqueloba*									*	
Globigerina spp.	1	*	25	3	2	6	71	1	2	*
Globogirina (*Zeaglobigerina*) *apertura*										
Globogerina (*Zeaglobigerina*) sp.	5			1						*
Globogerina (*Zeaglobigerina*) *woodi*										
Globogerina (*Zeaglobigerina*) cf *woodi*										
Globigerinita glutinata		3		2					*	
Globigerinita cf *glutinata*										
Globigerinita sp.										
Globigerinoides ruber										
Globigerinoides sp.										
Globigerinoides trilobus										
Globorotalia conomiozea										
Globorotalia crassaconica										
Globorotalia aff *crassaconica* (unkeeled)										
Globorotalia cf *crassaconica*										*1D*
Globorotalia crassaformis		*2S*			1				1S *3S*	*6S*
Globorotalia inflata		*	13	?2	?1	3	29		*4S*	*S*
Globorotalia inflata triangula										*S*
Globorotalia miotumida										
Globorotalia pliozea										
Globorotalia puncticulata	5	4			2		2S		1S *5S*	*S*
Globorotalia aff *puncticulata*										
Globorotalia cf *puncticulata*										
Globorotalia puncticuloides										
Globorotalia scitula		*								
Globorotalia sp.					2		2			
Globorotalia cf *subconomiozea*										
Globorotalia truncatulinoides tosaensis										*?*
Globorotalia tumida										*?*
Globorotaloides punticuloides										
Neogloboquadrina pachyderma			1	1			5	1	1 *2S*	
Neogloboquadrina cf pachyderma										
Neogloboquadrina sp.										
Orbulina bilobata										
Orbulina universa						1	1			*
AGGLUTINATED										
Bathysiphon sp.										
Haeuslerella finlayi										
Haeuslerella cf *finlayi*										
Haeuslerella morgani									?*	*

Waikato Univ. No.	W962344	W962346	W962348	W962355	W962356	W962358C	W962361	W962366	W962373	W962375A
Sample No.	59	58	3	51	50	393	396	401	408	
Stratigraphic height (m)	2260	2269	2277.5	2296	2300	2315	2330	2360	2394	2395
Haeuslerella parri	5	74	9	42	15	17	24	37		*
Haeuslerella aff *parri*									25	
Haeuslerella *cf* parri										
Haeuslerella pliocenica	28					27				
Haeuslerella sp.										
Karreriella cylindrica	8				11					*
Karreriella bradyi										
Martinotiella sp.										
Martinottiella communis	6								*	*
Sigmoilopsis zeaserus										
Siphonaperta macbeathi		?*								
Siphonaperta aff *macbeathi*										
Textularia kapitea										
Textularia lythostrota										
Textularia cf *mestayeri*										
Thalmannammina sp.										
RADIOLARIANS										
Total		36	4		2			24	8	

Waikato Univ. No.	W962380	W962393	W962395	W962398	W962406	W962409	W962412	W962420	W962432	W962442
Sample No.	440	453	455	458	463	542	464	492	565	553
Stratigraphic height (m)	2410	2459	2468	2547	2610	2625	2640	2667	2725	2775
BENTHICS										
Alabamina sp.					1					
Ammonia beccarii										
Ammonia sp.								*		
Amphicoryna cf *bortonica*										
Amphicoryna hirsuta			2	1	5	14		5	25	2
Amphicoryna aff *hirsuta*								*		
Amphicoryna cf *hirsuta*							2			
Amphicoryna scalaris										
Amphicoryna sp.	4			3	3	12	6		49	3
Anomalina spherica			1		*					
Anomalinoides alazanensis										
Anomalinoides parvumbilius	3		4	4	12	9	5	2	2	9
Anomalinoides cf *parvumbilius*										
Anomalinoides sp.										
Anomalinoides sphericus	2									
Anomalinoides subnonionoides	8		20		13	1	30	9	23	8
Astrononion kickinskii								2		
Astrononion neefi										
Astrononion cf *neefi*										
Astrononion novozealandicum										
Astrononion cf *novozealandicum*										
Astrononion parki			?1		*	12	6			18
Astrononion sp.										
Bolivina affiliata										
Bolivina aff *affiliata*										
Bolivina cf *affiliata*										
Bolivina albatrossi					*?*		1	*		
Bolivina aff *albatrossi*										
Bolivina lapsus										
Bolivina numerosa										
Bolivina spathulata					*?*					
Bolivina sp.										
Bolivina watti										
Bolivina zigzag										*
Bolivinita finlayi										
Bolivinita aff *finlayi*										
Bolivinita cf *finlayi*										
Bolivinita pliobliqua							?2		21	32
Bolivinita pliozea	55									
Bolivinita pohana										
Bolivinita pseudocompressa										
Bolivinita aff *pseudocompressa*										

Waikato Univ. No.	W962380	W962393	W962395	W962398	W962406	W962409	W962412	W962420	W962432	W962442
Sample No.	440	453	455	458	463	542	464	492	565	553
Stratigraphic height (m)	2410	2459	2468	2547	2610	2625	2640	2667	2725	2775
Bolivinita quadrilatera										
Bulimina aculeata	9									
Bulimina aff *aculeata* (reduced spines)			2		5	6		4	40	15
Bulimina cf *aculeata*					*					
Bulimina elongata										
Bulimina *cf* elongata						3			7	
Bulimina marginata										
Bulimina aff *marginata*				2						
Bulimina cf *marginata*										
Bulimina sp.										
Bulimina striata										
Bulimina cf *striata*	3		2		*	1	1	*		2
Bulimina cf *vella*										
Cassidulina neocarinata				1	*		1	1		11
Ceratocancris sp.										*
Chilostomella ovoidea										
Chrysalogonium verticale									?2	
Cibicides amoenus										
Cibicides deliquatus			3		2		5	*	3	2
Cibicides cf *deliquatus*	22		6	8	2	4		13	13	13
Cibicides finlayi										?1
Cibicides aff *finlayi*										
Cibicides cf *finlayi*										
Cibicides molestus	10		19		6		21	48	34	11
Cibicides aff *molestus*	6									
Cibicides neoperforatus										
Cibicides cf *notocenicus*										
Cibicides novozealandicus										
Cibicides spp.							11			
Cibicides subhaidingeri										
Dentalina obliquecostata										
Dentalina sp.	1		1		1	1	3	1	1	7
Dentalina soluta										
Dentalina substrigata								?2		
Discorbinella bertheloti										
Discorbinella cf *bertheloti*										
Discorbinella sp.										3
Discorbis dimidiatus										
Discorbis sp.										
Dyocibicides primitiva										
Dyocibicides sp.										
Elphidium advenum										
Elphidium charlottensis	1				*			?1		

Waikato Univ. No.	W962380	W962393	W962395	W962398	W962406	W962409	W962412	W962420	W962432	W962442
Sample No.	440	453	455	458	463	542	464	492	565	553
Stratigraphic height (m)	2410	2459	2468	2547	2610	2625	2640	2667	2725	2775
Elphidium cf *charlottensis*										
Elphidium simplex aoteanum										
Elphidium sp.										
Epistomella sp.										
Evolvocassidulina orientalis	18				2	10		*		19
Evolvocassidulina cf *orientalis*										
Evolvocassidulina cf *orientalis* (carinate var)			31	16						
Fissurina sp.					2			*	1	1
Gavelinopsis hamatus										
Gavelinopsis cf *hamatus*										
Gavelinopsis sp.										
Globocassidulina laevigata										
Globocassidulina subglobosa								*		
Gyroidina danvillensis										1
Gyroidina sp.										
Gyroidinoides sp.										
Gyroidinoides zelandicus			2							
Hoeglundina elegans	9		4	4	*					1
Lagena sp.				1			1		1	1
Lagena striata					*					
Lagena aff *striata*										
Lagena cf *striata*					*					
Laticarinina pauperata										
Lenticulina calcar			2	?8	*	25	3	3		*
Lenticulina aff *calcar*									8	
Lenticulina cf *calcar*										
Lenticulina costatus					*					
Lenticulina gyroscalpra										2
Lenticulina loculosus					*?*					
Lenticulina mamilligera										
Lenticulina orbicularis										
Lenticulina spp.	10		7	26	20	13	5	11	5	19
Marginulina sp.					1					
Margmulina subbullata										1
Mucronina sinalata										
Mucronina sp.										
Mucronina multicostales								1		
Mucronina sinalata										
Nodosaria longiscata					*			*		
Nodosaria sp.				1	1			*	2	*
Nodosaria substrigata					*?*					
Nonionella flemingi	2				*	2		*		1
Notorotalia depressa grp										

Waikato Univ. No.	W962380	W962393	W962395	W962398	W962406	W962409	W962412	W962420	W962432	W962442
Sample No.	440	453	455	458	463	542	464	492	565	553
Stratigraphic height (m)	2410	2459	2468	2547	2610	2625	2640	2667	2725	2775
Notorotalia cf *depressa*										
Notorotalia finlayi					18			14	3	26
Notorotalia cf *finlayi*										
Notorotalia finlayi grp										
Notorotalia finlayi/hurupiensis			15			35				
Notorotalia hurupiensis				?10	*?*					
Notorotalia cf *hurupiensis*	4									
Notorotalia hurupiensis/depressa							7			
Notorotalia macinnesi										
Notorotalia pliozea					*					
Notorotalia aff *pliozea*										3
Notorotalia spp.							2			
Notorotalia taranakia										
Notorotalia aff *taranakia*										
Notorotalia cf *taranakia*										
Oolina hexagona										
Oolina sp.										
Oolina squamosa					*					
Oridorsalis tenera	3		6	5	4	16	7	10	1	4
Parafissurina sp.										
Patellinella inconspicua										
Pileolina sp.										
Plectofrondicularia pellucida			1		*			*		
Plectofrondicularia cf *pellucida*										
Plectofrondicularia pohana										
Proxifrons advena								*		
Pseudonodosaria sp.										
Pullenia bulloides	1				*		1			
Pullenia quinqueloba										
Pullenia cf *quinqueloba*										
Pullenia sp.										
Pullenia subcarinata										
Rectobolivina striatula					*			?*		
Rectouvigerina striatula										
Rosalina bradyi										
Rotalia sp.										
Saracenaria italica			?1		1			1		
Saracenaria cf *italica*										
Saracenaria latifrons										
Saracenaria sp.										
Sigmoilopsis sp.					*					
Sigmoilopsis zeaserus										
Sigmomorphina sp.										

Waikato Univ. No.	W962380	W962393	W962395	W962398	W962406	W962409	W962412	W962420	W962432	W962442
Sample No.	440	453	455	458	463	542	464	492	565	553
Stratigraphic height (m)	2410	2459	2468	2547	2610	2625	2640	2667	2725	2775
Siphonia australis										
Siphotextularia wairoana										
Siphouvigerina belluda								*		
Siphouvigerina canariensis										
Siphouvigerina eketahuna										
Siphouvigerina cf *eketahuna*										
Siphouvigerina sp.										
Sphaeroidina bulloides			2			4				1
Spheroidinellopsis seminulina										
Spheroidinellopsis sp.										
Spiroloculina kennetti										
Stainforthia concava										*
Stilostomella hochstetteri										
Stilostomella lepidula								?1		
Stilostomella sp.					*			*		*
Trifarina bradyi					*					
Trifarina sp.										
Uvigerina (*Euuvigerina*) *miozea* grp			5	37	50		109	38	31	35
Uvigerina (*Siphouvigerina*) sp.										
Uvigerina cf *pliozea* (*miozea* grp)	76									*
Uvigerina cf *poroporoensis* (*miozea* grp)										
Uvigerina rodleyi				7		37				
Vagulina elegans										
Vaginulina sp.					1			1		
Vaginulina vagina					*?*					
Virgulopsis parri										
Virgulopsis patiae										
Virgulopsis pustulata	1									
Virgulopsis sp.										*
Virgulopsis subspinescens										
Virgulopsis *aff* subspinescens										
Virgulopsis turris						2				
Virgulopsis wanganuiensis					*?*	3		*		
Virgulopsis aff *wanganuiensis*										
Virgulopsis cf *wanganuiensis*										
Zeaflorilis parri										
PLANKTICS										
Globigerina bulloides					*					1
Globigerina falconensis					*			?1		
Globigerina quinqueloba	2			3		1				4
Globigerina aff *quinqueloba*										

Waikato Univ. No.	W962380	W962393	W962395	W962398	W962406	W962409	W962412	W962420	W962432	W962442
Sample No.	440	453	455	458	463	542	464	492	565	553
Stratigraphic height (m)	2410	2459	2468	2547	2610	2625	2640	2667	2725	2775
Globigerina cf *quinqueloba*										
Globigerina spp.	3		6		2	2	3	7	4	22
Globogirina (*Zeaglobigerina*) *apertura*										
Globogerina (*Zeaglobigerina*) sp.					*					
Globogerina (*Zeaglobigerina*) *woodi*					*	?1				
Globogerina (*Zeaglobigerina*) cf *woodi*										
Globigerinita glutinata										2
Globigerinita cf *glutinata*										
Globigerinita sp.	1									
Globigerinoides ruber										
Globigerinoides sp.										
Globigerinoides trilobus					*					
Globorotalia conomiozea										
Globorotalia crassaconica										3D *4D*
Globorotalia aff *crassaconica* (unkeeled)										
Globorotalia cf *crassaconica*					*10*					
Globorotalia crassaformis		*4S*			*5D*		3D	*1D*		2D
Globorotalia inflata	1	*	4		*		15	*1S*	8	5S *9S*
Globorotalia inflata triangula					*			1S *1S*		12S *9S*
Globorotalia miotumida										
Globorotalia pliozea										
Globorotalia puncticulata	3	*	3		*	?3	1			1S
Globorotalia aff *puncticulata*										
Globorotalia cf *puncticulata*										
Globorotalia puncticuloides										
Globorotalia scitula										*1S*
Globorotalia sp.	1									
Globorotalia cf *subconomiozea*										
Globorotalia truncatulinoides tosaensis										
Globorotalia tumida										
Globorotaloides punticuloides										
Neogloboquadrina pachyderma							1	*2D*		*1S*
Neogloboquadrina cf pachyderma										
Neogloboquadrina sp.										
Orbulina bilobata										
Orbulina universa					*					*
AGGLUTINATED										
Bathysiphon sp.										
Haeuslerella finlayi										
Haeuslerella cf *finlayi*										
Haeuslerella morgani										

Waikato Univ. No.	W962380	W962393	W962395	W962398	W962406	W962409	W962412	W962420	W962432	W962442
Sample No.	440	453	455	458	463	542	464	492	565	553
Stratigraphic height (m)	2410	2459	2468	2547	2610	2625	2640	2667	2725	2775
Haeuslerella parri	56		32	1	11	11	47		9	28
Haeuslerella aff *parri*										
Haeuslerella *cf* parri								8		
Haeuslerella pliocenica										
Haeuslerella sp.										
Karreriella cylindrica										
Karreriella bradyi										
Martinotiella sp.							1			
Martinottiella communis	5				*			8		
Sigmoilopsis zeaserus										1
Siphonaperta macbeathi										*
Siphonaperta aff *macbeathi*										
Texturlria kapitea										
Textularia lythostrota										
Texturlria cf *mestayeri*										
Thalmannammina sp.										
RADIOLARIANS										
Total					5	23			12	14

Waikato Univ. No.	W962449B	W962475	W962496	W962510	W962511	W962550	W962559
Sample No.	469	471	480	594	502	606	525
Stratigraphic height (m)	2810	2939	3105	3200	3202	3395	3440
BENTHICS							
Alabamina sp.							
Ammonia beccarii				*?			
Ammonia sp.							
Amphicoryna cf *bortonica*							
Amphicoryna hirsuta			*				
Amphicoryna aff *hirsuta*		2					
Amphicoryna cf *hirsuta*							
Amphicoryna scalaris							
Amphicoryna sp.		*					
Anomalina spherica			*				
Anomalinoides alazanensis							
Anomalinoides parvumbilius			1	*	*		
Anomalinoides cf *parvumbilius*							
Anomalinoides sp.		1					
Anomalinoides sphericus		1					
Anomalinoides subnonionoides							
Astrononion kickinskii		*			*		
Astrononion neefi							
Astrononion cf *neefi*							
Astrononion novozealandicum		3				1	
Astrononion cf *novozealandicum*							
Astrononion parki	8	17	*	13	*	27	
Astrononion sp.							
Bolivina affillata							
Bolivina aff *affiliata*							
Bolivina cf *affiliata*							
Bolivina albatrossi							
Bolivina aff *albatrossi*							
Bolivina lapsus							
Bolivina numerosa							
Bolivina spathulata							
Bolivina sp.						1	
Bolivina watti							
Bolivina zigzag							
Bolivinita finlayi							
Bolivinita aff *finlayi*							
Bolivinita cf *finlayi*							
Bolivinita pliobliqua		1	3	4			
Bolivinita pliozea	?1						
Bolivinita pohana							
Bolivinita pseudocompressa							
Bolivinita aff *pseudocompressa*							

Waikato Univ. No.	W962449B	W962475	W962496	W962510	W962511	W962550	W962559
Sample No.	469	471	480	594	502	606	525
Stratigraphic height (m)	2810	2939	3105	3200	3202	3395	3440
Bolivinita quadrilatera		*					
Bulimina aculeata	1						
Bulimina aff *aculeata* (reduced spines)		23	6	22			21
Bulimina cf *aculeata*			*			35	
Bulimina elongata							
Bulimina *cf* elongata							
Bulimina marginata							
Bulimina aff *marginata*		1					
Bulimina cf *marginata*							
Bulimina sp.							
Bulimina striata							
Bulimina cf *striata*							
Bulimina cf *vella*							
Cassidulina neocarinata		32		10		19	2
Ceratocancris sp.							
Chilostomella ovoidea							
Chrysalogonium verticale							
Cibicides amoenus							
Cibicides deliquatus		*	3	*	*		
Cibicides cf *deliquatus*		1					
Cibicides finlayi							
Cibicides aff *finlayi*							
Cibicides cf *finlayi*							
Cibicides molestus			*				
Cibicides aff *molestus*							
Cibicides neoperforatus							
Cibicides cf *notocenicus*							
Cibicides novozealandicus							
Cibicides spp.		*				9	
Cibicides subhaidingeri							
Dentalina obliquecostata							
Dentalina sp.		*		*		3	
Dentalina soluta							
Dentalina substrigata							
Discorbinella bertheloti							
Discorbinella cf *bertheloti*						1	
Discorbinella sp.							
Discorbis dimidiatus						1	
Discorbis sp.							
Dyocibicides primitiva							
Dyocibicides sp.							
Elphidium advenum							
Elphidium charlottensis		19	3	8	*	60	2

Waikato Univ. No.	W962449B	W962475	W962496	W962510	W962511	W962550	W962559
Sample No.	469	471	480	594	502	606	525
Stratigraphic height (m)	2810	2939	3105	3200	3202	3395	3440
Elphidium cf *charlottensis*							
Elphidium simplex aoteanum							
Elphidium sp.							
Epistomella sp.				6			
Evolvocassidulina orientalis	83	21	1	13		18	
Evolvocassidulina cf *orientalis*							
Evolvocassidulina cf *orientalis* (carinate var)							
Fissurina sp.						1	
Gavelinopsis hamatus							
Gavelinopsis cf *hamatus*							
Gavelinopsis sp.		*				6	
Globocassidulina laevigata							
Globocassidulina subglobosa						2	
Gyroidina danvillensis						1	
Gyroidina sp.							
Gyroidinoides sp.							
Gyroidinoides zelandicus			*				
Hoeglundina elegans		1	*				
Lagena sp.				2			1
Lagena striata			*	*			
Lagena aff *striata*							
Lagena cf *striata*			*				
Laticarinina pauperata							
Lenticulina calcar	3	*	2		*		
Lenticulina aff *calcar*		*	*				
Lenticulina cf *calcar*							
Lenticulina costatus			*				
Lenticulina gyroscalpra							
Lenticulina loculosus							
Lenticulina mamilligera							
Lenticulina orbicularis							
Lenticulina spp.			1	*		2	1
Marginulina sp.							
Margmulina subbullata							
Mucronina sinalata							
Mucronina sp.							
Mucronina multicostales							
Mucronina sinalata							
Nodosaria longiscata							
Nodosaria sp.			1				
Nodosaria substrigata							
Nonionella flemingi		12	1	4		40	
Notorotalia depressa grp						160	

Waikato Univ. No.	W962449B	W962475	W962496	W962510	W962511	W962550	W962559
Sample No.	469	471	480	594	502	606	525
Stratigraphic height (m)	2810	2939	3105	3200	3202	3395	3440
Notorotalia cf depressa							
Notorotalia finlayi		64	5	28	*		
Notorotalia cf finlayi							
Notorotalia finlayi grp							
Notorotalia finlayi/hurupiensis							
Notorotalia hurupiensis							4
Notorotalia cf hurupiensis			*				
Notorotalia hurupiensis/depressa							
Notorotalia macinnesi							
Notorotalia pliozea			*				
Notorotalia aff pliozea							
Notorotalia spp.	2						
Notorotalia taranakia							
Notorotalia aff taranakia							
Notorotalia cf taranakia	?1						
Oolina hexagona							
Oolina sp.		*					
Oolina squamosa		*		*		3	
Oridorsalis tenera	19	5	1	*			
Parafissurina sp.							
Patellinella inconspicua							
Pileolina sp.		3				1	
Plectofrondicularia pellucida							
Plectofrondicularia cf pellucida							
Plectofrondicularia pohana							
Proxifrons advena							
Pseudonodosaria sp.							
Pullenia bulloides							
Pullenia quinqueloba							
Pullenia cf quinqueloba							
Pullenia sp.			*				
Pullenia subcarinata							
Rectobolivina striatula			*	4			
Rectouvigerina striatula							
Rosalina bradyi		*					
Rotalia sp.							
Saracenaria itallica			*				
Saracenaria cf itallica							
Saracenaria latifrons							
Saracenaria sp.							
Sigmoilopsis sp.						1	
Sigmoilopsis zeaserus							
Sigmomorphina sp.							

Waikato Univ. No.	W962449B	W962475	W962496	W962510	W962511	W962550	W962559
Sample No.	469	471	480	594	502	606	525
Stratigraphic height (m)	2810	2939	3105	3200	3202	3395	3440
Siphonia australis							
Siphotextularia wairoana		*					
Siphouvigerina belluda							
Siphouvigerina canariensis							
Siphouvigerina eketahuna							
Siphouvigerina cf *eketahuna*							
Siphouvigerina sp.							
Sphaeroidina bulloides		7	2	*		1	
Spheroidinellopsis seminulina							
Spheroidinellopsis sp.							
Spiroloculina kennetti							
Stainforthia concava							
Stilostomella hochstetteri							
Stilostomella lepidula							
Stilostomella sp.							
Trifarina bradyi							
Trifarina sp.							
Uvigerina (*Euuvigerina*) *miozea* grp	1	4				4	3
Uvigerina (*Siphouvigerina*) sp.							
Uvigerina cf *pliozea* (*miozea* grp)							
Uvigerina cf *poroporoensis* (*miozea* grp)							
Uvigerina rodleyi		1	151	*	*		
Vagulina elegans							
Vaginulina sp.							
Vaginulina vagina			*				
Virgulopsis parri							
Virgulopsis patiae							
Virgulopsis pustulata						2	
Virgulopsis sp.							
Virgulopsis subspinescens							
Virgulopsis *aff* subspinescens							
Virgulopsis turris			1	2			
Virgulopsis wanganuiensis		3		17		40	3
Virgulopsis aff *wanganuiensis*				12			
Virgulopsis cf *wanganuiensis*							
Zeaflorilis parri		*		*			
PLANKTICS							
Globigerina bulloides		1	*				
Globigerina falconensis							
Globigerina quinqueloba							
Globigerina aff *quinqueloba*		2					

Waikato Univ. No.	W962449B	W962475	W962496	W962510	W962511	W962550	W962559
Sample No.	469	471	480	594	502	606	525
Stratigraphic height (m)	2810	2939	3105	3200	3202	3395	3440
Globigerina cf *quinqueloba*							
Globigerina spp.		5	*				
Globogirina (*Zeaglobigerina*) *apertura*							
Globogerina (*Zeaglobigerina*) sp.							
Globogerina (*Zeaglobigerina*) *woodi*							
Globogerina (*Zeaglobigerina*) cf *woodi*							
Globigerinita glutinata		*					
Globigerinita cf *glutinata*							
Globigerinita sp.		*					
Globigerinoides ruber							
Globigerinoides sp.							
Globigerinoides trilobus							
Globorotalia conomiozea							
Globorotalia crassaconica		*2D*					
Globorotalia aff *crassaconica* (unkeeled)							
Globorotalia cf *crassaconica*							
Globorotalia crassaformis		*1D*					
Globorotalia inflata		*12S:1D*	*5S*				
Globorotalia inflata triangula		*1S*	*20S*				
Globorotalia miotumida							
Globorotalia pliozea							
Globorotalia puncticulata		3	*6S*				
Globorotalia aff *puncticulata*							
Globorotalia cf *puncticulata*							
Globorotalia puncticuloides		*1S:1D*					
Globorotalia scitula							
Globorotalia sp.							
Globorotalia cf *subconomiozea*							
Globorotalia truncatulinoides tosaensis							
Globorotalia tumida							
Globorotaloides punticuloides							
Neogloboquadrina pachyderma		1 *3S:7D*					
Neogloboquadrina cf pachyderma							
Neogloboquadrina sp.							
Orbulina bilobata							
Orbulina universa			*	*			
AGGLUTINATED							
Bathysiphon sp.							
Haeuslerella finlayi							
Haeuslerella cf *finlayi*							
Haeuslerella morgani				*			

Waikato Univ. No.	W962449B	W962475	W962496	W962510	W962511	W962550	W962559
Sample No.	469	471	480	594	502	606	525
Stratigraphic height (m)	2810	2939	3105	3200	3202	3395	3440
Haeuslerella parri		8	*	1		11	
Haeuslerella aff *parri*							
Haeuslerella *cf* parri		*					
Haeuslerella pliocenica							
Haeuslerella sp.					*		
Karreriella cylindrica							
Karreriella bradyi							
Martinotiella sp.							
Martinottiella communis			*				
Sigmoilopsis zeaserus							
Siphonaperta macbeathi							
Siphonaperta aff *macbeathi*							
Texturlria kapitea							
Textularia lythostrota							
Texturlria cf *mestayeri*							
Thalmannammina sp.							
RADIOLARIANS							
Total							1

(3) Particle Size

All particle size information is presented on the accompanying CD ROM, from where it may be viewed directly or down loaded as required. Basic particle size data is contained in the summary section.

Sieve data where available is presented as sand and mud percentages.

Laser sizer data is presented in 0.5 phi increments, with the mean (μm), standard deviation, sand % and mud % values also given.

(4) ISOTOPE DATA

This section contains the results of the isotope analyses undertaken on the Europa 20/20 mass spectrometer during this study

This information is also available in electronic form (viewable and down loadable) from the CD ROM in the back of this thesis.

Appendix 2: Isotope Data

	STANDARDS									
SAMPLE	D-45	D-46	d-C13	d-O18						
TSS103	0.337	-4.705	1.953	-2.136						
TSS104	0.320	-4.769	1.937	-2.200						
TSS105	0.327	-4.626	1.939	-2.057						
TSS108	0.315	-4.722	1.930	-2.153						
TSS109	0.321	-4.644	1.933	-2.075						
TSS110	0.310	-4.764	1.926	-2.195						
TSS192m	0.365	-4.678	1.982	-2.109						
TSS193m	0.344	-4.834	1.965	-2.265						
TSS194m	0.375	-4.695	1.993	-2.126						
TSS195m	0.317	-4.850	1.937	-2.282						
TSS196m	0.330	-4.824	1.950	-2.255						
TSS197m	0.333	-4.801	1.952	-2.232						
TSS198m	0.364	-4.661	1.981	-2.092						
TSS199m	0.312	-4.537	1.920	-1.968						
TSS200m	0.349	-4.826	1.970	-2.257						
TSS219	0.301	-4.720	1.915	-2.151						
TSS221	0.342	-4.724	1.959	-2.155						
TSS222	0.346	-4.729	1.964	-2.160						
TSS236	0.362	-4.508	1.860	-2.211						
TSS237	0.327	-4.530	1.936	-1.961						
TSS238	0.373	-4.469	1.983	-1.899						
TSS239	0.310	-4.770	1.927	-2.201						
TSS240	0.321	-4.712	1.936	-2.143						
TSS241	0.324	-4.628	1.936	-2.059						
TSS242	0.272	-4.751	1.885	-2.182						
TSS243	0.338	-4.311	1.940	-1.740						
TSS244	0.332	-4.502	1.942	-1.932						

University No.	Strat. Height		*Uvigerina miozea* group							
	(m)		d-C13	d-O18	C13 vpdb	O18 vpdb	Volume	Error C13	Error O18	
W962333	2204		0.093	1.22	0.097	1.175	2E-08	0.018	0.03	
W962334	2208		0.024	1.119	0.028	1.074	2E-08	0.008	0.014	
W962335	2213		-0.095	0.995	-0.091	0.95	1E-08	0.006	0.014	
W962336	2223		-0.096	1.905	-0.076	1.846	1E-08	0.009	0.017	
W962337	2228		-4.365	-1.255	-4.376	-1.262	9E-09	0.013	0.025	
W962338	2233		-0.055	0.933	-0.051	0.888	2E-08	0.011	0.02	
W962339A	2240		-0.521	1.502	-0.517	1.457	7E-09	0.013	0.015	
W962339B	2244		-5.946	0.458	-5.939	0.389	6E-09	0.011	0.028	
W962340	2249		-6.24	-1.98	-6.251	-1.987	9E-09	0.008	0.022	
W962341	2253.5		-0.059	1.225	-0.055	1.18	2E-08	0.005	0.023	
W962344	2260		-4.541	-0.054	-4.521	-0.113	1E-08	0.016	0.021	
W962346	2269		0.006	1.619	-0.024	1.586	1E-08	0.009	0.014	
W962348	2277.5									
W962355	2296		-2.698	0.433	-2.691	0.364	1E-08	0.009	0.017	
W962356	2300		0.221	1.343	0.191	1.31	2E-08	0.016	0.02	
W962358A	2306		-0.068	1.101	-0.064	1.056	2E-08	0.009	0.021	
W962358B	2310		-0.253	1.451	-0.249	1.406	1E-08	0.004	0.011	
W962358C	2315		-1.841	0.932	-1.852	0.925	1E-08	0.027	0.043	
W962359	2320		-1.135	1.402	-1.115	1.343	2E-08	0.009	0.019	
W962360	2325		-0.924	1.232	-0.935	1.225	1E-08	0.008	0.021	
W962361	2330									
W962362	2335									
W962364	2350		-3.152	0.176	-3.182	0.143	8E-09	0.01	0.022	
W962366	2360		0.073	1.468	0.101	1.219	1E-08	0.006	0.007	
W962369	2376		0.189	1.509	0.213	1.333	3E-08	0.01	0.015	
W962370	2381		0.429	1.551	0.446	1.485	3E-08	0.015	0.017	
W962371	2386		0.437	1.63	0.454	1.564	1E-08	0.005	0.006	
W962372	2391		0.423	1.422	0.44	1.356	1E-08	0.008	0.011	
W962377	2404.5		0.376	1.52	0.404	1.271	2E+08	0.005	0.01	
W962384	2420.5		0.456	1.464	0.473	1.398	2E-08	0.007	0.014	
W962392	2450		0.448	1.435	0.476	1.186	1E-08	0.01	0.012	
W962393	2459		0.275	1.421	0.292	1.355	1E-08	0.007	0.021	
W962394	2466									
W962395	2468		0.519	1.438	0.547	1.189	1E-08	0.013	0.021	
W962398	2547		0.363	1.514	0.38	1.448	1E-08	0.01	0.022	
W962399	2548		0.096	1.287	0.12	1.111	1E-08	0.01	0.019	
W962406	2610		0.034	1.276	0.058	1.1	8E-09	0.011	0.016	
W962407	2615		0.008	1.088	0.025	1.022	2E-08	0.01	0.013	
W962408	2620		-0.042	1.846	-0.018	1.67	1E-08	0.006	0.018	
W962409	2625		-0.024	1.031	0.004	0.782	6E-09	0.007	0.021	
W962410	2630		0.095	1.322	0.119	1.146	1E-08	0.007	0.026	
W962411	2635		0.207	1.827	0.224	1.761	1E-08	0.005	0.007	
W962412	2640		-0.108	1.617	-0.091	1.551	2E-08	0.009	0.011	
W962414	2645		0.363	1.104	0.38	1.038	2E-08	0.012	0.026	
W962419	2661		0.071	1.319	0.088	1.253	1E-08	0.006	0.032	
W962424	2685		0.148	1.285	0.176	1.036	1E-08	0.01	0.023	

Appendix 2: Isotope Data

University No.	Strat. Height		*Cibicides delicatus*						
	(m)		d-C13	d-O18	C13 vpdb	O18 vpdb	Volume	Error C13	Error O18
W962333	2204								
W962334	2208		0.695	0.5	0.699	0.455	1.3E-08	0.008	0.008
W962335	2213		0.601	0.277	0.605	0.232	1.1E-08	0.005	0.009
W962336	2223		0.58	0.613	0.6	0.554	1.4E-08	0.004	0.025
W962337	2228		0.785	0.286	0.789	0.241	1E-08	0.01	0.021
W962338	2233		-2.23	-0.949	-2.241	-0.956	4.8E-09	0.013	0.037
W962339A	2240		-5.636	-1.3	-5.666	-1.333	4.2E-09	0.011	0.039
W962339B	2244		0.405	0.556	0.409	0.511	5.3E-09	0.01	0.023
W962340	2249		-8.542	-3.309	-8.553	-3.316	6.5E-09	0.005	0.03
W962341	2253.5		0.531	0.777	0.535	0.732	7.3E-09	0.012	0.01
W962344	2260		-3.488	-0.004	-3.468	-0.063	1.2E-08	0.007	0.017
W962346	2269		0.519	0.904	0.523	0.859	7E-09	0.011	0.018
W962348	2277.5		0.799	0.326	0.819	0.267	1.2E-08	0.005	0.016
W962355	2296		0.709	0.637	0.713	0.592	1.5E-08	0.012	0.025
W962356	2300		0.371	0.53	0.341	0.497	1.6E-08	0.004	0.01
W962358A	2306		-3.154	-0.761	-3.165	-0.768	4.4E-09	0.011	0.02
W962358B	2310		-0.986	0.51	-0.997	0.503	4.2E-09	0.019	0.031
W962358C	2315								
W962359	2320		-0.697	1.829	-0.69	1.76	1.3E-08	0.012	0.025
W962360	2325		0.547	1.268	0.536	1.261	7E-09	0.006	0.024
W962361	2330		0.4	-0.872	0.389	-0.879	6.8E-08	0.012	0.021
W962362	2335								
W962364	2350								
W962366	2360								
W962369	2376								
W962370	2381								
W962371	2386								
W962372	2391								
W962377	2404.5		0.889	1.052	0.917	0.803	9.8E-09	0.009	0.019
W962384	2420.5		0.922	1.208	0.939	1.142	1.5E-08	0.007	0.008
W962392	2450								
W962393	2459		0.919	1.111	0.936	1.045	1.8E-08	0.007	0.023
W962394	2466		1.18	0.912	1.204	0.736	1.6E-08	0.011	0.02
W962395	2468		1.142	1.041	1.17	0.792	1.1E-08	0.008	0.008
W962398	2547								
W962399	2548								
W962406	2610		0.759	0.789	0.783	0.613	9.9E-09	0.005	0.013
W962407	2615								
W962408	2620		1.034	0.865	1.058	0.689	2.5E-08	0.013	0.013
W962409	2625								
W962410	2630		1.029	0.904	1.053	0.728	1.2E-08	0.013	0.011
W962411	2635								
W962412	2640		1.08	1.497	1.097	1.431	3.4E-09	0.028	0.035
W962414	2645								
W962419	2661								
W962424	2685		0.803	0.876	0.831	0.627	9.3E-09	0.008	0.024

	University No.	Strat. Height		*Globigerina* sp.						
		(m)		d-C13	d-O18	C13 vpdb	O18 vpdb	Volume	Error C13	Error O18
	W962333	2204								
	W962334	2208								
	W962335	2213								
	W962336	2223								
	W962337	2228								
	W962338	2233								
	W962339A	2240								
	W962339B	2244								
	W962340	2249								
	W962341	2253.5								
	W962344	2260								
	W962346	2269								
	W962348	2277.5		0.05	-0.51	0.039	-0.517	3.2E-09	0.014	0.034
	W962355	2296								
	W962356	2300								
	W962358A	2306								
	W962358B	2310		-0.9	0.692	-0.911	0.685	2.6E-09	0.028	0.061
	W962358C	2315								
	W962359	2320		-1.376	0.075	-1.387	0.068	1.9E-09	0.075	0.136
	W962360	2325		-1.011	0.611	-1.022	0.604	7.4E-09	0.007	0.018
	W962361	2330		-0.23	-1.797	-0.241	-1.804	7.8E-09	0.016	0.044
	W962362	2335		-0.699	0.98	-0.71	0.973	3.5E-09	0.028	0.032
	W962364	2350								
	W962366	2360								
	W962369	2376								
	W962370	2381								
	W962371	2386								
	W962372	2391								
	W962377	2404.5								
	W962384	2420.5								
	W962392	2450								
	W962393	2459								
	W962394	2466								
	W962395	2468								
	W962398	2547								
	W962399	2548								
	W962406	2610								
	W962407	2615								
	W962408	2620								
	W962409	2625								
	W962410	2630								
	W962411	2635								
	W962412	2640								
	W962414	2645								
	W962419	2661								
	W962424	2685								